Genome, mutational and RNA-seq analyses of *Janthinobacterium* and *Duganella* strains reveal the presence of a single α-hydroxyketone-like quorum sensing system involved in bacterial-fungal interactions

Dissertation

for obtaining the degree Doctor rerum naturalium (Dr. rer. nat.)

at the Department of Biology
Subdivision of the Faculty of Mathematics, Informatics and Natural Sciences
of the University of Hamburg

by

Frederike Svenja Haack

from Itzehoe

Hamburg 2016

Approved by the Department of Biology, University of Hamburg at the request of
Prof. Dr. Wolfgang Streit
Second evaluator of the dissertation: Prof. Dr. Wilhelm Schäfer
Date of defense (Disputation): 24. October 2016

This is a corrected version.

Declaration on oath

I hereby declare, on oath, that I have written the present dissertation by my own and have not used other than the acknowledged resources and aids.

Hamburg,

_____

Frederike Haack

English Language Declaration

I hereby declare as a native English speaker that I have checked the thesis “Genome, mutational and RNA-seq analyses of *Janthinobacterium* and *Duganella* strains reveal the presence of a single α-hydroxyketone-like quorum sensing system involved in bacterial-fungal interactions” by Frederike Svenja Haack for grammatically correct English and the scientific accuracy of the language. I also confirm that I am a native English speaker.

Sincerely,

_____

Carla Haslauer

Following publications contribute to this research

Frederike S. Haack, Anja Poehlein, Cathrin Kröger, Christian A. Voigt, Meike Piepenring, Helge B. Bode, Rolf Daniel, Wilhelm Schäfer and Wolfgang R. Streit (2016). „**Molecular Keys to the *Janthinobacterium* and *Duganella* spp. Interaction with the Plant Pathogen *Fusarium graminearum*".** Front. Microbiol. 7:1668. doi: 10.3389/fmicb.2016.01668

Claudia Hornung, Anja Poehlein, Frederike S. Haack, Martina Schmidt, Katja Dierking, Andrea Pohlen, Hinrich Schulenburg, Melanie Blokesch, Laure Plener, Kirsten Jung, Andreas Bonge, Ines Krohn-Molt, Christian Utpatel, Gabriele Timmermann, Eva Spieck, Andreas Pommerening-Röser, Edna Bode, Helge B. Bode, Rolf Daniel, Christel Schmeisser and Wolfgang R. Streit (2012). **"The *Janthinobacterium* sp. HH01 genome encodes a homologue of the *V. cholerae* CqsA and *L. pneumophila* LqsA autoinducer synthases".** PLoS One. **8**(2): e55045. doi: 10.1371/journal.pone.0055045

Table of content

Figures

Tables

Data submission to public databases

The sequences of the rRNA genes of the isolates HH01, HH100 – HH107 were deposited at GenBank under the accession numbers KJ855978 (HH01), KJ855970 (HH100), KJ855971 (HH101), KJ855972 (HH102), KJ855973 (HH103), KJ855974 (HH104), KJ855975 (HH105), KJ855976 (HH106) and KJ855977 (HH107). The whole genome DNA sequences have been deposited at GenBank under the following accession numbers: *D. phyllosphaerae* DSM23865 (LROM00000000), *D*. sp. HH101 (LRON00000000), *D.* sp. HH105 (LRHV00000000), *J.* lividum DSM1522 (LRHW00000000), *J.* sp. MP5059B (LRHX00000000), *J.* sp. HH100 (LRHY00000000), *J.* sp. HH102 (LRHZ00000000), *J.* sp. HH103 (LRIA00000000), *J.* sp. HH104 (LRIB00000000), *J.* sp. HH106 (LRIC00000000) and *J.* sp. HH107 (LRID00000000). The RNA-seq data have been deposited in the SRA archieve under the accession number SRP073418 (*J.* sp. HH102) and SRP073365 (*D*. sp. HH01), respectively.

1 Introduction

1.1 The family *Oxalobacteraceae*

The family *Oxalobacteraceae* belongs to the order Burkholderiales of the β-proteobacteria and contains twelve genera. Based on 16S rRNA sequence similarity, the genera *Janthinobacterium* and *Duganella* are closely related to *Herbaspirillum* and *Oxalobacter* (Lincoln *et al.*, 1999). The *Oxalobacteraceae* family consists of Gram-negative, heterotrophic and mesophilic bacteria and is characterized by a wide range of phenotypic and ecological properties. These allow the bacteria to colonize diverse environmental habitats like water, soil or plants. One representative of an aquatic habitat, *D*. sp. HH01 (HH01), was shown to control the synthesis of the secondary metabolite violacein by quorum sensing (QS, Hornung *et al.*, 2012). Interestingly, this molecule was linked to an antifungal activity observed for *Oxalobacteraceae* (Lincoln *et al.*, 1999, Brucker *et al.*, 2008). Nevertheless, most members of this family are non-pathogenic, even though antifungal activities were described for cutaneous-, plant- and soil associated family members (Lincoln *et al.*, 1999, Brucker *et al.*, 2008, Wiggins *et al.*, 2011, Ramsey *et al.*, 2015).

1.1.1 The genus *Janthinobacterium*

Janthinobacterium was first described by De Ley *et al.* (1978). It is a purple-colored and rod shaped bacterium with a width of 0.8 - 1.5 µm and length of 1.8 – 6 µm. *Janthinobacterium* strains are commonly isolated from aquatic habitats such as rivers, lakes and springs and from the microbiota of soils (Sneath 1984, Johnson *et al.*, 1990, Osullivan *et al.*, 1990, Rossolini *et al.*, 2001). This group of bacteria can grow to remarkably high titers in marine habitats, as a winter bloom of *Janthinobacterium* in the Arctic Ocean showed (Alonso-Saez *et al.*, 2014). Consulting the National Center for Biotechnology Database (NCBI, June 2016), three *Janthinobacterium* species are described. This include *J. agaricidamnosum* (Graupner *et al.*, 2015), *J. lividum* (Sneath, 1956, De Ley *et al.*, 1978) and *J. svalbardensis* sp. nov., which was recently isolated from arctic glacier ice samples (Ambrozic Avgustin *et al.*, 2013). Besides *J. svalbardensis,* various strains are affiliated with these species, including 455 *J*. sp. strains. *J. agaricidamnosum* DSM9628, *J. lividum* DSM1522 as well as *J. svalbardensis* DSM25734 are considered as type strains. The genomes of the two type strains display an average size of 6.3 Mbp with a genus specific high GC-content of 61.7% and a median of 5,722 protein counts.

Characteristic for this genus is the expression of different pigments. For instance, the eponymous purplish color (janthinus is latin for “purple”) derives from the expression of the *vioABCDE* operon, which code for enzymes synthesizing the water-insoluble pigment violacein (Figure 1.1). Violacein is produced by the condensation of two modified L-tryptophan molecules (Balibar & Walsh, 2006). This secondary metabolite has anitimicrobial, antiviral, antitumorigenic, antifungal, antitrypanosomatid, antiulcerogenic, antiprotozoal and anticandida activities. However, the mechanisms remain unknown (Balibar & Walsh, 2006, Pantanella *et al.*, 2007, Brucker *et al.*, 2008). The synthesis of violacein and biofilm development of *J. lividum* is connected, suggesting an important role in overcoming environmental stresses (Pantanella *et al.*, 2007).

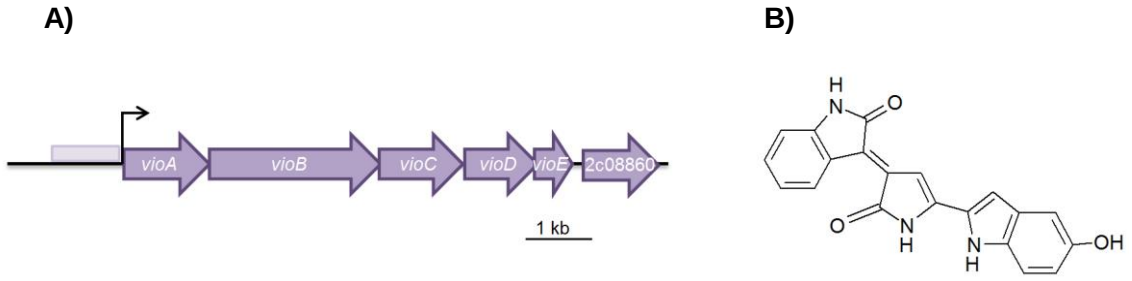

Figure 1.1 **Violacein biosynthesis operon and violacein molecule. A)** The violacein operon of HH01 consists of the genes *vioA, vioB, vioC, vioD, vioE* and Jab_2c08860. The arrow indicates the potential transcriptional start of the operon and the light purple box shows the predicted promoter sequence of the violacein operon. **B)** Bisindolepyrrolidone alkaloid violacein. This molecule is synthesized by the condensation of two modified L-tryptophan molecules.

Besides violacein, members of the genus *Janthinobacterium* synthesize the red pigment prodigiosin (Schloss *et al.*, 2010) and the purple violet pigment (PVP; Mojib *et al.*, 2010). Additionally, the antifungal virulence factor jagaricin (Graupner *et al.*, 2012, Graupner *et al.*, 2015) and the peptide lactone antibiotics janthinocin A, B and C (Johnson *et al.*, 1990, Osullivan *et al.*, 1990) were identified and seem to be specific for this genus.

1.1.2 The genus *Duganella*

Typical for bacteria of the Gram-negative, motile and nonspore-forming genus *Duganella* is the rod shape with a width of 0.6 - 0.8 µm and a length of 1.8 - 3.0 µm. The colonies are yellowish. Up to now six different species are described, namely *D. ginsengiosoli* (Yin *et al.*, 2013), *D. nigrescens* (Dohrmann *et al.*, 2013), *D. phyllosphaerae* (Kampfer *et al.*, 2012), *D. saccari* (Madhaiyan *et al.*, 2013), *D. radicis* (Madhaiyan *et al.*, 2013) and *D. zoogloeoides* (Dugan & Lundgren, 1960, Hiraishi *et al.*, 1997). Besides these strains, various strains are affiliated with these

species, including 156 *D*. sp. strains (NCBI, June 2016). The strain *D. violaceinigra* was recently reclassified to *Pseudoduganella violaceinigra,* due to 16S rRNA gene sequence analysis and the moderate similarity to *D. phyllosphaearae* of 96.8% (Kampfer *et al.*, 2012). Nevertheless, *Duganella* species thrive in diverse ecological niches, like wastewater sewage systems, soils, roots or appear leaf associated (Dugan & Lundgren, 1960, Aranda *et al.*, 2011, Kampfer *et al.*, 2012). *D. zoogloeoides* DSM16928 and *D. phyllosphaerae* DSM23865 are considered as type strains.

Duganella was first isolated from a zoogloeal matrix from wastewater and was named *Zoogloea ramigera* IAM 12760T (Dugan & Lundgren, 1960). The name derived from the characteristic cell aggregates, surrounded by a gelatinous zoogloeal matrix (Sneath 1984). However, further phenotypic and phylogenetic information reclassified the strain in the *Duganella* taxon (Hiraishi *et al.*, 1997), with *D. zoogloeoides* as type strain. *D. zoogloeoides* has a genome of 6.27 Mbp, a GC content of 63.7% and 5,291 genes coding for proteins. Besides *D. zoogloeoides*, *D. phyllosphaerae* was isolated from the leaf surface of *Trifolium repens* and is classified as type strain as well (Kampfer *et al.*, 2012). *D. phyllosphaearae* displays a genome size of 6.2 Mbp, a GC content of 63.9%, 5,390 coding genes and it shows a similarity of 99.3% to *D. zoogloeoides*. Furthermore, the strains *D. sacchari* and *D. radicis* were isolated from rhizosphere soil and rhizoplane of field-grown sugar cane. Interestingly *D. saccari* and *D. radicis* are claimed to promote plant growth in a not yet identified manner (Madhaiyan *et al.*, 2013).

1.2 *Janthinobacterium* and *Duganella* interact with eukaryotes

Living in ecological niches, like the members of the genera *Janthinobacterium* and *Duganella*, enforces the interaction with other organisms colonizing the corresponding habitat. Within these environments the organisms live closely together and thus compete for resources, promote growth, provide nutrients or interfere with the pathogenicity. One example for an interaction of *Oxalobactereacea* with eukaryotes is the interaction with fungi.

1.2.1 Bacterium-fungus interaction

A bacterium-fungus interaction (BFI) can occur symbiotic, commensalistic or antagonistic and in different habitats, which includes soils, animals and food. So far, various molecular interactions have been described, necessitating the communication between the involved partners. For this, density dependent expressed and secreted

molecules are used (Peleg *et al.*, 2010). Moreover, a BFI can occur in three different physical associations: (1) the bacterial cells colonize the fungal hyphae, (2) both organisms form a mixed biofilm or (3) the cells stay planktonic in direct proximity (Figure 1.2, Frey-Klett *et al.*, 2011).

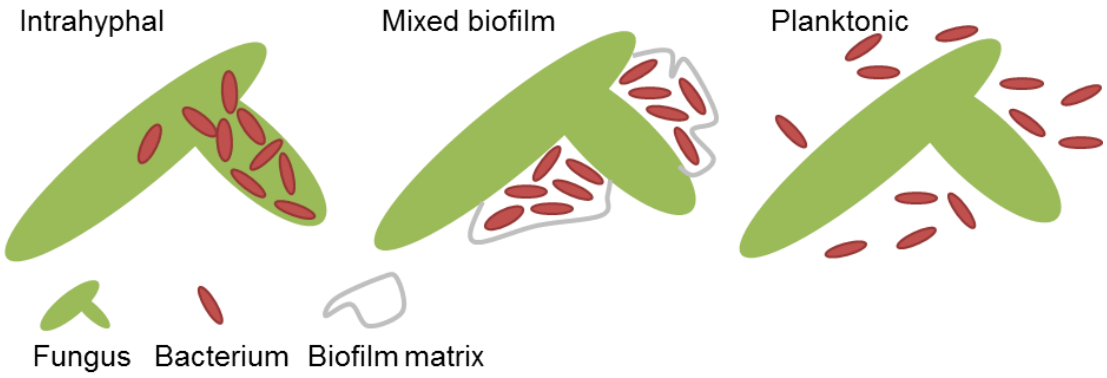

Figure 1.2 **Physical association of bacteria and fungi**. The bacterial cells (red) can enter the fungal cell (green) and live inside the hyphae (intrahyphal, left), the bacterial cells can form a mixed biofilm with the fungal cells (middle) or bacteria and fungi stay planktonic (right).

In general, BFIs are involved in plant and animal nutrition or pathology and play a role in ecology and food procession (Tarkka *et al.*, 2009, Frey-Klett *et al.*, 2011). The BFI includes the interaction via antibiosis, the modulation of the physiochemical environment, e.g. pH changes, the interaction via cellular contacts or the signaling-based interaction (Frey-Klett *et al.*, 2011). These interactions can impact bacterial and fungal growth, the secondary metabolite synthesis in terms of competition mediated increase or suppression, the virulence and the survival by protecting against competitors (Tarkka *et al.*, 2009). This BFI is mostly pathogenic and harms, weakens or kills the invading organism by inhibiting cell wall synthesis or the integrity of cell membranes (Frey-Klett *et al.*, 2011). Nevertheless, bacteria produce mixtures of antagonistic metabolites to compete with fungi. Attacking invading fungi with a multitude of secondary metabolites, volatile substances or even by the presence of QS molecules, helps to prevent the development of resistances and thereby protects the environmental niche (Tarkka *et al.*, 2009).

1.2.2 *Oxalobacteraceae*-fungus interaction

Most members of the *Oxalobacteraceae* are non-pathogenic and so far no humanpathogenic *Janthinobacterium* or *Duganella* strains were identified. Nonetheless, the best studied *Janthinobacterium* strain *J. lividum*, which was isolated from the gastrointestinal tract of the salamander *Plethodon cinereus* (Wiggins *et al.*, 2011), enhances the survival of nanoflagellates by protecting these against protozoans.

For this protective and probiotic effect, *J. lividum* must remain indigested by nanoflagellates (Matz *et al.*, 2004). Moreover, *J. lividum* as part of the human skin microbiota displays an antifungal activity on the humanpathogenic fungus *Trichophyton rubrum.* The mechanism remains unknown, even though an involvement of the secondary metabolite violacein and indole-3-carboxaldehyde is hypothesized (Ramsey *et al.*, 2015). Additionally, *J. lividum* displays antifungal activities on the skin of *P. cinereus*. This antifungal activity is promoted by the synthesis of violacein, which significantly reduces the mortality and morbidity of the host (Brucker *et al.*, 2008). Interestingly, it could be shown that HH01 regulates the synthesis of violacein by the JQS (*Janthinobacterium* QS) system (Hornung *et al.*, 2012). Besides, the type strain *J. agaricidamnosum* acts antifungal on the fungus *Agaricus bisporus* by causing soft rot disease (Lincoln *et al.*, 1999). Moreover, supplementing soil top layers with chitin showed a shift of abundance, including an increase of *Oxalobacteraceae*. While the number of *Massila* and *Duganella* increases, the number of *Janthinobacterium* decreaes. This is most likely due to a soil temperature shift and the availability of chitin (Cretoiu *et al.*, 2013). Additionally, infecting the rhizosphere of sugar beet seedlings with the plantpathogenic fungus *Rhizoctonia solani* resulted as well in a shift of bacterial abundance. Amongst others, members the *Oxalobacteraceae* family became predominant. At this condition, the expression of the sec translocase system to secrete extracellular lytic enzymes was enhanced (Chapelle *et al.*, 2015). This was in line with former studies, showing that *Oxalobacteraceae* and *Actinobacteria* decrease the number of fungi detected in soil (Cretoiu *et al.*, 2013). It was shown that in this environment the chitin degradation activity is enhanced. Since the hyphae of pathogenic fungi consist of chitin, the cell wall of the fungi could be hydrolyzed by the bacteria as hypothesized and this would result in the soil pathogen suppressive environment observed (Weller *et al.*, 2002, Mendes *et al.*, 2011, Cretoiu *et al.*, 2013).

Taking these aspects together, some *Oxalobacteraceae* display an antifungal activity. This effect might be linked to an enhanced chitin degradation activity and/or the synthesis of the antifungal pigment violacein. Interestingly, the expression and secretion of hydrolytic enzymes as chitinases are QS regulated in various bacteria (Chapon-Herve *et al.*, 1997, Schuster *et al.*, 2003, Wagner *et al.*, 2003, Goo *et al.*, 2010). Most intriguing, a connection between the CAI-1_{Vc} autoinducer of the CQS (*Cholerae* QS) system of *V. cholerae* and chitin was shown as well. In this case, CAI-1_{Vc} and chitin induce the expression of the transcriptional regulator TfoX, which regulates the expression of QstR. QstR is required for the expression of the competence genes. Therefore, CAI-1_{Vc} and chitin act together to induce natural competence (Suckow *et al.*, 2011, Beier & Bertilsson, 2013, Lo Scrudato & Blokesch,

2013, Dalia *et al.*, 2014, Sun *et al.*, 2015). At this point the question remains whether QS is involved in the observed pathogenicity of *Oxalobacteraceae* family members.

1.3 Bacterial communiation – quorum sensing

Bacteria continously alter levels of gene expression in order to adapt to stadily changing environmental conditions. However, gene expression is a costly mechanism, which consumes nutrients, energy and other valuable ressources. Therefore, coordinating gene expression helps to overcome environmental stresses and saves ressources by expressing genes only when needed. One mechanism to control gene expression is the coordination by cell densitiy perception. This regulation mechanism has the main advantage that it prevents single cells from producing costly extracellular public goods, beneficial for the population but non-essential for a single cell at low cell densities. These compounds produced at single cell level disperse in the environment before being absorbed by neighboring recipient cells (Figure 1.3). As a result, the production of public goods is more beneficial and efficient at higher population densities (Darch *et al.*, 2012).

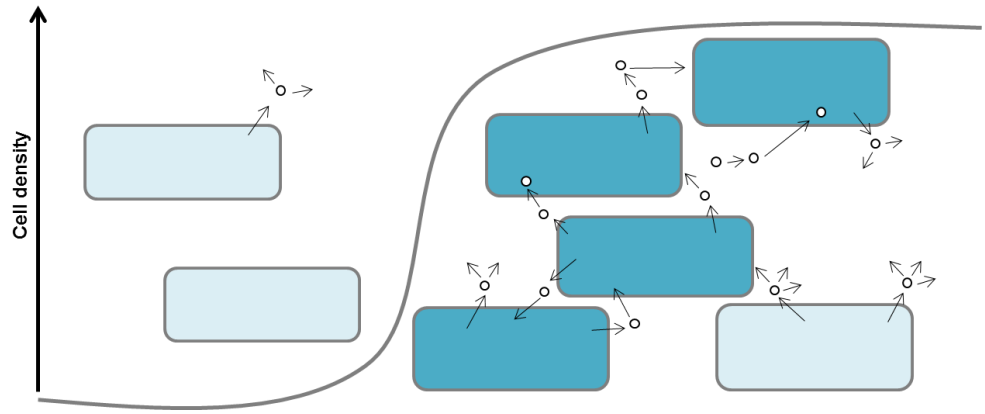

Figure 1.3 **Social benefit aspect of quorum sensing**. While extracellular public goods (circle) produced at low cell densities would disperse from the producing as well as the neighboring recipient cell (light blue rectangle), the cells do not have any advantage of producing these goods (light blue cells). At high cell densities, dispersing extracellular public goods are absorbed by neighboring recipient cells (dark blue rectangle), enhancing the efficiency of the population (Darch *et al.*, 2012).

In general, QS describes the minimum number of bacteria necessary to conduct the business of a group. One example and the first described QS mechanism is the bioluminescence of the marine bacterium *Aliivibrio fischeri,* formerly known as *Vibrio fischeri* (Urbanczyk *et al.*, 2007). This bacterium is found predominantly in symbiosis with various marine animals, e.g. in light-organs of specific squid. Within these

organisms the bioluminescence of *A. fischeri* camouflages the squids at night by eliminating its shadow. The expression of the bioluminescence genes is directly linked to the cell density within the light-organs and this coordination hinders gene products to diffuse and dilute (Geszvain & Visick, 2006, Verma & Miyashiro, 2013). This explicit mechanism, the turning-on of bioluminescence in the marine bacterium *A. fischeri*, was meant by the first usage of the term QS (Verma & Miyashiro, 2013). Further identified QS-controlled mechanisms include the biofilm and exopolysaccharide production of the opportunistic pathogen *Pseudomonas aeruginosa* (Sauer *et al.*, 2002) or the swimming and swarming motility of *Yersinia enterocolitica* (Tsai & Winans, 2011) and secondary metabolite synthesis in *Chromobacterium violaceum* (Morohoshi *et al.*, 2010) to name only a few examples.

1.4 How bacteria talk – the language

Bacteria coordinate gene expression in a cell density dependent manner. But the question remains, how bacteria determine the cell density in the sourrounding environment. The communication between bacteria of the same species, family or even with other microorganisms is based on small molecules. These molecules are used to sense the presence of bacteria in the environment and are called autoinducers (AI). This term is applied, since the presence of AIs mostly results in an autoinduction of the AI expression (Bassler, 1999). In general, AIs are small molecules that are synthesized by the AI synthase inside the cell and disperse into the surrounding by diffusion (Figure 1.4, Bassler, 1999). At low cell densities the AI concentration is low and not able to induce gene expression. As the cell density increases, the AI concentration rises as well. At this specific threshold concentration, the AI binds to an AI sensorkinase/phosphatase and this recognition event leads to a phosphorylation reaction that relays this AI-recognition event to a regulator protein. This regulator induces gene expression of target genes by binding to the specific promoter region (Figure 1.4, Garg *et al.*, 2014). Altogether, coordinating gene expression with the cell density, allows a target-orientated expression. The cells do not function as single cell, but respond to various environmental changes as a population. Certainly the usage of the same QS molecules by many different bacteria would lead to false-positive gene expression inductions. This is one of the reasons, why different QS molecules have evolved in different bacteria. This helps to eliminate the sourrounding noise, but allows the response to relevant signals.

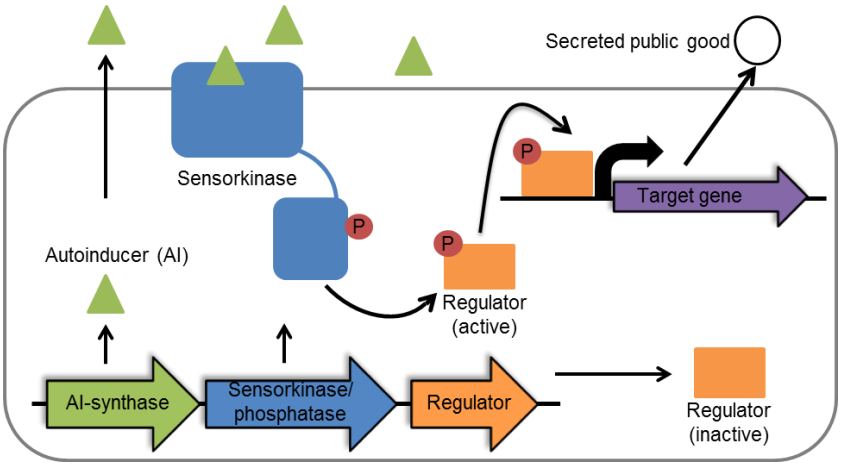

Figure 1.4 **Principle of a quorum sensing mechanism.** The autoinducer (AI) synthase synthesizes the AI (green), which is recognized by the sensorkinase/phosphatase (blue). Due to this recognition, the senorkinase/phosphatase autophosphorylates (red). This phosphate is transferred to the regulator (orange, inactive). The phosphorylated regulator (orange-red, active) binds to specific promoter regions of target genes (purple) and expresses these genes. Some gene products may be secreted as public good (circle, Bassler, 1999, Garg *et al.*, 2014).

One QS mechanism of Gram-negative bacteria is the synthesis and detection of acylated homoserine lactones (AHLs, Figure 1.5 A, Eberhard *et al.*, 1981, Fuqua & Greenberg, 1998). While the AHL backbones are structurally similar, the side chains differ. These molecule alterations enable intraspecific communication by preventing cross-talk events and reducing environmental noise. AHLs are synthesized by LuxI-type AI synthases and detected by cognate cytoplasmic LuxR proteins. After the binding of the AHL to the LuxR receptor, this complex binds to specific DNA promoters and thereby activates the expression of target genes (Bassler & Losick, 2006). In contrast to AHLs, the autoinducer-2 molecule (AI-2, Figure 1.5 B) is a widespread molecule used for interspecies communication. The AI synthase LuxS synthesizes the precursor 4,5-dihydroxy-2,3-pentanedione (DPD) that undergoes a spontaneous rearrangement. The resulting interconverted molecule allows the response to endogenously and exogenously produced AI-2. Therefore, AI-2 is considered as universal bacterial language (Bassler & Losick, 2006). But besides the role of LuxS to synthesize AI-2, LuxS possesses an important metabolic role in the activated methyl cycle. Because of this ambiguous function of LuxS, the corresponding *luxS* gene is widely distributed within bacteria (Vendeville *et al.*, 2005). Next to the interspecific communication with AI-2 and the intraspecific communication using AHL, a third QS mechanism has evolved. This system uses α-hydroxyketones (AHKs, Figure 1.5 C) as relatively small QS molecules. The molecule class was formerly only known as insect pheromone (Tiaden *et al.*, 2010). Recent studies have identified this molecule as QS molecule used by *Vibrio cholerae* (Higgins *et al.*, 2007), *V. harveyi* (Anetzberger *et al.*, 2012), *Legionella pneumophila* (Spirig *et al.*, 2008) and *Duganella* sp. HH01 (Hornung

et al., 2012). However, bacteria often use more than one QS system. For example *V. harveyi* codes for four different QS systems within its genome (Anetzberger *et al.*, 2012). These include the AI-2, the AHL HAI-1, the AHK CAI-1_{Vh} and a nitric oxide sensing system called H-NOX/HqsK. All these systems direct the signal to LuxU, a two-component phosphorelay protein that regulates QS in *V. harveyi* (Freeman & Bassler, 1999, Henke & Bassler, 2004, Anetzberger *et al.*, 2012).

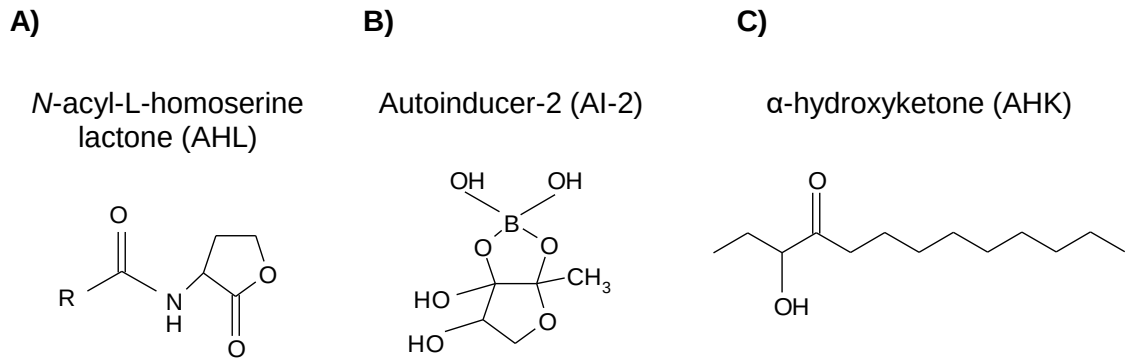

Figure 1.5 **Examples for the structural diversity of Gram-negative QS signaling molecules. A)** *N*-acyl-homoserine-lactone (AHL). R represents the diverging side chain synthesized by the LuxI AI synthases (Fuqua *et al.*, 1996). **B)** Autoinducer-2 (AI-2) of *V. harveyi* synthesized by LuxS (Ng & Bassler, 2009) and **C)** α-hydroxyketone (AHK) CAI-1 of *V. cholera* and synthesized by CqsA (Higgins *et al.*, 2007).

1.5 Using α-hydroxyketones for bacterial communication

With identifying AHKs as QS molecules used by bacteria, a new research field emerged. The tasks were to identify the AHK molecules synthesized, the QS circuit necessary to synthesize the AI, detect and respond to it and to identify the mechanisms controlled by this QS system. These points of interest were first deciphered for the two humanpathogenic bacteria *V. cholerae* and *L. pneumophila*. The marine bacterium *V. cholerae* uses the CQS system for bacterial communication (Tiaden & Hilbi, 2012). This is thought to be the most important system to induce competence (Antonova & Hammer, 2011). Within this bacterium, the CQS system controls gene expression in a density dependent regulatory circuit at the transition from exponential to stationary phase (Tiaden *et al.*, 2010). The likewise pathogenic bacterium *L. pneumophila* uses a similar AHK signaling system, the *Legionella* QS (LQS) system (Tiaden & Hilbi, 2012). In this case, LQS controls the switch from the replicative to the transmissive life cycle and induces the virulence in the stationary growth phase (Tiaden *et al.*, 2010, Schell *et al.*, 2015).

The CQS system consists of an AI synthase CqsA (A5E_A0527) and a membrane-bound sensorkinase/phosphatase CqsS (A5E_A0526, Figure 1.6 A, Tiaden & Hilbi, 2012). The CQS system synthesizes the CAI-1_{Vc} autoinducer and is necessary for maintaining pathogenicity and biofilm formation of this bacterium (Miller *et al.*, 2002, Higgins *et al.*, 2007). *L. pneumophila* harbors one additional protein necessary for the signaling process. Besides the AI synthase LqsA (lpg2731) and the sensorkinase/phosphatase LqsS (lpg2732), the response regulator LqsR (lpg2732, Figure 1.6 A) is present in the LQS system. LqsR functions as an element of the virulence regulatory network and promotes the pathogen-host interaction (Tiaden & Hilbi, 2012). Recently it could be shown that LAI-1, the AI of LQS, modulates eukaryotic cell migration by inter-kingdom signaling (Simon *et al.*, 2015).

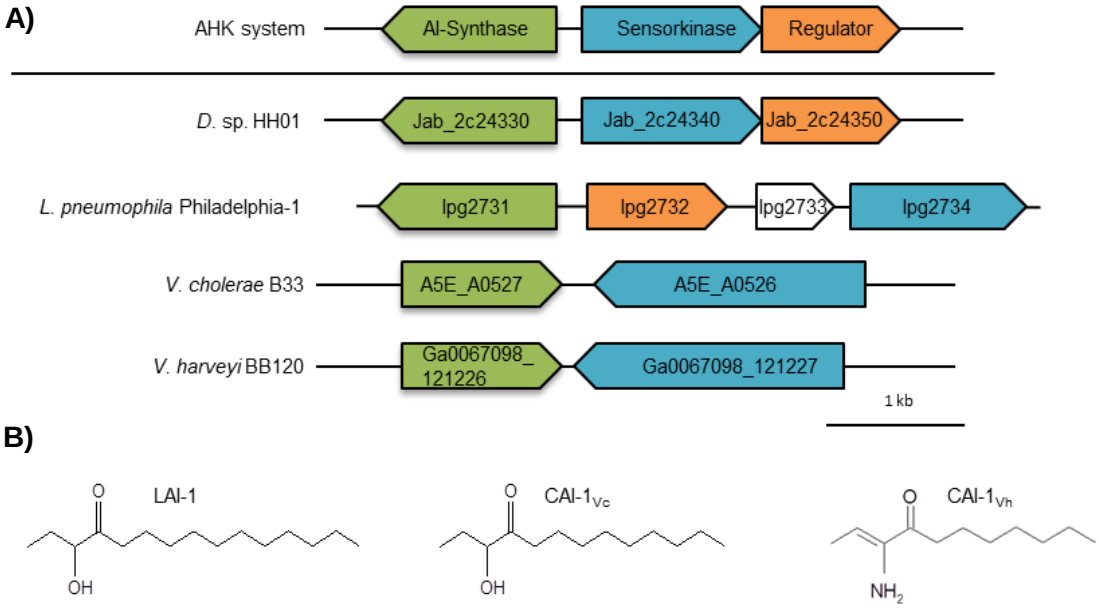

Figure 1.6 **Genes and autoinducers of the α-hydroxyketone signaling systems of HH01, *L. pneumophila* Philadelphia-1, *V. cholerae* B33 and *V. harveyi* BB120. A)** The AI synthase (green), the sensorkinase/phosphatase (blue) and the response regulator (only present in HH01 and Philadelphia-1; orange) are shown. **B)** LAI-1 of *L. pneumophila*, CAI-1_{Vc} of *V. cholerae* and CAI-1_{Vh} of *V. harveyi* (Higgins *et al.*, 2007, Spirig *et al.*, 2008, Hornung *et al.*, 2012, Tiaden & Hilbi, 2012).

For AHK-QS in general, a pyridoxal-(PLP)-dependent acyl-CoA transferase AI synthase synthezises the CAI-1 and LAI-1 AIs (Figure 1.6 B, Kelly *et al.*, 2009). LAI-1 and CAI-1_{Vc} share the hydroxygroup at the third carbon atom, but differ in the chain length (Tiaden & Hilbi, 2012), resulting in 3-hydroxypentadecan-4-one as LAI-1 (Spirig *et al.*, 2008) and (*S*)-3-hydroxytridecan-4-one as CAI-1_{Vc} (Higgins *et al.*, 2007). In case of $CqsA_{Vc}$, the synthesized amino-CAI-1_{Vc} hydrolyzes spontaneously and is then converted to CAI-1 by a short chain dehydrogenase (Kelly *et al.*, 2009, Ng *et al.*, 2011, Wei *et al.*, 2011). Besides LAI-1 and CAI-1_{Vc}, a third AHK-QS molecule could be

identified so far. This molecule is synthesized by *V. harveyi* and is a (*Z*)-3-aminoundec-2-en-4-one. It is referred to as CAI-1_{Vh} and differs in chain length and in the head group from CAI-1_{Vc} and LAI-1 (Ng *et al.*, 2011). Nonetheless, CAI-1_{Vh} can complement a *cqsA*$_{Vc}$ gene deletion (Higgins *et al.*, 2007, Ng *et al.*, 2011).

Interestingly, whereas exponentially growing *L. pneumophila* represses transmissive traits, e.g. virulence, post-exponential growing bacteria induce these, leading to pathogenicity (Schell *et al.*, 2015). This switch is controlled via a phosphorylation cascade, schematically depicted in Figure 1.7.

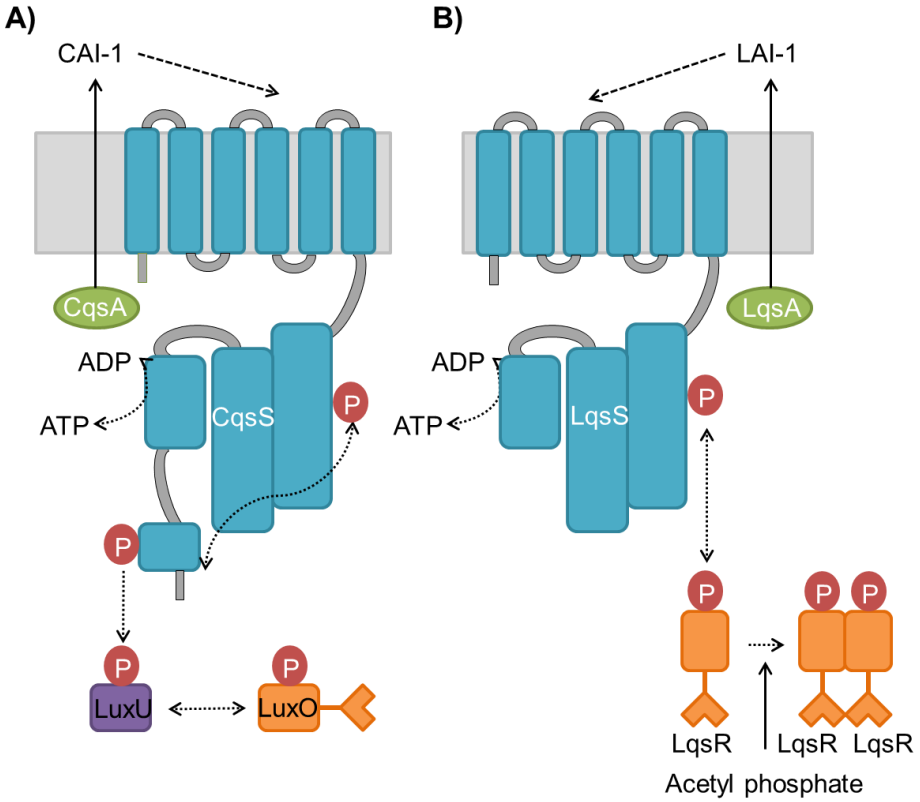

Figure 1.7 **α-hydroxyketone QS systems. A)** CAI-1 of *V. cholerae* is synthesized by the AI synthase CqsA (green). The AI is recognized concentration dependently by the sensorkinase/phosphatase CqsS (blue) outside of the cell. The HisKA/HATPase_C domain (histidine kinase A domain with a conserved histidine phospho-acceptor site / catalytic ATP binding and a transferase domain, C-terminal) catalyzes the autophosphorylation by ATP at H_{194} and transfers the phosphate to D_{618} in the C-terminal REC domain. The phosphate is afterwards shuttled via the phosphorelay protein LuxU (purple) to the REC domain of the response regulator LuxO (orange) and regulates QS-dependent gene expression. **B)** LAI-1 is synthesized by LqsA (green) and diffuses outside the cell. LAI-1 is recognized by the membrane-bound sensorkinase and phosphatase LqsS (blue). The histidine kinase output domain transfers the phosphate moiety to the receiver REC domain (receiver domain with conserved aspartate) of LqsR (orange), by binding to LqsS. After phosphorylation and in the presence of acetyl-phosphate, LqsR dimerises and regulates LAI-1 dependent gene expression (Hornung *et al.*, 2012, Tiaden & Hilbi, 2012, Schell *et al.*, 2014).

Up to now, the AHK-QS system has been identified in several other environmental bacteria, e.g. family members of the *Legionellaceae*, *Vibrionaceae*, *Burkholderiaceae*,

Chlorobiaceae and *Oxalobacteraceae* (Hornung *et al.*, 2012, Tiaden & Hilbi, 2012). As first described for *Oxalobactereacea*, this system was identified in HH01 and named *Janthinobacterium* QS (JQS, Hornung *et al.*, 2012). JQS comprises the AI-synthase JqsA (Jab_2c24330), the sensorkinase/phosphatase JqsS (Jab_2c24340) and the response regulator JqsR (Jab_2c24350, Figure 1.6 A). It was shown that a loss of the synthesized JAI-1 AI led to a decrease of the biosynthesis rate of the purple-pigment violacein. Since this effect is prominent in the stationary growth phase, the synthesis of violacein is QS-controlled (Hornung *et al.*, 2012). Interestingly, violacein is a secondary metabolite for which an antifungal activity is hypothesized (Balibar & Walsh, 2006, Pantanella *et al.*, 2007, Brucker *et al.*, 2008). Investigating this JQS system and the effect of JAI-1 on gene expression, the role of the AHK-QS system in bacterium-fungus interactions can be addressed in detail and in the backround of a non-humanpathogenic and genetically accessible bacteria.

1.6 Intention of this work

The intention of this work was to identify molecular keys involved in the *Oxalobacteraceae*-fungus interaction. Therefore, I isolated purple-pigmented *Janthinobacterium* and *Duganella* strains from diverse environments, established their genomes and compared these to publicly available genomes. MLS analyses as well as ANIm calculation were used for phylogenetic classification. Further analyses of the core- and pangenome should give clues to the overall genetic content of these two *Oxalobacteraceae* genera. Emphasis was set on potential quorum sensing systems.

Since previous work had suggested an interaction of *Janthinobacterium* species with fungi, part of this work should focus on the identification of first molecular keys of the interaction of *Janthinobacterium*/*Duganella* species with the plant pathogenic fungus *Fusarium graminearum*. Therefore, mutational analysis of a AI synthase gene and the phenotypic characterisation of the mutant was performed. Together with this, a global analysis of bacterial transcriptomes using RNA-seq was used to identify possible links between bacterial quorum sensing and the *Janthinobacterium/Duganella*-*F. graminearum* interaction.

2 Material and methods

Standard molecular cloning techniques were conducted as described in the Green and Sambrook Molecular Cloning laboratory manual (Sambrook, 2001). Thermostable solutions, glass vessels and other instruments were autoclaved at 121 °C for 20 min. Not-autoclavable instruments were washed with 70% EtOH and flamed. Chemicals were ordered from Sigma-Aldrich (Hamburg, Germany) or Carl Roth (Karlsruhe, Germany). Primers used in this study and sequencing reactions were ordered and carried out by Eurofins Genomics (Ebersberg, Germany). Producers of consumable materials or used equipment were only named if the experiments required specific materials or equipment.

2.1 Bacterial strains

Bacterial strains used in this study are listed in Table 2.1.

Table 2.1. Bacterial strains used in this study

Strain	Characteristics[1]	Reference/Source
Escherichia coli		
DH5α	Cloning strain *supE*44 Δ*lacU*169 (Φ80 lac*Z* ΔM15) *hsdR*17 *recA*1 *endA*1 *gyrA*96 *thi*-1 *relA*1	Hanahan, 1983
S17-1λpir	Modified RP4 plasmid integrated into genome	Simon *et al.*, 1983
Duganella		
sp. HH01	Wild type isolate, amp^R, tet^R, gen^S, kan^S	Hornung *et al.*, 2012
sp. HH01Δ*jqsA*	*jqsA* genedeletionmutant of HH01, gen^R	Hornung *et al.*, 2012
sp. HH101	Wild type isolate, amp^R, tet^R, gen^S, kan^S	This work
sp. HH105	Wild type isolate, amp^R, tet^R, gen^S, kan^S	This work
phyllosphaerae	Type strain DSM23865	Leibniz Institute DSMZ (Braunschweig, Germany)
zoogloeoides	Type strain DSM16928	Leibniz Institute DSMZ (Braunschweig, Germany)
Janthinobacterium		
sp. HH100	Wild type isolate, amp^R, tet^S, gen^S, kan^S	This work
sp. HH102	Wild type isolate, amp^R, tet^S, gen^S, kan^S	This work
sp. HH102Δ*jqsA*	*jqsA* (JAN4_00966) gene deletionmutant of HH102	This work
sp. HH103	Wild type isolate, amp^R, tet^S, gen^S, kan^S	This work

sp. HH104	Wild type isolate, amp^R, tet^S, gen^S, kan^S	This work
sp. HH106	Wild type isolate, amp^R, tet^S, gen^S, kan^S	This work
sp. HH107	Wild type isolate, amp^R, tet^S, gen^S, kan^S	This work
sp. MP5059B	Wild type isolate, amp^R, tet^S, gen^S, kan^S	This work
agaricidamnosum	Type strain DSM9628	Leibniz Institute DSMZ (Braunschweig, Germany)
lividum	Type strain DSM1522	Leibniz Institute DSMZ (Braunschweig, Germany)

[1] Abbreviations describing geno- and phenotypes were made according to Bachmann (Bachmann, 1983). amp: ampicillin, tet: tetracyclin, gen: gentamycin, kan: kanamycin

2.2 Vectors and constructs

The following table summarizes the vectors and constructs used and designed in this study (Table 2.2).

Table 2.2 Vectors and constructs used in this study

Vector / Construct	Characteristics	Reference / Source
pDrive	TA cloning vector, amp^R, kan^R	QIAGEN, Hilden, Germany
pDrive::*vioABCDE*	pDrive vector harboring the *vioABCDE* genes of HH01	Hornung *et al.*, 2012
pGEM-T	T cloning vector, amp^R	Promega, Mannheim, Germany
pNPTS138-R6KT	Suicide vector for generating gene deletion mutants	Lassak *et al.*, 2010
pK18mobII_pKOScvm	Plasmid to amplify the mCherry gene	Schluter *et al.*, 2015
pTS-21	pET-28a(+) harboring the *lqsA* gene from *Legionella pneumophila* El Tor	Spirig *et al.*, 2008
pBBR1MCS-2	Broad host-range vector, kan^R	Kovach *et al.*, 1995
pBBR1MCS-2::mCherry	mCherry derived from pK18mobII_pKOScvm, promoterless	This work
pBBR1MCS-2::PmCherry	mCherry derived from pK18mobII_pKOScvm under the constitutive pBBR1MCS-2 *lac* promoter	This work
pBBR1MCS-2::pvioHH107::mCherry	pBBR1MCS-2::mCherry with promoter of the *vioA* gene (JAB9_09370), with JAI-1 motif	This work
pBBR1MCS-2::pvioHH107-JAI-1::mCherry	pBBR1MCS-2::mCherry with promoter of the *vioA* gene (JAB9_09370), without JAI-1 motif	This work

pBBR1MCS-2::pchiA::mCherry	pBBR1MCS-2::mCherry with 5' region of the *chiA* gene (Jab_2c26490)	This work
pNPTS138-R6KT::*jqsA*UpDs	Suicide vector for generating a *jqsA* gene deletion mutant in HH102 (JAB4_14950)	This work
pBBR1MCS-2::$jqsA_{01}$	pBBR1MCS-2 harboring an extra chromosomal copy of the *jqsA* gene of HH01 (Jab_2c24330)	Hornung *et al.*, 2012
pBBR1MCS-2::$jqsA_{102}$	pBBR1MCS-2 harboring the *jqsA* gene of HH102 (JAB4_14950)	This work
pBBR1MCS-2::$cqsA_{Vc}$	pBBR1MCS-2 harboring the *cqsA* gene of *V. cholerae*	Hornung *et al.*, 2012
pBBR1MCS-2::$cqsA_{Vh}$	pBBR1MCS-2 harboring the *cqsA* gene of *V. harveyi*	Hornung *et al.*, 2012
pBBR1MCS-2::*lqsA*	pBBR1MCS-2 harboring the *lqsA* gene of *L. pneumophila*	This work

amp: ampicillin, kan: kanamycin

2.3 Primer

Primers used for PCR and sequencing are listed in Table 2.3.

Table 2.3. Primers used in this study

Primer	Sequence (5'-3' direction)	Function	Reference
oFH91	GTGGATCCGCGCCTTGCAGACGACAACTA	FP *vioA* promoter (JAB9_09370) with JAI-1 motif	This work
oFH92	GGCGAATTCCGTGCTCATACGAAATTCCT	RP *vioA* promoter (JAB9_09370) with JAI-1 motif	This work
oFH105	GACTCGAGATACCCGGGCTATTGTCGGTG	FP *vioA* promoter (JAB9_09370) without JAI-1 motif	This work
oFH93	GCGAATTCATGGTGAGCAAGGGCGAGGA	FP mCherry gene from pK18mobII_pKOScvm	This work
oFH94	GGCAAGCTTTTACTTGTACAGCTCGTCCAT	RP mCherry gene from pK18mobII_pKOScvm	This work
oFH106	AACGGCAGTTCGAAGGTCAG	FP UP to proof the *jqsA* gene deletion (JAB4_14950)	This work
oFH107	AATCTGCACGGCCTGAGCTT	RP DS to proof the *jqsA* gene deletion (JAB4_14950)	This work
oFH108	AATCGGCGCAAGCCGTG	FP to proof the *jqsA* gene deletion (JAB4_14950)	This work
oFH109	AGCGACGCCGTGCGGAA	RP to proof the *jqsA* gene deletion (JAB4_14950)	This work
oFH113	GTTCTAGACGCCTCGCCGGCGATGTTCAGGTAA	RP UP for the *jqsA* knockout (JAB4_14950)	This work
oFH114	GCTCTAGATGACGGATCTCGGCTACAAC	FP DS for the *jqsA* knockout (JAB4_14950)	This work

oFH115	GCGAATTCCGCTACACCAGC GCCAGCTT	RP DS for the *jqsA* knockout (JAB4_14950)	This work
oFH120	GCGGATCCTGTTGGACGCGG TAGTTCCCAC	FP UP for the *jqsA* knockout (JAB4_14950)	This work
oFH121	GCGGATCCTCCAGTTGCTGA TGGTATTG	FP *chiA* promoter of HH01 (Jab_2c26490), with JAI-1 motif	This work
oFH122	GCGAATTCGCTATCTCCTCCT GGGTTGATC	RP *chiA* promoter of HH01 (Jab_2c26490), with JAI-1 motif	This work
oFH99	AGTCTCGAGGCACAATATCG GCACAACTG	FP for $jqsA_{102}$ (JAB4_14950) complementation	This work
oFH100	GATCTAGAGCTACACCAGCG CCAGCTTGC	RP for $jqsA_{102}$ (JAB4_14950) complementation	This work
616V	AGAGTTTGATYMTGGCTCAG	16S rRNA analyses	Brosius *et al.*, 1981
1492 R	CGGYTACCTGTTACGAC	16S rRNA analyses	Kane *et al.*, 1993

Restriction sites are underlined, forward primer are abbreviated FP and reverse primer RP. DS refers to downstream and UP to upstream. Pyrimidine bases are abbreviated as Y and amino bases as M.

2.4 Bacterial cultivation

Liquid cultures were either inoculated by single colonies from agar plates, by inoculation with an optical density of 0.05 at 600nm (OD_{600nm}) of an overnight grown culture or by glycerol stocks (33% (v/v) final glycerol concentration, stored at -70 °C). Liquid cultures were grown in deep well plates, test tubes or Erlenmeyer flasks at 140 – 200 rpm in shakers. Supplements used for cultivation are summarized in Table 2.4. Heat sensitive supplements and antibiotics were sterile filtered (pore size0.22 µm). 10 mg chitin derived from shrimp shells (Sigma-Aldrich, Germany) were used for supplementation.

Escherichia coli (Table 2.1) was grown on solid or LB medium (Sambrook, 2001) overnight at 37 °C and *Janthinobacterium* (Table 2.1) were cultivated for three days on solid R2A medium (Reasoner & Geldreich, 1985) or overnight in liquid R2A medium at 22 °C. R2A –G refers to R2A media without glucose (G). Additionally, the cells were grown on TY (Sambrook, 2001) for 3 days at 22 °C.

Table 2.4. Antibiotics and supplements used in this study

Substance	Abbreviation	Stock solution	Final concentration	Solvent
Antibiotic				
Ampicillin	amp	100 mg/ml	100 µg/µl	H_20_{bidest}
Gentamycin	gen	25 mg/ml	25 µg/µl	H_20_{bidest}
Kanamycin	kan	25 mg/ml	25 µg/µl	H_20_{bidest}
Tetracyclin	tet	10 mg/ml	5 µg/µl	50% (v/v) EtOH
Supplement				
Glycerol	-	96% (v/v)	3.5% (v/v)	-
D-glucosamine	DG	1 M	10 mM	H_20_{bidest}
N-acetyl-D-glucosamine	NADG	0.1 M	10 mM	H_20_{bidest}

2.5 Violacein measurement

The violacein quantification was performed following a previously published protocol with minor modifications (Hornung *et al.*, 2012). Instead of water-satured butanol, 100% ethanol (EtOH) was used for the extraction and the absorbance was measured at 575 nm. The amount of synthesized violacein per ml was calculated as the ratio of the absorbance of the EtOH extract versus the culture density at OD_{600nm}. For calculating the molarity of synthesized violacein, the molar extinction coefficient of pure violacein of 0.05601 μg^{-1} cm^{-1} (Mendes, Carvalho et al. 2001), dissolved in EtOH and measured at 575 nm, was used. The cells were grown for 24 h in R2A or 48 h in TY as described in 2.4. To determine the amount of violacein expressed by the isolates, amp and glycerol were added to the R2A to enhance violacein expression (Table 2.4).

2.6 Bacterial characterization

Environmental samples were collected from a rainwater-cistern at the Botanical Garden Klein Flottbek (Hamburg, Germany). Strain MP5059B (abbreviated 5059) was isolated as a contaminant during an attempt to obtain a culture from fruiting bodies of *Ruzenia spermoides* collected in the Stadtwald Frankfurt close to the Jacobi Weiher (Germany). This strain was isolated by the working group of Prof. Dr. Meike Piepenbring of the department of mycology of the Goethe University of Frankfurt (Germany) and provided by the working group of Prof. Dr. Helge B. Bode of the Merck-Stiftungsprofessur for molecular biotechnology of the Goethe University of Frankfurt (Germany). Bacterial

samples were incubated on solid R2A as described above (2.4). Purple-pigmented colonies were repetitively isolated and microscopical surveyed to obtain pure cultures. Scanning electron microscopic (SEM) pictures were perfomed as previously described (Krohn-Molt *et al.*, 2013) and in cooperation with the research group morphological structure analyses of Dr. Frank Friedrich of the University of Hamburg (Germany). The two type strains *J. lividum* (De Ley *et al.*, 1978) and *D. phyllosphaerae* (Kampfer *et al.*, 2012) were included for analysis purposes (2.1). To distinguish the bacteria, isolates were named as HH100 – HH107 and 5059 (2.1).

2.6.1 Growth conditions

The generation time was calculated to determine growth behavior of the strains. The following formula was used, with *t2 – t1* as considered time interval of the exponential growth and *N2* and *N1* as cell concentration at the corresponding time points (2.4).

$$gt = \frac{\log 2\ (t2 - t1)}{\log N2 - \log N1}$$

Growth curves were calculated via measuring the OD_{600nm} hourly. To monitor the effect of JAI-1 on the violacein expression, the strains HH01 and HH102 and *jqsA* gene deletion mutants (2.8.1) were transformed with a *vio*-promoter fusion (pBBR1MCS-2::pvioHH107::mCherry, 2.10, Table 2.2). The increase of the mCherry fluorescence (590/20, 645/40 nm) was equated with the increase of the JAI-1 concentration.

The antibiotic resistance and susceptibility of the strains was determined by plating 1 x 10^7 cells / ml on solid R2A supplemented with antibiotics (amp, gen, kan and tet, Table 2.4). Susceptible strains showed no growth at the corresponding antibiotic concentration. Cells were incubated as described previously (2.4).

For flagellum mediated motility (swimming), R2A agar was supplemented with 0.2% (w/v) agar, and incubated as described above (2.4).

2.6.2 Hydrolytic and chitin degradation activities

For amylase, protease or lipase activity R2A medium was supplemented with 1% (w/v) starch, 4% (w/v) skimmilk or 1% (Vol.-%) tritutyrin (TBT), and strains were incubated as described (2.4). For TBT-R2A agar, R2A was heated prior to TBT addition, homogenized for 3 min and autoclaved immediately. Clear halos surrounding colonies indicate the presence of digesting enzymes. In case of amylase activity the clear halo is visualized after addition of Gram´s iodine. The chitinoclastic activity was determined by restoring the growth of the strains in M9 media (33.7 mM Na_2HPO_4, 22.0 mM KH_2PO_4, 8.55 mM NaCl, 9.35 mM NH_4Cl, 1 mM $MgSO_4$, 0.3 mM $CaCl_2$, 1 µg biotin,

1 µg thiamin and 1x trace solution (100 x trace solution: 13.4 mM EDTA, 3.1 mM $FeCl_3$ x $6H_2O$, 0.062 mM $ZnCl_2$, 76 µM $CuCl_2$ x 6 H_2O, 42 µM $CoCl_2$ x 2 H_2O, 162 µM H_3BO_3, 8.1 µM $MnCl_2$ x 4 H_2O) lacking glucose and supplemented with chitin from shrimp. The OD_{600nm} was measured after one week of incubation at 22 °C.

To test the influence of NADG on the biofilm formation of strains HH102 and HH102Δ*jqsA*, 2 ml R2A –G was supplemented with 10 mM NADG (Table 2.4) and inoculated with an OD_{600nm} of 0.05 with the bacterial strains. Incubation was performed for 72 h at 22 °C, not shaking.

2.7 Phylogenetic classification and genome analyses

To classify the isolated strains phylogenetically, 16S rRNA analysis as well as whole genome sequencing and comparative genomics were performed.

2.7.1 16S rRNA analysis

To determine the phylogenetic relationship of the strains, genomic DNA of pure cultures of the strains HH100 - HH107, 5059, *J. lividum* and *D. phyllosphaerae* (2.1, 2.4) was extracted using the peqGOLD Bacterial DNA Kit (PEQLAB Biotechnologie GmbH, Erlangen, Germany) according to manufacturer's instructions. The 16S rRNA genes were amplified via PCR using the universal bacterial 16S rRNA primer 616V and 1492R (Table 2.3). The Pfu DNA Polymerase from Thermo Scientific™ Oxoid™ (Oxoid®, Hampshire, United Kingdom) with following conditions was used: 95 °C for 30 s, 55 °C for 30 s and 72 °C for 2 min (34 cycles). The PCR products were cloned in the pGEM-T cloning vector (pGEM®-T Vector Systems Kit, Promega, Mannheim, Germany), following manufacturer´s instruction. Competent cells and transformation of these by heat shock were performed as described (Sambrook, 2001). Clones containing vectors with DNA inserts were selected by amp supplementation (Table 2.4) and positive tested clones were used for plasmid isolation using a HighYield® Plasmid Mini Kit (Real Genomics, RBCBioscience, Taipei, Taiwan) according to manufacturer's instruction. Sequencing was performed by Eurofins MWG Operon (Ebersberg, Germany) and the phylogenetic tree was constructed using the neighbor-joining algorithm of MEGA5 with bootstrap analysis from 1000 repeats (Tamura *et al.*, 2011). 16S rRNA sequence of *Nitrosomonas europaea* ATCC25978 (HE862405) was used as outgroup. Additionally, 16S rRNA sequences of *J. lividum* GA01 (DQ473538), *J. lividum* (JF970593), *J. agaricidamnosum* (AB681849), *J. lividum* Acam (EU275366), *J. lividum* CG3 (2516626029), *D. zoogloeoides* LB-H (AB495150), *D. zoogloeoides*

NBRC_102465 (AB681807), *D. ramigera* ATCC_25935 (X74914) and *D. zoogloeoides* DSM16928 (NR_025833) were included for analysis purposes.

2.7.2 Whole genome sequencing

The whole genome sequencing was performed by the Göttingen Genomics Laboratory (Georg-August University, Göttingen, Germany) using the Genome Analyzer II (Illumina, San Diego, CA, USA) (2x112 bp) and additionally the 454 GS-FLX Titanium XL pyrosequencing system (Titanium Chemistry, Roche Life Science, Mannheim, Germany) for the strains HH101 and HH105. Preparation of shotgun libraries was performed according to manufacturer's protocols. The genome of HH102 was sequenced on a MiSeq instrument (2x300 bp). Illuminia assemblies were performed with the SPAdes genome assembler software 3.5 (Bankevich *et al.*, 2012). The MIRA software (Checreux B, Wetter T et al. 1999) was used for initial hybrid *de novo* assembly and the software tool prodigal (Hyatt *et al.*, 2010) were used for automatic gene prediction. rRNA and tRNA identification was done with RNAmmer (Lagesen, Hallin et al. 2007) and tRNAscan (Lowe and Eddy 1997), respectively. For automatic annotation the Integrated Microbial Genomes/Expert Reviews (IMG-ER) system (https://img.jgi.doe.gov/cgi-bin/er/main.cg, Markowitz *et al.*, 2009, Mavromatis *et al.*, 2009, Markowitz *et al.*, 2012, Markowitz *et al.*, 2014) was used, followed by a manual revision using the BLASTP, Swiss-Prot, TrEMBL and InterPro databases (Zdobnov and Apweiler 2001).

2.7.3 Comparative genomics

For comparative genomics and next to the sequences of the nine isolates and two type strains, the following genomic data was included: Strain *J. agaricidamnosum* DSM9628 (9628, HG322949, Lincoln *et al.*, 1999), *J. lividum* strains PAMC 25724 (25724, AHHB00000000, Kim *et al.*, 2012), RIT308 (JFYR00000000, Gan *et al.*, 2014), MTR (JRRH00000000, Valdes *et al.*, 2015), *J.* species Marseille (Mars, CP000269, Audic *et al.*, 2007), RA13 (JQNP01000001, McTaggart *et al.*, 2015), CG3 (APFF00000000, Smith *et al.*, 2013), KBS0711 (LBCO00000000, Shoemaker *et al.*, 2015), Ant5-2 (LNCE00000000, Mojib *et al.*, 2010), *Pseudoduganella violaceinigra* DSM15887 (AUDI00000000, Li *et al.*, 2004, Kampfer *et al.*, 2012), *D. zoogloeoides* DSM16928 (16928, AX110134, Dugan & Lundgren, 1960, Hiraishi *et al.*, 1997) and *D*. sp. HH01, formerly known as *J*. sp. HH01 (HH01, AMWD00000000, Hornung *et al.*, 2012). Abbreviations in parenthesis refer to shortcuts and numbers to GenBank accession numbers used in this study. Genome information of *J.* species OK676 (60134), 344 (57625), 551a (57361), NFR18 (57185) and *D*. species CF402 (61889) and OV458

(60275) were extracted from the permanent and unpublished drafts available at http://www.jgi.doe.gov/ using the IMG software. Numbers in parenthesis refer to the IMG submission ID. Data from *J.* sp. B9-8 (CP014222) and *J.* sp. CG23_2 (CYSS00000000) were extracted from NCBI. *J. lividum* DSM1522 (1522, Sneath, 1956, De Ley *et al.*, 1978) and *D. phyllosphaereae* DSM23865 (23865, Kampfer *et al.*, 2012) sequenced in this study were ordered at the DMSZ, Braunschweig, Germany. HH100 – HH107 and MP5059B (5059) refers to the isolates of our lab. Abbreviations of the strains and accession numbers are written in parenthesis.

Pan- and coregenome analysis, MLSA detection and ANIm were calculated by the Göttingen Genomics Laboratory (Georg-August University, Göttingen, Germany). The Pan- and coregenome analysis was done as published previously (Poehlein *et al.*, 2015). To calculate the MLSA tree with 500 bootstraps RaxML (Stamatakis, 2014) in combination with an in house pipeline (PO-2_MLSA.py, https://github.com/jvollme) was used. Pyani.py (https://github.com/widdowquinn/pyani) was used to analyze the average nucleotide identity (ANIm). To further investigate the phylogenetic relationship of the strains used for MLS analysis, the ANIm was calculated at genomic level, replacing DNA-DNA hybridization (Goris *et al.*, 2007, Richter & Rossello-Mora, 2009). ANIm calculations are based on the comparison of the genome of one organism against another, identifying the matching regions and calculating the percentage nucleotide identity of these.

Additionally, for an extensive analysis of the genomes the IMG database was used. For example, to identify all genes involved in protein secretion of the strains the genes of one strain were sorted in view of their function and using the KEGG pathway analysis operation and all KEGG numbers of genes involved in bacterial secretion systems were displayed (status: January 2016). The gene clusters potentially synthesizing secondary metabolites were found by the AntiSMASH program (http://antismash.secondarymetabolites.org/, Medema *et al.*, 2011). Secondary metabolites include non-ribosomal peptide synthetases (NRPS), NRPS-polyketide synthases (PKS) hybrids clusters and compounds.

2.8 Mutagenesis of *Janthinobacterium* sp. HH102

2.8.1 Generating a *jqsA* gene deletion mutant

Cloning steps were carried out with standard methods (Sambrook, 2001). For the construction of the *jqsA* (JAB4_14950) gene deletion, a 583 bp fragment containing the sequence regions flanking the JqsA active center, were cloned in the suicide vector

pNPTS138-R6KT (Table 2.2, Lassak *et al.*, 2010), using oFH120/oFH113 (317 bp), oFH114/oFH115 (266 bp, Table 2.3) and the Pfu polymerase at following conditions: 95 °C for 30 s, 56.5 °C for 30 s and 72 °C for 40 s (34 cycles). After constructing pNPTS138::*jqsA*UpDs (Table 2.2), HH102 was transformed by electroporation (Hornung *et al.*, 2012). Single recombinant clones carrying this construct were selected on R2A. To obtain double recombinant mutants, heterogenotes were streaked on R2A in the presence of 10% (w/v) sucrose. The identity of the obtained *jqsA* mutant was verified by PCR, using oFH106/107, oFH107/108, oFH108/109 and oFH115/120 (Table 2.5). The obtained PCR fragment of oFH106/107 was sequenced to verify the correctness of the mutation.

Table 2.5 Primers, annealing temperatures and PCR product sizes to verify HH102Δ*jqsA*

Primer	Annealing temperature	Size of PCR fragment	
		WT	Δ
oFH106/107	59 °C	2083 bp	1344 bp
oFH120/115	59 °C	1289 bp	550 bp
oFH108/109	60 °C	280 bp	-
oFH108/107	59 °C	1150 bp	-

Additionally, HH01, HH102 and their respective gene deletion mutants were investigated in terms of violacein synthesis (2.5) in liquid R2A, on solid TY, the amylolytic, lipolytic and proteolytic activity and the attachment and utilization of chitin derived from shrimp shells (2.6.2).

2.8.2 Complementation of the *jqsA* gene deletion mutant

To complement the *jqsA* gene deletion, pBBR1MCS-2::$jqsA_{102}$ (Table 2.2) was constructed. To amplify the gene JAB4_14950, primer oFH99/oFH100 (Table 2.3) and the Pfu polymerase were used at following conditions: 95 °C for 30 s, 59 °C for 30 s and 72 °C for 2:45 min (34 cycles). The PCR product of 1363 bp was digested with XbaI and XhoI and ligated in pBBR1MCS-2. The resulting construct pBBR1MCS-2::$jqsA_{102}$ was introduced in the strain HH102Δ*jqsA* by electroporating the cells (Hornung *et al.*, 2012). Additionally, HH102Δ*jqsA* was transformed with pBBR1MCS-2::$cqsA_{Vc}$, pBBR1MCS-2::$cqsA_{Vh,}$ pBBR1MCS-2::$jqsA_{01}$ (Hornung *et al.*, 2012) and pBBR1MCS-2 and pBBR1MCS-2::*lqsA* constructed in this study (Table 2.2). For pBBR1MCS-2::*lqsA* construction, pTS21 (Table 2.2) was digested using EcoRI and NotI restriction enzymes. The desired *lqsA* was subcloned in pBluescriptKSII+ and digested with SacII at 37 °C in 1x Tango buffer for 1.5 h followed by a second digestion

step using EcoRI and an incubation in 2x Tango buffer for 1.5 h at 37 °C. Afterwards, the *lqsA* was cloned in pBBR1MCS-2 and sequenced to verify the correctness. To test the complementation potential of the cloned AI synthases and the pBBR1MCS-2 negative control, violacein measurements in R2A medium was performed (2.5).

2.8.3 Identification of JAI-1

To investigate the AI molecule JAI-1 *in silico* methods were used. The *in silico* analyses included the ClustalW alignment of multiple sensorkinases *J. agaricidamnosum* (GJA_1196), *J. lividum* (JALI_03520), HH102 (JAB4_14940), HH01 (Jab_2c24340), *D. phyllosphaerae* (DUPY_10340), *D. zoogloeoides* (F460DRAFT_03280), *L. pneumophila* Philadelphia-1 (lpg2734) and *V. cholerae* B33 (A5E_A0526, Hall, 2013). Additionally, a ClustalW alignment was performed with genes encoding for AI synthases (Hall, 2013). Therefore, protein sequenced of the strains *J. agaricidamnosum* (GJA_1197), *J. lividum* (JALI_03530), HH102 (JAB4_14950), HH01 (Jab_2c24330), *D. phyllosphaerae* (DUPY_10350), *D. zoogloeoides* (F460DRAFT_03279), *L. pneumophila* Philadelphia-1 (lpg2731) and *V. cholerae* B33 (A5E_A0527) were used.

2.9 RNA-seq analyses

2.9.1 RNA analyses of HH01 and HH01Δ*jqsA* in late stationary phase

The cells were cultivated in 20 ml R2A media with enhanced violacein synthesis conditions as described (2.4, 2.5) until a slight purple-stain was observed (22 h). The amount of synthesized violacein was quantified via ethanol extraction. For the extraction of the total RNA of the samples, the Ultra Clean™ Microbial RNA Isolation Kit (Mo Bio Laboratories, Inc., Carlsbad, CA, USA) was used. The removal of simultaneously extracted DNA was achieved by using the RTS DNase™ Kit (Mo Bio Laboratories, Inc., Carlsbad, CA, USA). The RNA was cleaned and concentrated via the RNA Clean & Concentrator™ -5 Kit and verified on a 1.2% formaldehyde-agarose gel (1.2% agarose dissolved in 1x FA gelbuffer; for 10x FA gelbuffer use 200 mM MOPS, 50 mM sodium acetate and 10 mM EDTA, dissolved in 0.1% DEPC-treated water, supplemented with 0.25% formaldehyde). Using the Fermentas RiboRuler High Range RNA Ladder and supplied 2X RNA Loading Dye (MBI Fermentas, St. Leon-Rot, Germany), the gel was run for 70 min at 120 volt in 1x FA electrophoresis buffer (1x FA gelbuffer, 2% formaldehyde). The concentration was defined spectrophotometically on a Take3 Micro-Volume-Plate, read by the Synergy HT Multi-Detection-Reader (Biotek,

Winooski, VT, USA). The rRNA was depleted using the Ribo-Zero™ Magnetic Kit for Gram-Negative Bacteria (Epicentre, Madison, WI, USA), cleaned via the RNA Clean & Concentrator™-5 Kit, spectrophotometically characterized and controlled on a 1.2% formaldehyde-agarose gel.

The single read transcriptome analysis was performed by GATC Biotech (GATC Biotech, Konstanz, Germany) according to proprietary methods (http://www.gatc-biotech.com/en/sequencing/transcriptomes.html). Briefly, the random primed cDNA libraries of the six samples were prepared with a fragment length of 50 bp and sequenced in the genome sequencer Illumina HiSeq2000 on one lane. The reads were processed bioinformatically using Bowtie, TopHat, Cufflinks and Cuffmerge. For tracking the mapped reads and determining the fragment per kilobase per million mapped reads – value (FPKM) of each primary transcript Cuffdiff was used. The differential expression of the grouped samples HH01 (HH01_1, HH01_2 and HH01_3) and HH01Δ*jqsA* (HH02_1, HH02_1 and HH02_3) such as the fold change and the p-value were computed at gene level.

2.9.2 RNA analyses of HH01, HH01Δ*jqsA,* HH102 and HH102Δ*jqsA* in early stationary phase

The cells were cultivated in 20 ml R2A media as described above (2.4). HH102 and HH102Δ*jqsA* were grown for 11 hours and HH01 and HH01Δ*jqsA* for 13 hours, corresponding to the early stationary phase. To extract the total RNA of the sample triplicates of HH01, HH01Δ*jqsA*, HH102 and HH102Δ*jqsA*, the hot phenol method was used with minor modifications (Aiba *et al.*, 1981). Therefore, 20 ml of a bacterial culture was mixed with 25 ml ice-cold killing buffer (20 mM Tris-HCl, pH 7.5, 5 mM $MgCl_2$), centrifuged for 10 min at 4 °C and shock frozen in liquid nitrogen. Cells were resuspended in 125 µl ice-cold 300 mM sucrose / 10 mM sodium acetate solution (pH 5.2) and mixed with 125 µl 2% (w/v) SDS / 10 mM sodium acetate (pH 5.2). The cells were incubated for 90 s at 65 °C before supplementation of 400 µl hot phenol and vigorous mixture, followed by an incubation for 3 min at 65 °C with a brief mixture of the suspension every minute. The suspension was shock frozen in liquid nitrogen and spun down for 10 min at RT, the supernatant was mixed again with 400 µl hot phenol and the steps were repeated. Afterwards 400 µl of (50:45:2 v/v) phenol/chloroform/isoamylalcohol was added to the supernatant and spun down. This step was repeated, followed by the addition of 400 µl (96:4 v/v) chloroform/isoamylalcohol. The cells were centrifuged for 2 min at RT. To the supernatant, 40 µl 3 M sodium acetate (pH 5.2) and 1 ml 100% (v/v) EtOH were added for RNA precipitation at -20 °C overnight. Afterwards, the RNA was spun down for

20 min at 4 °C, washed twice with 70% (v/v) EtOH, dried and dissolved in 200 µl DEPC-treated H_2O. The removal of simultaneously extracted DNA was achieved by using the RTS DNase™ Kit. The RNA was cleaned and concentrated via the RNA Clean & Concentrator™ -5 Kit, verified on a 1.2% formaldehyde-agarose gel and the concentration was measured as described above (2.9.1). The RNA was send to the Göttingen Genomics Laboratory (Georg-August University, Göttingen, Germany) and further processed as published (Gao *et al.*, 2015).

2.9.3 Quantitative real time PCR

The quantitative real time PCR (qRT-PCR) method was used to verify the transcriptomic data of the three RNA-seq analyses (Table 2.6).

Table 2.6 Primers used for qRT-PCR

Gene	Forward Primer (5'-3' direction)	Reverse Primer (5'-3' direction)	Efficiency [%]
rpoD Jab_2c27560	GAACAGCTGGAAGCGTTGAA	CTTGACGTAGGCCTTGGAGTTGTAG	98.4
dnaG Jab_2c27570	AACCGAAGTACTTGAATTCTCCCGAAAC	TATAGCCTTCCGTCACCAGCACATAC	93.4
Jab_2c07990	GTCGTCCGACGCGCTCAATA	GATGCTGGCCGGATTCAGGT	94.2
Jab_2c08810	ACAATCCTCTGCGCAAGGTCTACTT	CAGGTAGACATCCTCGCCTTGTTC	95.4
Jab_2c10590	TCGACCTGGCCGATGTCTAC	TGGCGACGAAGGACACCTTG	90.5
Jab_2c16610	ACCTGATCCGCAGCTGGAAC	GGTGTCGGTGACGACCACTT	97.8
Jab_2c26580	TGACGTCGAGCGTGACCTTG	CCAGGTTCACGCGCACATTG	86.9
Jab_2c35400	TCGGCGATCCGATCGAGTTC	AGTCGAGGTGGCCGAGATTC	97.2
rpoD JAB4_42690	CCAACTTGCGCCTGGTCATT	GGCGGTACTCGAACTTGTCA	95.1
dnaB JAB4_01060	TTGACGAGGCCGAGTCGAAG	CTCTGGTTGTCGCGGCTGTA	96.4
JAB4_02850	ATCCGCAGCCGCCATCTGTT	AACCTGCCGTCAGCTTGTCC	89.0
JAB4_16300	AGATCGCCTATGCCGTGCTG	GCGCTTGTTGACGGTGTCCA	93.8
JAB4_20530	TTGCTGCTGCCGATGGTGTC	TGGTAGCCGCGGTCGCATA	89.3
JAB4_35690	TTCCTGTCGGCAGTACAGCA	GGCCAGCAAGTTGGTCTTGA	84.3
JAB4_35800	TCAAGACGGCGCACGAAGAG	AGCACGGCGATGACGAGGTA	95.7
JAB4_42080	CGATCTTCGGCGTGGATTCG	GCGTCTTCCAGCGCGTGATA	88.5

At first, the primer efficiency was tested with a dilution series of 100, 10, 1 and 0.1 ng genomic DNA in triplicate using the CFX96 Touch™ Real-Time PCR Detection System (Bio Rad, München, Germany). For this, 8 µl of SYBR Green SuperMix (Quanta Biosciences, Gaithersburg,MD, USA) was mixed with 0.4 µl of each primer (100 pmol/µl, Table 2.6), 0.4 µl template and 6.8 µl $H_20_{bidest.}$. The PCR protocol was set as follows: 1. 95 °C 3 min, 2. 95 °C 15 s, 3. 60 °C 20 s, 4. 72 °C 15 s, repeat steps 4 to 2 for 39 times and with a melting curve from 65 to 95 °C in 5 s steps. Data were processed with the Bio-Rad CFX Manager 3.1 software (Bio Rad, München, Germany). Primer efficiency is shown in Table 2.6. For the qRT-PCRs, 2 µg of DNase treated RNA was transcribed in cDNA using the SuperScript® VILO cDNA Synthesis Kit and Master Mix (Thermo Scientific, Hampshire, United Kingdom). The synthesized cDNA was diluted 1:10 with $H_2O_{bidest.}$ and 0.4 µl were used for qRT-PCR. Each biological sample was measured in triplicate. Primer efficiency was included in calculation. The mode normalized expression (ΔΔCq) was picked. As control the house keeping genes *rpoD* (OxaI and II), *dnaG* (OxaII) and *dnaB* (OxaI) were used. The relative quantity of the three biological samples composed of triplicate were shown in a graph with data relative to control. Only the biological replicates jan4t1 and jan4t2 of HH102 were used for calculation.

2.10 Promoter-fusion studies

A second approach to determine the JAI-1 autoinducer induced violacein synthesis and the impact of a conserved sequence of the promoter, was the fluorescence measurement of promoter-fusions. The promoter-fusions plasmids were constructed using pBBR1MCS-2 as backbone and the fluorescence protein mCherry derived from pK18mobII_pKOScvm (Table 2.2). mCherry was amplified via PCR using oFH93/oFH94 (Table 2.3) with the following conditions: 95 °C for 30 s, 56 °C for 30 s and 72 °C for 45 s, 34 cycles; Taq polymerase; 737 bp. For pBBR1MCS-2::mCherry, the mCherry-PCR product was cloned in pBBR1MCS-2 using EcoRI and HindIII restriction sites. For the constitutively expressed pBBR1MCS-2::PmCherry, the mCherry of pBBR1MCS-2::mCherry was subcloned using SacI and XhoI endonucleases. Using pBBR1MCS-2::mCherry as backbone, the *vioA* violacein promoterregion (5' of JAB9_09370) of HH107 (peqGOLD Bacterial DNA Kit; PEQLAB Biotechnologie GmbH, Erlangen, Germany) was amplified via PCR (oFH91/ oFH92; 95 °C for 30 s, 52 °C for 30 s and 72 °C for 25 s, 34 cycles; Taq polymerase; 300 bp; Table 2.3) and cloned in pBBR1MCS-2::mCherry using BamHI and EcoRI restriction sites. This vector was designated as pBBR1MCS-2::pvio107::mCherry (Table 2.2). The

amplification with this construct as template and oFH105/oFH94 (95 °C for 30 s, 55 °C for 30 s and 72 °C for 60 s, 34 cycles; Taq polymerase; 1010 bp; Table 2.3) led to the exclusion of the conserved sequence, designated as JAI-1 motif. The PCR product was integrated via XhoI and HindIII restriction sites in pBBR1MCS-2, obtaining pBBR1MCS-2::pvio107-JAI-1::mCherry. To investigate influences on the promoter of the endochitinase *chiA* (Jab_2c26490 of HH01, isolated via the peqGOLD Bacterial DNA Kit; PEQLAB Biotechnologie GmbH, Erlangen, Germany), the 5' region of the gene was amplified using oFH121/oFH122 (95 °C for 30 s, 52 °C for 30 s and 72 °C for 30 s, 34 cycles; Taq polymerase; Table 2.3) and the 457 bp PCR product was digested with BamHI and EcoRI and ligated in pBBR1MCS-2::mCherry to obtain pBBR1MCS-2::pchiA::mCherry (Table 2.2).

The strains HH01, HH01Δ*jqsA*, HH102 and HH102Δ*jqsA* were electroporated with the promoter-fusion constructs as described previously (Hornung *et al.*, 2012). To test the impact on chitin degradation products on the *chiA* expression, the cells were grown in R2A -G supplemented with 0.05% (w/v) G, 10 mM DG, or 10 mM NADG for 24 h at 22 °C (2.4). To detect the fluorescence, 200 µl of the strains were transferred in a 96 well microtiter plate suitable for fluorescence assays and excited with 587 nm. The emitted fluorescence (610 nm) was detected via Synergy™ HAT SIAFRTD and the Gen5™ software. The relative fluorescene unit (RFU) was calculated as the ratio of the fluorescene versus the culture density at OD_{600nm}.

2.11 Coincubation studies of bacteria and fungi

Tests with the filamentous, necrotrophic fungus *Fusarium graminearum* were performed in cooperation with the AG Schäfer of the Biocentrum Klein Flottbek, department molecular phytopathology of the University of Hamburg (Germany).

2.11.1 Plate assay of *Janthinobacterium* or *Duganella* with *Fusarium graminearum*

For growth assays on solid media, mycelial plugs of the strain *Fusarium graminearum* 8*I*1 (Kazan *et al.*, 2012, Bonnighausen *et al.*, 2015), harboring a constitutively expressed GFP (Jansen *et al.*, 2005) were taken from the edge of a 3-day-old colony on complete medium (Leach *et al.*, 1982). Mycelial plugs were placed in the middle of a R2A plate. For assay plates, 1 x 10^5 bacterial cells/ml were streaked on solid R2A. Cells were incubated for six days under bacterial growth conditions (2.4). Plates were photographed for documentation.

2.11.2 Liquid assay of *Janthinobacterium* or *Duganella* with *Fusarium graminearum*

To determine the impact of all bacterial isolates and type strains on the growth of *F. graminearum* 8/1 (2.11.1), the fungus was grown on solid SNA (Nirenberg, 1981), for 1.5 – 2 weeks. The conidia were rinsed from the solid plate with 4 ml ice-cold $H_2O_{bidest.}$ and separated from mycelia (100 µm filter). 400 conidia solved in 20 µl CM were provided in one well of a black 96 microtiter plate suitable for fluorescence measurements. The bacteria were grown in R2A -G. 1 x 10^3 cells/µl were mixed with 400 fungal conidia, solved in a total volume of 200 µl R2A -G. Bacterial cells were provided with a constitutely expressed mCherry on a self-replicable plasmid (pBBR1MCS-2::PmCherry, 2.10).

For QS dependent fungal inhibition, cells were grown in R2A -G supplemented with 0.05% (w/v) G, 10 mM DG, 10 mM NADG or 10 mg chitin (C) for 24 h at 22 °C (2.4), diluted to a concentration of 1 x 10^9 cells/ml and filtered using a 0.22 µm pore filter. 0.05% (w/v) G was used as it corresponds to the concentration of R2A. The final concentrations of 10 mM DG and 10 mM NADG showed the best results from a 0.1 - 100 mM concentration range tested in preliminary experiments (not shown). For the liquid assay, 180 µl of bacterial supernatant was added to 400 conidia, solved in 20 µl R2A -G. To test the influence of proteins, bacterial supernatant of strains HH102 and HH102Δ*jqsA* with pretreated with NADG were denatured for 10 min at 95 °C, cooled and added to fungal conidia. Moreover, HH102Δ*jqsA* harboring the pBBR1MCS-2::$jqsA_{102}$ plasmid (Table 2.2) and grown in R2A –G and 10 mM NADG was used for complementation. The larger skale assay was performed in 5 ml R2A –G, 10 mM NADG, 1600 conidia and 1 x 10^5 bacterial cells pretreated with NADG for 24 h. The liquid assay was incubated for 72 h at 22 °C, shaking, prior to the GFP induced fluorescence measurement at 485/20 nm excitation and 530/25 nm emission. To show the inhibitory effect of the bacterial strains, the measured fluorescence at the start point was subtracted from the fluorescence at 72 h.

Additionally, the coincubated bacteria and fungi were surveyed light microscopically using bright field, GFP (485/20 nm, 530/25 nm) and mCherry (590/20 nm, 645/40 nm) filter. Confocal laser-scanning microscopy was performed in cooperation with Christian Voigt as published (Haack *et al.*, 2016) and SEM pictures were perfomed as previously described (Krohn-Molt *et al.*, 2013) and in cooperation with the research group morphological structure analyses of Dr. Frank Friedrich and the department of biodiversity, evolution and ecology, AG Jürgens, of the University of Hamburg (Germany).

3 Results

Previous studies have shown the importance of α-hydroxyketone based bacterial cell-cell communication as intragenus system, seemingly more important as AI-2 in *V. cholerae* (Higgins *et al.*, 2007). Interestingly, strain HH01 induces the biosynthesis of the purple-pigment violacein via QS (Hornung *et al.*, 2012). As this molecule synthesized by *J. lividum* is hypothesized to affect fungi (Lincoln *et al.*, 1999, Brucker *et al.*, 2008), nine purple-pigmented bacteria were isolated, sequenced and characterized to further investigate the QS system in non-pathogenic bacteria. Additionally, the influence of the JAI-1 dependent gene expression network was investigated by RNA-seq and physiological tests. Therefore, one existing QS mutant of *Duganella* (Hornung *et al.*, 2012) was compared to a *Janthinobacterium* QS mutant constructed in this study. To identifiy the effect of the isolates on the fungus, two coincubation assays of the isolates and the fungus *F. graminearum* were established in this study. Further, the impact of QS, chitin and chitin degradation products on the effect on the fungus were analyzed.

3.1 Isolates are affiliated with the family *Oxalobacteraceae*

In order to determine the phylogenetic classification, nine strains were isolated and characterized comparatively to the *Janthinobacterium* and *Duganella* type strains (2.6). Additionally, the strains were surveyed with respect to morphology, physiology, the phylogentic classification, genomic features and their effect on fungal growth (2.7, 2.11).

3.1.1 Morphology

The bacteria were isolated and incubated as described (2.6). When grown on solid R2A, the isolates displayed a purple colony colour to varying degrees (Figure 3.1). HH100, HH101, HH102, HH104, HH106, 5059 and *J. lividum* showed a dark purple colony colour, whereas the colony colour of the isolates HH105 and HH107 was brighter, comparable to HH01. The colonies of the two *Duganella* type strains *D. phyllosphaerae* and *D. zoogloeoides* as well as *J. agaricidamnosum* were not purple. In contrast, *Duganella* type strains displayed a yellowish colony color (Figure 3.1).

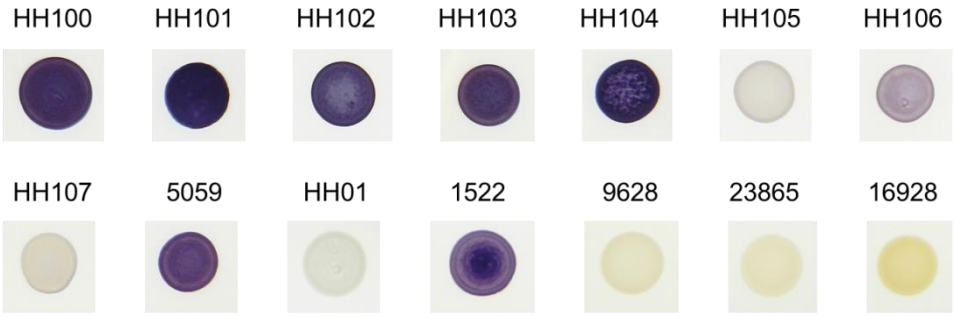

Figure 3.1 **Colony color of the 9 isolates, HH01 and the type strains.** 5 µl of an overnight culture of the isolates HH100 – HH107, 5059, the strain HH01 and the *Oxalobactereacea* type strains *J. lividum* (1522), *J. agaricidamnosum* (9628), *D. phyllosphaearae* (23865) and *D. zoogloeoides* (16928) were dropped on solid R2A medium and incubated for 3 days at 22 °C (isolates) or 28 °C (type strains).

To quantify the amount of synthesized violacein, the pigment was extracted (2.5). Similar to the growth on solid R2A (Figure 3.1), strains HH100, HH101, HH102, HH104 and HH106 synthesized violacein when grown in liquid R2A (Table 3.1).

Table 3.1 Violacein extraction of the isolates and type strains

Violacein synthesis [µg/ml]	**HH100**	**HH101**	**HH102**	**HH103**	**HH104**	**HH105**	**HH106**
R2A	1.27 ± 0.12	6.33 ± 0.15	1.54 ± 0.4	1.19 ± 0.02	1.83 ± 0.08	3.36 ± 0.76	0.15 ± 0.07
TY	1.09 ± 0.42	0.06 ± 0.06	2.33 ± 0.11	1.48 ± 0.54	0.78 ± 0.24	0.00 ± 0.01	1.21 ± 0.49
	HH107	**5059**	**1522**	**9628**	**23865**	**16928**	**HH01**
R2A	0.93 ± 0.26	0.37 ± 0.02	0.03 ± 0.01	0	0	0	1.98 ± 0.02
TY	2.34 ± 0.37	0.71 ± 0.06	0.01 ± 0.00	0.01 ± 0.02	0	0	0.01 ± 0.0

Strains sequenced in this study are marked dark gray. Abbreviations according to 2.7.3.

In contrast, the amount of violacein of strains 5059 and *J. lividum* (1522) was decreased and of strains HH105, HH102 and HH01 enhanced, when the same medium in a different aggregate state was used. Additionally, OxaI affiliated strains synthesized violacein when grown in TY, whereas OxaII affiliated strains did not. None of the type strains produced significant amounts of violacein, when grown at 22 °C, indicating a temperature dependent violacein expression. In general, HH101, HH104, HH105 and HH01 produced more violacein, when grown in R2A compared to TY. The violacein synthesis of the strains HH102, HH103, HH106, HH107 and 5059 increased when TY was used. The medium composition had no significant influence on the strains HH100 and *J. lividum* (1522). Even though HH105 and HH01 showed a slight purplish colony color on solid R2A, the highest amounts of violacein were extracted when grown in

liquid R2A. Again, the cultures of the two *Duganella* type strains *D. phyllosphaerae* (23865) and *D. zoogloeoides* (16928) as well as *J. agaricidamnosum* (9628) were not purple.

Surveying the isolates microscopically, the cells displayed a rod-shape. SEM pictures were taken to confirm the form and determine the size of the isolates (Figure 3.2, 2.6).

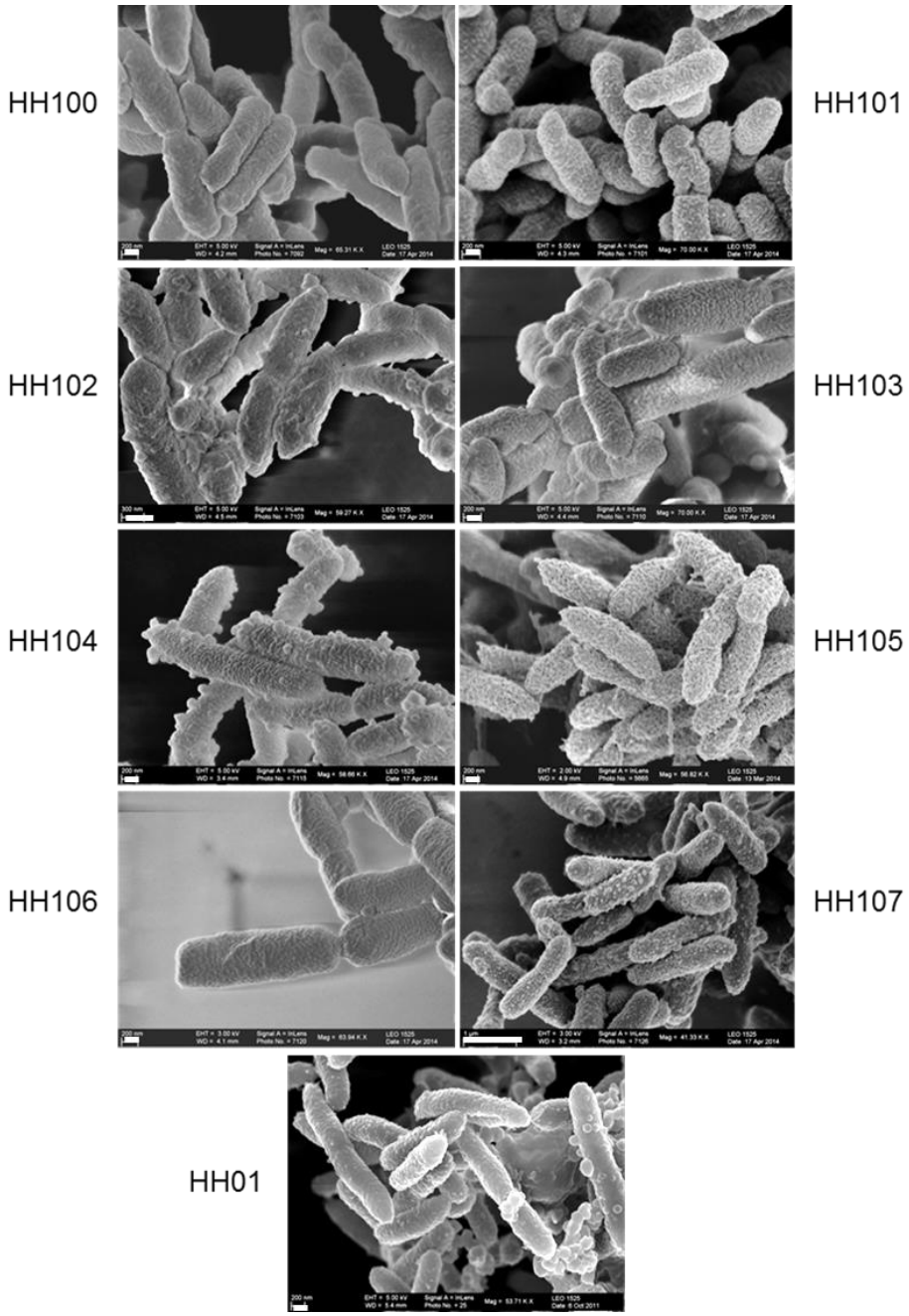

Figure 3.2 **Scanning electron microscopy images**. SEM pictures of the strains HH100 – HH107 and HH01. Scale bars of 200 nm (HH100, HH101, HH103 – HH106, HH01), 300 nm (HH102) and 1 µm (HH107) are indicated in the images by a white bar.

All isolates displayed a length that fitted in the range of *Janthinobacterium* (0.8 – 1.5 x 1.8 – 6 µm) and *Duganella* (0.6 – 0.8 x 1.8 – 3 µm). Additionally, the cell surface of

HH102, HH104 and HH107 were coated with small vesicle-like structures. The described occurrence on HH01 led to the presumption that the occurrence is an inherent property of some strains (Hornung *et al.*, 2012).

3.1.2 Phylogenetic classification

The phylogenetic classification was performed as described in 2.7. For the classification, 16S rRNA analyses (2.7.1), whole genome sequencing (2.7.2), pan- and coregenome analysis, MLSA and ANIm calculations were performed (2.7.3).

3.1.2.1 16S rRNA gene analyses

The result of the 16S rRNA gene analysis is shown in Figure 3.3. All isolates clustered within the two genera *Janthinobacterium* and *Duganella* of the family *Oxalobacteraceae*. Within this phylogenetic tree, two distinct branches were identified. Considering the isolates, the clusters were designated as OxaI and OxaII. As OxaI isolates, strains HH100, HH102 – HH104, HH106, HH107 and 5059 were grouped and as OxaII isolates, the strains HH101, HH105 and HH01 were grouped (Figure 3.3).

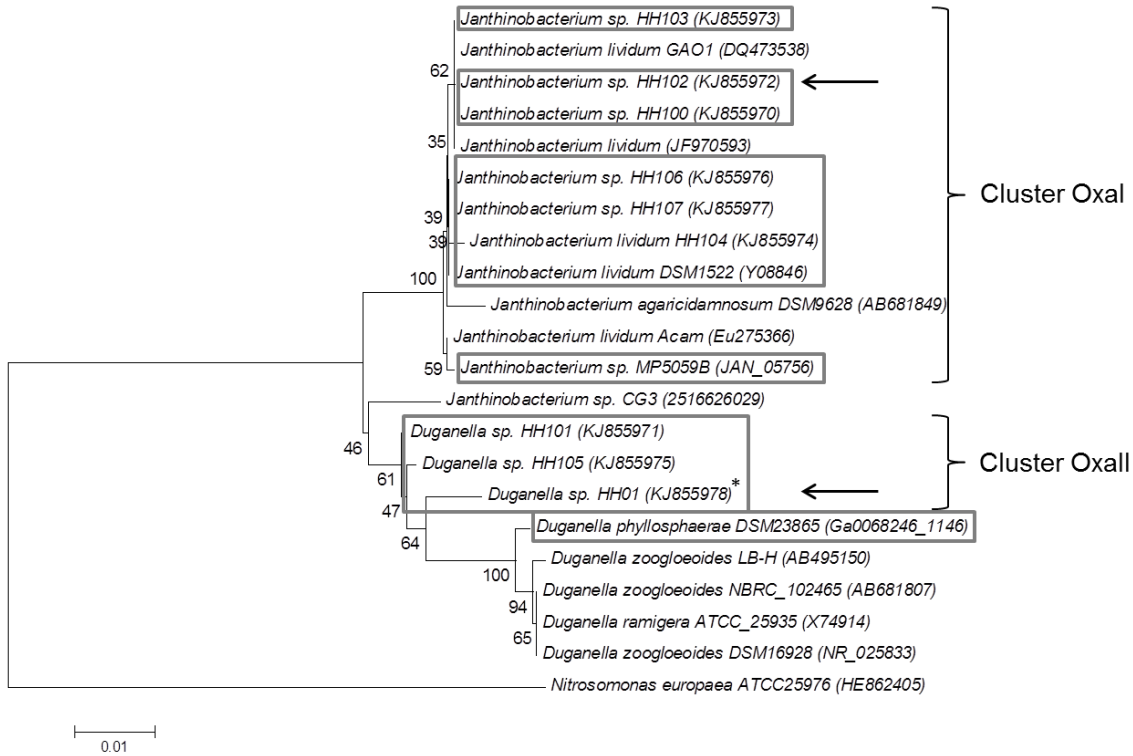

Figure 3.3 **Phylogenetic relationship,** sorted by universal bacterial 16S rRNA primer. The tree was constructed using the neighbor-joining algorithm of MEGA5 (Tamura *et al.*, 2011) with bootstrap analysis from 1000 repeats. The number at each branch point represents the bootstrap support percentage and the scale bar the sequence divergence. *N. europaea* was used as outgroup. GenBank accession numbers or respective IMG locus tags are listed in parentheses. Strains sequenced in this study are boxed in gray and strains used as group representatives are marked with an arrow. HH01 (marked with an asterisk) was formerly named *J.*sp. HH01.

It is most likely that OxaI isolates belong to the genus *Janthinobacterium*, whereas OxaII isolates are affilitated with the genus *Duganella*. According to this classification, the strain HH01 might affiliate with the genus *Duganella* and was therefore clustered to the *Duganella* genus. Nevertheless, due to overall low bootstrap percentages at the branchpoints, further genomic analyses were performed.

3.1.2.2 Phylogenetic classification according to comparative genomics

The whole genome sequencing was performed as described in 2.7.2 and the result of the analysis is summarized in Table 3.2 (analysis was performed in January 2016). The genomes sequenced and analyzed in this study ranged from 5.5 to 7.4 Mbp encoding between 5,467 to 6,535 predicted functions, as shown for HH107 and HH101 (Table 3.2). The G+C content of the nine isolates and two type strains ranged from 62.4 to 65.6%, with a mean value of 63.3% (Table 3.2). The number of RNA coding genes deviated significantly. Whereas HH104 harbored the lowest number of rRNA genes (6), isolate 5059 coded for the most rRNA and tRNA genes with 32 and 82, respectively (Table 3.2). In general, the amount of rRNA genes range from 6 (HH104) to 32 (5059), or tRNA genes from 57 (HH101) to 82 (5059) and 11 (HH104, HH106) to 23 (HH102) other RNA genes were present in the genomes (Table 3.2). This classification was based on the IMG annotation. Furthermore, all sequenced strains encoded synthesis clusters to produce secondary metabolites to differing extents. 1.04 (HH100) to 1.41% (5059) of the genomes of OxaI affiliated strains coded for the synthesis of secondary metabolites. In contrast, OxaII strains encoded a higher percentage, with 4.21 (HH101) and 6.78% (HH105) (Table 3.2). The two sequenced type strains encoded 8.1 (9628) and 1.46% (23865, Table 3.2). Currently the genomes of the 11 sequenced strains are available as draft genomes with 65 (HH104) to 223 (HH101) scaffolds.

Table 3.2 General genomic features of the strains sequenced and related *Oxalobacteraceae*

	Janthinobacterium										*Duganella*									
Genome traits	**HH100**	**HH102**	**HH103**	**HH104**	**HH106**	**HH107**	**5059**	**1522**	**9628**	**Mars**	**25724**	**RA13**	**CG3**	**OK676**	**344**	**551a**	**RIT308**	**HH101**	**HH105**	**23865**	**16928**	**HH01**
size [Mbp]	6.7	6.7	6.6	6.4	6.3	5.5	6.4	6.7	5.9	4.1	4.98	6.4	6.3	6.3	6.4	6.5	6.2	7.4	7.4	6.2	6.3	7.1
G+C content [%]	65.6	62.4	62.5	62.6	62.9	63	62.8	62.4	61	54.23	60.6	62.5	65.5	62.8	63.7	63.6	62.8	64.4	64.1	63.9	63.6	64.2
rRNAs	9	8	8	6	8	8	32	11	7	6	21	25	15	15	13	9	10	10	24	8	14	20
tRNAs	64	69	73	61	64	66	82	72	73	46	80	92	81	65	68	70	83	57	71	58	69	84
other RNA genes	22	23	22	11	11	14	12	17	0	14	13	9	13	14	12	12	-	14	12	14	13	0
coding genes	5970	5987	5873	5657	5604	5467	5645	5820	5493	3697	4432	5650	5426	5502	5526	5541	5431	6535	6277	5390	5342	5996
with function	4757	4776	4673	4647	4575	4481	4596	4760	4634	2813	3540	4612	4369	4594	4572	4594	4668	5340	5140	4375	4431	4323
% secondary metabolites	1.04	1.19	1.11	1.39	1.24	1.34	1.41	3.59	8.1	n.d.	n.d.	n.d.	n.d.	n.d.	n.d.	n.d.	n.d.	4.21	6.78	1.46	2.33	6.14
scaffolds	150	121	141	65	73	116	100	127	1	1	48	1	7	31	27	28	44	223	89	158	25	2

"n.d.": not determined, "-":no information available, abbreviations according to 2.7.3. Strains sequenced in this study are marked dark gray. Table modified from Haack *et al*., 2016.

Furthermore, the genomes of the 11 sequenced strains were aligned according to the OxaI and OxaII classification. The map is based on investigation of the amino acid identity by BLASTP analysis (NCBI), giving a graphical comparison of the isolates with the sequenced *J. lividum* and *D. phyllosphaerae* type strains. The comparison of the OxaI affiliated strains indicated a high level of synteny among these strains and *J. lividum* (Figure 3.4 A). Especially the sequences of HH102, HH103 and HH100 display a high level of synteny (Figure 3.4 A). In general, only two regions, marked with a numbered asterisk, display a genome divergence (Figure 3.4 A).

In contrast, the OxaII afiiliated strains showed more divergence in the sequence, according to the alignment and in comparison with *D. phyllosphaereae* (Figure 3.4 B). The three strains HH01, HH101 and HH105 showed the highest level of synteny.

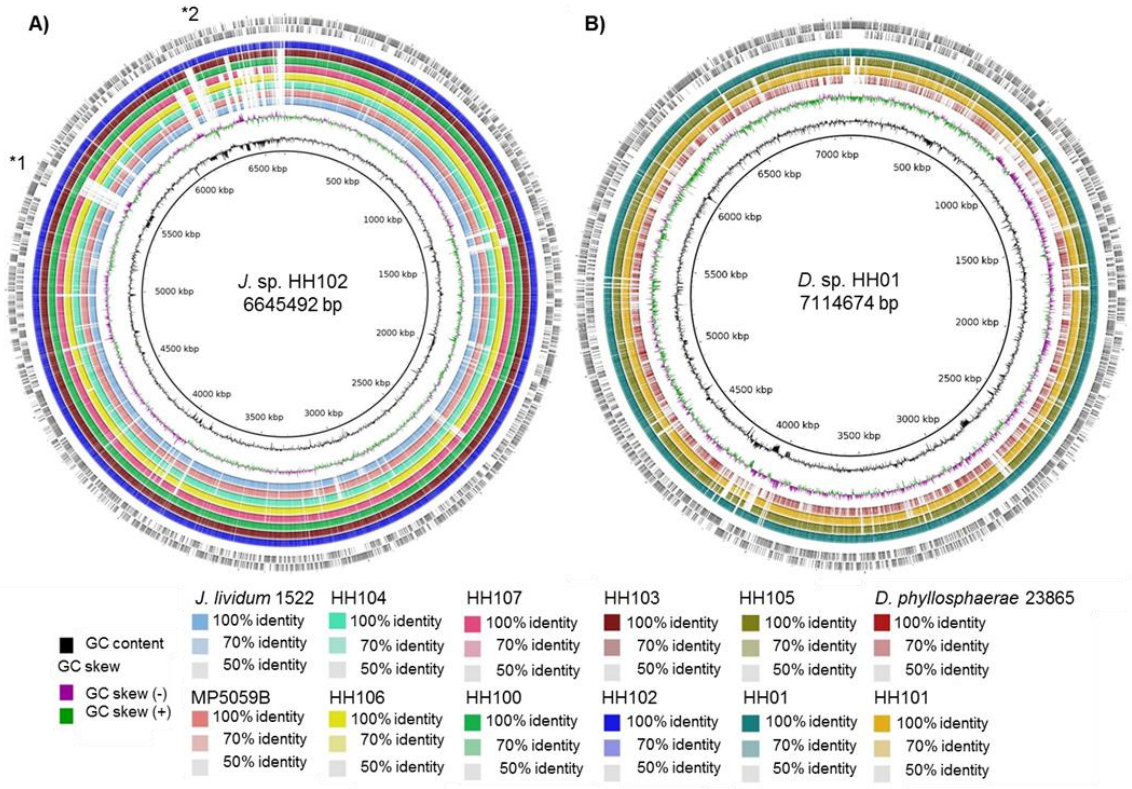

Figure 3.4 **Genome maps of the eleven strains sequenced in this study and HH01.** The innermost rings indicate the GC content (black) and GC skew (purple/green). The outer rings represent the genomes of the following isolates and two type strains in different colorings: **A)** *J. lividum* (1522, bright blue), MP5059B (bright red), HH104 (turquoise), HH106 (yellow), HH107 (pink), HH100 (green), HH103 (wine red), HH102 (blue) of the OxaI group, related to the genus *Janthinobacterium* and **B)** the OxaII strains, HH105 (green), HH01 (petrol), HH101 (organge) and *D. phyllosphaerae* (23865, red), affiliated with *Duganella*. Regions with high levels of divergence are marked with a numbered asterisk. The genome map was created using BRIG (Blast Ring Image Generator; http://sourceforge.net/projects/brig, Alikhan *et al.*, 2011). Figure was extracted from Haack *et al*.,2016.

For further analyses, the pan- and coregenome of the eleven sequenced strains and 20 strains affiliated with *Oxalobacteraceae* were calculated (2.7.3). The coregenome

comprised 1,058 genes with a pangenome of 23,628 genes. This calculation included genomic information of four *Duganella* strains, three OxaII affiliated strains, seven OxaI isolates, two *Janthinobacterium* type strains, 12 *Janthinobacterium* strains and the *Pseudoduganella violaceinigra* strain DSM15887. Extracting Marseille from the calculations due to the low gene number, the coregenome added up to 1,669 genes with a pangenome of 22,640 genes. Additionally, the core- and pangenome was used as basis for the MLSA and ANIm calculations (2.7.3).

Investigating the phylogenetic classification of the strains in this MLSA tree of 29 *Oxalobacteraceae* family members (Figure 3.5), again, a deviation in a *Duganella* and a *Janthinobacterium* branch was obvious.

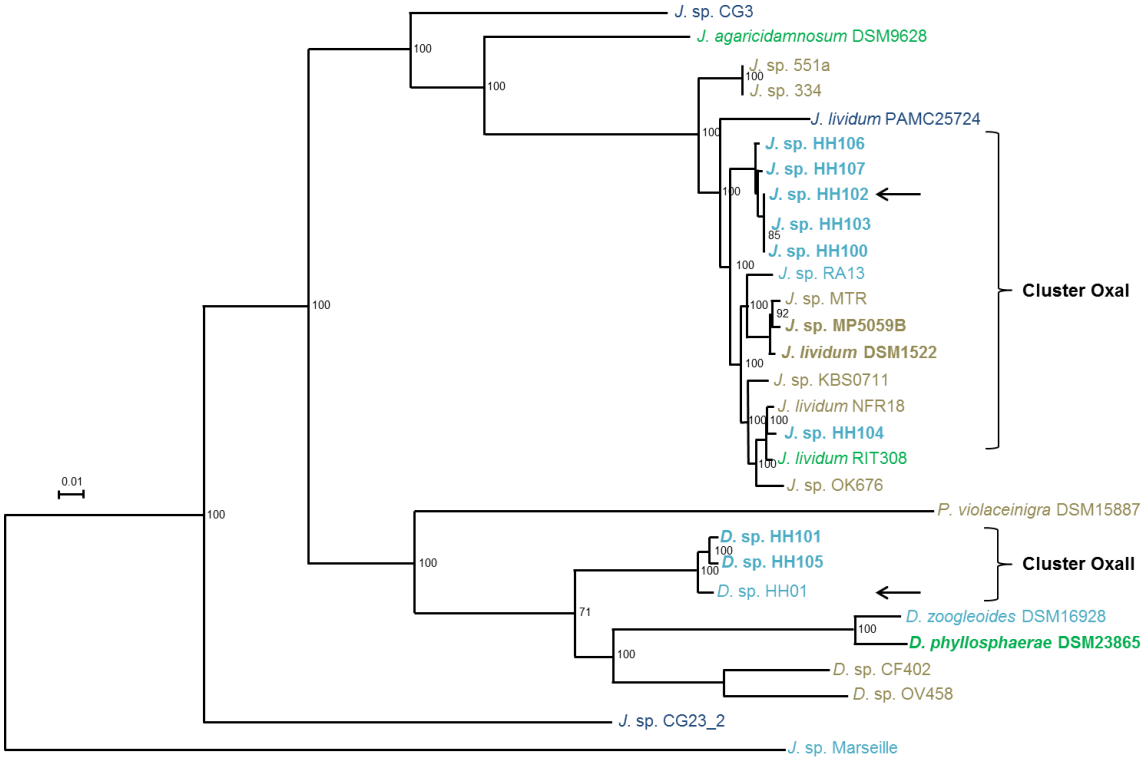

Figure 3.5 **Phylogenetic MLSA tree of 29 *Oxalobacteraceae* family members**. The isolates affiliated with the genus *Janthinobacterium* are grouped as cluster OxaI and isolates clustering within the *Duganella* branch as cluster OxaII. Strains sequenced in this study are written in bold, see 2.7.3 for strain information. Strains isolated from a cold watery source are written dark blue, strains isolated from leaf surfaces are written in green, brown are soil associated isolates and bright blue are isolates isolated from an aqueous source. Figure modified from Haack *et al*., 2016.

Due to the increased number of strains considered for the MLSA calculation, this phylogenetic tree was very diverse. Overall, the bacteria clustering in the *Janthinobacterium* branch diverged in three subbranches (Figure 3.5). These included one CG3 branch, one *J. agaricidamnosum* branch, both with a single strain, and one diversified branch, including the *J. lividum* type strain, nine *Janthinobacterium* strains

and seven OxaI affiliated isolates, namely HH100, HH102, HH103, HH104, HH106, HH107 and 5059 (Figure 3.5). Furthermore, the OxaII isolates classified in the *Duganella* branch. This cluster differed from the two type strains *D. zoogloeoides* and *D. phyllosphaerae* and displayed the highest similarity to themselves, as well as to the two isolates *D*. species CF402 and OV458 (Figure 3.5). Again, strain HH01 clustered within the *Duganella* branch, as shown for the 16S rRNA analysis (3.1.2.1). Considering this MLSA phylogenetic tree, *P. violaceinigra* differs from the other *Duganella* affilitated bacteria, indicating a distant relationship (Figure 3.5). Additionally, due to the low affiliation with either genera, Marseille can be seen as outgroup (Figure 3.5). Another method used in this study to answer the phylogenetic question of the nine isolates was the ANIm calculation (2.7.3, Figure 3.6).

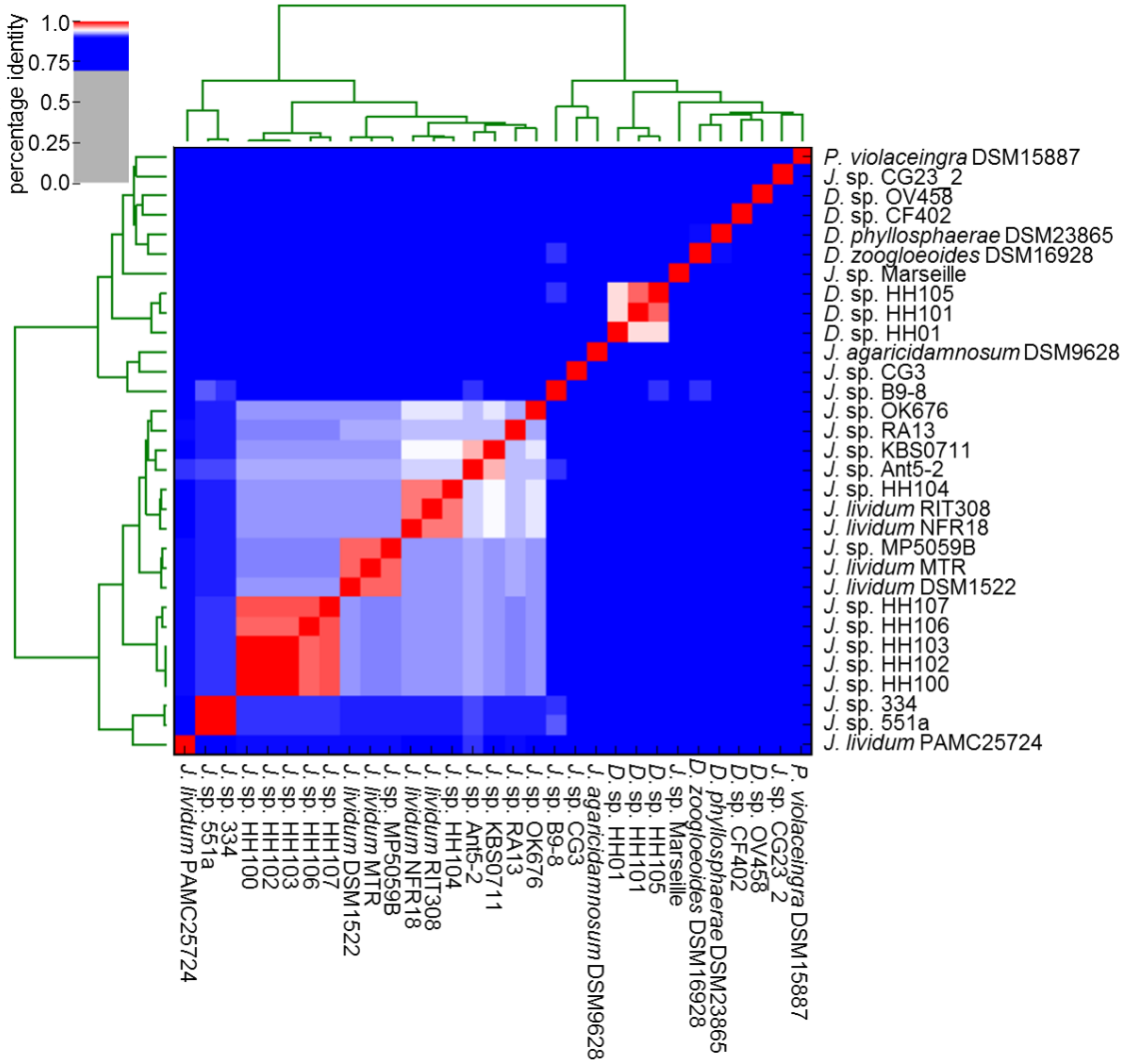

Figure 3.6 **ANIm percentage identity of sequenced *Duganella*, *Pseudoduganella* and *Janthinobacterium* strains.** The ANIm was constructed using genomic data published or extracted from http://www.jgi.doe.gov/ using the IMG database. For further strain information, consult 2.7.3. Figure extracted from Haack *et al*., 2016.

Considering the phylogenetic tree of this calculation, the *Duganella* and *Janthinobacterium* isolates divided in two distinct branches (Figure 3.6). Within the Duganella branch, the strains *P. violaceinigra*, *J*. sp. CG23_2, *D*. sp. OV458, *D*. sp. CF402, *D. phyllosphaerae*, *D. zoogloeoides, J*. sp. Marseille, HH105, HH101, HH01, *J. agaricidamnosum*, *J*. sp. CG3 and *J*. sp. B9-8 clustered (Figure 3.6). Within this branch, the OxaII affiliated strains HH101, HH105 and HH01 displayed a high synteny to each other (Figure 3.6). In contrast to MLSA, the tree sorted the three *J*. sp. strains Marseille, CG23_2 and CG3 as well as *J. agaricidamnosum* within this branch (Figure 3.6). However, the strains affiliated to the *Janthinobacterium* branch displayed a higher synteny (Figure 3.6). Especially HH104, *J. lividum* RIT308 and *J. lividum* NFR18 were closely related, as well as 5059, *J. lividum* MTR and the *J. lividum* type strain (Figure 3.6). Additionally, HH100, HH102 and HH103 showed a very high synteny, with a close relationship to HH106 and HH107 (Figure 3.6). This result underlined the classification of the OxaI isolates HH100, HH102- HH104, HH106, HH107 and 5059 to the genus *Janthinobacterium*.

3.2 Physiological characterization of the isolates

For a detailed classification of the isolates, the strains HH100 - HH107, 5059, HH01, *Janthinobacterium* and *Duganella* type strains (2.6) were investigated according to the generation time, resistances to antibiotics, swimming capacity (2.6.1), hydrolytic enzyme and chitin degradation activities (2.6.2) and protein translocation systems (2.7.3).

3.2.1 Bacterial growth

Doubling time ranged from 1.3 (HH100) to 1.8 (HH101) generations per h (Table 3.3). The OxaI grouped isolates as well as the *Janthinobacterium* type strains showed an average generation time of 1.4 h, whereas the OxaII isolates and the *Duganella* type strains displayed a slightly higher value with an average of 1.7 (Table 3.3). Overall, with respect to the phylogenetic classification, the generation time of the *Janthinobacterium* and the *Duganella* affiliated strains were very consistent.

Furthermore, the swimming capacity was determined for the isolates and the four type strains (Table 3.3). While all 14 strains were capable of flagella mediated motility, the swimming degree varied (Table 3.3). Whereas the OxaI isolates displayed a high (HH100, HH102, HH103, 5059) or medium (HH104, HH106, HH107) swimming motility, the *Janthinobacterium* type strains as well as the OxaII representatives

HH101, HH105 and HH01 displayed a slight swimming ability. In constrast, the *Duganella* type stains showed a high swimming ability, compareable to the above mentionened members of the OxaI group (Table 3.3).

Table 3.3 Generation time, swimming capacity and antibiotic susceptibility of the isolates, HH01 and type strains investigated in this study

	Janthinobacterium						
Feature	**HH100**	**HH102**	**HH103**	**HH104**	**HH106**	**HH107**	**5059**
Generation time	1.30 ± 0.09	1.42 ± 0.15	1.36 ± 0.06	1.32 ± 0.10	1.47 ± 0.21	1.32 ± 0.13	1.58 ± 0.08
Swimming	+++	+++	+++	++	++	++	+++
Resistance to							
Ampicillin (amp)	R	R	R	R	R	R	R
Gentamycin (gen)	S	S	S	S	S	S	S
Kanamycin (kan)	S	S	S	S	S	S	S
Tetracyclin (tet)	S	S	S	S	S	S	S

			Duganella				
Feature	**1522**	**9628**	**HH101**	**HH105**	**23865**	**16928**	**HH01**
Generation time	1.46 ± 0.02	1.58 ± 0.10	1.79 ± 0.43	1.77 ± 0.31	1.43 ± 0.02	1.49 ± 0.03	1.66 ± 0.14
Swimming	+	+	+	+	+++	+++	+
Resistance to							
Ampicillin (amp)	R	S	R	R	R	S	R
Gentamycin (gen)	S	S	S	S	S	S	S
Kanamycin (kan)	S	S	S	S	S	S	S
Tetracyclin (tet)	S	S	R	R	S	S	R

+: refers to a observed swimming ability. Doubling and tripling to the enhanced swimming degree. R: resistant, S: susceptible. Strains abbreviation according to 2.7.3.Strains sequenced in this study are marked dark gray. Table modified from Haack *et al.*, 2016.

Using the anitbiotics amp, gen, kan and tet, the strains were tested for antibiotic susceptibility (Table 3.3). Testing 30 µg/ml gen and 25 µg/ml kan, all isolates were susceptible against these two antibiotics (Table 3.3). In the case of 100 µg/ml amp, only *J. agaricidamnosum* and *D. zoogloeoides* were susceptible, all other investigated strains were resistant against this amp concentration (Table 3.3). Additionally, only the OxaII representatives showed a phylogenetically uniform behaviour in terms of resistance against 10 µg/ml tet (Table 3.3). Despite this uniformity, the *Duganella* type strains, as well as the OxaI representatives and the *Janthinobacterium* type strains displayed no resistance against this tet concentration (Table 3.3).

3.2.2 Secondary metabolite synthesis

Genome analyses revealed a large number of gene clusters linked to the biosynthesis of secondary metabolites (2.7.3, Table 3.2). In this study, three of the sequenced strains, namely HH101, HH105 and *J. lividum* (1522), encode 4.21%, 6.78% and 3.59% of their genome for the biosynthesis of secondary metabolites. In all other sequenced strains 1% of each genome coded for genes involved in the synthesis of secondary metabolites. Additionally, the genomes of the type strains *J. agaricidamnosum* (9628) and *D. zoogloeoides* (16928) as well as HH01, encode 8.1%, 2.33% and 6.14% for the synthesis of secondary metabolites, respectively (Table 3.2). Besides NRPS and NRPS/PKS hybrids (HH01, HH101, HH105, *J. agaricidamnosum* and *J. lividum*), clusters encoding for proteinaceous toxin bacteriocin (all strains), the terpene class of organic compounds (all strains), siderophores (*D. phyllosphaerae*), a cluster connected for the synthesis of butyrolactone (HH105) and hserlactone (*J. lividum*), the peptides linaridin and thiopeptide-lantipeptides (*J. agaricidamnosum*), and two compounds linked to the synthesis of pigments (indole and aryl-polyene, Table 9.1) were found within the strains. The presence of the indole structure was consistent with the presence of the violacein operon. Therefore, the purple colony color of the strains HH01, HH100, HH101, HH102, HH103, HH104, HH105, HH106, HH107, *J. agaricidamnosum*, *J. lividum* and 5059 can be explained by the expression of violacein (3.1.1). Instead of violacein, the two *Duganella* strains *D. phyllosphaerae* and *D. zoogloeoides* have the genetic potential to synthesize a yellow pigment, potentially an aryl-polyene.

3.2.3 Hydrolytic activity

The majority of the tested strains showed multiple hydrolytic activities in terms of amylolytic, lipolytic, proteolytic and chitinoclastic activities (Table 3.4). Furthermore, the genomes of the strains were analyzed according to genes potentially involved in these activities (Table 9.3, Table 9.4, Table 9.5 and Table 9.6).

Considering the amylolytic activity, no *Janthinobacterium* strain but *J. agaricidamnosum* showed an amylolytic activity. In contrast, all OxaII isolates and the two *Duganella* type strains displayed an amylolytic activity, indicating a phylum associated amylolytic activity. Comparing the physiological results with α-amylase genes present in the genomes, it was obvious that all *Duganella* affiliated strains shared two α-amylase genes (dark and medium gray, Table 9.3). Moreover, the OxaII group encoded one extra copy (bright gray, Table 9.3). The α-amylase genes of the OxaI isolates and *J. lividum* shared some similarities with the DUPY_33670 α-amylase

gene of *D. phyllosphaerae* and the corresponding ones from the *Duganella* affiliated strains. However, these genes were not active under tested conditions. Even though *J. agaricidamnosum* displayed an amylolytic activity, no annotated and homologous α-amylase genes were identified.

Table 3.4 Amylolytic, chitinoclastic, lipolytic and proteolytic activity of all isolates, HH01 and type strains

	Janthinobacterium						
Activity	**HH100**	**HH102**	**HH103**	**HH104**	**HH106**	**HH107**	**5059**
Amylolytic	-	-	-	-	-	-	-
Lipolytic	+	+	+	+	+	+	+
Proteolytic	++	++	++	++	++	++	++
Chitinoclastic	++	++	++	++	++	++	++

			Duganella				
Activity	**1522**	**9628**	**HH101**	**HH105**	**23865**	**16928**	**HH01**
Amylolytic	-	+	+	+	+	+	+
Lipolytic	++	+	+++	+++	+++	+	+++
Proteolytic	-	+	(+)	(+)	-	-	(+)
Chitinoclastic	++	++	+	+	-	-	+

+: activity observed, doubling and tripling indicated an increased degree of the activity, brackets a slight activity and -: no activity. Strain abbreviations according to 2.7.3. Strains sequenced in this study are marked dark gray. Table extracted from Haack *et al*., 2016.

Considering lipolytic/esterolytic activity, all strains showed a moderate lipolytic/esterolytic activity (Table 3.4). Comparing the activities with each other, the OxaI isolates and *J. agaricidamnosum* as well as *D. zoogloeoides* displayed a moderate lipolytic activity. *J. lividum* showed a slightly enhanced activity and OxaII isolates and *D. phyllosphaerae* displayed a comparable high lipolytic activity (Table 3.4). Nonetheless, comparing this physiological trait with the altogether 82 annotated and potentially secreted lipases and esterases, no pattern was identified (Table 9.4). All isolates, despite the lipolytic activity degree, harbored four (HH101 and HH105) to seven (HH100, HH102, HH103, HH106, HH107) genes potentially involved in this hydrolytic activity (Table 3.4). Taking these results together, the lipolytic and the amylolytic activities are in part characteristic for the two goups. Additionally, all but *J. lividum* and *D. pyhllosphaerae* showed proteolytic activities on skimmilk plates (Table 3.4). Whereas members of the OxaI group show a high skimmilk degrading activity, *J. agaricidamnosum* and *D. zoogloeoides* had a moderat activity. The OxaII grouped strains displayed a slight activity (Table 3.4). Unfortunately, 750 genes are linked to annotated proteases in the 14 strains, making it impossible to identify the

skimmilk degrading proteases. However, the protease activity is in line with the phylogeny.

In contrast to the amylase activity, all but the *Duganella* type strains were able to degrade chitin under the tested conditions (Table 3.4). This indicated a dependency on the phylogenetic classification. The OxaI affiliated strains and the *Janthinobacterium* type strains displayed a high chitin utilizing ability. The ability to use chitin as sole C-source was reduced for OxaII strains and not identified for the *Duganella* type strains. Comparing the chitinoclastic activity with the number of chitin degradation enzymes present in the genomes, it is noteworthy that in *D. phyllosphaerae* and *D. zoogloeoides* no annotated, predicted and potentially secreted chitinases were identified. In contrast, OxaI isolates and *Janthinobacterium* type strains harbored one (HH106), two (HH104, HH107, *J. lividum*), three (HH100, HH102, HH103) or four (*J. agaricidamnosum*, 5059) corresponding chitinase genes (Table 9.5). Members of the OxaII group harbored three (HH101, HH105) or four (HH01) genes, even though the chitin degradation capacity was slightly reduced. Further investigations of the genomes revealed another group of genes potentially involved in chitin degradation, namely deacetylases. Again, these results confirmed the phylogenetic classification. These annotated, predicted and potentially secreted peptidoglycan/xylan/chitin deactylases were present in a higher number in OxaII isolates (HH01: five, HH101 and HH105: four) compared to the *Duganella* type strains with two and three for *D. phyllosphaearae* and *D. zoogloeoides*, respectively (Table 9.6). Whereas HH100, HH102, HH103, HH106, HH107, 5059 and *J. lividum* encoded for one predicted deacetylase and HH104 for two associated genes, no deacetylase were identified in *J. agaricidamnosum*.

3.2.4 Protein translocation

Considering the genomic data, the strains were investigated for protein translocation systems, necessary to export proteins to their final destination outside of the cell (2.7.3). Genes present and potentially involved in the expression of functional transportsystems are summarized in Table 9.2. The genes were identified via a function search and KEGG pathway analyzis of the IMG database (2.7.3). 58 to 92 (*D. zoogloeoides* and *J. agaricidamnosum*) genes were linked to protein secretion. Table 3.5 summarizes the secretion systems identified in the fourteen investigated strains.

In general, most proteins are translocated by the secretion (sec) system, which transports unfolded proteins (Driessen *et al.*, 1998). All strains harbored nine to ten genes necessary for the sec system. Only SecM, a regulatory protein that functions as

secretion-responsive control of SecA, the peripheral membrane ATPase was not identified in all 14 investigated strains (Sijbrandi *et al.*, 2003). Considering the OxaI strains as well as the *Janthinobacterium* type strains, in all but HH103, HH107 and *J. agaricidamnosum* the inner membrane protein (IMP) SecE was not identified. The absence of SecM and SecE assumes the functional replacement by another gene or the lack of necessity of this protein. Despite this observation, OxaII isolates as well as *D. phyllosphaerae* harbored this gene, indicating a phylogenetic distribution of this system. Only in the second type strain *D. zoogloeoides* no SecD/F, SecE or SecG genes were identified, coding for inner membrane translocases. Besides the sec system, the tat (twin arginine transporter) system is used in bacteria to translocate folded proteins (De Buck *et al.*, 2008). This system consists of the TatABC proteins and was present in all strains.

Table 3.5 Predicted secretion systems present in all isolates and type strains

	Strain	Secretion system		Strain	Secretion system
Janthinobacterium	**HH100**	sec, tat, T2SS, T6SS		**1522**	sec, tat, T2SS, T6SS
	HH102	sec, tat, T1SS, T4SS, T2SS, T6SS		**9628**	sec, tat, T2SS, T6SS
	HH103	sec, tat, T1SS, T2SS, T6SS	*Duganella*	**HH101**	sec, tat, T2SS, T4SS, T6SS
	HH104	sec, tat, T1SS, T2SS, T6SS		**HH105**	sec, tat, T2SS, T4SS, T6SS
	HH106	sec, tat, T1SS, T2SS, T6SS		**23865**	sec, tat, T2SS, T4SS, T6SS
	HH107	sec, tat, T1SS, T2SS, T6SS		**16928**	sec, tat, T2SS, T4SS, T6SS
	5059	sec, tat, T1SS, T2SS, T6SS		**HH01**	sec, tat, T2SS, T6SS

Bright gray written secretion systems refer to a truncated system. Strain abbreviations according to 2.7.3. Strains sequenced in this study are marked dark gray.

Due to the outer membrane of Gram-negative bacteria, additional translocation systems are required. They are divided in two groups, sec-dependent and sec-independent pathways. The most common and broadly conserved sec-dependent system is the type-II-secretion system (T2SS) to translocate exoproteins (Maria, 2001). Contemplating the T2SS, all strains harbored the *gspCDEFGHIJKLMO* genes to assemble this secretion system, with the exception of HH105. Only the *gspS* gene, encoding an outer membrane protein (OMP), was not identified. Additionally, no *gspC* gene was identified in HH105, coding for an IMP, a generell secretion pathway protein. However, the presence of the T2SS in almost all strains is significant for the group of *Oxalobacteraceae*. The second sec-dependent secretion system, the type V secretion system (T5SS, Henderson *et al.*, 2004), was not identified in any of the strains. Therefore, T5SS does not play a role for protein secretion in this family.

In contrast to the T2SS and T5SS, the type-I- and type-III-secretion systems (T1SS and T3SS) functions sec-independent, with the T1SS functioning as an ABC-export system mainly used for toxin secretion (Henderson *et al.*, 2004). For the analysis of the presence of this secretion system in the strains, the IMG database were analyzed for TolC, HlyD and HlyB homologues according to the KEGG numbers. Whereas the OxaI representatives with the exception of HH100 and the two *Janthinobacterium* type strains encoded all three genes, none of the *Duganella* type strains and OxaII isolates displayed a potential T1SS (Table 9.2). Analyzing the *Janthinobacterium* strains, strains HH100, *J. lividum* and *J. agaricidamnosum* lacked the membrane fusion protein HlyD, and *J. agaricidamnosum* additionally the ABC transporter HlyB. Whereas all OxaII isolates and *Duganella* affiliated type strains encoded *tolC*, *hlyB* was only present in HH101 and *hlyD* was not identified in any of the investigated *Duganella* affiliated strains. This indicated a linkage between the T1SS and the phylogeny. In contrast to the T1SS, only one gene of the T3SS was identified in all strains, namely the ATPase YscN (Henderson *et al.*, 2004). Therefore, this ATPase might be involved in another system than T3SS. Moreover, only *J. agaricidamnosum* expressed ten genes for the assembly of the T3SS, suggesting an incomplete and non-functional T3SS, which is in general necessary for the pathogenicity of bacterial strains.

Two further secretion systems are the type-IV secretion-system (T4SS) potentially derived from the DNA translocation apparatus of conjungable-bacteria and the type-VI-secretion system (T6SS, Wallden *et al.*, 2010). Examining the T4SS, a linkage to the phylogeny was identified. Analyzing the KEGG pathways of the strains in the IMG database (2.7.3), strains HH102 and *J. lividum* encoded some T4SS genes and the two OxaII isolates HH101 and HH105 encoded ten out of twelve genes necessary for T4SS. VirB1 and VirB7, a periplasmic protein and an OMP, were not identified so far, leading to the question, if this system is functional in these two strains. In contrast to *D. phyllosphaearae*, which harbors seven genes linked to the T4SS, no genes were identified in *D. zoogloeoides* as well as in HH01, indicating T4SS as no *Duganella* specific protein secretion system. In contrast, the T6SS was present in all strains. The T6SS transports effectors into eukaryotic host cells during a pathogen-host interaction. However, proteins translocated remain mainly unidentified (Bingle *et al.*, 2008, Filloux *et al.*, 2008). The T6SS is characterized by a high diversity of genes involved in the assembly of this system and six genes were identified as non-essential hallmark proteins, namely VgrG, Hcp, Lip, IcmF, DotU and ClpV (Filloux *et al.*, 2008). With the exception of *J. agaricidamnosum* and the *Duganella* strains HH101, HH105, *D. zoogloeoides* and *D. phyllosphaearae*, all proteins but Lip were identified in the

strains. Again, this indicated a phylogenetic dependency of the presence of specific T6SS genes.

Summarizing these results, all strains shared genes encoding the sec, tat, T2SS and T6SS secretion systems and no strains coded for the T3SS or the T5SS (Table 3.5). The expression of the T1SS was limited to the OxaI affiliated *Janthinobacterium* strains, whereas some *Duganella* strains (partly) encode the T4SS (3.2.4), following the phylogenetic distribution. Figure 3.7 illustrates the protein secretion systems of the OxaI and OxaII representative strains HH102 and HH01.

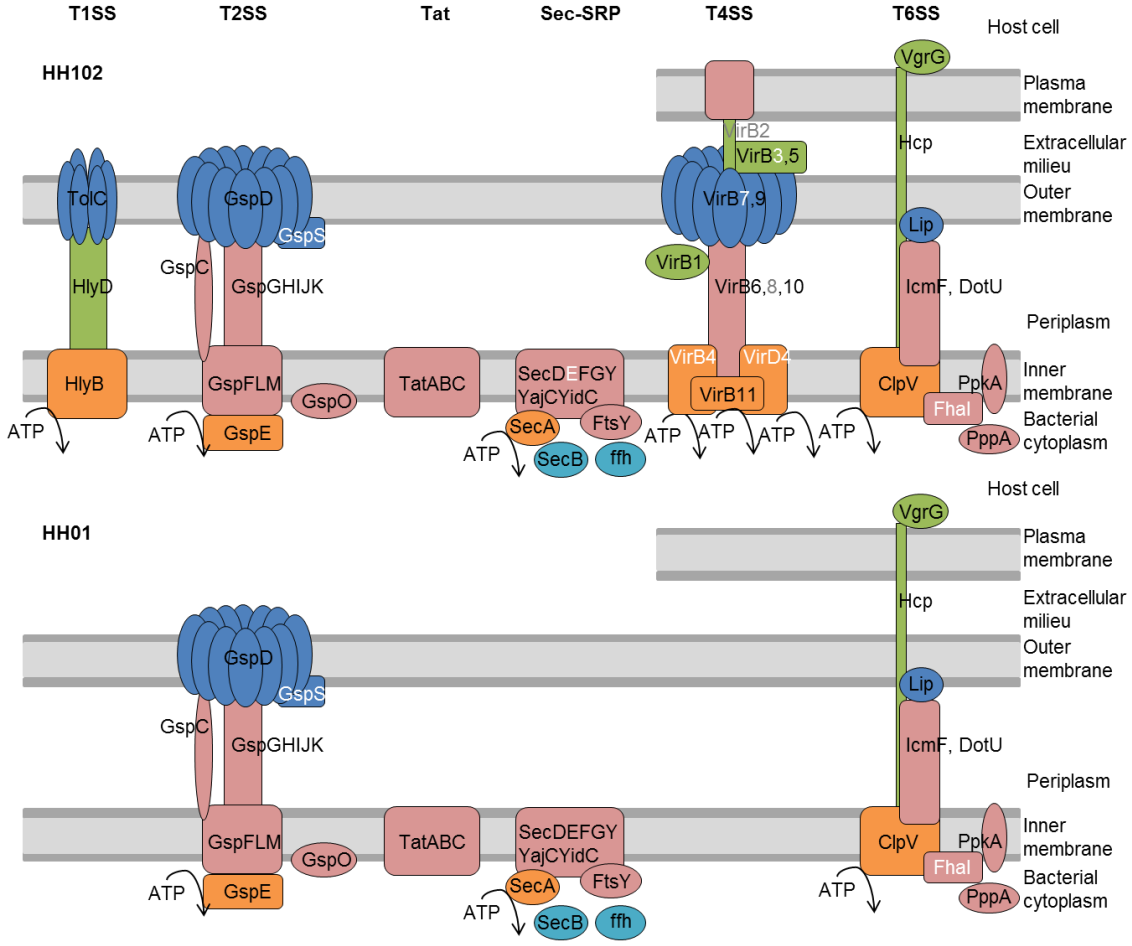

Figure 3.7 **Protein secretion systems of the strains HH102 and HH01**. Shown are the T1SS, T2SS, sec, tat, T4SS, T6SS of HH102 and T2SS, sec, tat, T6SS of HH01. Proteins involved and their schematical location within the outer and inner membrane, the periplasm of the bacteria, the extracelluar millieu and the plasma membrane of the host cell is shown. Proteins not identifed are written in white/gray.

3.3 *Oxalobacteraceae* isolates inhibit the growth of the fungus *Fusarium graminearum*

The characterization of the newly isolated strains and the four *Janthinobacterium* and *Duganella* type strains revealed the potential to synthesize secondary metabolites,

hydrolytic enzymes and the ability to secrete them in the environment (3.2). As these metabolites are well known to be involved in pathogenicity of bacteria, the influence of these members of the *Oxalobacteraceae* on the growth of the plant pathogenic fungus *F. graminerarum* was investigated in this study. Therefore, a plate assay as well as a liquid assay was established as described in material and methods (2.11.1, 2.11.2).

3.3.1 *Oxalobacteraceae* inhibit fungal growth

The influence of the HH01, HH100 – HH107, 5059, *J. agaricidamnosum, J. lividum*, *D. phyllosphaerae* and *D. zoogloeoides* strains (2.1) as well as two *E.coli* strains harboring an empty pDrive plasmid or the pDrive plasmid encoding the *vioABCDE* genes (2.1, 2.2) on solid R2A is summarized in Figure 3.8.

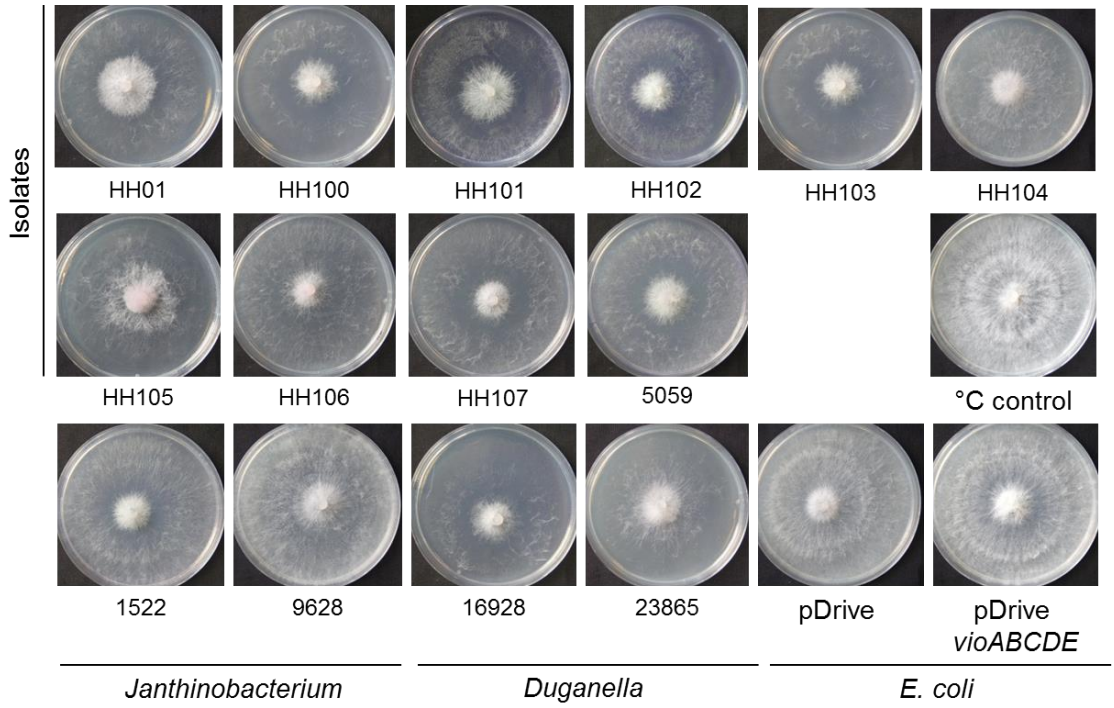

Figure 3.8 **Plate assay to test the growth inhibition of *F. graminearum*** by the isolates HH100 – HH107 and 5059, the strain HH01, the type strains *D. phyllosphaerae* (23865), *D. zoogloeoides* (16928), *J. agaricidamnosum* (9628) and *J. lividum* (1522). Included are the temperature control and *E. coli* comparison strains. *E. coli* strains harbor either an empty pDrive plasmid or a pDrive::*vioABCDE* plasmid (derived from HH01, Jab_2c00810-50). Coincubation studies were performed with 1 x 10^9 bacterial cells/ml and hyphae from *F. graminearium*. The solid R2A plates were incubated for six days at 22 °C. The test was repeated four times. This figure was extracted from Haack *et al*., 2016.

All tested *Janthinobacterium* and *Duganella* isolates and type strains reduced growth of *F. graminearum* at different extent (Figure 3.8). While *F. graminearum* alone and coincubated with *E. coli* strains spread over the entire plate after six days of incubation, the sixteen investigated strains caused a reduction of fungal growth. Interestingly, the purple *E. coli* pDrive::*vioABCDE* strain did not lead to a significant alteration in fungal

growth compared to the temperature control or the *E. coli* harboring the empty pDrive plasmid. Furthermore, despite the lack of genes coding for violacein synthesis in the *Duganella* type strains, these strains displayed an effect on fungal growth. However, testing the effect of these strains on a plate did not allow a quantification of the growth reduction. Therefore, the liquid assay correlating GFP fluorescence with the growth and presence of the fungus was established in this study (2.11.2, Figure 3.9).

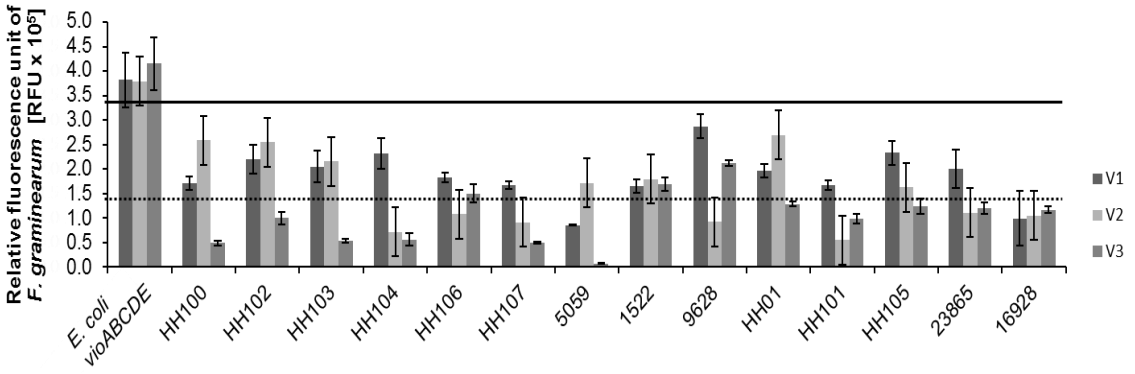

Figure 3.9 **Liquid assay to test the growth inhibition of *F. graminearum*** by the isolates HH100 – HH107 and 5059, the strain HH01, the type strains *D. phyllosphaerae* (23865), *D. zoogloeoides* (16928), *J. agaricidamnosum* (9628), *J. lividum* (1522) and *E. coli* pDrive::*vioABCDE*. The black line indicates the RFU of the GFP labeled *F. graminearum* without bacterial supernatant (RFU: 329,711 ± 74,129) and the black dashed line indicates the average of all isolates and type strains (RFU: 147,231). Filtered supernatant of 1 x 10^9 cells/ml and 400 fungal conidia were incubated in R2A –G in a total volume of 200 µl. Cells were incubated for 48 h at 28 °C prior to fluorescence measurement. Shown are the experiments numbered as V1, V2 and V3 with a mean from four samples each.

Considering the fungal growth reduction by the isolates, HH01 and the *Duganella* and *Janthinobacterium* type strains, all tested strains displayed an effect (Figure 3.9). Only the *E. coli* strain harboring the pDrive::*vioABCDE* plasmid did not reduce the RFU compared to the *F. gramineraum* control (391,947 ± 61,385 compared to 329,711 ± 74,129). HH101, HH104, HH107 and 5059 were the bacterial isolates with the highest effect along with the *Duganella* type strains *D. phyllosphaerae* and *D. zoogloeoides*. The mean RFU of all *Janthinobacterium* and *Duganella* strains averaged 147,231. Nevertheless, the individual experiments V1, V2 and V3 as well as the four biological quadruples of each experiment fluctuated significantly. This phenomenon might be explained with a non-uniform growth of the fungus, as even the fungal control varied significantly within each experiment (compare to Table 9.9). Thus, for further experiments the percentage of the RFU change of *F. graminearum* coincubated with the bacteria was normalized to the fungal control of each experiment to ensure the reproducibility and comparability of these experiments.

3.4 Despite phylogenetical differencies, various *Oxalobacteraceae* harbor functional homologues of the JQS system

Although the sequenced and examined *Oxalobacteraceae* strains differ with respect to the generation time or the expression of hydrolytic enzymes (3.2), all strains harbored a conserved gene cluster necessary for bacterial communication. Investigating altogether 22 strains according to the presence of AI systems in the genome, all but *J. lividum*, RA13 and CG3 lacked N-AHL synthesis genes, no strain synthesized the AI-2 and all but Marseille encoded genes necessary for a α-hydroxyketone-based QS system (Table 3.6). This system was first described for the two humanpathogenic bacteria *V. cholerae* and *L. pneumophila* and an involvement of this QS system in bacterial pathogenicity was hypothesized. Therefore, investigating the QS mechanisms present in *Janthinobacterium* and *Duganella* was of special interest. Understanding how bacteria communicate and interact with its environment might help to understand the BFI of the *Oxalobacteraceae* with the fungus *F. graminerarum* in terms of a fungal growth reduction (3.3).

Table 3.6 QS systems in selected *Oxalobacteraceae*

	QS system					QS system			
	Strain	**N-AHL**	**AI-2**	**JAI-1**		**Strain**	**N-AHL**	**AI-2**	**JAI-1**
Janthinobacterium	**HH100**	-	-	+		**RA13**	+	-	+
	HH102	-	-	+		**CG3**	+	-	+
	HH103	-	-	+		**OK676**	-	-	+
	HH104	-	-	+		**344**	-	-	+
	HH106	-	-	+		**551a**	-	-	+
	HH107	-	-	+		**RIT308**	-	-	+
	5059	-	-	+	***Duganella***	**HH101**	-	-	+
	1522	+	-	+		**HH105**	-	-	+
	9628	-	-	+		**23865**	-	-	+
	Mars	-	-	-		**16928**	-	-	+
	25724	-	-	+		**HH01**	-	-	+

+: genes encoding for QS system present in the genome, -: not present. Strains abbreviations according to 2.7.3. Strains sequenced in this study are marked dark gray.

Considering the genome sequences of the strains, *J. lividum* (1522) harbored one *luxI/luxR* cluster (JALI_51420 and JALI_51430), one additional *luxI* homologue (JALI_55550) and two further *luxR* homoglues (JALI_57870 and JALI_31370). The

LuxI AI synthase is necessary to synthesize N-AHL QS molecules and the LuxR receptor recognizes the produced N-AHL. Moreover, both RA13 and CG3 strains encoded for one *luxI/luxR* cluster, with the corresponding locus tags FG13DRAFT_1957/FG13DRAFT_1956 and JANGC3DRAFT_0717/ JANGC3DRAFT_0712, respectivley. CG3 harbored one extra *luxR* homologue (JANGC3DRAFT_0091) and the isolate 5059 encoded for a *luxR* receptor gene (JAB1_14880) without any identified LuxI AI synthase present in the genome. These genes might function as *luxR* solos, characterized by the lack of an *luxI* gene in chromosomal proximity, but being possibly involved in the recognition of internal or external produced N-AHL (Hudaiberdiev *et al.*, 2015). Besides N-AHL, all 22 genomes were examined with respect to the presence of *luxS* AI-2 synthase homologous genes. The *luxS* gene was absent in all strains (Table 3.6). Instead of these two well characterized QS systems for intraspecific (N-AHL) and interspecific (AI-2) communication, all strains but Marseille harbored the JQS system, used for AHK based bacterial communication (Table 3.6).

3.4.1 The JQS system

The JQS system consists of an autoinducer synthase JqsA to synthesize the *Vibrio* and *Legionella*-like JAI-1 AI, a sensorkinase/ phosphatase JqsS and a response regulator JqsR (Hornung *et al.*, 2012). This system was present in all strains with slight alterations (Figure 3.10). Whereas the *jqsA* gene of all strains differed barely, with a size of 1244 (OxaI isolates) to 1259 bp (OxaII isolates), the intergenic region between *jqsA* and *jqsS* as well as the size of *jqsS* varied slightly and with respect to the phylogenetic classification (Table 9.7, Figure 3.10). In case of the OxaI isolates HH100, HH102, HH103, HH106 and HH107, the intergenic region consisted of 43 bp and the predicted *jqsS* coding sequence amounted 1442 bp (Table 9.7). In contrast, the intergenic regions of all further investigated *Oxalobacteraceae* had a size of 153 to 184 bp and the *jqsS* differed from 1271 to 1319 bp (Table 9.7). However, considering the size from the *jqsA* stoppcodon to the *jqsS* stoppcodon, two groups were identified. The OxaI isolates and *J. agaricidamnosum* on the one hand and with a size of 1485 to 1479 bp, and on the other hand the OxaII representatives (1452 bp), *Duganella* type strains *D. phyllosphaerae* (1448 bp) and *D. zoogloeoides* (1447 bp) and the two *Janthinobacterium* strains 5059 and *J. lividum* (1451 bp). Since the differences of the OxaI isolates evened out, this effect depicted in Figure 3.10 for OxaI isolates, might be caused by annotation discrepancies. Moreover, for the intergenic region between *jqsS* and *jqsR* as well as the *jqsR* gene, slight alterations were observed (Table 9.7). All OxaI and OxaII isolates as well as *J. lividum* displayed a size of 4 bp, the *Duganella*

type strains of 3 bp and *J. agaricidamnosum* of 9 bp. The *jqsR* gene, only present in the *Legionella* LQS system and not in the *Vibrio* CQS system (Figure 3.10), varied from 1007 bp (OxaI isolates and 1522) to 1010 bp (OxaII isolates) to 1076 and 1091 bp of *D. phyllosphaereae* and *D. zoogloeoides,* respectively.

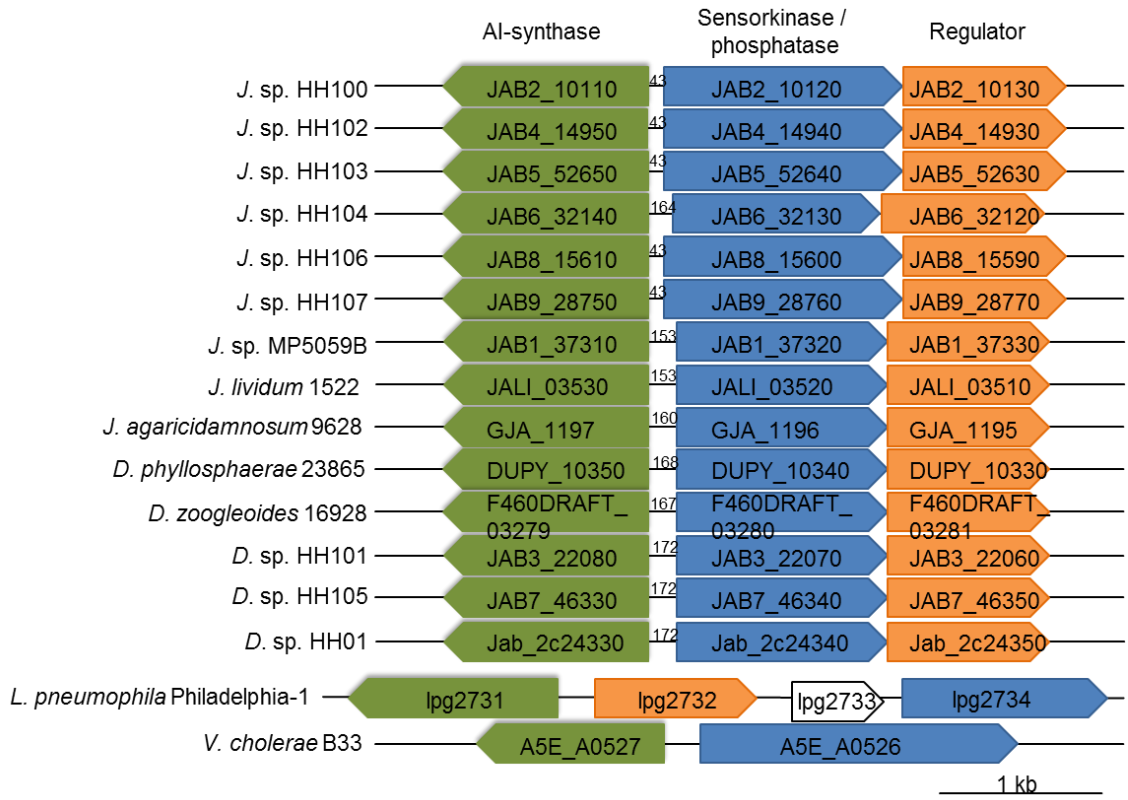

Figure 3.10 **JQS system and intergenic regions of all investigated *Oxalaboactereacea*, *L. pneumophila* Philadelphia-1 and *V. cholerae* B33 strains.** The JQS autoinducer systems include the autoinducer synthase shown in green, the sensor kinase / phosphatase in blue and a response regulator in orange, if present. Numbers in the genes indicate the corresponding locus tag used in the IMG database. The number between the AI synthase and the sensorkinase correlates with the bp lenght of the intergenic region. The intergenic region length between the sensorkinase and the response regulator is 4 bp, with the exception of *D phyllosphaerae* (23865) and *D. zoogloeoides* (16928) with only 3 bp and *J. agaricidamnosum* (9628) with 9 bp.

However, aligning the JqsA sequences of the isolates and related *Oxalobacteraceae* strains as well as from *V. cholerae* B33 and *L. pneumophila* Philadelphia-1, again the distribution of the JqsA sequences according to the phylogentic classification was observed (Figure 3.11). The autoinducer synthase sequences of strains and isolates affiliated with the *Janthinobacterium* genus showed homologies to each other, as well as the AI synthases of *Duganella* affiliated strains itself (Figure 3.11).

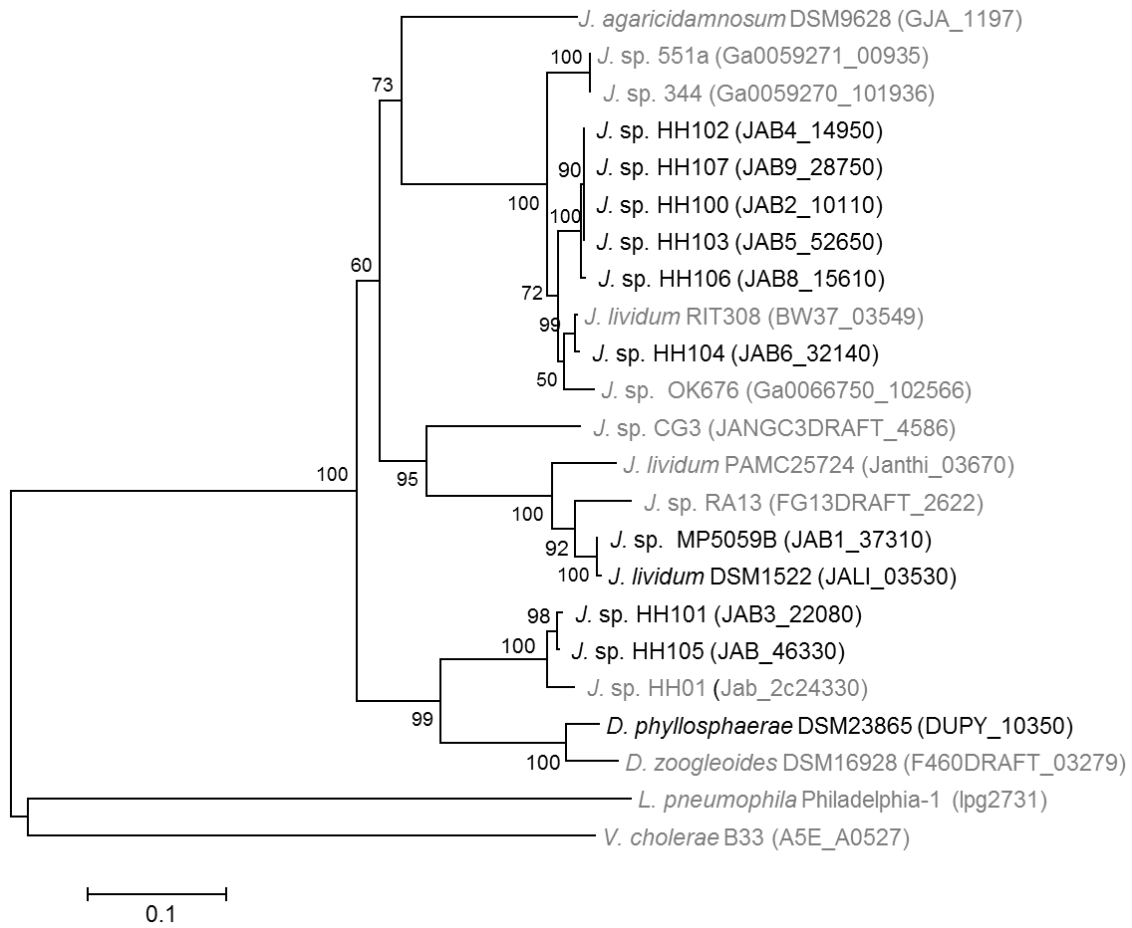

Figure 3.11 **Alignment of AI synthases of 21 *Oxalobacteraceae*, *L. pneumophila* Philadelphia-1 and *V. cholerae* B33.** For analysis, the GenBank accession numbers or respective IMG locus tags (written in parenthesis) were extraced via IMG or NCBI and aligned using the BioEdit software (Hall, 1999). The phylogentic tree was constructed using the neighbor-joining algorithm of MEGA5 (Tamura *et al.*, 2011) with bootstrap analysis from 1000 repeats. The number at each branch point represents the bootstrap support percentage and the scale bar the sequence divergence. The AI synthases of *L pneumophila* Philadelphia-1 and *V. cholerae* B33 were used as outgroups. Strains sequenced in this study are written in black.

Within the *Janthinobacterium* strains, three main branches separated the AI synthase sequences (Figure 3.11). Therefore, the AI synthase of the first *J. agaricidamnosum* branch differed from the ones of the strains HH102, HH107, HH100, HH103, HH106 and HH104, affiliated with *J.* sp., and the ones of the strains *J. lividum* and 5059 (Figure 3.11). Whereas the sequences of the AI of the OxaII representatives shared the most homologies, the ones of *D. phyllosphaerae* and *D. zoogloeoides* formed a second group within this genus (Figure 3.11). Additionally, due to minor similarities to the AI synthases of *L. pneumophila* Philadelphia-1 and *V. cholerae* B33, these proteins were used as outgroups (Figure 3.11).

3.4.2 Phenotypical impact of JAI-1 on HH102

To examine the influence and structure of JAI-1 of HH102 (JAI-1_{102}), a *jqsA* gene deletion mutant was constructed and verified in this study (2.8). Figure 3.12 summarizes expected PCR product length from HH102 and the HH102Δ*jqsA* gene deletion mutant, as well as the PCR products obtained and separated on a 0.8% agarose gel. The PCR product of the primer pair oFH115/120 (Table 2.5) was sequenced additionally to verify the gene deletion mutation (data not shown). The deletion of *jqsA* did not have a significant influence on the growth of this strain, with a generation time of 1.5 ± 0.04 compared to 1.4 ± 0.15 of HH102 (2.6.1).

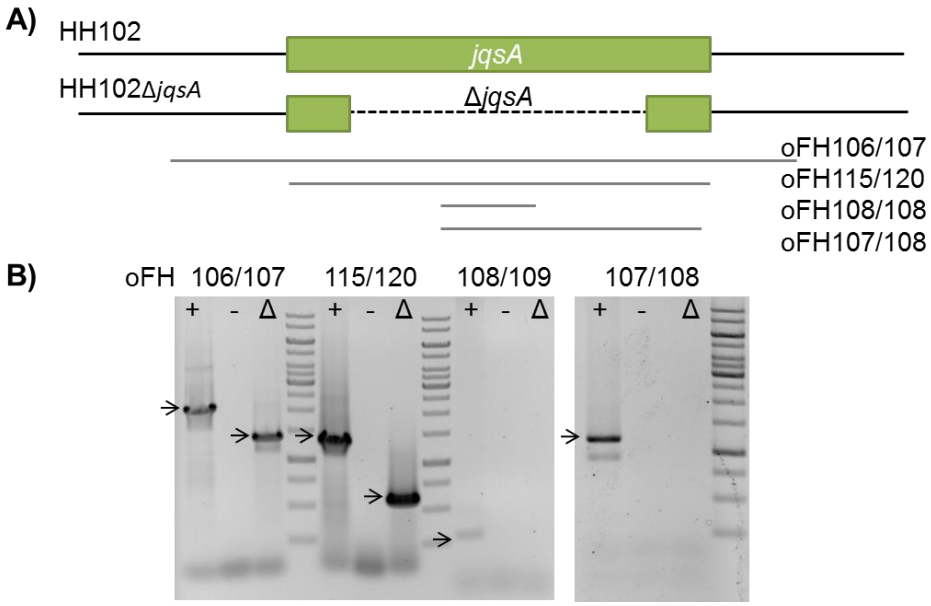

Figure 3.12 **HH102Δ*jqsA* gene deletion verification. A)** Schematic primer binding and product length (gray lines) of the pairs oFH106/107, oFH115/120, oFH108/109 and oFH107/108 in *jqsA* of HH102 and HH102Δ*jqsA.* **B)** PCR products using HH102 (+), a no template control (-) and the HH102Δ*jqsA* mutant (Δ) as template separated on a 0.8% agarose gel. Arrows indicate the desired product length accroding to the expected product length.

To test the effect of a *jqsA* gene deletion on the strains HH102 and HH01, the strains were investigated according to the growth in R2A, on TY, in M9 lacking a C-source and supplemented with shrimp shell chitin, the amylolytic, lipolytic, chitinoclastic and proteolytic activity (2.6.2). Figure 3.13 presents the growth of the HH01 and HH102 strains with respective *jqsA* gene deletion mutants in liquid R2A and on solid TY. All four strains grew and synthesized violacein to different extents in R2A and on TY medium (Figure 3.13). A *jqsA* gene deletion in strain HH102 decreased the amount of synthesized violacein compared to the wild type. For strain HH01 and its respective *jqsA* gene deletion mutant it was already shown by Hornung et al. (2012) and proved in this study. Interestingly, on solid TY the colonies of the OxaII representative HH01 and its corresponding gene deletion mutant were not continously pigmented. Only bacteria

at the colony edge synthesized violacein. This effect was not observed for HH102 and HH102Δ*jqsA*. These colonies were continiously pigmented.

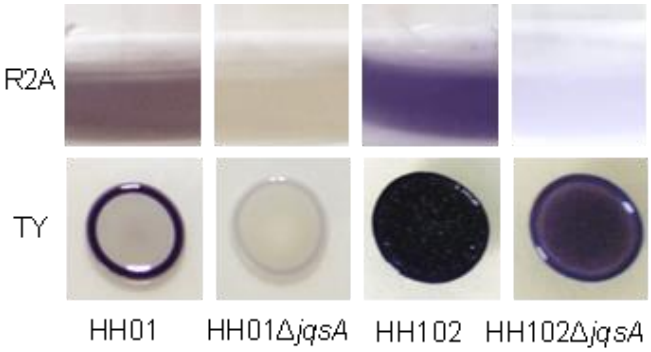

Figure 3.13 **Growth of HH01, HH01Δ*jqsA*, HH102 and HH102Δ*jqsA* on solid TY and in liquid R2A.** Cells were incubated for 72 h (TY) and 24 h (R2A) at 22 °C. Figure modified from Haack *et al*., 2016.

Furthermore, the strains were tested with respect to an altered expression and secretion of hydrolytic enzymes. For this, the amylolytic, lipolytic, proteolytic and chitinoclastic enzymatic activity was tested (2.6.2).

Table 3.7 Amylolytic, lipolytic, proteolytic and chitinoclastic activity of HH102, HH01 and the corresponding gene deletion mutants

Activity	**HH102**	**HH102Δ*jqsA***	**HH01**	**HH01Δ*jqsA***
Amylolytic	-	-	+	+
Lipolytic	+	+	+++	+++
Proteolytic	++	-	(+)	(+)

+: activity observed, doubling and tripling indicates an increased degree of the activity, brackets a slight activity and -: no activity could be observed.

The *jqsA* gene deletion did not have an influence on the amylolytic and lipolytic activity of HH102 or HH01 (Table 3.7). The protease acitivity of HH01 was not affected by JAI-1_{01}. In contrast, a lack of JAI-1_{102} resulted in a decrease of the protease activity of HH102 (Figure 3.14).

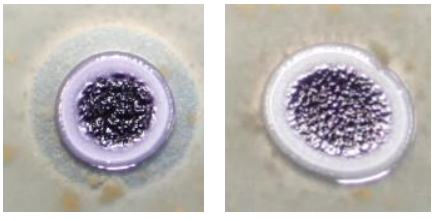

Figure 3.14 **Protease activity of the strain HH102 and its *jqsA* gene deletion mutant.** Cells were grown on R2A supplemented with 4% (w/v) skimmilk and indcubated at 22 °C for 72 h. Figure modified from Haack *et al.*, 2016.

Additionally, the effect of JAI-1 of HH01 and HH102 was tested by comparison of the wild types with its respective *jqsA* mutants. The ability to attach to chitin and utilize degradation products as sole C-source was tested by complementing the growth of cells in M9 lacking a C-source and supplemented with chitin (2.6.2, Figure 3.15). Regardless of the presence of lack of JAI-1 and the OxaI or OxaII affiliation, the strains did not grow in M9 lacking a C-source (Figure 3.15). Providing shrimp shell chitin, all strains restored growth at different values (Figure 3.15). HH102 and HH102Δ*jqsA* attached to the chitin flakes and restored growth. A difference was seen for the violacein synthesis of HH102 and HH102Δ*jqsA.* Whereas HH102 cells produced violacein in the culture supernatant by planktonic cells as well as cells attached to chitin, the planktonic cells of HH102Δ*jqsA* produced less violacein (Figure 3.15). In contrast, no significant attachment and violacein synthesis of the strains HH01 and HH01Δ*jqsA* was detected (Figure 3.15). However, HH01 and HH01Δ*jqsA* partly restored growth regardless of the presence or lack of *jqsA*.

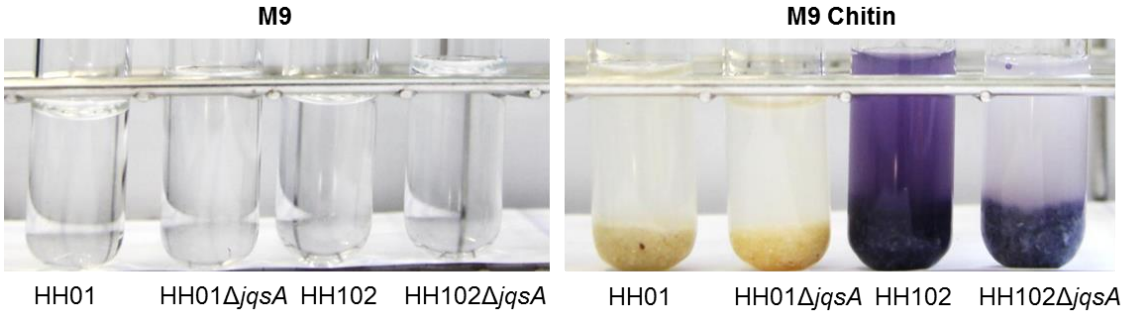

Figure 3.15 **Influence of chitin on the growth of HH01, HH01Δ*jqsA*, HH102 and HH102Δ*jqsA* in M9 minimal media, lacking a C-source**. The strains were incubated for 1 week at 22 °C in M9 –G medium, with and without chitin derived from shrimp shell.

3.4.3 CAI-1 and LAI-1 complement a *jqsA* gene deletion of OxaI and OxaII representatives

After establishing the HH102Δ*jqsA* gene deletion mutant, the mutation was complemented using different AI synthases. This helped to identify the recognition potential and usage of AI synthases of various strains to synthesize an AI. The AI synthases derived from the strains *L. pneumophila* (pBBR1MCS-2::*lqsA*), *V. cholerae* (pBBR1MCS-2::$cqsA_{Vc}$), *V. harveyi* (pBBR1MCS-2::$cqsA_{Vh}$) and the OxaI and OxaII representatives HH102 (pBBR1MCS-2::$jqsA_{102}$) and HH01 (pBBR1MCS-2::$jqsA_{01}$) was tested and compared to a pBBR1MCS-2 negative control (2.8.2, Figure 3.16). As a *jqsA* gene deletion in strain HH102 decreased the amount of synthesized violacein by 72.2 ± 3.7% compared to HH102, the extraction of synthesized violacein was used to

determine the complementation potential of the investigated AI synthases. Figure 3.16 summarizes the complementation assay using HH102, its corresponding *jqsA* gene deletion mutant established in this study, as well as HH01 and HH01Δ*jqsA* (Hornung *et al.*, 2012). The violacein synthesis of the OxaII representative HH01 was likewise JAI-1_{01} dependent and displayed a reduction of synthesized and extracted violacein of 81.4 ± 5.6% (Figure 3.16).

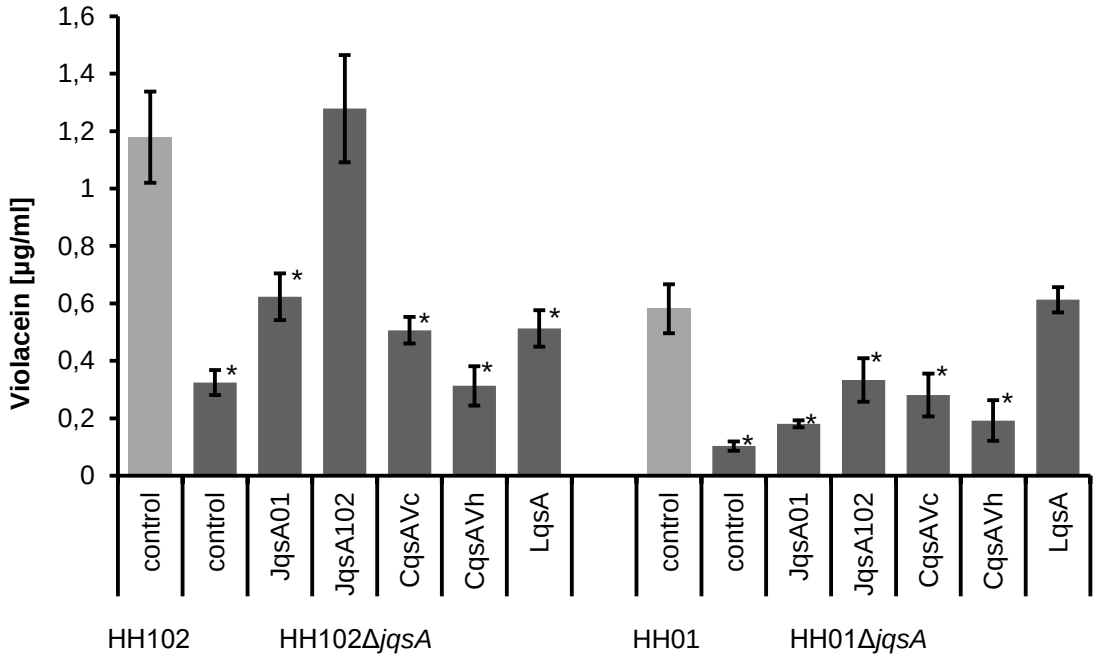

Figure 3.16 **Complementation assay of HH102Δ*jqsA* and HH01Δ*jqsA*** using AI synthases derived from HH01 (JqsA01), HH102 (JqsA102), *V. cholerae* (CqsAVc), *V. harveyi* (CqsAVh) and *L. pneumophila* (LqsA). Cells were grown for 48 h in R2A media at 22 °C. Wild types (light gray) and gene deletion mutants harboring the empty pBBR1MCS-2 plasmid were used as negative controls (control). Experiments were performed thrice. Two-tailed P-value of the unpaired t tests ≤ 0.037, n = 3 of three individual experiments is marked with an asterisk. Figure modified from Haack *et al*., 2016.

Providing an extrachromosomal copy of the innate $JqsA_{102}$ AI synthase in strain HH102Δ*jqsA*, the phenotype of a reduced violacein synthesis was restored to wild type level (Figure 3.16). Complementing HH102Δ*jqsA* with the AI synthases derived from HH01, *V. cholerae* and *L. pneumophila*, the violacein synthesis was reduced by half compared to the wild type. In contrast, providing the $cqsA_{Vh}$ gene of *V. harveyi* in HH102Δ*jqsA* no effect on the violacein synthesis was observed. Moreover, the overall violacein synthesis of the OxaI representative HH102 was as twice as high as the violacein synthesis of the OxaII strain HH01, when grown in R2A media without supplements (Figure 3.16). Interestingly, the *jqsA* gene deletion of HH01 was not complemented to wild type level using the innate $JqsA_{01}$. Instead, only 20% of the

reduced violacein synthesis was restored, when an extrachromosomal copy of *jqsA*$_{01}$ was provided. Complementing HH01Δ*jqsA* with its own AI synthase resulted in a decreased complementation compared to providing CqsA$_{Vh}$. In contrast, using JqsA$_{01}$, CqsA$_{Vc}$ and LqsA, the violacein synthesis was restored to 60.4 ± 22.4%, 47.5 ± 6.9% and 107.4 ± 15.1% to the wild type level (Figure 3.16).

3.4.4 Clues to the possible JAI-1 structure

Providing HH102Δ*jqsA* and HH01Δ*jqsA* with extrachromosomal copies of AI synthases derived from HH102, HH01, *V. cholerae, V. harveyi* and *L. pneumophila,* the complementation of the JAI-1 induced violacein synthesis was achieved (Figure 3.16). Since the complementation might be due to structurally similar AI molecules, the amino acid sequences of the AI synthases JqsA$_{01}$ and JqsA$_{102}$ and sensor kinases JqsS$_{01}$ and JqsS$_{102}$ were compared with the ones of the *Duganella* and *Janthinobacterium* type strains as well as the well known AI synthases and sensor kinases of *V. cholerae* and *L. pneumophila* (Figure 3.17). For both strains, the AI as well as the signaling mechanism was identified previously (Ng *et al.*, 2010, Bolitho *et al.*, 2011, Ng *et al.*, 2011, Tiaden & Hilbi, 2012). Therefore, the amino acid sequences of HH01 and HH102 were investigated according to the presence of essential amino acids identified in *V. cholerae* and *L. pneumophila*. Considering the ClustalW multiple alignments (Figure 3.17), all eight investigated AI synthases shared homologies in the area sourrounding the active center. This included amino acids necessary to form the pyridoxal 5' (PLP) binding pocket and a potentially involved lysine (Figure 3.17, Spirig *et al.*, 2008). Using the psi-BLAST tool of NCBI, amino acids used for PLP binding were identified. With the exception of *J. lividum*, all eight investigated AI synthases shared all amino acid sequences potentially conducting this function. Only *J. lividum* exhibited an amino acid exchange from a tryptophan (W) to methionine (M). Both amino acids are classified as unpolar and hydrophobe (Figure 3.17), decreasing a potential impact of the exchange. Furthermore, all strains harbored one lysine (K236), which was identified in *V. cholerae* as involved in forming the hydrogen bond between the amino group of the AI synthase and the free aldehyde of PLP (Spirig *et al.*, 2008). The function of K236 could be taken over by the amino acids K253 (HH01), K248 (HH102), K249 (*J. agaricidamnsoum*), K249 (*J. lividum*), K252 (*D. phyllosphaereae*) or K253 (*D. zoogloeoides*) as shown for K258 of *L. pneumophila*.

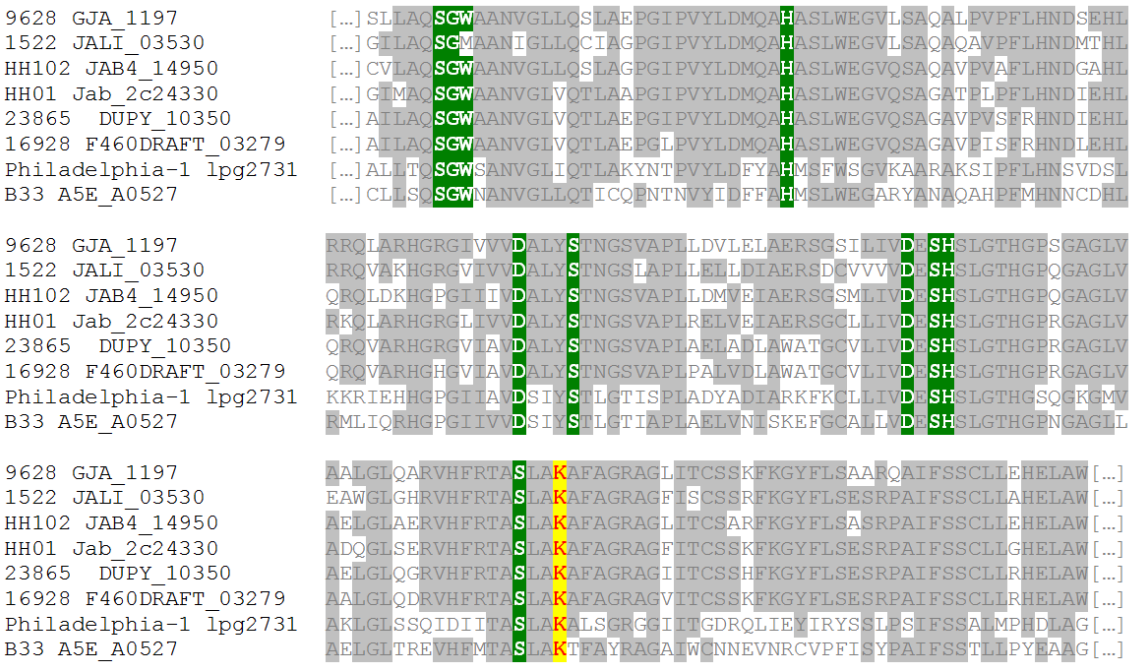

Figure 3.17 **AI synthases ClustalW multiple alignment** of *J. agaricidamnosum* (9628, GJA_1197), *J.* lividum (1522, JALI_03530), HH102 (JAB4_14950), HH01 (Jab_2c24330), *D. phyllosphaerae* (23865, DUPY_10350), *D. zoogloeoides* (16928, F460DRAFT_03279), *L. pneumophila* Philadelphia-1 (lpg2731) and *V. cholerae* B33 (A5E_A0527). Marked in green and written in white are the amino acids essential for binding pyridoxal 5'-phosphate (PLP). Marked in yellow and written in red are the lysines (K) potentially involved in the hydrogen bond between the amino group of the AI synthase and the free aldehyde of PLP, identified for K236 of *V. cholerae* (Spirig *et al.*, 2008). This position is considered as active site. Amino acids present in 50% of the strains were marked bright gray. Numbers in brackets refer to strain numbers and gene locus tags.

Besides the JqsA sequence, the amino acid sequences of the sensorkinases $JqsS_{01}$ (Jab_2c24340) and $JqsS_{102}$ (JAB4_14940) were compared with the ones of the *Duganella* and *Janthinobacterium* type strains as well as the described $CqsS_{Vc}$ (VCA0522) and LqsS (lpg2734) sensorkinases (Figure 3.18). Comparing these sequences the first amino acid important for AHK recognition is a serine at position 107 of $CqsS_{Vc}$. At this position two tryptophan amino acids were identified in $JqsS_{01}$ (W116) and $JqsS_{102}$ (W160), respectively. To determine the length of the hydrophobic acyl chain and the polar head group, three phenylalanines (F160, F162, F166) and one cysteine (C170) are necessary in $CqsS_{Vc}$ of *V. cholerae* (Tiaden & Hilbi, 2012). This motif altered in $JqsS_{01}$ and $JqsS_{102.}$ Histidine and valine replaced two of the phenylalanines of the $CqsS_{Vc}$ sensorkinase, leading to H171/F173/V177 ($JqsS_{01}$) and H215/F217/V212 ($JqsS_{102}$). Additionally, the cysteine C170 was replaced by an alanine (A181, $JqsS_{01}$) or a valine (V225, $JqsS_{102}$).

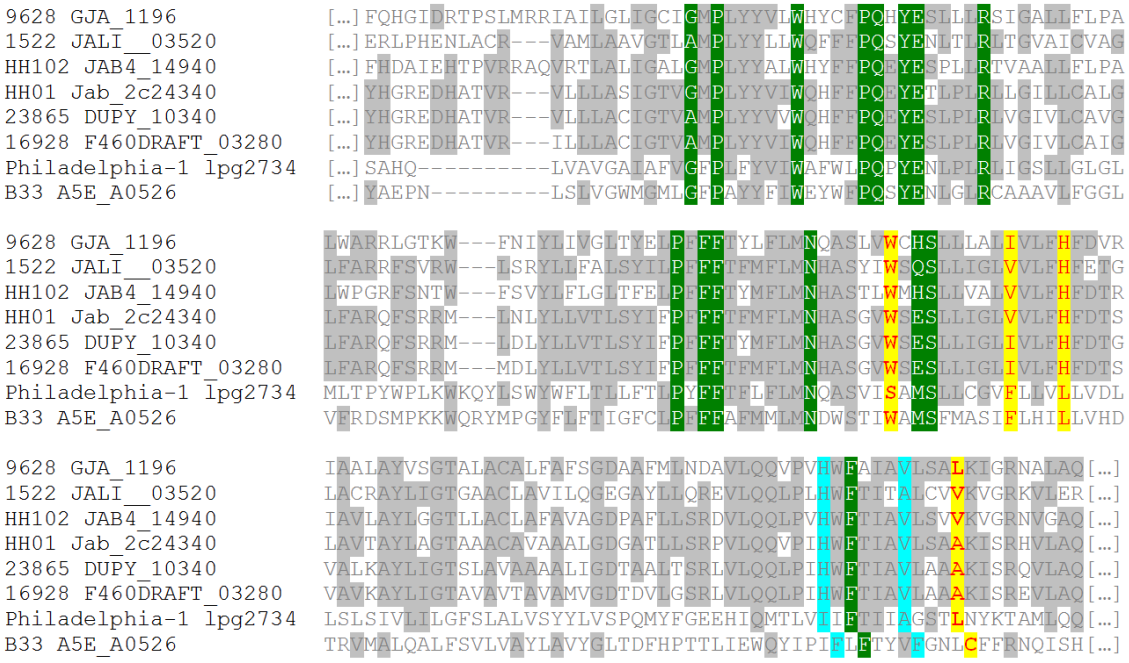

Figure 3.18 **ClustalW multiple sensorkinase alignment** of *J. agaricidamnosum* (9628, GJA_1196), *J. lividum* (1522, JALI_03520), HH102 (JAB4_14940), HH01 (Jab_2c24340), *D. phyllosphaerae* (23865, DUPY_10340), *D. zoogloeoides* (16928, F460DRAFT_03280), *L. pneumophila* Philadelphia-1 (lpg2734) and *V. cholerae* B33 CqsS (A5E_A0526). Shown are the amino acids essential for AHK binding and signal transduction (green highlighted), for recognition of the hydroxyl or amino group at the C_3 (marked yellow written in red) and essential amino acids for recognition of the acyl tail length are marked in bright blue. Amino acids present in 50% of the strains were marked bright gray. Numbers in brackets refer to strain numbers and gene locus tags.

Accompanying this study, Katrin Petersen overexpressed during her master thesis the recombinant AI synthase JqsA of strain HH01 in *E. coli*. This appoach was executed to determine the structure of the JAI-1 molecule of HH01. The purified JqsA protein was used for an *in vitro* enzyme assay to produce artifical JAI-1 molecules with varying acyl chain length. As substrates were myristol-, octanoyl-, dodecyl or decanoyl-CoA and (S)-2-aminobutyrate (SAB) used to synthesize artifical JAI-1 with the acyl chain length of C11, C13, C15 and C17. These artifical JAI-1 should have been used for downstream identification of JAI-1. However, even though JqsA was successfully overexpressed and purified, it was not possible to detect artifical JAI-1 molecules with varying acyl tail length. Further work will be done to identify the molecule and one approach would be the repetition using another substrate as SAB.

3.5 RNA-seq analyses reveal the regulation of nine distinct gene clusters of HH01 and HH102

RNA-seq analyses were performed to determine further effects of the loss of JAI-1 on HH01 and HH102 (2.9). For this purpose, the presence of JAI-1 was monitored with a growth curve, correlating the growth phase with the JAI-1 induced violacein expression. This was measured with a *vio*-promoter fusion (2.6.1, Figure 3.19). RNA-seq analyses were carried out at early stationary phase of the strains HH01, HH01Δ*jqsA*, HH102 and HH102Δ*jqsA* as illustrated in Figure 3.19. This timepoint corresponds to the transition from exponential to stationary growth phase. At this growth phase many of QS-dependent processes are turned on, as shown for *V. cholerae* (Tiaden *et al.*, 2010). Additionally, the effect of JAI-1 on HH01 compared to its gene deletion mutant HH01Δ*jqsA* in late stationary phase (24 h) was investigated in this study.

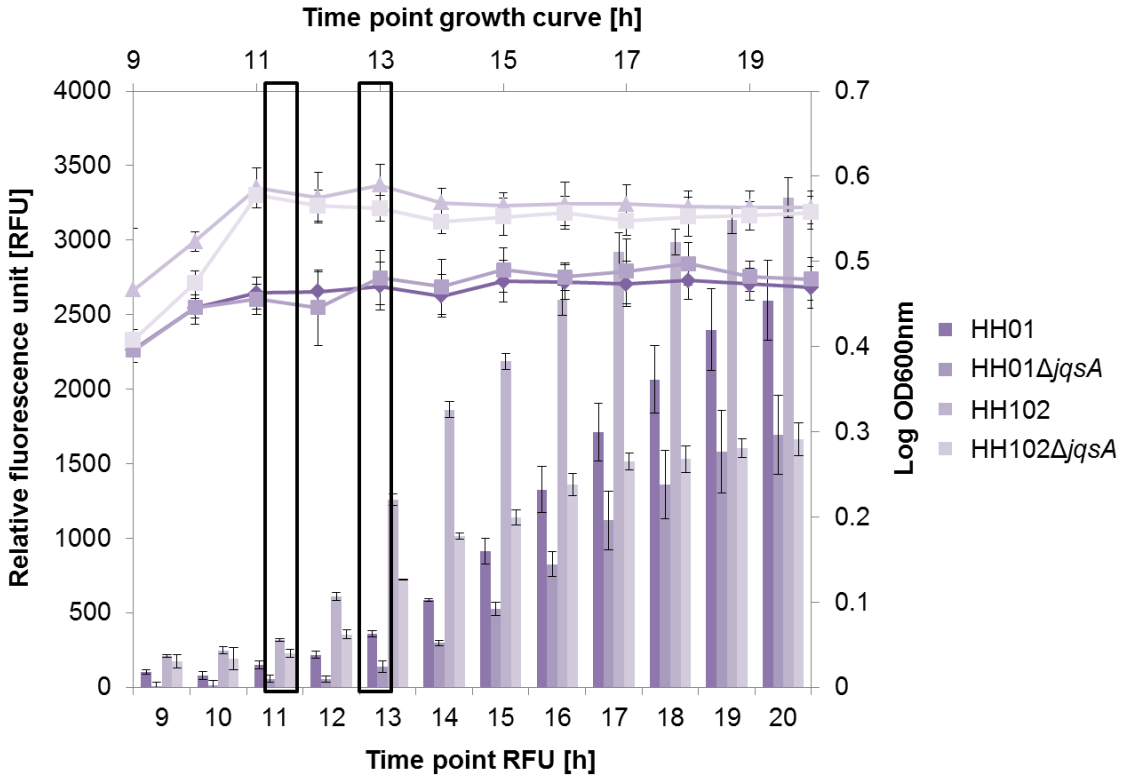

Figure 3.19 **Violacein-promoter controlled mCherry expression** in dependence of growth phase. Selected timepoints of the transciptomic analysis at early stationary phase of the strains HH01, HH01Δ*jqsA*, HH102 and HH102Δ*jqsA* are shown.Timepoints are black boxed.

For the early stationary growth phase RNA-seq analysis, twelve individual samples were analyzed, representing three independent biological samples of the strains HH01, HH01Δ*jqsA*, HH102 and HH102Δ*jqsA* (2.9.2). For each strain a minimum of 19,660,352

reads mapped uniquely after tRNA and rRNA depletion. Data were considered as statistically significant with a log fold-change (FC) of ≥ 2.0, a likelihood value ≥ 0.9 and a FDR-value of ≤ 0.05. Since the RNA-seq data of the third biological replica of strain HH102 (jan4t3) deviate significantly from the other two repilcates jan4t1 and jan4t2, these two samples were averaged and this value was used as third replicate for calculation. Likewise to the early stationary growth phase, three independent biological samples of the strains HH01 and HH01Δ*jqsA* were analyzed to obtain RNA-seq data of the late stationary growth phase of these strains (2.9.1). A minimum of 25,074,703 reads mapped uniquely. This corresponds to at least 39.13% of mRNA. qRT-PCR technique was used to confirm parts the RNA-seq data (2.9.3).

Table 3.8 summarizes significant regulated gene clusters. In early stationary phase, JAI-1_{01} of HH01 alters the gene expression of four distinct gene clusters what corresponds to 31 genes in total 0.52% of all genes present in the genome. The regulation was verified via qRT-PCR for six genes (Table 3.8, Figure 9.1). Additionally, three gene clusters with altogether 14 genes were significantly altered in gene expression when JAI-1_{102} of HH102 was missing. This corresponds to 0.23% of the genes present in this strain. Six genes were verified via qRT-PCR (Table 3.8, Figure 9.2). In late stationary growth phase, four gene clusters were significantly regulated by JAI-1_{01} of HH01. This corresponds to nine genes (0.15% of the genes present in the genome). One regulated gene and the *vioA* gene were verified via qRT-PCR (Figure 9.3, Table 3.8). Whereas in late stationary phase of HH01 the majority of the genes (five) are upregulated and four genes are downregulated, 28 genes are downregulated and only three genes are upregulated by JAI-1_{01} in early stationary phase. JAI-1_{102} of HH102 affects the gene expression by downregulation of all 14 genes. However, despite the violacein operon no genes are regulated by JAI-1 of HH01 and HH102 as well, regardless of the phylogenetic affiliation to the coregenome or the presence in other strains (Table 3.8). Interestingly, the majority of genes are arranged in close proximity, indicating the organisation as operons.

Table 3.8 QS dependent genes of HH01 and HH102, including the log fold change, the phylogenetic classification, the presence of the JAI-1 motif and the verification via qRT-PCR

HH01 late stationary phase					
Locus tag	**predicted function**	**Log fold change**	**Phylogenetic classification**	**JAI-1 motif**	**fold change qRT-PCR**
Iron related gene cluster I					
Jab_2c05340	ferredoxin-NADP reductase	1.48	C	no	
Jab_2c05350	fur family transcriptional regulator, ferric uptake	3.52	II		

Secondary metabolites					
Jab_2c08810	L-tryptophan oxidase, *vioA*	-0.23	I, II, J	yes	-7.27
Jab_2c08820	violacein biosynthesis protein, *vioB*	-0.24			
Jab_2c08830	monooxygenase, *vioC*	-0.31			
Jab_2c08840	tryptophan hydroxylase, *vioD*	-0.01			
Jab_2c08850	violacein biosynthesis protein, *vioE*	0.04			
Jab_2c08860	predicted arabinose efflux permease	-0.38			
Iron related gene cluster II					
Jab_2c17010	DNA-binding transcriptional regulator, LysR family	0.02	C -Marseille - PAMC	no	
Jab_2c17020	hypothetical protein	0.94	I, II		
Jab_2c17030	uncharacterized iron-regulated membrane protein	2.53	II		
Jab_2c17040	inorganic ion transport and metabolism	2.76	I, II		
SDR gene cluster					
Jab_2c26560	aldo/keto reductase	-5.98	unique	yes	
Jab_2c26570	LysR substrate binding domain-containing protein	-6.97			
Jab_2c26580	short-chain dehydrogenase/reductase	-7.35	II		-189.4
Jab_2c26590	transcriptional regulator AraC family	-3.14			
Jab_2c26600	hypothetical protein	-0.86			
Others					
Jab_2c02380	inorganic ion transport and metabolism	3.02	C - Marseille	no	
Jab_2c02390	posttranslational modification, protein turnover, chaperones; SCO1/SenC/PrrC family	2.70	I, II, D, J		
HH01 early stationary phase					
Locus tag	**predicted function**	**Log fold change**	**Phylogenetic classification**	**JAI-1 motif**	**fold change qRT-PCR**
Transport system					
Jab_2c10580	outer membrane protein, *oprM*	-1.71	I, II, J	yes	
Jab_2c10590	HlyD family secretion protein	-2.28			-1.77
Jab_2c10600	ATPase	-1.09			
Jab_2c10610	inner membrane transport permease, *yhhJ*	-2.37			
Lipopolysaccharide synthesis					
Jab_2c07990	lipopolysaccharide biosynthesis protein	-2.14	II, J	yes	-3.92
Jab_2c08000	tyrosine-protein kinase	-2.00			
Jab_2c08010	hypothetical protein	-1.97			
Jab_2c08020	UDP-N-acetylglucosamine 2-	-1.95	I -5059, II -		

	epimerase, *wecB*		105, J		
Jab_2c08030	polysaccharide deacetylase	-2.21	II, J		
Jab_2c08040	hypothetical protein	-2.09			
Jab_2c08050	glycosyl transferase	-1.97			
Jab_2c08060	eight transmembrane protein, *epsH*	-1.94			
Jab_2c08070	glycosyl transferase	-2.42			
Jab_2c08080	asparagine synthetase 1	-1.90	II		
Jab_2c08090	glycosyltransferase	-1.69	II, J		
Jab_2c08100	putative capsular polysaccharide biosynthesis protein	-1.94			
Secondary metabolites					
Jab_2c08810	L-tryptophan oxidase, *vioA*	-2.61	I, II, J	yes	-5.97
Jab_2c08820	violacein biosynthesis protein, *vioB*	-2.41			
Jab_2c08830	monooxygenase, *vioC*	-2.32			
Jab_2c08840	tryptophan hydroxylase, *vioD*	-2.34			
Jab_2c08850	violacein biosynthesis protein, *vioE*	-2.45			
Jab_2c08860	predicted arabinose efflux permease	-2.54			
Jab_2c16610	kynureninase, *kynU*	2.67	I, II - 105	yes	+5.40
Jab_2c16620	tryptophan 2,3-dioxygenase, *kynA*	2.40	I, II - 101		
Jab_2c35330	hypothetical protein	-1.18	unique	n.a.	
Jab_2c35360	polyketide synthase	-2.39			
Jab_2c35370	homoserine O-succinyltransferase, *metA*	-3.68			
Jab_2c35380	non-ribosomal peptide synthetase/amino acid adenylation protein	-3.34			
Jab_2c35390	glycine/serine hydroxymethyltransferase, *glyA*	-3.04			
Jab_2c35400	non-ribosomal peptide synthetase	-3.49			-7.76
Jab_2c35410	non-ribosomal peptide synthetase	-3.68			
Locus tag	**predicted function**	**Log fold change**	**Phylogenetic classification**	**JAI-1 motif**	**fold change qRT-PCR**
SDR gene cluster					
Jab_2c26560	aldo/keto reductase	-7.77	unique	yes	
Jab_2c26570	LysR substrate binding domain-containing protein	-3.58			
Jab_2c26580	short-chain dehydrogenase/reductase	-8.77	II		-353.35
Jab_2c26590	transcriptional regulator AraC family	-3.96			
Jab_2c26600	hypothetical protein	-1.14			

Other					
Jab_1c10070	putative serine/threonine protein kinase	-2.48	II	no	
Jab_1c13730	porin	-2.24	I, II - 104	no	
Jab_1c18190	putative polysaccharide deacetylase	2.30	II	yes	
Jab_1c09990	tetracycline resistance protein	-3.18	I, II - 104	yes	
Jab_2c08460	histidine kinase	-2.17	I, II, D, J	yes	
Jab_2c08470	diguanylat cyclase	-2.21			
Jab_2c19720	TIR domain containing protein	-2.29	C - Marseille	yes	
HH102 early stationary phase					
Locus tag	**predicted function**	**Log fold change**	**Phylogenetic classification**	**JAI-1 motif**	**fold change qRT-PCR**
Type VI secretion system					
JAB4_02740	type VI secretion system protein, *impL*	-3.91	I, II, D, J-1522	yes	
JAB4_02750	type VI secretion system protein, *impM*	-3.29	C -M-Pd		
JAB4_02760	OmpA-OmpF porin	-4.22			
JAB4_02770	type VI secretion system protein, *impK*	-2.53	I, II, D -16928, J	yes	
JAB4_02780	type VI secretion system protein, *impJ*	-2.09	C -M		
JAB4_02790	type VI secretion system protein, *vasD*	-2.12	I, 01, J-9628		
JAB4_02800	hypothetical protein	-3.73	C -M	yes	
JAB4_02810	type VI secretion system protein, *impB*	-3.40	C -M,-9628		
JAB4_02820	type VI secretion system protein, *impC*	-3.64	C -M		
JAB4_02830	type VI secretion system secreted protein, *hcp*	-3.99			
JAB4_02840	type VI secretion system protein, *impF*	-3.44			
JAB4_02850	type VI secretion system protein, *vasG*	-3.44	C -M, J-9628		-13.86
JAB4_02860	type VI secretion system protein, *impA*	-3.35	C -M		
Flp pilus assembly					
JAB4_35690	flp pilus assembly protein, *flp/pilA*	-2.58	I, J	yes	-5.07
JAB4_35700	prepilin peptidase, *cpaA*	-2.50	C -M		
JAB4_35710	hypothetical protein	-3.07			
JAB4_35720	flp pilus assembly protein, *cpaB*	-3.21			
JAB4_35730	flp pilus assembly protein, *cpaC*	-3.01	C -M. -CG23		
JAB4_35740	hypothetical protein	-3.13	I, J		

JAB4_35750	tight adherence protein, *tadG*	-3.02	C -M		
JAB4_35760	tight adherence protein, *tadE*-like	-3.58	I, J		
JAB4_35770	tight adherence protein, *tadE*-like	-3.56	C -M		
JAB4_35780	flp pilus assembly protein, *cpaE*	-3.35	I -5059, II, D, J-1522		
JAB4_35790	flp pilus assembly protein, *cpaF*	-3.60	C		
JAB4_35800	tight adherence protein, *tadB*	-3.49	C -M		-10.53
JAB4_35810	tight adherence protein, *tadC*	-3.37			
JAB4_35820	TPR repeat-containing protein	-3.22	I, J		
Secondary metabolites					
JAB4_20480	inner membrane transport protein YdhP	-1.76	I, II, J	yes	
JAB4_20490	hypothetical protein	-1.70			
JAB4_20500	tryptophan hydroxylase, *vioD*	-1.79			
JAB4_20510	monooxygenase, *vioC*	-1.84			
JAB4_20520	violacein biosynthesis protein, *vioB*	-2.09			
JAB4_20530	L-tryptophan oxidase, *vioA*	-2.22			-6.48
Others					
JAB4_03960	phospholipase	-2.90	I - 5059	no	
JAB4_13490	hypothetical protein	-2.60	I, J	yes	
JAB4_13500	hypothetical protein	-3.22	I, J		
JAB4_16300	PRC-barrel domain protein	-2.67	I, II, J, D	yes	-6.25
JAB4_23200	hemerythrin-like metal-binding domain protein	-2.58	I, II, J-9628	yes	
JAB4_30510	response regulator receiver domain-containing protein	-2.52	I, J-9628	yes	
JAB4_42080	aminoglycoside 3-N-acetyltransferase	-2.89		yes	-3.57
JAB4_42090	hypothetical protein	-3.21			
JAB4_42320	hypothetical protein	-2.81	I, J	no	
JAB4_42330	hypothetical protein	-2.83			
JAB4_54620	soluble aldose sugar dehydrogenase	-3.04	I, J-9628	yes	
Locus tag	**predicted function**	**Log fold change**	**Phylogenetic classification**	**JAI-1 motif**	**fold change qRT-PCR**

We considered genes with a fold-change of ≥ 2.0, a likelihood value ≥ 0.9 and a FDR-value of ≤ 0.05 as statistically significant. Significant regulated genes are written in black, non significant in gray. “Yes” referrs to the presence, “no” to the absence of the JAI-1 motif and n.a. to not available as the promoter lies within a contig border. For phylogenetic classification, isolates are classified according to the OxaI (I) or OxaII (II) affiliation and type strains were abbreviated with J (*Janthinobacterium*) and D (*Duganella*). 9628 refers to *J. agaricidamnosum*, 1522 to *J. lividum*, 23865 to *D. phyllosphaerae*, 16928 to *D. zoogloeoides,* 5059 to *J*. sp. MP5059B, M to *J*. sp. Marseille and PD to *P. violaceinigra*. - indicates the lack of this gene within the genome of the following strain, C refers to the core genome and unique to the unique presence within this strain. Genes verified via qRT-PCR are either down- (-) or upregulated (+). Table was modified from Haack *et al*., 2016.

3.5.1 JAI-1_{01} influences the secondary metabolite and lipopolysaccharide synthesis

As the RNA-seq data gave new insights in the genes regulated by JAI-1 of the OxaII representative HH01, a very diverse group of genes are regulated via QS and with respect to the growth phase observed. Only the highest regulated group, a so called short chain dehydrogenase (SDR) gene cluster, was regulated at both growth conditions (Table 3.8). At late stationary phase it was the only gene cluster repressed by JAI-1. This is not as striking at early growth phase. Considering the phylogenetic affiliation of the reductase and its potential transcriptional regulator gene pair Jab_2c26560 and Jab_2c26570, these genes are unique to HH01. The other potential pair Jab_2c26580 and Jab_2c26590 was only identified in the OxaII strains. No homologues to the OxaI affiliated strains were identified. However, the function of these genes remain unknown.

Most intriguing, JAI-1_{01} induced the synthesis of secondary metabolites in early stationary phase. Besides the secondary metabolite cluster to synthesize violacein (Jab_2c08810 – Jab_2c08860) in all OxaI, OxaII and *Janthinobacterium* type strains, another non-ribosomal peptide synthetases (NRPS) and NRPS-polyketide synthase (PKS) hybrid cluster (Jab_2c35160 – Jab_2c35410) unique to HH01 was partly JAI-1_{01} regulated (Table 3.8). The QS regulated genes included the three NRPS (Jab_2c35380, Jab_2c35400 and Jab_2c35410), one PKS (Jab_2c35360), the homoserine O-succinyltransferase MetA gene (Jab_2c35370) and the glycine/serine hydroxymethyltransferase GlyA (Jab_2c35390). These six genes are potentionally regulated in an operon, indicated by the genomic organization and underlined by the steady and high differentially expression of a log FC of -2.39 to -3.68 (Table 3.8). Interestingly, even though the violacein synthesis of HH01 is evidentially controlled by JAI-1 at late stationary phase and a change of color was observed between HH01 and HH01Δ*jqsA,* the *vioABCDE* operon does not seem to be regulated at transcriptional level only. Nevertheless, verifying this RNA-seq data via qRT-PCR showed a reduction of the expression level of *vioA* (Figure 9.3).

Additionally, five genes of a twelve gene cluster (Jab_2c07990 – Jab_2c08100) necessary to synthesize lipopolysaccharides were significantly regulated by JAI-1_{01} in early stationary phase. This gene cluster is mostly unique to the OxaII and *Janthinobacterium* type strains. No homologous gene cluster were identified for HH102. Moreover, strain HH01 regulates one not otherwise specified transport system via JAI-1. The lack of JAI-1_{01} in early stationary phase decreased the expression of this putative secretion system significantly as shown in Table 3.8. However, nothing is

known on the mode of action or the substrates transported. Even though this gene cluster displayed homologous genes in the OxaI strains, this gene cluster was not JAI-1_{102} QS controlled in HH102 under tested conditions. Besides the mentioned genes and gene clusters regulated in early stationary phase by HH01 derived JAI-1, two gene clusters were regulated in late stationary phase regarding iron. This included a fur family transcriptional regulator (Jab_2c05350), the iron-regulated membrane protein (Jab_2c17030) and a protein involved in inorganic ion transport and metabolism (Jab_2c17040). These genes were upregulated when JAI-1 is missing. However, no uniform phylogenetic distribution was distinguishable and the functions of these genes remain unknown.

3.5.2 JAI-1_{102} affects the secondary metabolite synthesis, type VI secretion system and flp pilus assembly

Investigating the influence of JAI-1_{102} on the gene expression on the OxaI representative HH102, the involvement of JAI-1 on the violacein expression was verified at transcriptomic level (Table 3.8). But more intriguing was the observation that JAI-1_{102} affects the expression of type VI secretion system (T6SS) related genes (JAB4_02740 – JAB4_02860), mainly affiliated with the coregenome of the investigated strains (Table 3.8). Three genes out of the 13 gene cluster were statistically and significantly regulated by JAI-1. The remaining genes were non-statistically significant but regulated as well. However, due to the affiliation of the genes to this gene cluster it is most likely that this whole gene cluster is altered in its expression by QS. Interestingly, even though the first T6SS cluster JAB4_02740 – JAB4_02860 of HH102 shows homologies to the T6SS Jab_2c19030 – Jab_2c19150 of the OxaII representative HH01, no influence of the QS molecule JAI-1_{01} on the gene expression was measured, indicating a constitutive expression of the T6SS of the strain HH01.

In contrast to the type IV secretion system (T4SS), which shares two genes with the T6SS (*icmF* and *dotU)*, all other genes are mostly unique to the T6SS of each bacteria (Filloux *et al.*, 2008). In general, the T6SS consists of about 12 – 25 genes and can be found in multiple complete and incomplete T6SS loci, which cooperate with each other. Six functions and genes could be identified as hallmarks for T6SS. For example DotU, a transmembrane protein with or without a C-terminal OmpA porine extension and what interacts with the second hallmark transmembrane domain containing protein IcmF. Moreover, the two T6SS components and potential effector proteins Hcp and VgrG, the T6SS motor ClpV, an ATPase potentially necessary to fold/unfold T6SS components or effectors, and Lip, a putative outer-membrane lipoprotein could be identified (Filloux *et al.*, 2008). In HH102, two gene clusters were identified for T6SS expression, encoding

for all six hallmark proteins. The two T6SS associated gene clusters are JAB4_02740 – JAB4_02860 and JAB4_06710 – JAB4_06770 (Table 3.9). Whereas the first T6SS cluster seems to be characteristic for these investigated strains of the *Oxalobacteraceae* family, the second T6SS cluster is more affiliated with the OxaI strains (Table 3.9).

Table 3.9 Genes involved in type VI secretion

Name	Locus tag	KEGG number	log fold change	Phylogenetic classification
IcmF	JAB4_02740	KO:K11891	-3.91	OxaI, OxaII, D, J-1522
ImpM	JAB4_02750	KO:K11890	-3.29	core -M-Pd
	JAB4_02760		-4.22	core -M-Pd
DotU	JAB4_02770	KO:K11892	-2.53	OxaI, OxaII, D-16928, J
ImpJ	JAB4_02780	KO:K11893	-2.09	Core -M
Lip	JAB4_02790	KO:K11906	-2.12	OxaI, 01, J-9628
	JAB4_02800		-3.73	Core -M
ImpB	JAB4_02810	KO:K11901	-3.40	Core -M,-9628
ImpC	**JAB4_02820**	**KO:K11900**	**-3.64**	**Core -M**
Hcp	JAB4_02830	KO:K11903	-3.99	Core -M
ImpF	**JAB4_02840**	**KO:K11897**	**-3.44**	**Core -M**
ClpV	**JAB4_02850**	**KO:K11907**	**-3.44**	**Core -M, J-9628**
ImpA	JAB4_02860	KO:K11902	-3.35	Core -M
VgrG	JAB4_06720	KO:K11904	-1.41	OxaI, J
	JAB4_06730		-2.13	OxaI, J
ImpH	JAB4_06740	KO:K11895	-1.14	OxaI, J-9628
ImpG	JAB4_06750	KO:K11896	-2.26	OxaI, OxaII, J
ImpJ	JAB4_06760	KO:K11893	-2.73	OxaI, J -9628
PpkA	JAB4_00290	EC:2.7.11.1	0.15	OxaI, OxaII -HH105, D-23865, J
	JAB4_30930		-0.195	OxaI, OxaII, D, J-9628
	JAB4_57910		0.0271	OxaI -HH106, -HH107, OxaII -HH101, D, J
PppA	JAB4_54850	EC:3.1.3.16	-0.042	HH100, HH102, HH103
	JAB4_56450		0.1989	Core -M
σ54	JAB4_40520	KO:K03092	-0.047	Core

Shown are the corresponding protein names, the gene loci, KEGG or EC enzyme numbers, the log fold change of the RNA-seq analysis at early stationary phase and the phylogenetic distribution of these genes. Significant regulated genes are written in bold. Genes with a log FC of ≥ 2.0, a likelihood value ≥ 0.9 and a FDR-value of ≤ 0.05 were considered as statistically significant. For phylogenetic classification, strains were abbreviated, with “J” referring to *Janthinobacterium* type strains and “D” to *Duganella* type strains. Numbers according to strain abbreviations, “M” to Marseille and “Pd” to *Pseudoduganella* (2.7.3). Strains were classified as OxaI and OxaII affiliated. “-“ indicates the lack of this gene in these strains.

Considering the genes, five of the six hallmark proteins are encoded in the first T6SS cluster, with JAB4_02740 encoding DotU, JAB4_02740 for IcmF, JAB4_02830 for Hcp, JAB4_02850 for ClpV and JAB4_02790 for Lip. Additionally, JAB4_02750, JAB4_02780, JAB4_02810, JAB4_02820, JAB4_02840 and JAB4_02860 showed homologies to the genes *impM*, *impJ*, *impB*, *impC*, *impF* and *impA* of the Imp system of *R. leguminosarum*, with unknown functions (Filloux *et al.*, 2008). The majority of the genes of this gene cluster belonged to the coregenome of the *Oxalobacteraceae* strains investigated, excluding Marseille (Table 3.9) and were not organized in genomic islands. Interestingly, the expression of the genes was reduced by 2-4-fold, when JAI-1 was missing (Table 3.9). However, even though *clpV*, *impC* and *impF* were reduced significantly by a FDR value ≤ 0.05 and a likelihood of ≥ 0.9 (data not shown), this T6SS cluster was most likely regulated in a QS dependent way. The second T6SS cluster, JAB4_06710 - JAB4_06770, comprises of the hallmark protein VgrG (JAB4_06720), the *impJ* homologue JAB4_06760, the two T6SS genes JAB4_06740 and JAB4_06760 and the two flanking hypothetical proteins JAB4_06710 and JAB4_06730. Nonetheless, all genes were not regulated significantly, with a reduced expression by 1.1-2.7-fold (Table 3.9).

Moreover, the RNA-seq data of the strain HH102 displayed the regulation of a flp pilus assembly cluster by JAI-1_{102}. Flp pili belong to the class of the broad distributed type IV pili (T4P) with the major subjunit type IV pilin. The tight adherence pili (Tad) as the flp pili are called as well, were first identified in *Aggregatibacter (Actinobacillus) actinomycetemcomitans* and belong to the T4b subgroup (Giltner *et al.*, 2012). The function of T4P varies and includes motility, attachment, acquisition of DNA and even an involvement in the virulence of *Pectobacterium atrosepticum* and *P. wasabiae* on potato tubers was shown recently (Nykyri *et al.*, 2013). The flp pili cluster of HH102 comprised 14 genes, with all genes regulated, but only three genes statistically significant. Nevertheless, due to the chromosomal arrangement in a gene cluster, it is most likely that this whole gene cluster was regulated by JAI-1_{102}. Interestingly, even though these genes were present in the coregenome (excluding Marseille) of all 31 genes belonging to the *Oxalobacteraceae* family and investigated in this study, the homologous genes in HH01 were not regulated by JAI-1_{01} under tested conditions (Table 3.8).

3.5.3 JAI-1 regulated genes harbor a conserved nucleotide motif

Comparing the 5’ regions of the JAI-1 regulated genes of the strains HH01 and HH102 with each other, a conserved palindromic sequence in almost all of the QS dependent genes and operons were found (Table 3.8). This conserved TTGA$_{N6/7}$TCAA sequence

was identified 243 bp upstream of the *vioA* translational start site. Altering sequences could be identified in almost all QS regulated genes of the strains HH01 and HH102 received by RNA-seq analysis (Table 3.10).

Table 3.10 JAI-1 motif and log fold change of regulated genes in HH01 and HH102

Locus tag	predicted function	JAI-1 motif in 5' gene region	Log fold change
HH01			
Jab_1c09990	tetracycline resistance protein	**TTGA** ACACGG **TCAT**	-3.18
Jab_1c18190	polysaccharide deacetylase	**CTGA** AACGCA **TCAA**	2.3
Jab_2c07990	lipopolysaccharide biosynthesis protein	**TTGA** TCTGTC **TCAA**	-2.14
Jab_2c08810	L-tryptophan oxidase *vioA*	**TTGA** CATTTA **TCAA**	-2.61
Jab_2c08460	histidine kinase	**TTGA** TATTCC **ACAA**	-2.17
Jab_2c10580	outer membrane protein *oprM*	**TTTG** ATCTACA **TCAA**	-1.71
Jab_2c16610	kynureninase	**TTGA** AAAAAA **TCGA**	2.67
Jab_2c19720	TIR domain-containing protein	**TTGA** CATCGA **TCAC**	-2.29
Jab_2c26560	helix-turn-helix domain-containing protein	**TTGA** CCAGCACA **TCAA**	-7.77
HH102			
JAB4_02740	intracellular multiplication and human macrophage-killing	**TTGC** GCAGCG **TCAA** **TTGT** CGTATG **TCAA**	-3.91
JAB4_02770	hypothetical protein	**TTGA** GATTAA **TCAG**	-2.53
JAB4_02800	hypothetical protein	**CTGA** TTAATC **TCAA**	-3.73
JAB4_13500	hypothetical protein	**TTGA** TACCAA **TCAA**	-3.22
JAB4_16300	PRC-barrel domain protein	**TTGA** GGCAGA **TCAA**	-2.67
JAB4_23200	bacteriohemerythrin	**TTGA** TCCAGA **TCAT**	-2.58
JAB4_35690	flp/fap pilin component	**TTGT** GGCGCG **TCAA**	-2.58
JAB4_42090	hypothetical protein	**TTGC** GGTAAG **TCAA**	-3.21

Regulation refers to the fold change of the mutant strains compared to the wild types HH01 and HH102 (Table 3.8). Non-statistical significant genes are written in gray. Table was modified from Haack *et al.,* 2016.

Investigating the predicted promoter sequences of the genes *chiA*, a GH18 chitinase, *vioA* of the violacein operon and the AI synthase gene *jqsA* of the 14 *Oxalobacteraceae* strains sequenced and analyzed in this study, the JAI-1 motif could be identified in all of these strains (Table 9.8). However, since the sequences varyed slightly from each other within the conserved eight basepairs, a logo was created using all of the 28 sequences, which not extend 14 bp (Figure 3.10, http://skylign.org/, Wheeler *et al.*, 2014). Considering the JAI-1 motifs identified in this study, the position

in the 5’ region differed from 80 to 339 bp upstream of the translational start codon ATG.

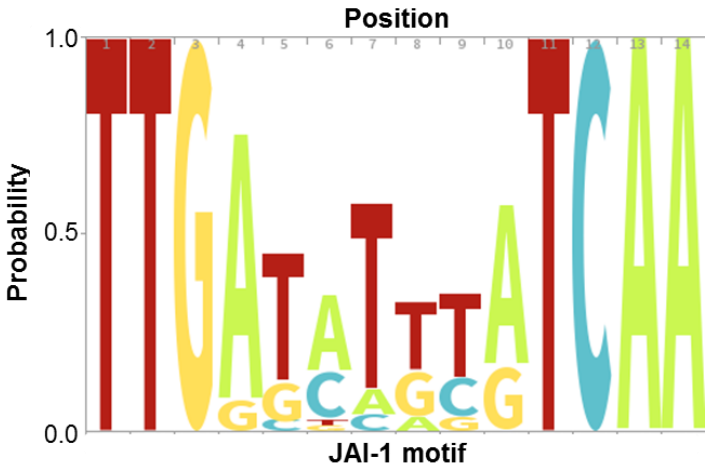

Figure 3.20 **Conserved JAI-1 motif** predicted by sequence analysis of 5’ upstream regions. Data analysis included the promoter regions of the genes *chiA*, *jqsA* and *vioA* (Table 9.8). The logo was created with http://skylign.org/ (Wheeler et al., 2014), excluding sequences extending 14 bp. Figure extracted from Haack *et al*., 2016.

To identify the importance of this conserved JAI-1 motif on the violacein expression, promoter fusion studies were performed within this study (2.10). Therefore, a 280 bp 5’ fragment of the *vioA* gene of the strain HH107 was fused to a mCherry fluorescence reporter gene on a self replicable plasmid. Additionally, the 49 bp truncated 5’ region, which eliminated the JAI-1 motif was fused to a mCherry as well (Figure 9.4). The influence of JAI-1 synthesized by HH01 or HH102 on the mCherry controlled by the *vioABCDE* promoter is impressively shown in Figure 3.21. Both OxaI and OxaII representatives expressed the mCherry fluorescence reporter protein when the JAI-1 motif was present and regardless of the presence or lack of JAI-1. Interestingly, the fluorescence was reduced by 34.7% (HH01) and 49.3% (HH102), when *jqsA* was deleted. The lack of a complete reduction of the violacein synthesis can be explained by abiotic and biotic influences on the violacein synthesis, e.g. the pH, ampicillin, glycerol and glucose (Balibar & Walsh, 2006, Ahmad *et al.*, 2012). Moreover, the deletion of the 49 bp fragment including the $TTGA_{N6/7}TCAA$ JAI-1 motif resulted in a 75 – 90% reduction of promoter activity (Figure 3.21). As this indicated a regulatory role of this conserved sequence on the JAI-1 dependent gene expression, this sequence was designated JAI-1 motif.

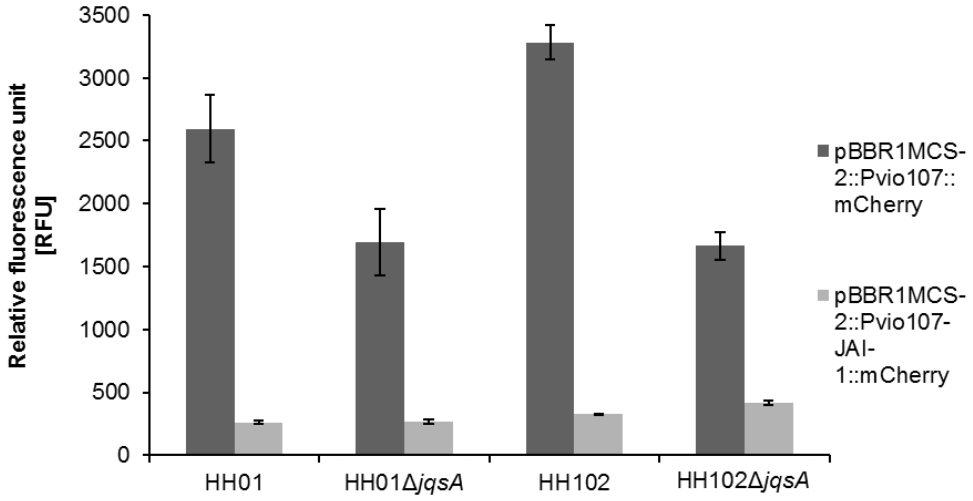

Figure 3.21 **Influence of the conserved JAI-1 motif on the violacein expression in dependency on JAI-1**, investigated using the *vioA*::mCherry promoter fusion. The RFU of the strains HH01, HH01Δ*jqsA,* HH102 and HH102Δ*jqsA* were determined by measuring the fluorescence at 587/610 nm per OD_{600nm} = 1. For pBBR1MCS-2::Pvio107-JAI-1::mCherry (bright gray) the JAI-1 bp was exluded from pBBR1MCS-2::Pvio107::mCherry (gray). Cells were grown at 22 °C for 24 h in R2A Mean values of a minimum of three independent experiments are shown. Standard deviations are indicated by bars. Figure extracted from Haack *et al*., 2016.

3.6 Chitin degradation products interfere with conserved JAI-1 signaling motif

As shown by RNA-seq analysis various distinct gene clusters linked to bacterial pathogenicity are present and were QS controlled in strains HH01 and HH102. This included the synthesis of the secondary metabolite violacein and a yet unidentified secondary metabolite, the T6SS as well as genes involved in the assembly of the flp pilus (3.5.1, 3.5.2). Even a JAI-1 motif present in the 5' region of influenced genes was identified (3.5.3). Additionally, it could be shown in this study that JAI-1_{102} influenced the proteolytic activity of strain HH102 as well as the attachment to shrimp shell chitin and its utilization as sole energy source (3.4.2). Considering the chitinoclastic pathway used by these two bacteria, the chitinases present in the genomes of the two strains were analyzed regarding to the presence of a JAI-1 motif. Indeed, the 5' region of the endochitinase *chiA* (Jab_2c26490) contained the JAI-1 motif (Table 9.8). Interestingly, this gene was not significantly regulated considering the RNA-seq approaches. However, it is a well described phenomenon that the expression of chitinases is induced by chitin degradation products (Beier & Bertilsson, 2013). For this reason, a *chiA*-mCherry promoter fusion was constructed (2.10) and the induction potential of chitin degradation products (N-acetyl-D-glucosamine, NADG and D-glucosamine, DG) and glucose (G) on the promoter fusion was tested (Figure 3.22). This test

demonstrates that G has an inhibitory effect and the chitinase expression. Omitting G, the RFU of the strains is induced by twice. Therefore, further tests were performed with R2A -G as described in respective parts of this work. The concentration of 10 mM NADG had no significant influence on the *chiA* expression as well as DG on the expression of the HH01 derived *chiA* promoter in the strains HH01, HH01Δ*jqsA* or HH102Δ*jqsA*. In contrast, 10 mM DG induced the *chiA* expression in strain HH102. Hence a fold change of HH102 vs. HH102Δ*jqsA* of 2-fold was detected. Calculating the p-value in an unpaired t-test this result is statistically significant (Figure 3.22, bright gray bars).

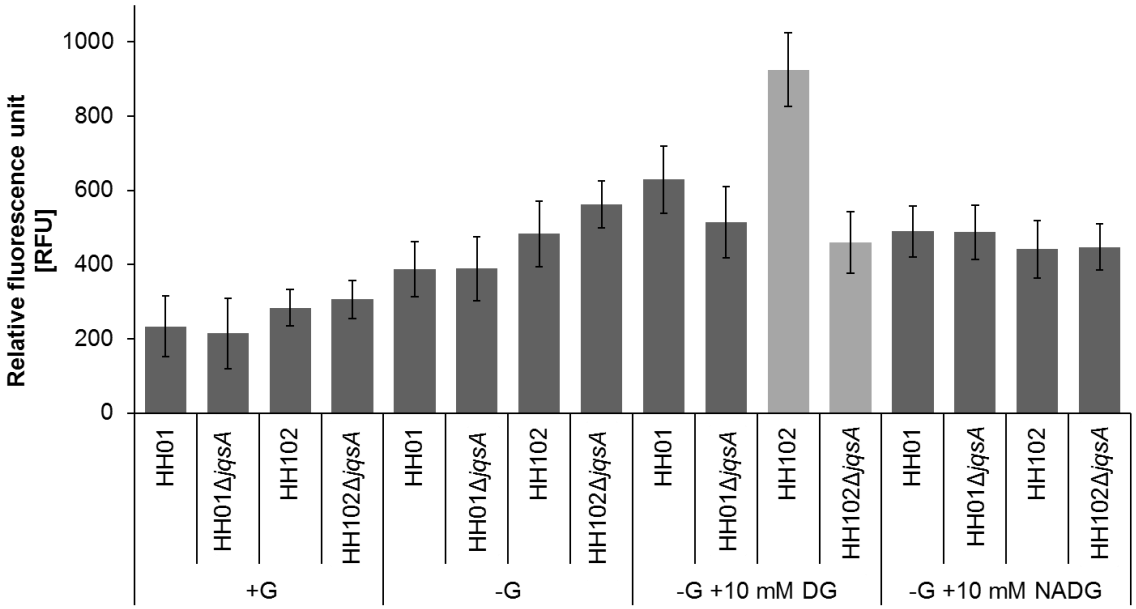

Figure 3.22 **Induction of the *chiA* promoter expression by the chitin degradation products NADG, DG and G.** The HH01, HH01Δ*jqsA,* HH102 and HH102Δ*jqsA* bacterial cells were incubated in R2A with 0.05% G, without G and with the supplementation of 10 mM DG or 10 mM NADG for 24 h at 22 °C. The RFUs of the strains were determined by measuring the fluorescence at 587/610 nm per OD_{600nm} = 1. Mean values of a minimum of three independent experiments are shown. Standard deviations are indicated by bars. The statistical significance of the bright gray bars was calculated with an unpaired t-test.The two-tailed p-value is less than 0.0001, making this change statistically significant.

To conclude Figure 3.22, this test explained why no JAI-1 effect was determined in the RNA-seq studies (2.9) and despite the presence of the JAI-1 motif (Table 9.8). On the one hand the *chiA* expression was partly reduced by G and on the other induced by DG. Under this condition, lacking G and supplemented with DG, a first connection of the chitin metabolic cycle and the lack or presence of HH102 derived JAI-1 was indicated. The influence of chitin was as well observed during the phenotypic characterization of the HH102Δ*jqsA* gene deletion mutant described in 3.4.2.

To test if chitin degradation products and JAI-1 somehow interfere, the influence of DG and NADG compared to the fluorescence of the cells grown in R2A –G was analyzed in this study. Therefore, the *vioA*-promoter fusion with and without the JAI-1 motif was used (2.10, Figure 3.23).

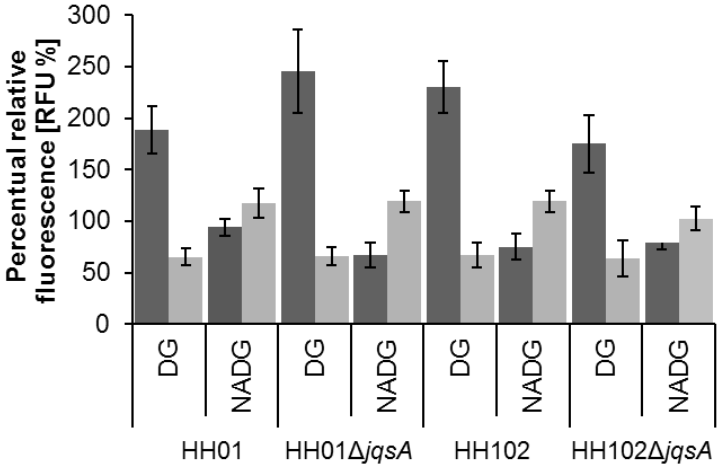

Figure 3.23 **Percentual influence of 10 mM DG and 10 mM NADG** on the pBBR1MCS-2::PvioHH107::mCherry (dark gray) and pBBR1MCS-2::PvioHH107-JAI::mCherry (bright gray) controlled mCherry expression of the strains HH01, HH01Δ*jqsA*, HH102 and HH102Δ*jqsA.* Cells were grown in R2A -G and with supplements for 24 hours at 22 °C. The RFUs of the strains were determined after incubation for 20 h at 22 °C by measuring the fluorescence at 587/610 nm per OD_{600nm} = 1. The RFU of the R2A -G condition was set as 100%. Standard deviations are indicated by bars.

Interestingly, DG induced the expression of HH01, HH01Δ*jqsA*, HH102 and HH102Δ*jqsA* by 89, 164, 130 and 75% (Figure 3.23). Moreover, eliminating the JAI-1 motif the effect was reversed. The mCherry expression was reduced to 65, 66, 67 and 64% of the R2A –G media control, which was set as 100%. Therefore, the chitin degradation product interfered with the JAI-1 motif of the *vioA*-promoter to induce mCherry expression. Next to the involvement of the JAI-1 motif, the JAI-1 molecule might play a role in fluorescence expression as well. The lack of JAI-1 in HH01Δ*jqsA* enhanced the RFU by 57% and reduced the RFU of HH102Δ*jqsA* by 55% compared to the respective wild type strains. Nevertheless, high standard deviations made these changes not statistically significant (as tested via an unpaired t-test), but enabled an indication for the JAI-1 molecule involvement. In case of the supplementation of NADG, the RFU displayed values of 94, 67, 75 and 79% for HH01, HH01Δ*jqsA*, HH102 and HH102Δ*jqsA* (Figure 3.23). The presence of the JAI-1 motif reduced the expression by 33, 25 and 21% for HH01Δ*jqsA*, HH102 and HH102Δ*jqsA*. Only the RFU of HH01 converged to the control of 100%. This indicated an potential involvement of JAI-1_{01} and NADG on the *vioA*-promoter controlled mCherry expression. Eliminating the JAI-1

motif and supplementing NADG, the effect evened out and the RFU displayed values of 117, 119, 120 and 103% for HH01, HH01Δ*jqsA*, HH102 and HH102Δ*jqsA* (Figure 3.23). No statistical significant difference were detected between wild type and mutant strains.

3.7 JAI-1_{102} is important for the growth suppression of the plant pathogen *F. graminearum*

Within this study, I investigated the influence of the presence or lack of JAI-1 of HH01 and HH102 on the growth of the plant pathogen *F. graminearum.* As apparently chitin played a role within the QS circuit, the HH01, HH01Δ*jqsA*, HH102 and HH102Δ*jqsA* strains were pretreated with chitin degradation products prior to the coincubation assay described in 2.11.2. Chitin degradation products were used, as it was shown that the chitinase expression was induced by the chitin degradation product DG (Figure 3.22), that DG influenced the violacein expression dependant on the presence or lack of the JAI-1 motif (Figure 3.23) and with respect to the fact that the fungal cell wall comprises of chitin, which consists of two 180° rotated (1→4)-β-linked NADG molecules.

3.7.1 NADG suppresses effect of JAI-1 on fungal growth

The influence of JAI-1 and chitin degradation products were investigated by performing coincubation studies and comparing the effects of the wild type and respective mutant strains on the fungus. OxaII representative HH01 and its mutant strain HH01Δ*jqsA* did not have a distinct inhibitory effect on *F. graminerarum* when preincubated with or without G or NADG (Figure 3.24 A). Only the preincubation with DG reduced fungal growth significantly. Treating fungal cells with DG resulted in an overall decreased fungal growth and the fungal growth inhibition was enhanced when DG pretreated bacterial cells were added (Figure 9.5). However, no impact of JAI-1_{01} on *F. graminearum* growth was measureable. Next to the influence of HH01 and HH01Δ*jqsA* on *F. graminearum*, the effect of the OxaI representative HH102 and its *jqsA* gene deletion mutant was investigated (Figure 3.24 B). As described for HH01/HH01Δ*jqsA*, the pretreatment with DG resulted in an overall higher fungal growth reduction (Figure 9.5) and the preincubation of the bacterial strains in R2A-G or supplemented with G did not have a significant effect on *F. graminearum.* Under these conditions and preincubated with DG, HH102 and HH102Δ*jqsA* displayed a similar effect on *F. graminearum*, regardless of the presence or lack of JAI-1.

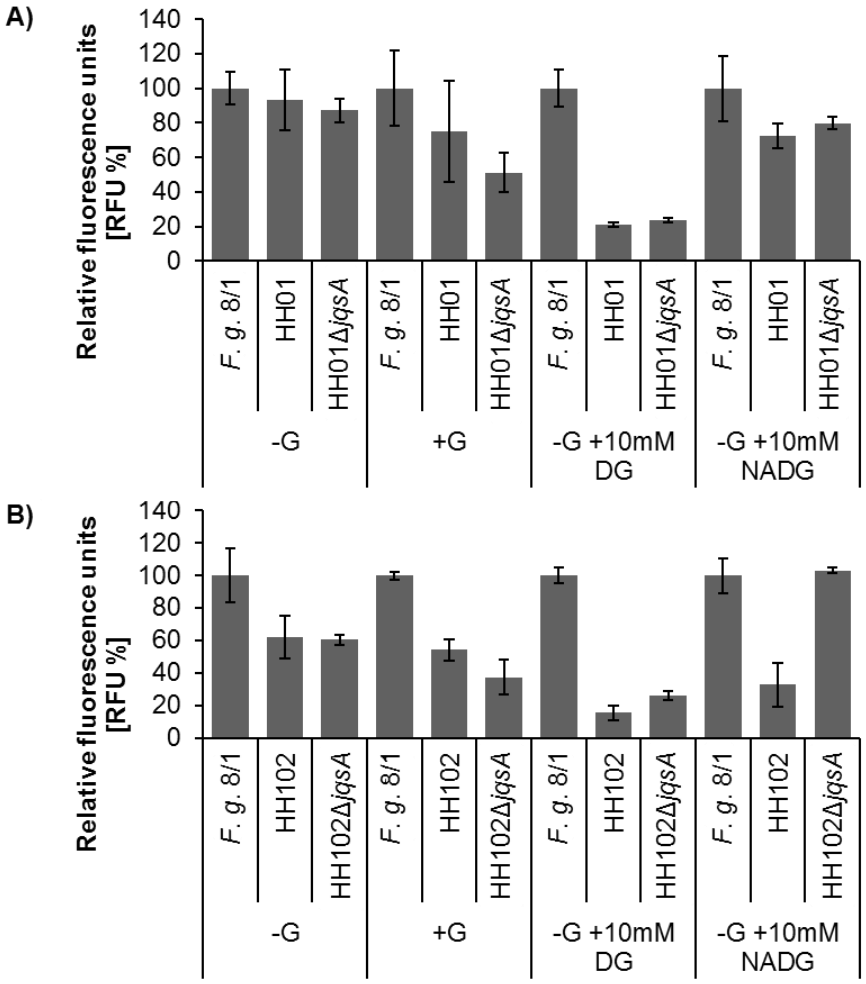

Figure 3.24 **Bacterial inhibition of *F. graminearum* growth.** Strains HH102, HH01, HH102Δ*jqsA* and HH01Δ*jqsA* were grown in R2A -G. Media were supplemented with 0.05% G, 10 mM DG or 10 mM NADG. Bacteria were incubated at 22 °C for 24 h. 180 µl of filtered supernatant (1 x 10^9 cells/ml) and 400 fungal conidia were incubated in a volume of 200 µl for 72 h at 28 °C. Expression of chromosomally integrated GFP in *F. gramineraum* was detected at 485/20; 528/20 nm. Experiments were performed at least thrice in quadruples. One individual experiment is shown. *gfp* expression of *F. graminearum* in different media was double normalized. First, results of coincubated bacteria with fungi were normalized to fungal samples without bacteria in respective media (set as 100%). Second, RFU-values were normalized to *F. graminearum* growth in R2A –G, which was set as 100%. This takes the direct influence of chitin degradation products on fungal growth into account. Figure extracted from Haack *et al*., 2016.

Most intriguing, the fungal growth reduction of HH102 was highly decreased, when *jqsA* was deleted and both stains were pretreated with NADG. Coincubating *F. graminearum* and HH102Δ*jqsA* pretreated with NADG evened the effect observed for HH102 out. The RFU of *F. graminearum* and *F. graminearum* with HH102Δ*jqsA* corresponded. Comparing the effect of HH102 and HH102Δ*jqsA* on *F. graminearum* with each other, the effect on the fungal growth was 2.5 ± 0.3-fold higher in the presence of JAI-1 (strain HH102). Repeating this assay, an overall difference of 3.1 ± 1.6-fold were calculated for strain HH102 compared to its gene deletion mutant

HH102Δ*jqsA* (Table 9.9). Providing HH102Δ*jqsA* with an extrachromosomal copy of the *jqsA* gene on a self replicable pBBR1MCS-2 plasmid resulted in the restorement of the fungal growth reduction, similar to the effect of HH102 on *F. graminearum* (2.11.2, Table 9.10).

3.7.2 Involvement of NADG, the biofilm synthesis and attachment to *F. gramineraum* in growth suppression

To further examine the HH102 – *F. graminearum* and HH102Δ*jqsA* – *F. graminearum* BFI and the influence of NADG and JAI-1 on the effect on fungal growth, these BFIs were microscopically surveyed (2.11.2, Figure 3.29). Prior to this, the influence of NADG on the biofilm synthesis (2.6.2, Figure 3.25) and the attachment of strains HH102 and HH102Δ*jqsA* to the fungus (2.11.2, Figure 3.26) was investigated.

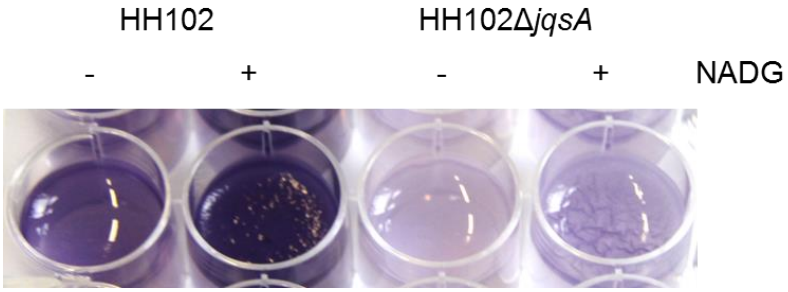

Figure 3.25 **Influence of NADG on the biofilm formation** of strains HH01, HH01Δ*jqsA*, HH102 and HH102Δ*jqsA* incubated for 72 h at 22 °C in R2A –G with 10 mM NADG.

Interestingly, the supplementation of NADG affected the biofilm synthesis of strains HH102 and HH102Δ*jqsA.* Both strains produced thicker biofilms. Coherent with this, the biofilms of HH102 and HH102Δ*jqsA* grown in R2A –G and 10 mM NADG appeared more purple than the controls grown in R2A –G and without NADG. This corresponded well to the thickness of the biofilms.

Moreover, a first test implied that HH102 and HH102Δ*jqsA* attach to fungal hyphae (2.11.2, Figure 3.26). This observation was consistent to results depicted in this work, including the the attachment to chitin (Figure 3.15) and the JAI-1-dependent expression of type IV pili (Table 3.8). Comparing the fungus grown without bacteria and the fungus grown with either HH102 or HH102Δ*jqsA*, the growth of the coincubated fungus was reduced in both BFI. Due to the lack of verifiability, no difference between the degree of fungal growth reduction was detectable for HH102 and HH102Δ*jqsA*. Most intriguing, while the fungal hyphae grew dense and were colored white, the hyphae of *F. graminearum* coincubated with HH102 or HH102Δ*jqsA* were from lighter structure

and appeared purple colored. As HH102 and HH102Δ*jqsA* produce violacein, this result hypothesized an attachment of these bacterial strains to the hyphae of the fungus.

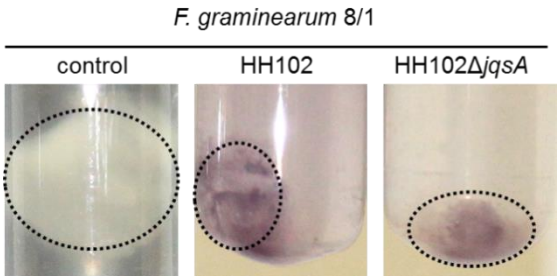

Figure 3.26 **Coincubation of *F.* graminearum 8/1 (control) with strains 1 x 10^5 cells HH102 or HH102Δ*jqsA***. Assay was incubated at 28 °C for 72 h in 5 ml R2A –G with 10 mM NADG. Circles mark the fungal hyphae at the three conditions: without bacteria (control), coincubated with HH102 or HH102Δ*jqsA*.

To learn more about the interaction between HH102 and *F. gramineraum*, the BFI was inspected microscopically (Figure 3.27) regarding the biofilm formation and attachment to the fungal hyphae. Most impressively, the bacterial cells formed biofilms around the fungal hyphae. Moreover, hyphae covered with bacteria were not able to express *gfp* anymore, what might correspond to the reduced fungal growth measured (Figure 3.9).

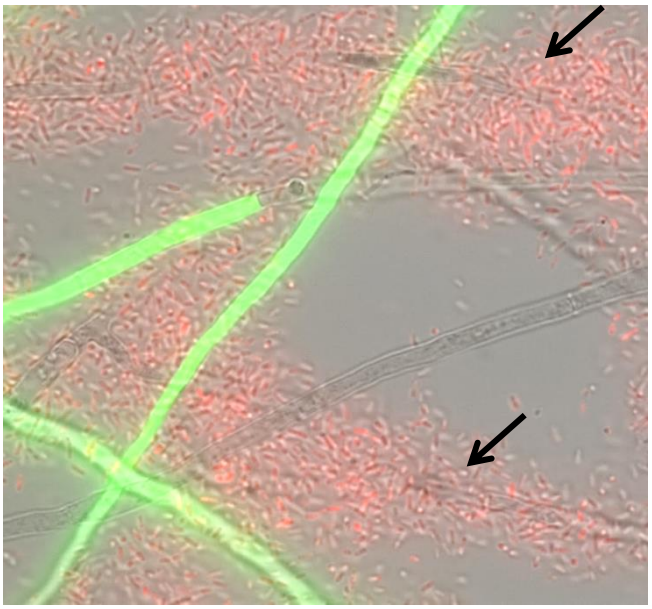

Figure 3.27 **Light-microscopic image of a coincubation assay of strain HH102 and *F. gramineraum*** in R2A –G. Cells were coincubated for 72 h at 28 °C in liquid media. Due to chromosomally integrated *gfp* the fungal cells appear green and HH102 harbor a constitutive expressed mCherry fluorescence protein (red) on a self replicable pBBR1MCS-2 plasmid. Fungal hyphae covered by bacteria (marked by arrows) are not expressing *gfp*.

Surveying the interaction of strains HH102 or HH102Δ*jqsA* pretreated with NADG and *F. graminearum* via SEM techniques, the attachment of these bacterial strains to fungal hyphae was observed as well (Figure 3.28 B-D).

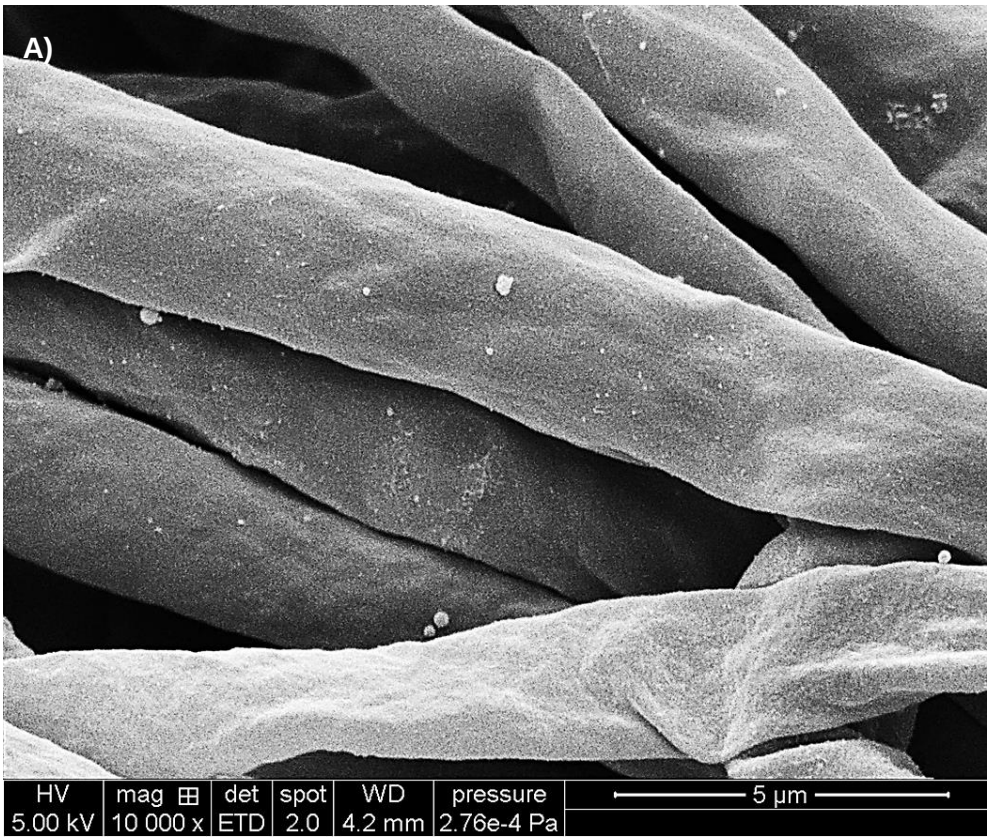
A)
HV
5.00 kV
mag
10 000 x
det
ETD
spot
2.0
WD
4.2 mm
pressure
2.76e-4 Pa
5 µm

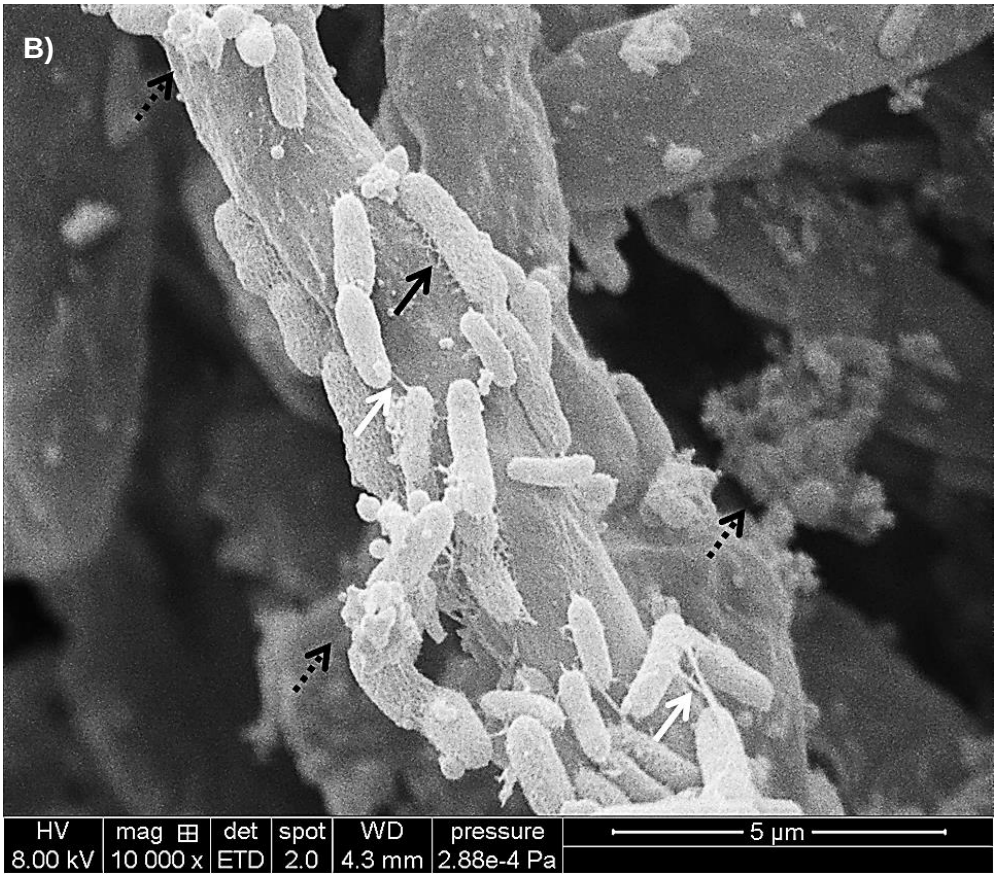
B)
HV
8.00 kV
mag
10 000 x
det
ETD
spot
2.0
WD
4.3 mm
pressure
2.88e-4 Pa
5 µm

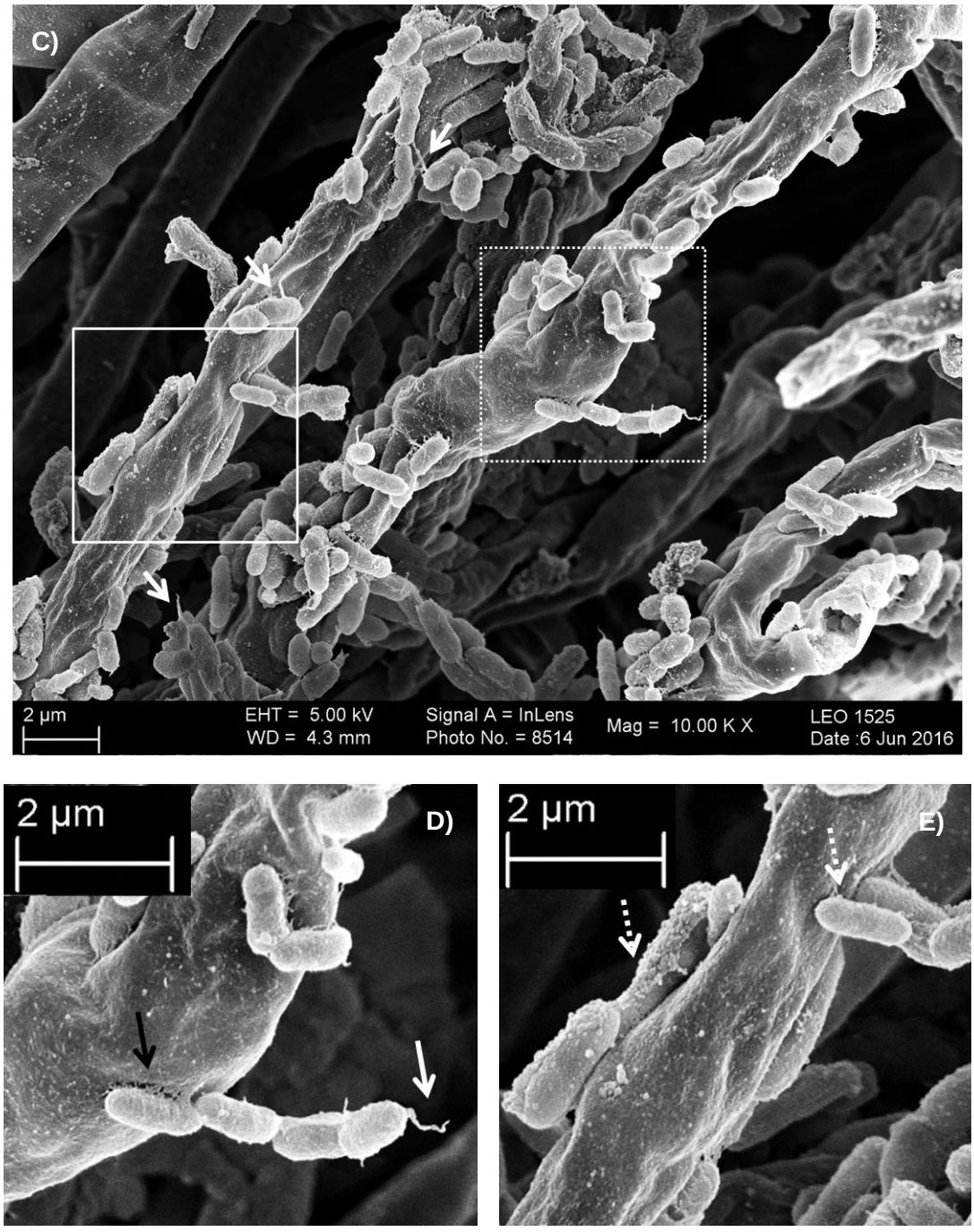

Figure 3.28 **SEM pictures of *F. graminearum* (A) and HH102/HH102Δ*jqsA*-*F. graminearum* BFI (B-E).** Bacterial cells were pretreated with NADG (A, B) or without NADG (C - E) prior to coincubation assay. For this, interaction was incubated for 72 h at 28 °C. Scale bar = 2 µm. A: *F. graminearum* control, B-E: *F. graminarum* BFI (B: HH102, C - E: HH102Δ*jqsA*). White dashed box and white box in **C** was enlarged for figures **D** and **E**. White arrows mark anchor-like structures at cell surfaces, black arrows point at tight attached bacteria to fungal hyphae, black dashed arrows mark potential exopolysaccharides necessary for the attachment and white dashed arrows point to phenotypical heterogenous bacterial cells.

Comparing hyphae coincubated with bacteria with hyphae non-coincubated, the hyphae of the *F. graminearum* control appeared firm with a smooth surface (Figure 3.28 A). In contrast, by the attachment of the bacterial strains HH102 or HH102Δ*jqsA*,

the fungal hyphae seemed to alter the firm structure and many hyphae appeared dent with a rough surface. Anaylsis of a *jqsA* deletion mutant did not reveal a significant difference in the apperance of the hyphae and no significant influence of NADG supplementation was observed so far. Surprinsingly, the bacterial surfaces of the wild type as well as *jqsA* mutant strains displayed phenotypical heterogeneous surface structures (Figure 3.28 E). Some of the cells appeared covered with outer membrane vesicles or other mucus-like structures. However, the composition and function of this cover for the BFI remain unknown and further analysis have to uncover a potential involvement of the JQS system on the occurrence. Further, the bacterial cells seemed to produce exopolysaccharides to attach to fungal hyphae (Figure 3.28, B, D, black arrows) as well as anchor-like structures (Figure 3.28 B-D, white arrows). Using BLASTP analyses of NCBI, genes possibly linked to exopolysaccharides were identified. These included the gene clusters JAB4_27350 – JAB4_27450, JAB4_10550 – JAB4_10580 and JAB4_01250 – JAB4_01280, which showed homologies to the *espA-M* genes of *Streptococcus thermophilus*, *rmlA-D* genes of *Stenotrophomonas maltophilia* and PA3552 – PA3558 genes of *P. aeruginosa* (Stingele *et al.*, 1996, Matsukawa & Greenberg, 2004, Huang *et al.*, 2006). Even though these genes were expressed in the RNA-seq approach comparing HH102 and HH102Δ*jqsA*, no significant effect of JAI-1 on these genes was observed. Interestingly, examining the HH102-*F. graminearum* interaction, this BFI produced undefined structures sourrounding fungal hyphae and bacterial cells. Moreover, HH102 wild type cells appeared to produce more exopolysaccharides necessary for the attachment to fungal cells compared to the strain HH102Δ*jqsA* (Figure 3.28 B, black dashed arrows).

To further investigate this interaction regarding the influence of JAI-1, confocal laser-scanning microscopy was performed (Figure 3.29). First, NADG had no influence on the growth of fungal hyphae when not coincubated with bacteria. The growth of the fungal hyphae remained linear and unidirectional with germination at the conidial poles (first panels of Figure 3.29 A). In contrast, the coincubation with strains HH102 and HH102Δ*jqsA* results in a reduced germination rate of the fungus and the hyphal growth was altered (Figure 3.29 A four lower panels). Instead of the linear growth, coincubated hyphae outgrew lateral and twisted. The germination of the hyphae was not restricted to conidial poles. Second, strain HH102 formed dense biofilms and cell assemblages around fungal hyphae (Figure 3.29 A two middle panels). HH102 covered the hyphae often completely and the pretreatment with NADG enhanced this effect. The positive influence of NADG on the biofilm formation of HH102 and HH102Δ*jqsA* was already shown in preliminary tests (Figure 3.25). However, strain HH102Δ*jqsA* did not form dense biofilms and did not cover the hyphae at the same extend as HH102,

regardless of the NADG supplementation (Figure 3.29 A two lower panels). Most intriguing, coincubating strain HH102 pretreated with NADG and *F. graminearum*, a thight attachment of the bacterial cells to fungal hyphae was observed (Figure 3.29 B, C). This was not observed to this extent for HH102 grown without NADG supplementation or for strain HH102Δ*jqsA* regardless of NADG presence. This observation corresponded well to the effect observed, as JAI-1 influenced the fungal growth significantly (Figure 3.24).

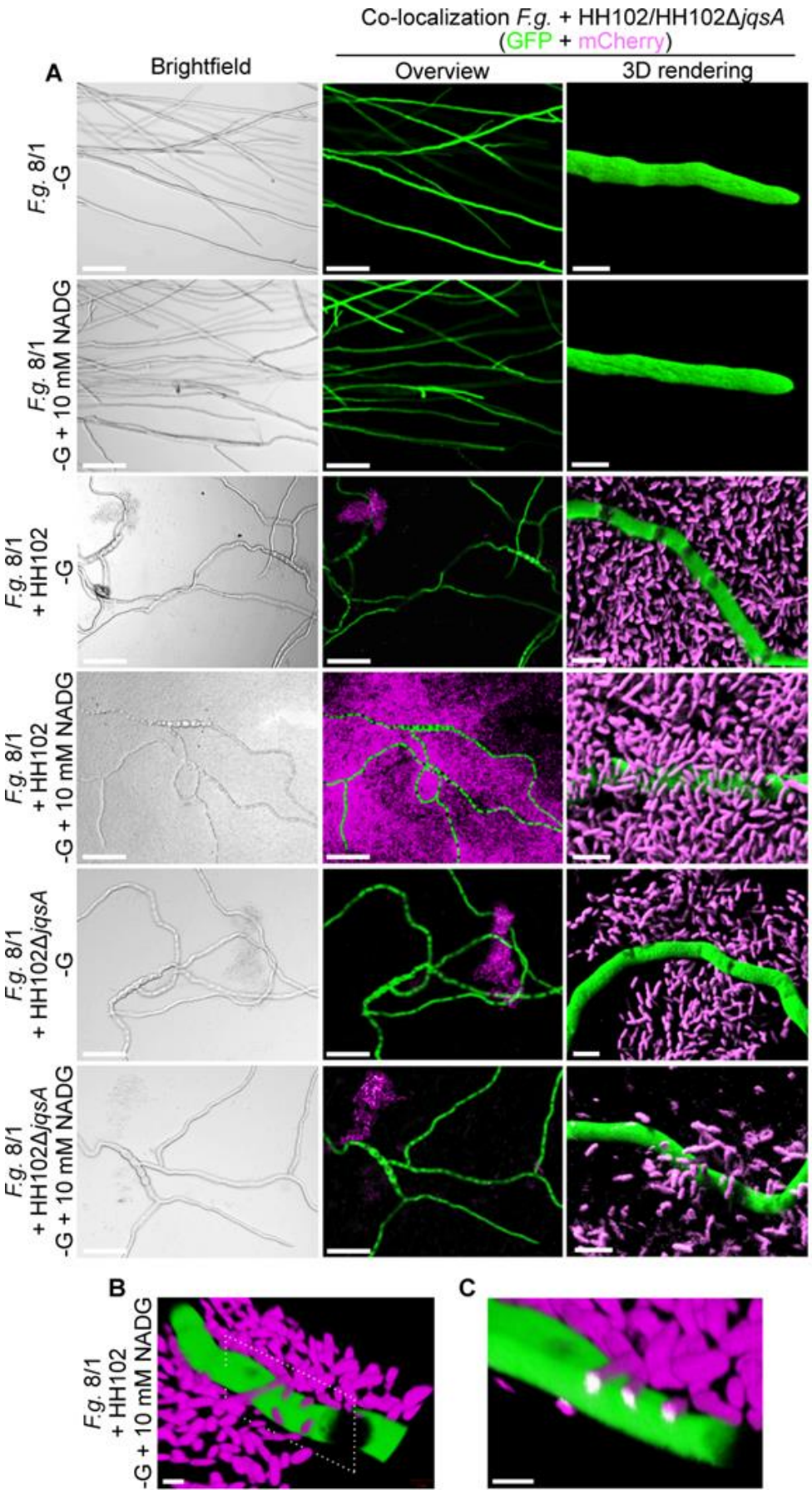

Figure 3.29 **Microscopic images reflecting the HH102 and HH102Δ*jqsA* interaction with *F. graminearum*. A)** Co-localization of mCherry-tagged HH102 or HH102Δ*jqsA* cells and GFP-

tagged *F. graminearum* in co-cultures. Left panels brightfield overview images; middle panels, same section image as on left side panel but using fluorescence detection for GFP (green) and mCherry (magenta); and right panels, 3D rendering of selected regions. Scale bars: overview (left and middle panels) micrographs = 100 µm; 3D-rendered micrographs = 5 µm (right panels). No mCherry-based fluorescence was visible in control cultures without bacteria. **B)** 3D-projection of HH102 cell attachment on *F. graminearum* hyphae in cultures supplemented with NADG. Dotted frame indicates plane of *in silico* cross section in C. Scale bar = 2 µm. **C)** *In silico* cross section at sites of bacterial attachment on *F. graminearum* hyphae. Bacterial interaction was indicated by white color. Scale bar = 2 µm. The HH102 and HH102Δ*jqsA* cells constitutively expressing mCherry were coincubated with *F. graminearum* expressing GFP in 200 µl R2A -G supplemented with or without 10 mM NADG at 22°C for 72 h. Micrographs were taken by confocal laser-scanning microscopy. Figure extracted from Haack *et al*., 2016.

3.7.3 Denaturation of bacterial supernatant leads to reduced fungal growth suppression

To identify possible factors leading to the growth effect in the presence of NADG and JAI-1, which is evened out in HH102Δ*jqsA*, the involvement of proteins was investigated within this study. This was of special interest, since this study indicated an involvement of the protinaceous structures of T4P (Table 3.8) and chitinases/chitin degradation products (3.6, 3.7), both linked to JAI-1. Therefore, the fungal conidia were coincubated with bacterial supernatant of the strains HH102 and HH102Δ*jqsA*. In contrast to previous tests, one part of the supernatant was denatured prior to the usage (2.11.2). Whereas denatured proteins lost their activity, thermostable chemical compounds as the bisindolepyrrolidone alkaloid violacein or the α-hydroxyketone JAI-1_{102} would remain in the active chemical form. When filtered bacterial supernatant was used, strains HH102 and HH102Δ*jqsA* reduced the fungal growth (Table 3.11). The usage of denatured and filtered bacterial supernatant did not effect the fungal growth, as indicated by RFU values comparable to the non-coincubated fungal wild type RFU values.

Table 3.11 RFU values of the inhibition of *F. graminerarum* growth by supernatant and denatured supernatant of HH102 and HH102Δ*jqsA*

	Relative fluorescence unit [RFU] of *F.graminearum*				
	***F. graminearum* control**	**HH102**		**HH102Δ*jqsA***	
Number experiment		**SN**	**SN***	**SN**	**SN***
1	6615 ± 230.6	351 ± 29.4	7617 ± 256.8	820 ± 45.1	7377 ± 240.0
2	6836 ± 417.2	548 ± 99.8	7713 ± 284.7	2280 ± 223.7	7241 ± 1628.4
3	15529 ± 315.3	3507 ± 155.1	14441 ± 2222.5	3822 ± 1639.5	13552 ± 825.3

SN refers to supernatant. *: denatured supernatant.

4 Discussion

4.1 Isolates are affiliated with the genera *Janthinobacterium* and *Duganella*

Within this study, eight purple-pigmented bacteria were isolated from aqueous and soil sources. The strains were affiliated with the genera *Janthinobacterium* and *Duganella* as 16S rRNA analyses revealed (Figure 3.3). Investigating the isolates physiologically, the strains displayed phenotypic characteristics for the genera *Janthinobacterium* and *Duganella* (3.1, 3.2). Therefore, the isolates HH100, HH102, HH103, HH104, HH106, HH107, 5059 were grouped as OxaI cluster with HH102 as selected representative and affiliation to the genus *Janthinobacterium* and isolates HH101, HH105 and HH01 as OxaII cluster with HH01 as representative and the affiliation to the genus *Duganella* (Figure 3.3). Additional analyses of 31 available genomic information *Janthinobacterium*, *Duganella* and *Pseudoduganella* genomes in terms of genome mapping (Figure 3.4), MLSA (Figure 3.5) and ANIm calculation (Figure 3.6), supported this classification. The core- and pangenome of the strains comprised 1,058 core and 23,628 pan genes. Thus, this study analyzed the largest gene pool of *Janthinobacterium*, *Duganella* and *Pseudoduganella* strains.

Comparing the MLSA and ANIm calculation, the *Janthinobacterium* branch consisted of the strains OK676, RA13, KBS0711, Ant5-2, HH104, RIT308, NFR18, 5059, MTR, 1522, HH107, HH106, HH103, HH102 and HH100 (Figure 3.6). Strains HH104, RIT308 and NFR18 formed one subgroup, 5059, MTR and *J. lividum* a second subgroup and HH100, HH102 and HH103 a third subgroup with close relationship to HH106 and HH107. According to these analyses, the classification of the strains HH100, HH102 – HH104, HH106, HH107 and 5059 as OxaI isolates was proven. In addition to the genus *Janthinobacterium*, the OxaII strains HH01, HH101 and HH105 displayed the highest level of synteny to each other (Figure 3.6) with close relationship to *D. phyllosphaerae* and *D. zoogloeoides* as well as the two strains OV458 and CF402 (Figure 3.5). According to these analyses, the classification of HH101, HH105 and HH01 within the OxaII group was verified. Moreover, the affiliation of HH01 to the genus *Duganella* was recommended. HH01 was former classified as *Janthinobacterium* (Hornung *et al.*, 2012). Furthermore, the detailed characterization of 31 *Oxalobacteraceae* affiliated strains underlined the classification of *D. violaceinigra* to *Pseudoduganella violaceinigra*, as previously identified by the low 16S rRNA gene sequence identity to *D. phyllosphaerae* of 96.8% (Kampfer *et al.*, 2012).

In contrast to the high synteny according to 16S rRNA and MLS analyses, the ANIm calculation of the strains clustered CG23_2, Marseille, CG3, B9-8 and the type strain *J. agaricidamnosum* within the *Duganella* branch. With the exception of B9-8, which is not included in the MLS analyses, these strains formed unique branches (CG3 and *J. agaricidamnosum*) or were considered as outgroup (Marseille and CG23_2). Considering the general genomic features of the strain Marseille, this strain diverged significantly from the other members of the family *Oxalobacteraceae*. The deviations included the low genome size of 4.1 Mbp, compared to the average genome size of the isolates of 6.45 Mbp, the low number of coding genes with function prediction of 2,813 compared to 5,467 to 6,535 genes and the low G+C content of 54.23% compared to 62.4 to 65.5% of the isolates (Table 3.2). This outsider role of the strain Marseille was reflected by the pan- and coregenome analysis (3.1.2.2). Whereas the pan- and coregenome of the 31 strains comprised 1,058 core and 23,628 pan genes, the exclusion of Marseille added the coregenome up to 1,669 genes and 22,640 pan genes. In case of CG3 and CG23_2, the discrepancy might be explained by the isolation source, as both organisms were isolated from an Antarctic supraglacial stream (Smith *et al.*, 2013, Smith *et al.*, 2016). Thus, these strains were presumably exposed to various environmental stresses and unfavorable conditions, evoking an adaption of the metabolism. Moreover, extremely high UV B radiation at the Antartica might have led to cell damaging, potentially corresponding to the phylogenetic distribution observed. Additionally, the *Janthinobacterium* type strain *J. agaricidamnosum* displayed a diverse classfication according to MLSA and ANIm as well, illustrating the necessity of interplay of phylogentic methods based on the genome sequence and an extensive phenotypic characterization.

4.2 *Janthinobacterium* and *Duganella* inhibit the growth of the plant pathogen *Fusarium graminearum*

Janthinobacterium, *Duganella* and *Oxalobacteraceae* family members colonize a wide range of ecological niches. These niches include aquatic habitats, as the isolates HH100 - HH107, soil habitats (5059), the Antarctic supraglacial stream (GC3 and CG23_2, Smith *et al.*, 2013, Smith *et al.*, 2016) and the occurrence on leaf surfaces (*D. phyllosphaerae,* Kampfer *et al.*, 2012). But besides the colonization of these habitats, competition for nutrients and space in these niches is of special interest. One mechanism to prevail against invading microorganisms, e. g. fungi, is the expression and secretion of secondary metabolites and hydrolytic enzymes, which allows the

adaption to various ecological niches and therefore opens a wide reservoir of resources. One example for inter-species microbial interactions in soil is the *Oxalobacteraceae* genus *Collimonas*. Bacteria affiliated with this genus have the ability to feed on fungi under nutrient-limited conditions and the involvement of secondary metabolites as terpenes and further (PKS-) NRPS gene cluster products as well as the exoenzymes chitinases or peptidases is suggested (Song *et al.*, 2015).

4.2.1 Effect of secondary metabolites on fungal growth

One mechanism to cope with crowded habitats is the synthesis and secretion of secondary metabolites, which are compounds typically synthesized in the stationary growth phase. These compounds are not necessary for growth, development or reproduction, but beneficial for the adaption to various enviroments. Since most enzymes that convert precursors to secondary metabolites arose by gene duplication and divergence of primary metabolism genes, numerous secondary metabolites are limited to major taxa and occur in varying numbers (Cavaliersmith, 1992). For example, the genus *Streptomyces* of the phylum Actinobacteria harbors 20 – 30 gene clusters for the synthesis of secondary metabolites, which corresponds to 5 – 7% of its genome (Bentley *et al.*, 2002, Ikeda *et al.*, 2003). Moreover, most secondary metabolites are aromatic compounds, isoprenes, oligosaccharides, peptides, polyketides or β-lactam rings. They are produced by bacteria, plants and fungi to provide protection against competitors, predators and parasites. Thus, the synthesis of secondary metabolites benefits their producers as poisons (Cavaliersmith, 1992). For example, the secondary metabolite violacein has anitimicrobial, antiviral, antitumorigenic, antitrypanosomatid, antiulcerogenic, antiprotozoal and anticandida activity (Balibar & Walsh, 2006, Pantanella *et al.*, 2007). Violacein is synthesized via the *vioABCDE* operon, which expresses enzymes that catalyze the condensation of two modified L-trypthophan molecules (Figure 1.1, Balibar & Walsh, 2006). Previous studies linked the synthesis of the purple-pigment violacein to the pathogenicity of specific *Janthinobacterium* species against fungi (Brucker *et al.*, 2008, Ramsey *et al.*, 2015). As the nine isolates were selected by the expression of the purple-pigment violacein, the question arose if these strains interact with fungi and alter fungal growth by the synthesis of secondary metabolites. Therefore, the strains were investigated with regard to the potential to synthesize and secrete secondary metabolites.

The investigated bacteria encoded 1 – 8% secondary metabolite associated genes in their genomes (Table 3.2, Table 9.2). Interestingly, the presence of a high percentage of such genes depended in part on the phylogeny. Whereas HH101, HH105 and HH01 as OxaII strains and *D. zoogloeoides* encoded 4.21, 6.78, 6.14 and 2.33% for genes for

the synthesis of secondary metabolites, only the two *Janthinobacterium* type strains *J. lividum* and *J. agaricidamnosum* encoded 3.59 and 8.1% for genes for the secondary metabolite synthesis. Considering the presence of NRPS and NRPS/PKS hybrids, only the OxaII strains HH01, HH101 and HH105 and the *Janthinobacterium* type strains encoded for these classes of enzymes. With the exception of *D. zoogloeoides*, this observation contributed to the high number of secondary metabolite clusters. In contrast, the OxaI affiliated strains encoded only 1% of their genome for genes to synthesize secondary metabolites. Considering the presence of secondary metabolite gene clusters in the bacterial strains (Table 3.2, Table 9.2), gene clusters for the synthesis of bacteriocins were present in all 14 investigated strains. Bacteriocins are a diverse group of antimicrobial peptides produced by bacteria expressed to inhibit the growth of similar or closely related bacteria (Dobson *et al.*, 2012). Throughout the high diversity and high number of gene clusters potentially encoding for bacteriocins within the investigated strains, no solely bacteriocin affecting fungal growth was identified. Futhermore, all 14 strains encoded a gene cluster potentially involved in the synthesis of a terpene. This class of chemical compound can be produced by all kingdoms of life, suggesting a role for long-distance interkingdom interactions and communication, as assumed for *Collimonas* (Song *et al.*, 2015). Analyzing the strains according to homologues sequences of the epimerase Jab_2c05650 and the Clp protease Jab_2c05890 genes, these genes are present in all strains. This implies the synthesis of an alike terpene by the *Oxalobacteraceae* strains. However, up to date only few reports are available addressing the effect of terpenes of microbial origin on microorganisms (Song *et al.*, 2015) and one can only speculate an involvement of this class of compunds on the BFI observed. Further work has to unravel the involvement of terpenes within *Janthinobacterium/Duganella-F. graminearum* interactions.

Moreover, all strains synthesized either an indole or an aryl-polyene as pigment (Table 3.2 and Table 9.2). The aryl-polyene cluster present in the two *Duganella* strains *D. zoogloeoides* and *D. phyllosphaerae* was linked to the synthesis of a yellow pigment, possibly xanthomonadin (Jenkins & Starr, 1985). Previous studies indicated an important role of the carotenoid-like pigment for protection against photobiological damage (Rajagopal *et al.*, 1997) when synthesized by phytopathogenic *Xanthomonas* bacteria and exposed to toluidine blue and visible light (Poplawsky *et al.*, 2000). The presence of the indole structure was consistend with the presence of the violacein operon and the purple colony color of the investigated strains (Figure 3.1, Table 3.1). Strains HH01, HH100 - HH107, *J. lividum* and 5059 expressed this pigment (3.1.1). Only *J. agaricidamnosum* did not express violacein under tested conditions, even though the *vioABCDE* operon was identified within the genome. This indicated a high

degree of interference of biotic and abiotic factors on the violacein synthesis. The influence of the medium used was most prominent for HH01 and HH105, which synthesized the lowest amounts of violacein on solid R2A or liquid TY (Figure 3.1). In general, a supplementation of ampicilin and glycerol to R2A enhanced the violacein expression (Table 3.1). The media did not have a significant influence on the violacein synthesis of the OxaI isolates. Moreover, the influence of temperature on the amount of synthesized violacein was demonstrated for *J. lividum*. Incubating this strain at 28 °C enhanced the violacein synthesis but incubation at 22 °C prohibited the expression of the violacein operon, independent on the medium used.

Taking these results together, the synthesis of secondary metabolites and pigments seems to be a common feature of the investigated strains affiliated with the family *Oxalobacteracea*. This aspect might contribute to the pronounced ability of the strains to adapt to various environmental conditions and to enforce against invading microorganisms, as typical for members of these two genera. Therefore, these strains were studied with regard to the interaction and effect on the plant pathogenic fungus *F. graminearum*. Most intriguing, strains HH100 – HH107, 5059, HH01 and the type strains *J. agaricidamnosum*, *J. lividum*, *D. phyllosphaerae* and *D. zoogloeoides* reduced the growth of *F. graminearum* when coincubated on solid or in liquid medium (Figure 3.8 and Figure 3.9). This bacterial effect on the fungus was coherent with the presence of various gene clusters encoding bacteriocins and terpenes, suggesting an involvment of these chemical compounds in reducing fungal growth. Moreover and despite the antifungal effect of violacein, the presence of this secondary metabolite was not coherent with the effect on the fungus. Both *D. phyllosphaerae* and *D. zoogloeoides* did not harbor the violacein operon or synthesized this pigment, but reduced fungal growth (Figure 3.8 and Figure 3.9). Additionally, the purple *E. coli* pDrive::*vioABCDE* showed no significant inhibition of the fungus *F. graminearum* (Figure 3.8 and Figure 3.9). Even though it is hypothesized that the antifungal activity of *J. lividum* on the skin of *P. cinereus* as well as against the fungus *T. rubrum* is linked to the biosynthesis of violacein (Brucker *et al.*, 2008, Ramsey *et al.*, 2015), this was not shown for the *Janthinobacterium*/*Duganella*-*F. graminearum* interaction. Therefore, I concluded that violacein was not responsible for the growth suppression of *F. graminearum* by the isolates, the strain HH01 and the *Janthinobacterium* and *Duganella* type strains. Furthermore, comparing the effect of the *Oxalobacteraceae* genus *Collimonas* on fungi with the expression of violacein, an involement of this secondary metabolite was excluded as well (Song *et al.*, 2015). Moreover, testing denaturated bacterial supernatant of strain HH102 on the fungal growth, the effect of growth reduction was lost (Table 3.11). As violacein and terpenes as a second

secondary metabolite synthesized by the strains were considered as thermostable chemical compounds unaffected by prolonged heating, these observation excluded violacein and terpenes as solely defense factors of the investigated *Oxalobacteraceae-F. graminearum* BFI and suggests an involvement of proteins. Therefore, the potential to express and secrete hydrolytic enzymes, as chitinases or proteases and their role in reducing the fungal growth was investigated within this study (4.2.2).

4.2.2 Involvement of chitin degradation enzymes in fungal growth suppression

The expression and secretion of hydrolytic enzymes is of special interest. Especially the presence of chitinases was linked to the pathogenicity of specific *Oxalobacteraceae.* Studies proved an enhanced expression of chitinases in chitin supplemented and fungi decreased soils (Weller *et al.*, 2002, Mendes *et al.*, 2011, Cretoiu *et al.*, 2013, Kielak *et al.*, 2013, Ramsey *et al.*, 2015) . Moreover, chitinases are hypothesized to be one of the antifungal factors of the *Oxalobacteraceae* genus *Collimonas* (Song *et al.*, 2015). Therefore, the potential to express and secrete hydrolytic enzymes was investigated to identify the influence on the *Janthinobacterium*/*Duganella–F. graminearum* BFI. Emphasis was set one the expression and secretion of chitinases.

Considering the observed hydrolytic activities in combination with the phylogenetic distribution of the 14 strains investigated in this study, the ability to express and secrete hydrolytic enzymes (amylases, proteases and lipases) was in accordance with the genus (3.2.3). It was shown that the *Janthinobacterium* affiliated OxaI isolates displayed an amylolytic but no proteolytic activity and that the *Duganella* affiliated OxaII strains behaved *vice versa*. A similar result was detected for the lipolytic activity. *Janthinobacterium* affiliated OxaI isolates displayed a moderate lipolytic activity, the *Duganella* affiliated OxaII strains had a high activity. As none of these hydrolytic activities were expressed throughout all tested *Janthinobacterium* and *Duganella* strains to the same extent, these enzymes did not contribute to the observed fungal growth reduction provoked by HH100 - HH107, HH01, 5059, *J. lividum, J. agaricidamnosum, D. phyllosphaerae* and *D. zoogloeoides.* Main emphasis was set on the chitin degradation activity, as hypothesized to be involved in reducing fungal growth (Weller *et al.*, 2002, Mendes *et al.*, 2011, Cretoiu *et al.*, 2013, Kielak *et al.*, 2013, Ramsey *et al.*, 2015).

Investigating the ability to utilize chitin as sole C-source, a dependency on the genus was identified. Whereas OxaI affiliated strains, *J. lividum* and *J. agaricidamnosum*

utilized chitin, the ability was reduced for OxaII strains and not detectable for *D. phyllosphaereae* and *D. zoogloeoides* under tested conditions (Table 4.1).

Table 4.1 Chitinoclastic activity and number of potential chitinases and deacetylases identified in the analyzed genomes identified

	Janthinobacterium						
	HH100	**HH102**	**HH103**	**HH104**	**HH106**	**HH107**	**5059**
Chitinoclastic activity	++	++	++	++	++	++	++
Number of potential chitinases	3	3	3	2	1	2	4
Number of potential deacetylases	1	1	1	2	1	1	1
			Duganella				
	1522	**9628**	**HH101**	**HH105**	**23865**	**16928**	**HH01**
Chitinoclastic activity	++	++	+	+	-	-	+
Number of potential chitinases	2	4	3	3	0	0	4
Number of potential deacetylases	1	0	4	4	2	3	5

+: activity observed, ++ indicated an increased degree of the activity and -: no activity was observed. For strain abbreviations consult 2.7.3.

All strains encoded genes for the synthesis of chitin degradation enzymes, either chitinases or deacetylases (Table 4.1). Moreover, all strains encoded the T2SS, necessary for the secretion of hydrolytic enzymes, e.g. chitinases, proteases and lipases (Table 3.5, Johnson *et al.*, 2006). Considering the genes of potentially secreted chitinases, which are mainly used for chitin degradation in aquatic habitats (Hillman *et al.*, 1989, Gooday, 1990), all strains utilizing chitin encoded at least one chitinase (Table 4.1). However, the number of identified chitinases present in the genome did not correlate with the degree of chitin hydrolysis, with the exception of *D. phyllosphaeare* and *D. zoogloeoides*. Both strains displayed no chitin utilization activity and encoded no chitinase genes. Further investigations of the genomes revealed the presence of another group of genes, namely deacetylases that are potentially involved in chitin degradation. Genes coding for deacteylases were present in all strains but *J. agaricidamnosum*. The chitin deacetylation mechanism is preferably used by soil-associated bacteria (Hillman *et al.*, 1989, Gooday, 1990). Comparing the presence of genes encoding chitin degradation enzymes with the isolation sources of the strains, the observed discrepancy between the OxaI, OxaII and *Janthinobacterium* type strains to *D. phyllosphaerae* and *D. zoogleoides* could be explained. Whereas *Janthinobacterium* strains were commonly isolated from aquatic habitats such as

rivers, lakes and springs (Sneath 1984, Johnson *et al.*, 1990, Osullivan *et al.*, 1990, Rossolini *et al.*, 2001), *Duganella* affiliated strains were mostly isolated from soils (Dugan & Lundgren, 1960, Aranda *et al.*, 2011, Kampfer *et al.*, 2012). However, some exceptions occur, as 5059 and *J. lividum* were isolated from soils*, J. agaricidamnosum* from a leaf suface and *D. zoogloeoides* from a watery source (Figure 3.5). Nevertheless, the divergence might be linked to an adaption of these genera to the corresponding environmental niche to enhance the chance for survival. For example, especially in aquatic systems an excessive chitinase activity was observed, leading to an intra- and interspecific cross-feeding (Beier & Bertilsson, 2013). Even though 0.1 – 5.8% of aquatic bacteria degrade chitin (Cottrell *et al.*, 1999, Beier & Bertilsson, 2011) and 4 – 40% incorporate chitin hydrolysis products (Nedoma *et al.*, 1994, Riemann & Azam, 2002). In contrast, the *Duganella* genus is mostly affiliated with soil, plant surfaces and the rhizosphere and soil-borne strains prefer the mechanism of deacetylating chitin. Therefore, the *Duganella* strains might not be adapted to the aqueous environment, what contributed to the observed lack of chitin degradation by *D. phyllosphaerae* and *D. zoogloeoides* under tested conditions and despite encoding 2 and 3 deacetylases. However, as OxaII strains were classified as *Duganella* strains, these strains encoded chitinases and degraded chitin under tested conditions (Table 4.1). This might contributed to an adaption of these strains to the aquaous environment, as OxaII strains were isolated from a watery source.

In summary, all strains have the potential to express and secrete hydrolytic enzymes at different extents and in dependency on the genus. However, this chitin degradation activity might be involved in the observed fungal growth reducing effect of the strains (Figure 3.8 and Figure 3.9). For this, the attachment to and degradation of chitin would be essential steps, resulting in the destruction of the fungal cell wall. For example, bacteria attach to the fungal cell wall and use β-1,3-glucanases and secreted chitinases for the degradation of the fungal cell wall (Leveau & Preston, 2008). Additionally, previous studies indicated that the chitin degradation activity is enhanced in pathogen suppressive and *Oxalobacteraceae* abundant soils, resulting in the hydrolysis of chitinous fungal hyphae (Weller *et al.*, 2002, Mendes *et al.*, 2011, Cretoiu *et al.*, 2013). Characterizing the OxaI representative HH102 for its potential to attach to chitinous surfaces, this strain had the ability to attach to chitin and utilize chitin as C-source (Figure 3.15). Moreover, strain HH102 attached to *F. graminearum* hyphae (Figure 3.26). Therefore, the expression and secretion of chitin degradation enzymes of attached HH102 cells might have led to the observed growth reduction of *F. graminearum* (Figure 3.8 and Figure 3.9). An involvement of proteinaceous factors as chitin degradation products was implied by testing the influence of denaturated

bacterial supernatants on fungal growth (Table 3.11). Considering the fact that the expression and secretion of hydrolytic enzymes is described as QS regulated in different bacteria (Chapon-Herve *et al.*, 1997, Schuster *et al.*, 2003, Wagner *et al.*, 2003, Goo *et al.*, 2010, Hornung *et al.*, 2012), the question arose whether the observed effect of the *Janthinobacterium* and *Duganella* strains on *F. graminearum* were controlled by QS. To answer this question, the strains were investigated according to the QS systems present in the genomes, how QS effects gene expression and if QS is involved in the effect of these strains on *F. graminearum* (4.3).

4.3 *Janthinobacterium* QS system is used for bacterial communication

Investigating the above-characterized bacterial strains according to their QS systems present, all strains coded for the conserved JQS gene cluster (with the exception of strain Marseille, Hornung *et al.*, 2012). Since the genome of Marseille is from smaller size compared to family members (Table 3.2), the JQS system might be lost during evolution. Analyzing the occurrence of the AHK based QS system based on the amino acid similarities to the JqsA AI synthase by BLASTP analysis (NCBI), a very diverse distribution was observed (Figure 4.1). The most JQS homologues, including the AI synthase JqsA, the sensorkinase JqsS and the response regulator JqsR, were found within the proteobacterium phylum. This included species of the α-, β- and γ-proteobacteria, with the majority belonging to the β-proteobacteria (23 of 40 strains). The β-proteobacteria could be divided in three main families, namely *Comanonadaceae,Oxalobacteraceae* and *Burkholderiaceae*. Moreover, whereas the genomic arrangement of the JQS system correlated with the phylogentic distribution of the strains, the isolation sources did not seem to correlate within the β-proteobacteria. The strains were isolated from watery sources and sediments (eight strains), from soils (ten strains) or were associated with plants (five strains). Most interestingly, seven strains were shown to alter the growth of fungi significantly, all members of the *Oxalobacteraceae*. At this point it is tempting to speculate that JQS signaling does play a role in bacterial-fungal interactions within *Oxalobacteraceae*. Next to β-proteobacteria, JQS homologues were found in α- and γ-proteobacteria. The majority of these strains were isolated from a watery source (eight out of 13) and three strains from infections. No strains were isolated from soil or plant samples. Additionally, all four chlorobi strains were isolated from watery habitats. Moreover, in contrast to the most α- and γ-proteobacteria, the chlorobi lack the JqsR regulator genes, alike *V. cholerae*.

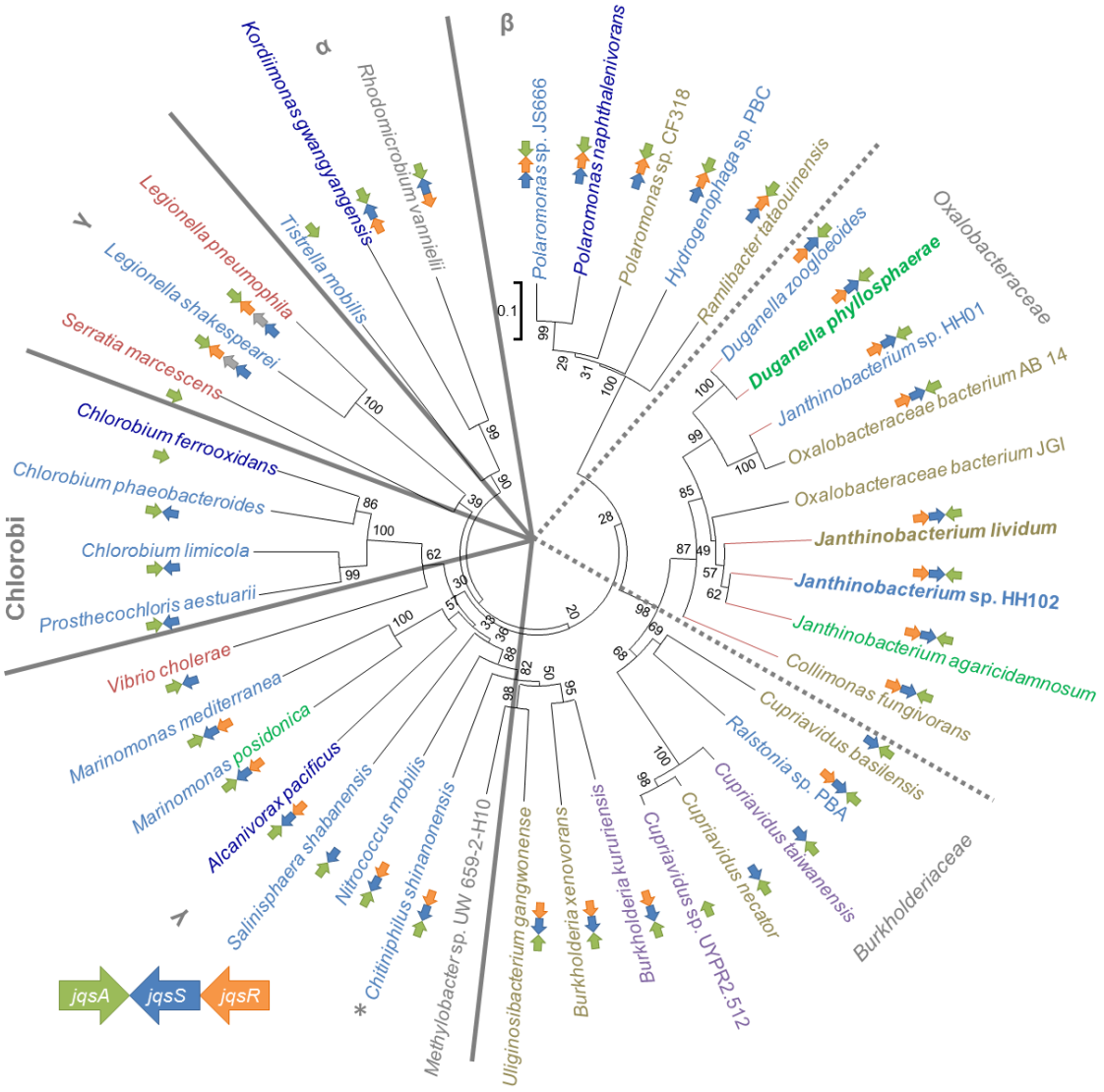

Figure 4.1 **Alignment of JqsA autoinducer synthase homologous genes.** JqsA homologues of strain HH102 were identified using the BLASTP tool of NCBI. The sequences were aligned using the BioEdit software (Hall, 1999). The phylogentic tree was constructed using the neighbor-joining algorithm of MEGA5 (Tamura *et al.*, 2011) with bootstrap analysis from 1000 repeats. The number at each branch point represents the bootstrap support percentage and the scale bar the sequence divergence. Numbers in brackets refer to the NCBI accession numbers of the amino acid sequences of the following strains aligned: *Alcanivorax pacificus* W11-5 (WP_008733540), *Burkholderia kururiensis* M130 (WP_017773076), *Burkholderia xenovorans* LB400 (WP_011493203), *Chitiniphilus shinanonensis* DSM23277 (WP_018748045), *Chlorobium ferrooxidans* DSM13031 (WP_006365391), *Chlorobium limicola* DSM245 (WP_012465459), *Chlorobium phaeobacteroides* DSM266 (WP_011745776), *Collimonas fungivorans* Ter331 (WP_014004148), *Cupriavidus basilensis* OR16 (WP_006160062), *Cupriavidus necator* N-1 (WP_013952137), *Cupriavidus* sp. UYPR2.512 (WP_018312629), *Cupriavidus taiwanensis* LMG 19424 (WP_012355169), *Duganella zoogloeoides* ATCC 25935 (WP_019922871), *Hydrogenophaga* sp. PBC (WP_009517083), *Janthinobacterium* sp. HH01 (renamed to *Duganella* sp. HH01 within this study, WP_008451424), *Kordiimonas gwangyangensis* DSM19435 (WP_020399303), *Legionella shakespearei* DSM23087 (WP_018575957), *Marinomonas mediterranea* MMB-1 (WP_013662838), *Marinomonas posidonica* IVIA-Po-181 (WP_013796753), *Methylobacter* sp. UW 659-2-H10 (WP_018054731), *Nitrococcus mobilis* Nb-231 (WP_005000375), *Oxalobacteraceae bacterium* AB_14 (WP_020701576), *Oxalobacteraceae bacterium* JGI 0001004-K23 (WP_020487418), *Polaromonas naphthalenivorans* CJ2 (WP_011802883), *Polaromonas* sp. CF318 (WP_007862578), *Polaromonas* sp. JS666 (WP_011484931), *Prosthecochloris aestuarii* DSM271 (WP_012505256), *Ralstonia* sp. PBA (WP_009523067), *Ramlibacter tataouinensis*

TTB310 (WP_013900164), *Rhodomicrobium vannielii* ATCC 17100 (WP_013418290), *Salinisphaera shabanensis* E1L3A (WP_006912311), *Serratia marcescens* W2.3 (WP_019453911), *Tistrella mobilis* KA081020-065 (WP_014747931) and *Uliginosibacterium gangwonense* DSM18521 (WP_018608770). Numbers in following strains refer to the locus tags of the sequences used: *Janthinobacterium lividum* DSM1522 (JALI_03530), *Janthinobacterium agaricidamnosum* DSM9628 (GJA_1197), *Janthinobacterium* sp. HH102 (JAB4_14950), *Duganella phyllosphaerae* DSM23865 (DUPY_10350), *Legionella pneumophila* Philadelphia-1 (lpg2731) and *Vibrio cholerae* B33 (A5E_A0527). These strains belong to the classes of Alpha- (α-), Beta- (β-), or Gamma- (γ-)proteobacteria of the phylum proteobacteria or to the phylum chlorobi, separated by gray lines and written in bold. Beta-proteobacteria are devided in the families *Comamonadaceae*, *Oxalobacteraceae* and *Burkholderiaceae* of the order Burkholderiales, depicted by dotted gray lines. *C. shinanonensis* (marked with an asterisk) belongs to Betaproteobacteria. Strains sequenced in this study are written in bold. Red branches indicate an effect on fungi. Color of bacterial names refer to the isolation source. Blue: aquatic environment, green: plant associated, brown: soil isolates, purple: isolated as endophyt, red: isolated from infection, dark blue: sediment of oceans or lakes, blue/green: isolated from a water plant, gray: isolation source unknown. The presence of a potential JQS system was depicted using arrows. Green: *jqsA*, blue: *jqsS* and orange: *jqsR* homologous genes. Gray genes are not further specified. The orientation of the arrows contribute to the genomic arrangement.

Taking these observations together, the JQS system is phylogenetically widely distributed. However, the system differs with respect to the *jqsR* regulator gene. As this gene is missing, the JqsS homologues protein might adopt the JqsR function, as described for *V. cholerae*. In *V. cholerae*, the REC domain of the sensorkinase catalyzes the autophosphorylation, making JqsR dispensable (Figure 1.7, Tiaden & Hilbi, 2012, Schell *et al.*, 2014). Nevertheless, the occurrence in diverse phyla and classes as well as habitats underlines the importance of this QS system. One can only speculate that this system either evolved evolutionary early and developed over time in the originating species or that this system was passed on via horizontal gene transfer. As the genomic arrangement, composition of the JQS system and occurrence in diverse families and species is coherent, the JQS system is most likely an ancient QS system used for bacterial communication within watery habitats.

To advance the knowledge about this QS system and to investigate a potential involvement of the JQS system on *Oxalobacteraceae*-fungi interactions, emphasis was set on the JQS system of the *Janthinobacterium* and *Duganella* strains characterized within this study. The JQS system of the *Janthinobacterium* and *Duganella* strains consisted of the JAI-1 AI synthase JqsA, the sensorkinase/phosphatase JqsS and the response regulator JqsR (Table 3.6, Figure 3.10). Deduced from *in silico* analysis and comparison with known AHK QS systems of *L. pneumophila* and *V. cholerae* (Hornung *et al.*, 2012, Tiaden & Hilbi, 2012, Schell *et al.*, 2014), a model how this JQS system might function was depicted in Figure 4.2.

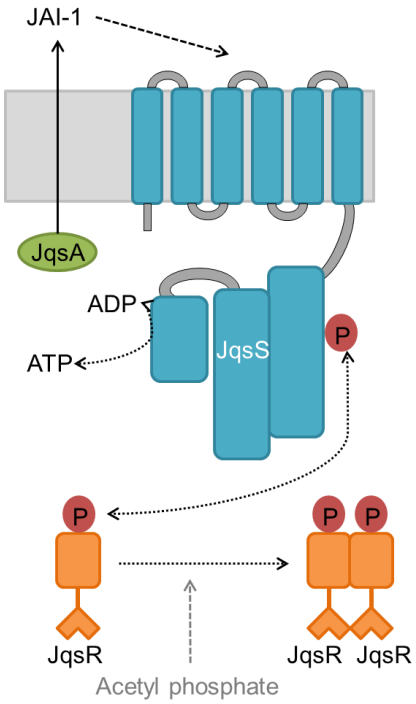

Figure 4.2 **Hypothetical JQS system.** JqsA (green) synthesizes the JAI-1 AI molecule which diffuses outside the cell. The membrane-bound sensorkinase and phosphatase JqsS (blue) recognizes JAI-1. This event may lead to a phosphate transfer from JqsS to the regulator JqsR (orange). After phosphorylation JqsR could dimerise and regulate JAI-1 dependent gene expression. Acetyl-phosphate (written in gray) might be involved in the dimerisation (Hornung *et al.*, 2012, Tiaden & Hilbi, 2012, Schell *et al.*, 2014).

Considering the genome sizes and intergenic regions (Figure 3.10), as well as the amino acid sequences of the AI synthases (Figure 3.11), slight differences were observed according to the phylogenetic distribution of the investigated *Oxalobacteraceae.*This variance might reflect and contribute to the adaption to various environments, as *Janthinobacterium* and *Duganella* affiliated strains were isolated from diverse habitats (Figure 3.5). Nevertheless, the JQS system appeared to be the main QS system of this gene pool, as only three out of 22 strains encoded AHL synthesis genes and no AI-2 synthesis genes were identified (3.3). To better understand this AHK-based QS system, the JQS systems of the OxaI and OxaII representatives HH102 and HH01 were analyzed in detail.

4.3.1 HH01 and HH102 use α-hydroxyketone-like molecules

To get a first hint on the impact of the AI molecules derived from HH102 and HH01 on gene expression, a gene deletion mutant of the OxaI representative HH102 was constructed (3.4.2) and analyzed in comparison to the OxaII representative gene deletion mutant HH01Δ*jqsA* (Hornung *et al.*, 2012). In both strains a loss of JAI-1 resulted in a decreased violacein synthesis (Figure 3.13), as previously published for

HH01Δ*jqsA* (Hornung *et al.*, 2012). Providing extrachromosomal copies of AI synthase genes derived from HH01, HH102, *V. cholerae*, *V. harveyi* and *L. pneumophila*, the reduced violacein synthesis was partly complemented (Figure 3.16). This necessitated two assumptions for both strains: First, the ability of the extrachromosomally provided AI synthases to synthesize the desired AHK and second, the potential of the JqsS sensorkinases to recognize these (Ng *et al.*, 2010, Bolitho *et al.*, 2011, Ng *et al.*, 2011, Tiaden & Hilbi, 2012).

Assuming that the provided AI synthases synthesized its correct AHK molecule, LAI-1 and CAI-1 derived from *V. harveyi* or *V. cholerae*, three individual molecules were recognized by the two JqsS sensorkinases of HH102Δ*jqsA* and HH01Δ*jqsA* (Table 4.2).

Table 4.2 Recognition of AHK molecules by *V. harveyi, V. cholerae*, HH01Δ*jqsA* or HH102Δ*jqsA*

Backbone	Molecule		*V. harveyi*	*V. cholerae*		*D.* sp.	*J.* sp.
			JMH626 / MR14*	WN1102	MM920 / A1552 Δ*cqsA**	HH01 Δ*jqsA*	HH102 Δ*jqsA*
C11	$CAI\text{-}1_{Vh}$	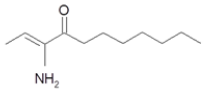	+ [4]	+ [4]	+ [2]	+ [1]	-
C13	$CAI\text{-}1_{Vc}$	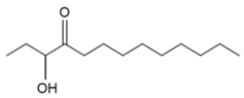	- [4]	+ [4]	+ [3]	+ [1]	+
C15	LAI-1	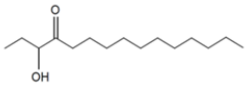	n.t.	n.t.	+ [3] - [3]	+ [1]	+
	$JAI\text{-}1_{01}$	?	-* [1]	n.t.	-* [1]	+ [1]	+
	$JAI\text{-}1_{102}$	?	n.t.	n.t.	n.t.	+	+

+: this molecule was recognized by the reporter strains *V. harveyi* JMH626 or MR14 (marked with an asterisk), *V. cholerae* WN1102, MM920 or A1552Δ*cqsA* (marked with an asterisk), *D.* sp. HH01Δ*jqsA* or *J*. sp. HH102Δ*jqsA*. -: no recognition of the molecules was observed and n.t. refers to: not tested. Number in brackets refers to respective publications. 1: Hornung *et al.*, 2012, 2: Higgins *et al.*, 2007, 3: Spirig *et al.*, 2008 and 4: Ng *et al.*, 2011.

The AI molecules varied with respect to the carbon backbone with 11 ($CAI\text{-}1_{Vh}$, (*Z*)-3-aminoundec-2-en-4-one), 13 ($CAI\text{-}1_{Vc}$, (*S*)-3-hydroxytridecan-4-one) and 15 (LAI-1, 3-hydroxapentadecan-4-one) carbon atoms and in the functional group at the third C atom. This functional group was either an amino group ($CAI\text{-}1_{Vh}$) or a hydroxy group ($CAI\text{-}1_{Vc}$, LAI-1). Considering the complementation potential, I hypothesize an AHK-like structure for $JAI\text{-}1_{102}$ as well as $JAI\text{-}1_{01}$. However, $JAI\text{-}1_{102}$ and $JAI\text{-}1_{01}$ must differ. This assumption was made, since providing extrachromosomal copies of the AI synthases of HH102 or HH01 in the contrarious gene deletion mutant ($JqsA_{102}$ in HH01 and

$JqsA_{01}$ in HH102) the violacein biosynthesis was not restored to wild type level (Figure 3.16). However, the $JAI\text{-}1_{102}$ induced violacein biosynthesis of HH01 was higher compared to the $JAI\text{-}1_{01}$ induced synthesis in HH102. This observation contributed to similar amino acid sequences of the JqsS sensorkinases of strains HH102 and HH01, which are necessary for JAI-1 recognition (Figure 3.18).

4.3.2 *In silico* characterization of JqsA and JqsS of HH01 and HH102

To identify the possible structures of the two JQS molecules $JAI\text{-}1_{01}$ and $JAI\text{-}1_{102,}$ further *in silico* analyses were performed within this study (3.4.4). Detailed *in silico* analyses were choosen, as different experimental approaches did not lead to the identification of the AHK-QS molecules (3.4.4). Moreover, previous studies showed that AI synthases were not strict in the selection of the acyl-coenzyme A (acyl-CoA) used as AHK backbone and that the synthesized enamine is not stable in aqueous solutions (Eliot & Kirsch, 2004, Kelly *et al.*, 2009, Wei *et al.*, 2011). Transfering these observations to the JQS system, the identification of $JAI\text{-}1_{01}$ and $JAI\text{-}1_{102}$ via biochemical approaches was hindered. Nevertheless, comparing the CqsA synthase sequence with the sequences of the JqsA synthases from HH01 and HH102, the amino acids necessary to catalyze a transamination reaction to produce AHK molecules were present (Figure 3.17). This mechanism was described for CAI-1 synthesis, with decanoyl-CoA (d-CoA) and S-adenosyl-methionine (SAM) as preferred substrates (Figure 4.3).

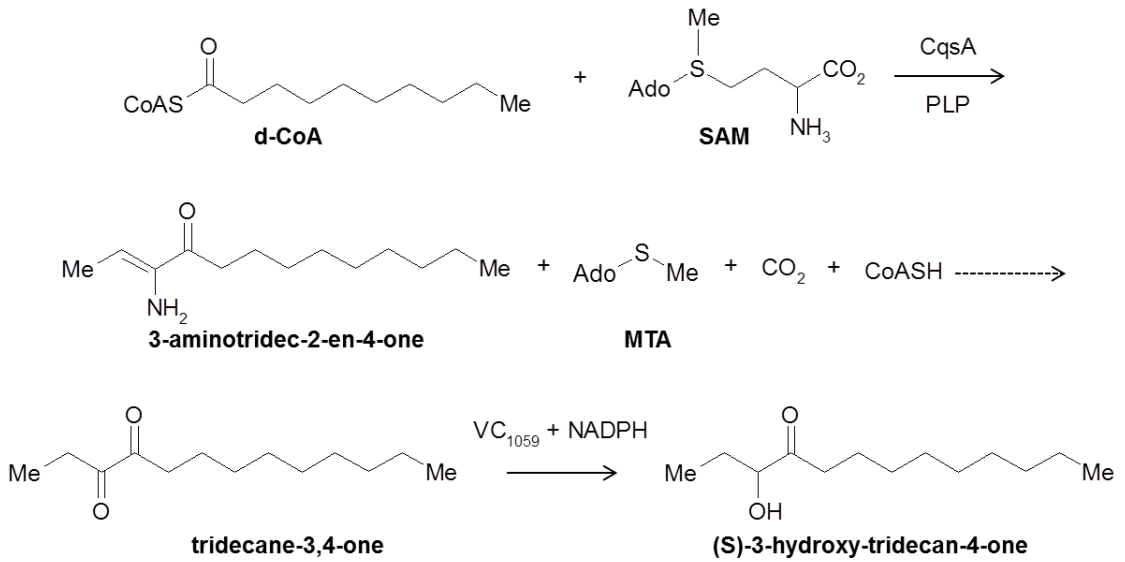

Figure 4.3 **CAI-1 synthesis of *V. cholerae***. For the CAI-1 synthesis, decanoyl-CoA (d-CoA) and S-adenosyl-methionine (SAM) are used as substrate. In a transamination reaction PLP acts as a carrier and transports the aminogroup from SAM to d-CoA by releasing MTA, CO_2 and coenzyme A (CoASH). The resulting 3-aminotridec-2-en-4-one enamine is not stable in water and hydrolyzes to tricecane-3,4-one. This molecule is reduced by the short chain dehydrogenase VC1059 to the $CAI\text{-}1_{Vc}$ molecule (*S*)-3-hydroxytridecan-4-one (Wei *et al.*, 2011).

The reaction is catalyzed by the 7-keto-8-aminopelargonate-like synthase CqsA, according to the COG classification. Within this reaction, a transamination reaction and nucleophilic addition takes place. The amino group of SAM is transferred to the ketogroup of the d-CoA, while SAM is bound to the cofactor PLP. The lysine (K) at position 236 of CqsA (VCA0523; K253 of $JqsA_{01}$, Jab_2c24330; K246 of $JqsA_{102}$, JAB4_14950) is necessary for the covalent linkage between the ε-amino group and the PLP cofactor, which is essential for the synthesis of the AI (Eliot & Kirsch, 2004, Kelly *et al.*, 2009). Moreover, Kelly et al. showed that (S)-2-aminobutyrate (SAB) is another suitable substrate for the the synthesis of CAI-1 (Kelly et al, 2009). Since the AI synthease JqsA is alike CqsA classified as 7-keto-8-aminopelargonate-like synthase, SAB was used for an *in vitro* enzyme assay accompanying this study (3.4.4). Unfortunately these tests were not conclusive. This might be caused by a disability of the JqsA AI synthase to use SAB as preferred substrate. Other amino donors might be the preferred substrate, as L-alanine, D-alanine, γ-aminobutyric acid or SAM. The length of the acyl-CoA might not be significant for this reaction (Eliot & Kirsch, 2004, Kelly *et al.*, 2009, Wei *et al.*, 2011).

Moreover, the length of the carbon backbone of the innate JAI-1_{01} and JAI-1_{102} molecules remain unknown. In analogy to the LqsA AI synthase, the potential to use different activated acyl-CoAs to conduct this function hindered the identification. For example, examining supernatants of bacterial cultures expressing LqsA, a composition of differing AHK molecules was identified. Only 66-68% of all LAI-1-like molecules synthesized displayed a chain length of 15 carbon atoms, the length of the specified LAI-1 molecule. Additionally, minor amounts of C_{13} (CAI-1), C_{14}, C_{16} and C_{17} were detected (Spirig *et al.*, 2008). Considering a potential promiscuous substrate selection of JqsA, as described for CqsA, which utilizes C_8-CoA and C_{10}-CoA (Wei *et al.*, 2011) or LqsA (Spirig *et al.*, 2008), other chain lengths, presumably shorter chains, might be synthesized. Moreover, CqsA synthesizes an enamine (3-aminotridec-2-en-4-one, Figure 3.17). However, this molecule is not stable in an aqueous environment and is spontaneously hydrolyzed to tridecane-3,4-one. A short chain dehydrogenase (VC1059) reduces this molecule to the CAI-1_{Vc} molecule described for *V. cholerae*: (*S*)-3-hydroxytridecan-4-one (Figure 3.17, Wei *et al.*, 2011). Since no significant homologous proteins of the short chain dehydrogenase were identified in HH102 or HH01, the question remains, if an amino-group, a keto-group or a via another short chain dehydrogenase reduced hydroxy group is present at the third C-atom of JAI-1_{01} or JAI-1_{102}. However, Wei *et al.* (2011) showed that even the amino form of CAI-1_{Vc}, synthesized by CqsA as an intermediate, potentially induces QS and that a conversion to the more stable hydroxy form of CAI-1_{Vc} is not required for its function.

Additionally, the identification of the JqsA potential to produce AHK molecules like JAI-1_{102} and JAI-1_{01}, the sensorkinases $JqsS_{01}$ and $JqsS_{102}$ were compared with $CqsS_{Vc}$ and LqsS to identify the recognition potential of the *Oxalobacteraceae* sensorkinases (Figure 3.18). To determine the functional group at the C_3, the amino acids tryptophan (W) and serine (S) at positions 104 and 107 and of $CqsS_{Vc}$ were identified as essential. $CqsS_{Vc}$ slightly prefers the amino modification over the hydroxy modification and an alteration of W104 resulted in an increased preference for a hydroxy modification, as present in LqsS (Ng *et al.*, 2010, Tiaden & Hilbi, 2012). In $JqsS_{01}$ and $JqsS_{102}$ the presence of the W116 and W160 amino acids indicated a preference for an amino modification at C_3. Additionally, amino acids (phenylalanine, F; cysteine, C) necessary to determine the acyl length were identified on the conserved N-terminal receptor region. In $CqsS_{Vc}$, F160, F162, F166 and C170 determine the size of the polar head group as well as the length of the hydrophobic chain (Tiaden & Hilbi, 2012). These three phenylalanines and the cysteine are thought to function as gatekeepers, a regulatory mechanism to control the access to the binding site. This prevents the recognition of related signals to prohibit inappropriate activation or inhibition of signaling due to cross-talk events or environmental signals (Ng *et al.*, 2010, Tiaden & Hilbi, 2012). Out of this, the *Vibrio* spp. conserved gatekeeper amino acid F162 has to be emphasized, which mediates the interaction of F162 with the head group of the CAI-1 molecule. $JqsS_{01}$ and $JqsS_{102}$ shared this phenylalanine at the positions 173 and 217, respectively. In fact, the second position of the gatekeeper was conserved in CqsS, $JqsS_{01}$ and $JqsS_{102}$. Nevertheless, even though the three gatekeepers of $JqsS_{01}$ and $JqsS_{102}$ were identical (H173/F173/V177 and H215/F217/V212), they differ from the $CqsS_{Vc}$ gatekeeper (F160/F162/F166). However, this analysis contributed to the observed fact that $JqsA_{102}$ led to an increased violacein biosynthesis in strain HH01 compared to its innate $JqsA_{01}$ AI synthase (Figure 3.18). This suggested an evolutional origin of the JQS system present in the *Janthinobacterium* and *Duganella* affiliated strains and investigated in this study. Analyzing another amino acid position essential to determine the acyl chain length, these amino acids varied (Figure 3.18). $CqsS_{Vc}$ harbors a cysteine at position 170, what fixes the maximal length of the acyl chain length to C_{10}, but nevertheless allows the detection of smaller chain lengths (Spirig *et al.*, 2008, Wei *et al.*, 2011). The acyl chain length of AI molecules recognized by $CqsS_{Vh}$ is limited to a maximum of eight C atoms. This is caused by a phenylalanine at position 166 (F166, Figure 3.18, Ng *et al.*, 2011). Comparing these positions with $JqsS_{01}$ and $JqsS_{102}$, an alanine (A) and a valine (V) were identified at positions 181 and 225, respectively. Neither alanine nor valine is as bulky as phenylalanine or able to

form disulfide bonds. This corresponded with the broader substrate spectrum in terms of the response to signals with varying acyl chain lengths (Figure 3.16).

To conclude the complementation studies as well as the *in silico* analyses, JAI-1 synthesized by HH01 and HH102 is most likely an AHK molecule. The chain length of JAI-1 might be longer as C_8, as indicated by the slight recognition of CAI-1_{Vh}. The functional group at the third C atom of the JAI-1 molecules might be an enamine or the hydrolyzed form, comparable to CAI-1_{Vh} and as indicated by the complementation assay (Figure 3.16). However, the structure depends on the substrate utilized by the JqsA synthases and the lack of short chain dehydrogenases present in HH01 and HH102 to reduce the hydrolyzed ketoform of the amino group. Moreover, the results indicated that the *Janthinobacterium* and *Duganella* representatives HH102 and HH01 expressed different extrachromosomally provided AI synthases, synthesized different AI molecules and recognized a broad spectrum of AHK molecules. This ability results on the one hand in a high potential to respond quickly to various environmental changes, but may lead on the other hand to nonspecific activations of the QS machinery by environmental noise. Nevertheless, colonizing diverse habitats and sharing these with competitors engenders the evolvement of defense mechanisms. Synchronizing the expression of defense factors with the presence of a high number of bacteria expressing these, help organisms to save energy and ressources. Therefore, whether the JQS systems of HH102 and HH01 coordinated the expression of defense factors to reduce the growth of *F. graminearum* in a BFI, was investigated within this study (4.4).

4.4 JQS signaling is involved in bacterium-fungus interaction

Colonizing different habitats and the survival in these various environments provokes an interaction with other organisms. Within the differing environments, bacteria and fungi interact in various forms, associated in a mixed biofilm, as planktonic cells in close proximity or with bacteria colonizing the fungus intrahyphal (Frey-Klett *et al.*, 2011). Nevertheless, within a BFI microorganisms often compete with each other and therefore develop mechanisms to weaken or kill the invading organisms. An important role in dealing with competing strains is the synthesis and secretion of various hydrolytic enzymes and secondary metabolites. Providing these classes of enzymes and compounds, help bacteria to colonize diverse habitats and to adapt to various environmental niches (Figure 3.5). Additionally, providing a multitude of different factors helps microorganisms to compete with invading microorganisms (Tarkka *et al.*, 2009,

Frey-Klett *et al.*, 2011). Since expressing these genes at single cell level does not aid the survival of the population but weakens the single cell and consumes rare metabolites, the expression is synchronized by QS. Examples are *Burkholderia glumae* and *P. aerugninosa*, which control and coordinate the expression of hydrolytic enzymes and the type II secretion system (T2SS) via the QS network (Chapon-Herve *et al.*, 1997, Schuster *et al.*, 2003, Wagner *et al.*, 2003, Goo *et al.*, 2010). Moreover, a recent study isolated *Pseudomonas* spp. from frog skins and showed the inhibition of the fungus *Batrachochytrium dendrobatidis* in a density dependent way. The authors hypothesized the QS-regulated bacterial compound synthesis as important for this antifungal effect (Yasumiba *et al.*, 2016). Interestingly, the *Janthinobacterium* and *Duganella* isolates expressed and secreted various hydrolytic enzymes and secondary metabolites (chapter 4.2). Furthermore, the strains HH102 and HH01 coordinated the expression of the pigment violacein (Figure 3.13), the proteolytic (Figure 3.14) and the chitinolytic (Figure 3.15) activities via QS. Whereas the QS-regulated expession of these potential defense factors is involved in affecting the growth of the fungus *F. graminearum*, was investigated within this study.

4.4.1 JAI-1 induces the synthesis of defense factors

The deletion of *jqsA* in HH01 and HH102 resulted in the decreased violacein synthesis of these strains as shown by phenotypic characterization (Figure 3.13) and via RNA-seq analysis (Table 3.8). As demonstrated (Figure 3.9) and discussed previously (4.2.1), violacein did not seem to be the major factor for *F. graminearum* growth inhibition for all investigated *Janthinobacterium* and *Duganella* strains. Nevertheless, investigating the 5' regions of the *vioA* promoter sequences of the 14 *Janthinobacterium* and *Duganella* strains examined in this study, a conserved palindromic sequence was identified (Figure 3.20). Deleting the $TTGA_{N6/7}TCAA$ sequence 243 bp upstream of the translational start site of the *vioA* gene led to a significant reduced violacein biosynthesis of HH01, HH01Δ*jqsA*, HH102 and HH102Δ*jqsA* (Figure 3.21). This JAI-1 motif was found 80 to 339 bp upstream of the translational start sites of the majority of genes regulated by JAI-1 (Table 3.8). Most genes regulated by JAI-1 were arranged in close promiximity, indicating the organization as operons and the regulation via the JAI-1 motif. Therefore, this JAI-1 motif was most likely involved in the induction of QS-regulated genes and operons. As the JAI-1 motif was not identified in the upstream region of few JQS-regulated genes and identified in the upstream region of non-regulated genes, e. g. the *chiA* chitinase (Table 9.8), the JAI-1 motif might not be the only factor involved JQS-dependent gene regulation.

Contemplating further genes associated with the synthesis of secondary metabolites, the interplay of the violacein operon and the *kynUA* cluster of HH01 has to be mentioned. This *kynUA* cluster was next to a putative polysaccharide deacetlyase (Jab_1c18190) the only upregulated cluster in early stationary growth phase of HH01 (Table 3.8). The upregulation might be explained as follows: the lack of JAI-1_{01} decreased the expression of the *vioABCDE* operon. As no condensation of the tryptophan molecules to violacein could be catalyzed any more, the amount of tryptophan would accumulate. Therefore, to prevent the accumulation of tryptophan, the *kynUA* cluster expression is simultaneously induced via JAI-1 and to express tryptophan degradation enzymes. The JAI-1 motif was identified in the 5' region of this cluster, supporting this hypothesis. However, assuming a storage function of violacein to regulate the intracellular amount of tryptophan, this amino acid could as well trigger the *kynUA* expression. This would imply another role of tryptophan, next to its usage as amino acid or for violacein biosynthesis.

Besides the *vioABCDE* and *kynUA* operons, one additional secondary metabolite synthesis cluster was regulated by JAI-1_{01} in early stationary phase (Table 3.8). This cluster was unique to strain HH01 and therefore did probably not contribute to the overall observed effect of the *Janthinobacterium* and *Duganella* strains on the fungus and investigated in this study (Figure 3.9). Regardless of this, the RNA-seq data strongly suggested a QS-dependent regulation of genes linked to the synthesis of secondary metabolites via JAI-1. This is of special interest, as understanding how the secondary metabolite synthesis was regulated and induced allows to enter an enormous reservoir of genetic and metabolic diversity, helping industry to find novel antibiotic compounds or anticancer agents (Demain & Fang, 2000, Paradkar *et al.*, 2003, Sanchez & Olson, 2005, Ruiz *et al.*, 2010). However, testing denaturated and non-denaturated supernatant of HH102 and HH102Δ*jqsA* on growth of *F. graminearum*, no differences provoked by the wild type and mutant strains were identified (Table 3.11). In fact, testing denaturated supernatant the bacterial effect on the fungus was abrogated. Therefore, thermostable chemical compounds might not contribute to the effect on this fungus. This might include constitutive expressed secondary metabolites, secondary metabolites whose synthesis was induced via JAI-1 as well as the JAI-1 molecule itself. Even though LAI-1 of *L. pneumophila* inhibited eukaryotic cell migration directly and was thereby used for inter-kingdom signaling (Simon *et al.*, 2015), the direct involvement of JAI-1 or JAI-1-induced secondary metabolites might not play a role in this *Oxalobacteraceae–F. graminearum* BFI. According to these observations, it was hypothesized that the fungal growth suppression was provoked by proteinacous factors.

For HH102 it was shown phenotypically that the proteolytic activity depended on the presence of the QS molecule JAI-1_{102} (Table 3.7). This effect might either be caused by the induction or repression of proteases or the secretion system. Since the T2SS is well known for the secretion of hydrolytic enzymes, e.g. chitinases, lipases or proteases (Chapon-Herve *et al.*, 1997, Schuster *et al.*, 2003, Wagner *et al.*, 2003, Goo *et al.*, 2010), the RNA-seq data were analyzed according to genes associated with T2SS genes and proteases. Nevertheless, no QS dependent proteases or T2SS genes were identified by RNA-seq. This might be due to an unfavorably selected time point for sampling. Coincubating HH102 and *F. graminearum* under conditions similar to the proteolytic test (2.11.2, 2.6.2), no difference between the wild type HH102 and the *jqsA* gene deletion mutant was observed (Figure 3.24 B, columns -G). To my knowledge, even though the virulence of some bacterial pathogens rely on the degradation of virulence regulators by conserved Clp and Lon proteases or the lysis of host tissue proteins could result in the destruction of tissue integrity (Lantz, 1997), caseases were not found to play a role in virulence. Therefore, regulating the expression and secretion of this exoprotease to hydrolyze casein via JAI-1, might not play a major role in reducing fungal growth within this BFI.

Analyzing the RNA-seq data for further fungal growth suppressing factors of the strains and a potential linkage to QS, the T6SS was found to be JAI-1_{102} controlled within the strain HH102 (Table 3.8). Even though this system was identified in all investigated strains (3.2.4), strain HH01 did not regulate T6SS gene expression via JAI-1_{01} under tested conditions (3.5.2). In general, the T6SS was first identified in *R. leguminosarum* and according to the lost ability to effectively nodulate pea (impaired for nodulation) the genes of this SS were called Imp genes (Roest *et al.*, 1997). The T6SS is structurally similar to an intracellular membrane-attached contractile phage tail (Ho *et al.*, 2014) and it transports effectors into prokaryotic and eukaryotic host cells during a pathogen-host interaction. Up to date, only a few proteins translocated were identified (Bingle *et al.*, 2008, Filloux *et al.*, 2008). One example is the VgrG1 protein of *V. cholerae*. This protein carries an enzymatically active domain, which cross-links actin and thereby kills eukaryotic cells. However, an involvement in pore formation can not be excluded. Comparing the T6SS found in about 100 Gram-negative bacteria (Dong *et al.*, 2013), this system consists of 12 - 25 genes with six genes identified as hallmarks for T6SS and the other genes as unique for each T6SS of each bacteria (Filloux 2008). Moreover, the genes can be arranged in multiple complete and incomplete T6SS loci. Within HH102, two gene clusters were identified and one of these clusters was JAI-1 regulated and the other not. The JAI-1 motif was present in all three potential operons of the induced gene cluster (Table 3.9). The phenomenon of regulated and non-

regulated clusters within one organism is described for other strains as well. While some strains constitutively express the T6SS genes, others restrict the expression, dependent on cell density, the post-translational phosphorylation modus or other factors (Miyata *et al.*, 2013). Especially *Vibrio* species, *P. aeruginosa* and *Yersinia pseudotuberculosis* regulate the T6SS expression by QS, with *V. alginolyticus* encoding two T6SS clusters, one regulated and one not (Sheng *et al.*, 2012, Miyata *et al.*, 2013). Inducing the T6SS gene expression during the pathogen-host interaction prevents cost-effective expression in other stages, e.g. the transport of effector proteins into an eukaryotic host (Bingle *et al.*, 2008, Filloux *et al.*, 2008). Interestingly, Borgeaud *et al*. (2015) suggested that the T6SS functions as predatory killing device in *V. cholerae*. As part of the competence regulon it is induced by the growth on chitin with CAI-1 acting as competence pheromone. The T6SS causes the killing of neighboring cells to release DNA, which can be incorporated and used for horizontal gene transfer. However, even though HH102 did not code for competence genes necessary to integrate foreign DNA, this strain regulated T6SS via JAI-1_{102}. Most intriguing, pretreating strain HH102 and its corresponding *jqsA* deletion mutant with the chitin degradation product NADG prior to an coincubation with the fungus *F. graminearum*, HH102Δ*jqsA* did not reduce fungal growth to the same extent as its wild type HH102 (Figure 3.24 B, columns +NADG). Therefore, even though HH102 might not integrate foreign DNA for horizontal gene transfer as *V. cholerae*, an interaction of the AHK molecule and chitin was observed within this study and alike *V. cholerae*. Considering that JAI-1 induced T6SS expression, this observation might indicate that the T6SS is one defense factor of the investigated *Oxalobacteraceae*.

Moreover, the RNA-seq data of the strain HH102 displayed the regulation of a flp pilus assembly cluster by JAI-1_{102}, with a JAI-1 motif 5’ of the translational start of this potential operon (Table 3.8). Even though most genes were identified in the coregenome of 30 strains belonging to the *Oxalobacteraceae* family and investigated in this study (excluding Marseille), the homologous genes in HH01 are not regulated by JAI-1_{01} under tested conditions. In general, Flp pili belong to the class of the broad distributed type IV pili (T4P). T4P belong to the T4b subgroup and are called tight adherence pili (Tad) as well. They were first identified in *Aggregatibacter (Actinobacillus) actinomycetemcomitans* (Giltner *et al.*, 2012). The function of T4P varies and includes motility, attachment and acquisition of DNA. Interestingly, a recent study implied that T4P are necessary for the attachment to chitin of *V. vulnificus* (Williams *et al.*, 2015). Within this study, strains HH102 and HH102Δ*jqsA* attached to chitin (Figure 3.15) as well as to the surface of *F. graminearum* (Figure 3.26). However, regulating the expression of T4P via JQS might not be the exclusive factor affecting

fungal growth, as no difference between the HH102 wild type and HH102Δ*jqsA* gene deletion mutant on *F. graminearum* was observed (Figure 3.24 B, columns -G). Therefore, T4P are presumably one of colluding factors involved in the growth reduction of *F. graminearum*.

To conclude, expressed T6SS and T4P are considered as potential defense factors of *Janthinobacterium* and *Duganella* against invading *F. graminearum* competitors. Especially the expression of T4P are of special interest, as T4P are described to be involved in the attachment to chitin (Williams *et al.*, 2015). With the knowledge that bacteria attach to chitinous fungi and hydrolyze the fungal cell wall (Leveau & Preston, 2008), the question remained if a similar mechanism resulted in the effect of HH102 and HH102Δ*jqsA* on *F. graminearum* growth. Therefore, the impact of chitin and chitin degradation products on QS and the fungal growth reduction effect of strains HH01, HH102 and respective JQS gene deletion mutants was investigated in this study.

4.4.2 JAI-1_{102} and NADG reduce *F. graminearum* growth

Within BFIs, microorganisms often compete with each other and examples for mechanisms to weaken or kill the invading organism are the inhibition of the cell wall synthesis or the changing of the integrity of fungal cell membranes (Frey-Klett *et al.*, 2011). As described, the OxaI representative HH102 attached to chitinous surfaces (Figure 3.15), induced the T4P expression necessary for the attachment via JQS (Table 3.8) and attached to *F. graminearum* (Figure 3.26 - Figure 3.29). These observations might contribute to the observed growth reducing effect of *Janthinobacterium* and *Duganella* strains investigated within this study (Figure 3.8, Figure 3.9). Moreover, these observations might link the growth reducing effect to the hydrolysis of the fungal cell wall (Leveau & Preston, 2008) or might contribute to the observed pathogen suppressive and *Oxalobacteraceae* abundant soils (Weller *et al.*, 2002, Mendes *et al.*, 2011, Cretoiu *et al.*, 2013). Necessary for the hydrolysis of fungal cell walls and pathogen suppressive soils, are next to the attachment, the expression and secretion of chitinases. Interestingly, the putative polysaccharide deacteylase (Jab_1c18190) of HH01 is one out of three upregulated genes in early stationary growth phase. This deacetylase belongs to the carbohydrate esterase 4 familiy and deacetylates its potential substrate chitin. The JAI-1 motif was found 5’ of the translational start codon, indicating a connection between JQS and chitin metabolism (Table 3.10). In contrast, even though strain HH102 harbored three potential chitinases and one deacetylase (Table 4.1), no JAI-1_{102} regualted chitin degradation enzymes were identified in HH102. Nevertheless, investigating the 5’ regions of *chiA* chitinase genes present in all strains, the JAI-1 motif was identified in all assumed promoter

sequences (Table 9.8). With the knowledge that the expression of chitinases is induced by chitin degradation products (Beier & Bertilsson, 2011) and the observation that this JAI-1 motif played a role in JQS signaling, a promoter-fusion was constructed. With this, the induction of the chitinase expression via chitin degradation products and glucose (G) was tested (Figure 3.22). Whereas G inhibited and N-acetyl-D-glucosamine (NADG) had no influence on the expression of the reporter fusion, the *chiA* expression was induced by D-glucosamine (DG) in strain HH102. Most intriguing, deleting *jqsA* of strain HH102 inhibited the induction. Neither G, NADG nor DG had a comparable effect on strains HH01 and HH01Δ*jqsA*. Concerning strains HH102 and HH102Δ*jqsA*, this was another evidence linking the JQS system with chitin metabolism. Moreover, testing the impact of chitin degradation products on the JAI-1 motif of the violacein promoter-fusion provided in HH102 and HH102Δ*jqsA*, DG enhanced the violacein expression. The deletion of the JAI-1 motif resulted in a loss of this effect (Figure 3.23). This was shown for strains HH01 and HH01Δ*jqsA* as well. Again, a potential linkage between the JQS system and the chitin metabolism was shown impressively.

As these tests suggested the necessity to induce chitinase expression, coincubation tests of pretreated HH01, HH01Δ*jqsA*, HH102 and HH102Δ*jqsA* cells with *F. graminearum* were performed. Treating the bacterial cells with DG, an overall high effect of the strains on *F. gramineraru*m was observed (Figure 3.24). A concentration of 10 mM of the monosaccharide DG harmed *F. graminearum* significantly (Figure 9.5). As the fungus was already weakened by DG, the growth reducing compounds synthesized by HH01, HH01Δ*jqsA*, HH102 and HH102Δ*jqsA* might have had a higher impact on the fungal growth. This was interesting, as the mixcellaneous component chitosan comprises of β-1,4-linked DG polymers. One can only hypothesize that this DG concentration was inhibiting to *F. graminearum* and not DG itself. Despite the influence of DG on fungal growth, no significant differences occured between the effect of the OxaI and OxaII representatives with the corresponding *jqsA* gene deletion mutants on *F. graminearum.* This was in contrast to preliminary experiments. Within these it was shown that DG induced *vioA* promoter-fusion expression in HH102 and HH102Δ*jqsA* (Figure 3.23) and *chiA* promoter-fusion expression in HH102 but not in HH102Δ*jqsA* (Figure 3.22). Nevertheless, these preliminary tests allowed an indication of the linkage between JQS and chitin metabolism. The absence of a difference between the growth reduction of HH102 and HH102Δ*jqsA* might be outperformed by the effect of DG (Figure 3.24 columns +DG).

Testing NADG as second chitin degradation product, the fungal growth reduction of HH102 was highly decreased when *jqsA* was deleted and both strains were pretreated with NADG. NADG is as well as DG a component of the fungal cell wall, in which the β-1,4-linked NADG homopolymers form the polysaccharide chitin. Providing *F. graminearum* with NADG, no influence of *F. graminearum* growth was observed (Figure 9.5). Most intriguing, NADG treated HH102 cells reduced the growth of *F. graminearum* 3.1 ± 1.6-fold higher, compared to NADG pretreated HH102Δ*jqsA* cells (Figure 3.24, Table 9.9). This is to my knowledge the first study providing evidence that the JAI-1 JQS AI of NADG pretreated cells was involved in reducing fungal growth. Surveying this BFI microscopically, the effect of JAI-1 and NADG is prominent. Even though both strains reduced fungal germination significantly and altered hyphal growth, HH102 and especially NADG pretreated HH102 cells formed dense biofilms around fungal hyphae and attached to fungal cells closely (Figure 3.29). Neither a comparable dense biofilm formation nor the close attachment to hyphae was observed for HH102Δ*jqsA*. This was astonishing, as NADG induced biofilm formation (Figure 3.25) and attachment to *F. graminearum* hyphae (Figure 3.26) for HH102 as well as HH102Δ*jqsA*. Moreover, surveying the *Janthinobacterium*-*F. graminearum* interaction microscopically, strains HH102 and HH102Δ*jqsA* appeared to alter the fungal surface by the attachment (Figure 3.28). Instead of firm and smooth hyphae, the hyphae appeared dent with a rough surface. Astonishing, the bacterial surfaces displayed phenotypical heterogeneous surface structures and the cells seemed to express and secrete expopolysaccharides and anchor-like structures to attach to the fungal hyphae. Evidently, the HH102 wild type strain appeared to produce slightly more exopolysaccharides and anchor-like structures. Since the questions remained, whether these surface and anchor-like structures are preparation artifacts, outer membrane vesicles, disrupted exopolysaccharides or correspond to T4P and if these facotors are QS-regulated, further tests are necessary to identify and characterize these factors. Another potential involvement of JAI-1 in this BFI was further indicated by the undefined structures sourrounding fungal hyphae and bacterial cells within a HH102-*F. graminearum* BFI. These were not observed at the same extent for the HH102Δ*jqsA*-*F. graminearum* BFI. To conclude, the attachment of the bacterial cells to fungal hyphae was confirmed and the involvement of JAI-1 indicated. No penetration of HH102 into fungal hyphae was observed via SEM techniques.

Considering the necessity of JAI-1 for fungal growth reduction, further QS-regulated proteinaceous factors despite T6SS, T4P or chitinases might be involved in reducing fungal growth. This was assumed, as HH102 and HH102Δ*jqsA* showed no difference except for the pretreatment with NADG and the fungal growth reduction was

independent on the presence of JAI-1_{01}. Therefore, a multitude of antagonistic metabolites produced might be the reason for the observed effect of strains HH100 – HH107, 5059, HH01, *J. agaricidamnosum, J. lividum, D. phyllosphaerae* and *D. zoogloeoides* on the growth of *F. graminearum* and as hypothesized in a previous study (Tarkka *et al.*, 2009). This assumption is assisted by the fact that these strains differed with respect to the phylogeny, the secondary metabolite and hydrolytic enzyme synthesis and secretion. However, in contrast to *J. livdium* or *L. pneumophila*, an involvement of chemical compounds as violacein or LAI-1 as the main growth reducing factor of these *Janthinobacterium* and *Duganella* strains were excluded (Brucker *et al.*, 2008, Ramsey *et al.*, 2015, Simon *et al.*, 2015).

Altogether, this study implied an involvement of JAI-1 in the interaction with *F. graminearum*. NADG enhanced the growth reduction of HH102 and led to a thight attachment to fungal hyphae and subsequent to fungal cell damage. As DG enhanced the violacein expression in dependency on the presence of the JAI-1 motif, an interference of DG and NADG in this complex regulatory circuit was suggested. These results fitted well with the RNA-seq data showing the JAI-1_{102} induced expression of the T6SS and T4P, both involved in the fungal growth suppression and somehow interfering with the chitin metabolism as described for *V. cholerae* and *V. vulnificus* (Borgeaud *et al.*, 2015, Williams *et al.*, 2015). Therefore, I hypothesize that strain HH102 uses JQS to attach tightly to *F. graminearum* hyphae via T4P and thereby induces the expression and secretion of chitinases by the presence of the cell component NADG. As the chitinases would hydrolyze the fungal cell wall, this would be one colluding factor leading to the fungal growth reduction. Further potential defense factors identified are the QS-regulated T6SS and the QS-independent synthesized secondary metabolite bacteriocin. This hypothesis would be in line with former studies, showing that the presence of *Oxalobacteraceae* reduce the number of fungi in soil and that in this environment the chitin degradation enzyme activity is enhanced (Weller *et al.*, 2002, Mendes *et al.*, 2011, Cretoiu *et al.*, 2013). To my knowledge, this is the first study hypothesizing an involvement of JQS on the growth reduction of the plant pathogenic fungus *F. graminearum*.

5 Abstract

Members of the family *Oxalobacteraceae* are widely distributed. Especially bacteria of the genera *Janthinobacterium* and *Duganella* colonize very diverse habitats and thereby interact with microorgansims. For example, within bacterial-fungal interactions invading organsims are often harmed, weakened or killed. Even though most *Oxalobacteraceae* are non-pathogenic, *J. lividum* is well known for its antifungal effects. For this, the involvement of the purple-pigment violacein has been discussed (Ramsey *et al.*, 2015). However, up to date the molecular aspects responsible of this bacterial-fungal interaction remain mostly unknown.

To advance this field and to identify first mechanisms involved in *Oxalobacteraceae*-fungus interactions, eight purple-pigmented aquatic bacteria and one soil bacterium were isolated, sequenced, phylogenetically classified and characterized with respect to four *Janthinobacterium* and *Duganella* type strains and one additional *Duganella* strain. Analyzing the genomes of these 14 strains and 17 publicly available genomes, a core- and pangenome of 1,058 and 23,628 genes were identified. This represents up to date the largest gene pool of *Janthinobacterium* and *Duganella* strains. Moreover, investigating the 14 *Janthinobacterium* and *Duganella* strains in *Oxalobacteraceae*-*Fusarium graminearum* interactions, all strains reduced the growth of the plantpathogenic fungus. To unravel molecular aspects responsible for the observed bacterial-fungal interactions, the genomes were analyzed with respect to the presence of possible defense mechanisms. Remarkably, all strains encoded the type II and type VI secretion systems, but none encoded a type III secretion system. Furthermore, the strains were physiologically characterized according to the ability to synthesize the identified defense factors. In fact, 12 out of 14 strains synthesized the secondary metabolite violacein and hydrolyzed chitin.

Astonishing, the majority of the investigated *Oxalobacteraceae* strains encoded the *Janthinobacterium* quorum sensing (JQS) system as the only QS system. The JQS system revealed homologies to the CQS and LQS systems of *Vibrio cholerae* and *Legionella pneumophila*, respectively and uses α-hydroxyketone-like autoinducer molecules for bacterial communication. To investigate the influence of JAI-1 on fungal growth, a *jqsA* deletion mutant was constructed in the *Janthinbacterium* strain HH102. This mutant and the previously constructed deletion mutant of strain HH01 were used for a global transcriptome analysis to unravel the effects of JAI-1. Using RNA-seq, a set of 45 QS-regulated genes were identified in the two strains analyzed. Among the regulated genes were secondary metabolites, type IV attachment pili and type VI secretion system gene clusters. The QS-dependent regulation of these genes were

partly verified by qRT-PCR technology and by using reporter fusions. Surprisingly, no genes were coregulated in both analyzed strains and besides violacein, suggesting different QS-regulons in the *Janthinobacterium* and *Duganella* affiliated strains.

Interestingly, analyses of the promoter regions of the QS-regulated genes identified a conserved 14 to 15 bp palindromic sequence in the 5' direction of almost all QS-regualted genes in the two strains. This motif was designated JAI-1 motif. Reporter studies strongly suggested this signaling motif to be involved in inducing violacein expression. Moreover, the chitin degradation product D-glucosamine was experimentally shown to induce violacein expression in the presence of the JAI-1 motif. Additionally, this motif was identified within the 5' region of *chiA* endochitinases genes. These aspects were first evidences linking JQS and chitin metabolism in *Oxalobacteraceae*. To further analyze the influence of JAI-1-regulated defense factors and the chitin metabolism on *Oxalobacteraceae-F. graminearum* interactions, the bacterium-fungus interactions were monitored in the presence of the chitin degradation product N-acetyl-D-glucosamine (NADG). Within these BFIs, the bacterial strains changed the fungal growth pattern as well as the microscopic appearance of the fungal hyphae. Most intriguing, pretreated HH102 wild type cells had a much stronger effect on fungal growth compared to the HH102Δ*jqsA* deletion mutant. This suggests an involvement of JQS signaling in bacterial-fungal interactions. Thus, this is the first study specifying JAI-1 and NADG as potential factors involved in *Janthinobacterium-F. graminearum* interactions.

6 Outlook

To better understand the *Oxaolobactereaceae*–fungus interaction further work has to unravel the molecular aspects of this interaction. The question remains how JAI-1 and N-acetyl-D-glucosamine (NADG) collude and reduce fungal growth. Therefore, microscopic analyses of the interaction of HH102 and HH102Δ*jqsA* should be performed and the role of bacterial attachment, biofilm formation and NADG on the fungal growth should be investigated. Additionally, gene deletion mutants of the type VI secretion system and the type IV pili genes should be genereated to investigate the role of these proteinaceous factors in bacterial-fungal interactions. It has to be unraveld whether and how proteins or chemical compounds interfere with the fungi. In this context, the role of bacteriocins and terpenes synthesized by the analyzed strains should be investigated.

The coincubation studies should be carried out with the wheat and bareley pathogenic fungus *F. graminearum* as well as other plantpathogenic fungi, e. g. *Stagonospora nodorum*. Testing this filamentous ascomycete and pathogen of wheat helps to identify whether the observed fungal growth reduction is limited to *F. graminearum*. RNA-seq data of bacterial wild type and quorum sensing (QS) mutant strains coincubated with fungi should be generated to identify factors involved in the bacterial effect on fungal growth. Moreover, the bacterium–fungus interaction should be investigated on fungus infected plants to simulate a natural interaction situation.

Furthermore, the QS molecule JAI-1 synthesized by *Janthinobacterium* and *Duganella* has to be identified. Therefore, the *in vitro* enzyme assay to synthesize artifical QS molecules should be established. Additionally, a potential direct involvement of this molecule in the interaction has to be investigated.

7 References

Ahmad WA, Yusof NZ, Nordin N, Zakaria ZA & Rezali MF 2012. Production and Characterization of Violacein by Locally Isolated *Chromobacterium violaceum* Grown in Agricultural Wastes. Applied Biochemistry and Biotechnology, 167**,** 1220-1234.10.1007/s12010-012-9553-7

Aiba H, Adhya S & De Crombrugghe B 1981. Evidence for two functional *gal* promoters in intact *Escherichia coli* cells. J Biol Chem, 256**,** 11905-10

Alikhan NF, Petty NK, Ben Zakour NL & Beatson SA 2011. BLAST Ring Image Generator (BRIG): simple prokaryote genome comparisons. BMC Genomics, 12**,** 402.10.1186/1471-2164-12-402

Alonso-Saez L, Zeder M, Harding T, Pernthaler J, Lovejoy C, Bertilsson S & Pedros-Alio C 2014. Winter bloom of a rare betaproteobacterium in the Arctic Ocean. Front Microbiol, 5**,** 425.10.3389/fmicb.2014.00425

Ambrozic Avgustin J, Zgur Bertok D, Kostanjsek R & Avgustin G 2013. Isolation and characterization of a novel violacein-like pigment producing psychrotrophic bacterial species *Janthinobacterium svalbardensis* sp. nov. Antonie Van Leeuwenhoek, 103**,** 763-9.10.1007/s10482-012-9858-0

Anetzberger C, Reiger M, Fekete A, Schell U, Stambrau N, Plener L, Kopka J, Schmitt-Kopplin P, Hilbi H & Jung K 2012. Autoinducers act as biological timers in *Vibrio harveyi*. PLoS One, 7**,** e48310

Antonova ES & Hammer BK 2011. Quorum-sensing autoinducer molecules produced by members of a multispecies biofilm promote horizontal gene transfer to *Vibrio cholerae*. FEMS Microbiol Lett, 322**,** 68-76.10.1111/j.1574-6968.2011.02328.x

Aranda S, Montes-Borrego M & Landa BB 2011. Purple-pigmented violacein-producing *Duganella* spp. inhabit the rhizosphere of wild and cultivated olives in southern Spain. Microbial ecology, 62**,** 446-59.10.1007/s00248-011-9840-9

Audic S, Robert C, Campagna B, Parinello H, Claverie JM, Raoult D & Drancourt M 2007. Genome analysis of *Minibacterium massiliensis* highlights the convergent evolution of water-living bacteria. PLoS Genet, 3**,** e138

Bachmann BJ 1983. Linkage map of *Escherichia coli* K-12, edition 7. Microbiol Rev, 47**,** 180-230

Balibar CJ & Walsh CT 2006. *In vitro* biosynthesis of violacein from L-tryptophan by the enzymes VioA-E from *Chromobacterium violaceum*. Biochemistry, 45**,** 15444-57.10.1021/bi061998z

Bankevich A, Nurk S, Antipov D, Gurevich AA, Dvorkin M, Kulikov AS, Lesin VM, Nikolenko SI, Pham S, Prjibelski AD, Pyshkin AV, Sirotkin AV, Vyahhi N, Tesler G, Alekseyev MA & Pevzner PA 2012. SPAdes: a new genome assembly algorithm and its applications to single-cell sequencing. J Comput Biol, 19**,** 455-77.10.1089/cmb.2012.0021

Bassler BL 1999. How bacteria talk to each other: regulation of gene expression by quorum sensing. Curr Opin Microbiol, 2**,** 582-7

Bassler BL & Losick R 2006. Bacterially speaking. Cell, 125**,** 237-46.10.1016/j.cell.2006.04.001

Beier S & Bertilsson S 2011. Uncoupling of chitinase activity and uptake of hydrolysis products in freshwater bacterioplankton. Limnology and Oceanography, 56**,** 1179-1188.10.4319/lo.2011.56.4.1179

Beier S & Bertilsson S 2013. Bacterial chitin degradation-mechanisms and ecophysiological strategies. Frontiers in Microbiology, 4.Artn 14910.3389/Fmicb.2013.00149

Bentley SD, Chater KF, Cerdeno-Tarraga AM, Challis GL, Thomson NR, James KD, Harris DE, Quail MA, Kieser H, Harper D, Bateman A, Brown S, Chandra G, Chen CW, Collins M, Cronin A, Fraser A, Goble A, Hidalgo J, Hornsby T, Howarth S, Huang CH, Kieser T, Larke L, Murphy L, Oliver K, O'neil S, Rabbinowitsch E, Rajandream MA, Rutherford K, Rutter S, Seeger K, Saunders D, Sharp S, Squares R, Squares S, Taylor K, Warren T, Wietzorrek A, Woodward J, Barrell BG, Parkhill J & Hopwood DA 2002. Complete genome sequence of the model actinomycete *Streptomyces coelicolor* A3(2). Nature, 417**,** 141-7.10.1038/417141a

Bingle LEH, Bailey CM & Pallen MJ 2008. Type VI secretion: a beginner's guide. Current Opinion in Microbiology, 11**,** 3-8.10.1016/j.mib.2008.01.006

Bolitho ME, Perez LJ, Koch MJ, Ng WL, Bassler BL & Semmelhack MF 2011. Small molecule probes of the receptor binding site in the *Vibrio cholerae* CAI-1 quorum sensing circuit. Bioorganic & Medicinal Chemistry, 19**,** 6906-6918.10.1016/j.bmc.2011.09.021

Bonnighausen J, Gebhard D, Kroger C, Hadeler B, Tumforde T, Lieberei R, Bergemann J, Schafer W & Bormann J 2015. Disruption of the GABA shunt affects mitochondrial respiration and virulence in the cereal pathogen *Fusarium graminearum*. Mol Microbiol, 98**,** 1115-32.10.1111/mmi.13203

Borgeaud S, Metzger LC, Scrignari T & Blokesch M 2015. The type VI secretion system of *Vibrio cholerae* fosters horizontal gene transfer. Science, 347**,** 63-7.10.1126/science.1260064

Brosius J, Ullrich A, Raker MA, Gray A, Dull TJ, Gutell RR & Noller HF 1981. Construction and fine mapping of recombinant plasmids containing the *rrnB* ribosomal RNA operon of E. coli. Plasmid, 6**,** 112-8

Brucker RM, Harris RN, Schwantes CR, Gallaher TN, Flaherty DC, Lam BA & Minbiole KP 2008. Amphibian chemical defense: antifungal metabolites of the microsymbiont *Janthinobacterium lividum* on the salamander *Plethodon cinereus*. J Chem Ecol, 34**,** 1422-9.10.1007/s10886-008-9555-7

Cavaliersmith T 1992. Origins of secondary metabolism. Ciba Foundation Symposia, 171**,** 64-87

Chapelle E, Mendes R, Bakker PA & Raaijmakers JM 2015. Fungal invasion of the rhizosphere microbiome. ISME J.10.1038/ismej.2015.82

Chapon-Herve V, Akrim M, Latifi A, Williams P, Lazdunski A & Bally M 1997. Regulation of the xcp secretion pathway by multiple quorum-sensing modulons in *Pseudomonas aeruginosa*. Mol Microbiol, 24**,** 1169-78

Chevreux B, Wetter T, Suhai S 1999. Genome sequence assembly using trace signals and additional sequence information, p 45-56. Wingender E (ed), Computer science and biology: proceedings of the German conference on bioinformatics (GCB) '99 Hannover, Germany. GBF-Braunschweig, Department of Bioinformatics, Braunschweig, Germany

Cottrell MT, Moore JA & Kirchman DL 1999. Chitinases from uncultured marine microorganisms. Applied and Environmental Microbiology, 65**,** 2553-2557

Cretoiu MS, Korthals GW, Visser JHM & Van Elsas JD 2013. Chitin amendment increases soil suppressiveness toward plant pathogens and modulates the *Actinobacterial* and *Oxalobacteraceal* communities in an experimental

agricultural field. Applied and Environmental Microbiology, 79**,** 5291-5301.10.1128/Aem.01361-13

Dalia AB, Lazinski DW & Camilli A 2014. Identification of a membrane-bound transcriptional regulator that links chitin and natural competence in *Vibrio cholerae*. Mbio, 5.ARTN e01028-1310.1128/mBio.01028-13

Darch SE, West SA, Winzer K & Diggle SP 2012. Density-dependent fitness benefits in quorum-sensing bacterial populations. Proceedings of the National Academy of Sciences of the United States of America, 109**,** 8259-8263.10.1073/pnas.1118131109

De Buck E, Lammertyn E & Anné J 2008. The importance of the twin-arginine translocation pathway for bacterial virulence. Trends in Microbiology, 16**,** 442-453

De Ley J, Segers P & Gillis M 1978. Intrageneric and intergeneric similarities of *Chromobacterium* and *Janthinobacterium* ribosomal ribonucleic-acid cistrons. Int J Syst Bacteriol, 28**,** 154

Demain AL & Fang A 2000. The natural functions of secondary metabolites. Adv Biochem Eng Biotechnol, 69**,** 1-39

Dobson A, Cotter PD, Ross RP & Hill C 2012. Bacteriocin production: a probiotic trait? Appl Environ Microbiol, 78**,** 1-6.10.1128/AEM.05576-11

Dohrmann AB, Kuting M, Junemann S, Jaenicke S, Schluter A & Tebbe CC 2013. Importance of rare taxa for bacterial diversity in the rhizosphere of Bt- and conventional maize varieties. ISME J, 7**,** 37-49.10.1038/ismej.2012.77

Dong TG, Ho BT, Yoder-Himes DR & Mekalanos JJ 2013. Identification of T6SS-dependent effector and immunity proteins by Tn-seq in *Vibrio cholerae*. Proc Natl Acad Sci U S A, 110**,** 2623-8.10.1073/pnas.1222783110

Driessen AJ, Fekkes P & Van Der Wolk JP 1998. The Sec system. Curr Opin Microbiol, 1**,** 216-22

Dugan PR & Lundgren DG 1960. Isolation of the floc-forming organism *Zoogloea-Ramigera* and its culture in complex and synthetic media. Applied Microbiology, 8**,** 357-361

Eberhard A, Burlingame AL, Eberhard C, Kenyon GL, Nealson KH & Oppenheimer NJ 1981. structural identification of autoinducer of *Photobacterium fischeri* luciferase. Biochemistry, 20**,** 2444-2449.Doi 10.1021/Bi00512a013

Eliot AC & Kirsch JF 2004. Pyridoxal phosphate enzymes: Mechanistic, structural, and evolutionary considerations. Annual Review of Biochemistry, 73**,** 383-415.10.1146/annurev.biochem.73.011303.074021

Filloux A, Hachani A & Bleves S 2008. The bacterial type VI secretion machine: yet another player for protein transport across membranes. Microbiology, 154**,** 1570-1583.10.1099/mic.0.2008/016840-0

Freeman JA & Bassler BL 1999. Sequence and function of LuxU: a two-component phosphorelay protein that regulates quorum sensing in *Vibrio harveyi*. Journal of Bacteriology, 181**,** 899-906

Frey-Klett P, Burlinson P, Deveau A, Barret M, Tarkka M & Sarniguet A 2011. Bacterial-fungal interactions: hyphens between agricultural, clinical, environmental, and food microbiologists. Microbiol Mol Biol Rev, 75**,** 583-609.10.1128/MMBR.00020-11

Fuqua C & Greenberg EP 1998. Self perception in bacteria: quorum sensing with acylated homoserine lactones. Current Opinion in Microbiology, 1**,** 183-189.Doi 10.1016/S1369-5274(98)80009-X

Fuqua C, Winans SC & Greenberg EP 1996. Census and consensus in bacterial ecosystems: The LuxR-LuxI family of quorum-sensing transcriptional regulators. Annual Review of Microbiology, 50**,** 727-751.DOI 10.1146/annurev.micro.50.1.727

Gan HY, Gan HM, Savka MA, Triassi AJ, Wheatley MS, Smart LB, Fabio ES & Hudson AO 2014. Whole-genome sequences of 13 endophytic bacteria isolated from shrub willow (salix) grown in geneva, new york. Genome Announc, 2.10.1128/genomeA.00288-14

Gao R, Krysciak D, Petersen K, Utpatel C, Knapp A, Schmeisser C, Daniel R, Voget S, Jaeger KE & Streit WR 2015. Genome-wide RNA sequencing analysis of quorum sensing-controlled regulons in the plant-associated *Burkholderia glumae* PG1 strain. Appl Environ Microbiol, 81**,** 7993-8007.10.1128/AEM.01043-15

Garg N, Manchanda G & Kumar A 2014. Bacterial quorum sensing: circuits and applications. Antonie Van Leeuwenhoek, 105**,** 289-305.10.1007/s10482-013-0082-3

Geszvain K & Visick KL 2006. Roles of bacterial regulators in the symbiosis between *Vibrio fischeri* and *Euprymna scolopes*. Prog Mol Subcell Biol, 41**,** 277-90

Giltner CL, Nguyen Y & Burrows LL 2012. Type IV pilin proteins: versatile molecular modules. Microbiol Mol Biol Rev, 76**,** 740-72.10.1128/MMBR.00035-12

Goo E, Kang Y, Kim H & Hwang I 2010. Proteomic analysis of quorum sensing-dependent proteins in *Burkholderia glumae*. J Proteome Res, 9**,** 3184-99.10.1021/pr100045n

Gooday GW 1990. The ecology of chitin degradation. Advances in Microbial Ecology, 11**,** 387-430

Goris J, Konstantinidis KT, Klappenbach JA, Coenye T, Vandamme P & Tiedje JM 2007. DNA-DNA hybridization values and their relationship to whole-genome sequence similarities. Int J Syst Evol Microbiol, 57**,** 81-91.10.1099/ijs.0.64483-0

Graupner K, Lackner G & Hertweck C 2015. Genome sequence of mushroom soft-rot pathogen *Janthinobacterium agaricidamnosum*. Genome Announc, 3.10.1128/genomeA.00277-15

Graupner K, Scherlach K, Bretschneider T, Lackner G, Roth M, Gross H & Hertweck C 2012. Imaging mass spectrometry and genome mining reveal highly antifungal virulence factor of mushroom soft rot pathogen. Angewandte Chemie-International Edition, 51**,** 13173-13177.DOI 10.1002/anie.201206658

Green MR and Sambrook J 2012. Molecular Cloning. A laboratory manual, forth edition. Cold Spring Harbor Laboratory Press, Cold Spring Harbor, New York.

Hall BG 2013. Building phylogenetic trees from molecular data with MEGA. Mol Biol Evol, 30**,** 1229-35.10.1093/molbev/mst012

Hall TA 1999. BioEdit: a user-friendly biological sequence alignment editor and analysis program for Windows 95/98/NT. Nucl. Acids. Symp. Ser. , 41**,** 95-98

Hanahan D 1983. Studies on transformation of *Escherichia coli* with plasmids. J Mol Biol, 166**,** 557-80

Henderson IR, Navarro-Garcia F, Desvaux M, Fernandez RC & Ala'aldeen D 2004. Type V protein secretion pathway: the autotransporter story. Microbiol Mol Biol Rev, 68**,** 692-744.10.1128/MMBR.68.4.692-744.2004

Henke JM & Bassler BL 2004. Three parallel quorum-sensing systems regulate gene expression in *Vibrio harveyi*. Journal of Bacteriology, 186**,** 6902-6914.10.1128/Jb.186.20.6902-6914.2004

Higgins DA, Pomianek ME, Kraml CM, Taylor RK, Semmelhack MF & Bassler BL 2007. The major *Vibrio cholerae* autoinducer and its role in virulence factor production. Nature, 450**,** 883-6.10.1038/nature06284

Hillman K, Gooday GW & Prosser JI 1989. The mineralization of chitin in the sediments of the Ythan-Estuary, Aberdeenshire, Scotland. Estuarine Coastal and Shelf Science, 29**,** 601-612.Doi 10.1016/0272-7714(89)90013-9

Hiraishi A, Shin YK & Sugiyama J 1997. Proposal to reclassify *Zoogloea ramigera* IAM 12670 (P. R. Dugan 115) as *Duganella zoogloeoides* gen. nov., sp. nov. International Journal of Systematic Bacteriology, 47**,** 1249-1252

Ho BT, Dong TG & Mekalanos JJ 2014. A view to a kill: the bacterial type VI secretion system. Cell Host Microbe, 15**,** 9-21.10.1016/j.chom.2013.11.008

Hornung C, Poehlein A, Haack FS, Schmidt M, Dierking K, Pohlen A, Schulenburg H, Blokesch M, Plener L, Jung K, Bonge A, Krohn-Molt I, Utpatel C, Timmermann G, Spieck E, Pommerening-Roser A, Bode E, Bode HB, Daniel R, Schmeisser C & Streit WR 2012. The *Janthinobacterium* sp. HH01 genome encodes a homologue of the *V. cholerae* CqsA and *L. pneumophila* LqsA autoinducer synthases. PLoS One, 8**,** e55045

Huang TP, Somers EB & Wong AC 2006. Differential biofilm formation and motility associated with lipopolysaccharide/exopolysaccharide-coupled biosynthetic genes in *Stenotrophomonas maltophilia*. J Bacteriol, 188**,** 3116-20.10.1128/JB.188.8.3116-3120.2006

Hudaiberdiev S, Choudhary KS, Alvarez RV, Gelencser Z, Ligeti B, Lamba D & Pongor S 2015. Census of solo LuxR genes in prokaryotic genomes. Frontiers in Cellular and Infection Microbiology, 5.Artn 2010.3389/Fcimb.2015.00020

Hyatt D, Chen GL, Locascio PF, Land ML, Larimer FW & Hauser LJ 2010. Prodigal: prokaryotic gene recognition and translation initiation site identification. BMC Bioinformatics, 11**,** 119.10.1186/1471-2105-11-119

Ikeda H, Ishikawa J, Hanamoto A, Shinose M, Kikuchi H, Shiba T, Sakaki Y, Hattori M & Omura S 2003. Complete genome sequence and comparative analysis of the industrial microorganism *Streptomyces avermitilis*. Nat Biotechnol, 21**,** 526-31.10.1038/nbt820

Jansen C, Von Wettstein D, Schafer W, Kogel KH, Felk A & Maier FJ 2005. Infection patterns in barley and wheat spikes inoculated with wild-type and trichodiene synthase gene disrupted *Fusarium graminearum*. Proc Natl Acad Sci U S A, 102**,** 16892-7.10.1073/pnas.0508467102

Jenkins CL & Starr MP 1985. Formation of halogenated aryl-polyene (Xanthomonadin) pigments by the type and other yellow-pigmented strains of *Xanthomonas maltophilia*. Annales De L Institut Pasteur-Microbiologie, 136B**,** 257-264.Doi 10.1016/S0769-2609(85)80071-5

Johnson JH, Tymiak AA & Bolgar MS 1990. Janthinocins A, B and C, novel peptide lactone antibiotics produced by *Janthinobacterium lividum*. II. Structure elucidation. J Antibiot (Tokyo), 43**,** 920-30

Johnson TL, Abendroth J, Hol WG & Sandkvist M 2006. Type II secretion: from structure to function. FEMS Microbiol Lett, 255**,** 175-86.10.1111/j.1574-6968.2006.00102.x

Kampfer P, Wellner S, Lohse K, Martin K & Lodders N 2012. *Duganella phyllosphaerae* sp. nov., isolated from the leaf surface of *Trifolium repens* and proposal to reclassify *Duganella violaceinigra* into a novel genus as *Pseudoduganella violceinigra* gen. nov., comb. nov. (vol 35, pg 19, 2012). Systematic and Applied Microbiology, 35**,** 278-278.DOI 10.1016/j.syapm.2012.02.001

Kane MD, Poulsen LK & Stahl DA 1993. Monitoring the enrichment and isolation of sulfate-reducing bacteria by using oligonucleotide hybridization probes designed from environmentally derived 16s ribosomal-RNA sequences. Applied and Environmental Microbiology, 59**,** 682-686

Kazan K, Gardiner DM & Manners JM 2012. On the trail of a cereal killer: recent advances in *Fusarium graminearum* pathogenomics and host resistance. Mol Plant Pathol, 13**,** 399-413.10.1111/j.1364-3703.2011.00762.x

Kelly RC, Bolitho ME, Higgins DA, Lu W, Ng W-L, Jeffrey PD, Rabinowitz JD, Semmelhack MF, Hughson FM & Bassler BL 2009. The *Vibrio cholerae* quorum-sensing autoinducer CAI-1: analysis of the biosynthetic enzyme CqsA. Nat Chem Biol, 5**,** 891-895

Kielak AM, Cretoiu MS, Semenov AV, Sorensen SJ & Van Elsas JD 2013. Bacterial chitinolytic communities respond to chitin and pH alteration in soil. Applied and Environmental Microbiology, 79**,** 263-272.10.1128/Aem.02546-12

Kim SJ, Shin SC, Hong SG, Lee YM, Lee H, Lee J, Choi IG & Park H 2012. Genome sequence of *Janthinobacterium* sp. strain PAMC 25724, isolated from alpine glacier cryoconite. J Bacteriol, 194**,** 2096.10.1128/JB.00096-12

Kovach ME, Elzer PH, Hill DS, Robertson GT, Farris MA, Roop RM, 2nd & Peterson KM 1995. Four new derivatives of the broad-host-range cloning vector pBBR1MCS, carrying different antibiotic-resistance cassettes. Gene, 166**,** 175-6.0378111995005841 [pii]

Krohn-Molt I, Wemheuer B, Alawi M, Poehlein A, Gullert S, Schmeisser C, Pommerening-Roser A, Grundhoff A, Daniel R, Hanelt D & Streit WR 2013. Metagenome survey of a multispecies and alga-associated biofilm revealed key elements of bacterial-algal interactions in photobioreactors. Appl Environ Microbiol, 79**,** 6196-206.10.1128/AEM.01641-13

Lantz MS 1997. Are bacterial proteases important virulence factors? J Periodontal Res, 32**,** 126-32

Lassak J, Henche AL, Binnenkade L & Thormann KM 2010. ArcS, the cognate sensor kinase in an atypical Arc system of *Shewanella oneidensis* MR-1. Appl Environ Microbiol, 76**,** 3263-74.10.1128/AEM.00512-10

Leach J, Lang BR & Yoder OC 1982. Methods for selection of mutants and i*n vitro* culture of *Cochliobolus heterostrophus*. Journal of General Microbiology, 128**,** 1719-1729

Leveau JH & Preston GM 2008. Bacterial mycophagy: definition and diagnosis of a unique bacterial-fungal interaction. New Phytol, 177**,** 859-76.10.1111/j.1469-8137.2007.02325.x

Li WJ, Zhang YQ, Park DJ, Li CT, Xu LH, Kim CJ & Jiang CL 2004. *Duganella violaceinigra* sp. nov., a novel mesophilic bacterium isolated from forest soil. Int J Syst Evol Microbiol, 54**,** 1811-4.10.1099/ijs.0.63141-0

Lincoln SP, Fermor TR & Tindall BJ 1999. *Janthinobacterium agaricidamnosum* sp. nov., a soft rot pathogen of *Agaricus bisporus*. Int J Syst Bacteriol, 49 Pt 4**,** 1577-89

Lo Scrudato M & Blokesch M 2013. A transcriptional regulator linking quorum sensing and chitin induction to render *Vibrio cholerae* naturally transformable. Nucleic Acids Research, 41**,** 3644-3658.10.1093/nar/gkt041

Madhaiyan M, Poonguzhali S, Saravanan VS, Hari K, Lee KC & Lee JS 2013. *Duganella sacchari* sp. nov. and *Duganella radicis* sp. nov., two novel species isolated from rhizosphere of field-grown sugar cane. International Journal of Systematic and Evolutionary Microbiology, 63**,** 1126-1131.Doi 10.1099/Ijs.0.040584-0

Maria S 2001. Biology of type II secretion. Molecular Microbiology, 40**,** 271-283

Markowitz VM, Chen IM, Chu K, Szeto E, Palaniappan K, Grechkin Y, Ratner A, Jacob B, Pati A, Huntemann M, Liolios K, Pagani I, Anderson I, Mavromatis K, Ivanova NN & Kyrpides NC 2012. IMG/M: the integrated metagenome data management and comparative analysis system. Nucleic Acids Res, 40**,** D123-9.10.1093/nar/gkr975

Markowitz VM, Chen IM, Chu K, Szeto E, Palaniappan K, Pillay M, Ratner A, Huang J, Pagani I, Tringe S, Huntemann M, Billis K, Varghese N, Tennessen K, Mavromatis K, Pati A, Ivanova NN & Kyrpides NC 2014. IMG/M 4 version of the integrated metagenome comparative analysis system. Nucleic Acids Res, 42**,** D568-73.10.1093/nar/gkt919

Markowitz VM, Mavromatis K, Ivanova NN, Chen IM, Chu K & Kyrpides NC 2009. IMG ER: a system for microbial genome annotation expert review and curation. Bioinformatics, 25**,** 2271-8.10.1093/bioinformatics/btp393

Matsukawa M & Greenberg EP 2004. Putative exopolysaccharide synthesis genes influence *Pseudomonas aeruginosa* biofilm development. J Bacteriol, 186**,** 4449-56.10.1128/JB.186.14.4449-4456.2004

Matz C, Deines P, Boenigk J, Arndt H, Eberl L, Kjelleberg S & Jurgens K 2004. Impact of violacein-producing bacteria on survival and feeding of bacterivorous nanoflagellates. Appl Environ Microbiol, 70**,** 1593-9

Mavromatis K, Ivanova NN, Chen IM, Szeto E, Markowitz VM & Kyrpides NC 2009. The DOE-JGI standard operating procedure for the annotations of microbial genomes. Stand Genomic Sci, 1**,** 63-7.10.4056/sigs.632

Mctaggart TL, Shapiro N, Woyke T & Chistoserdova L 2015. Draft genome of *Janthinobacterium* sp. RA13 isolated from lake Washington sediment. Genome Announc, 3.10.1128/genomeA.01588-14

Medema MH, Blin K, Cimermancic P, De Jager V, Zakrzewski P, Fischbach MA, Weber T, Takano E & Breitling R 2011. antiSMASH: rapid identification, annotation and analysis of secondary metabolite biosynthesis gene clusters in bacterial and fungal genome sequences. Nucleic Acids Research, 39**,** W339-W346.10.1093/nar/gkr466

Mendes R, Kruijt M, De Bruijn I, Dekkers E, Van Der Voort M, Schneider JHM, Piceno YM, Desantis TZ, Andersen GL, Bakker PaHM & Raaijmakers JM 2011. Deciphering the rhizosphere microbiome for disease-suppressive bacteria. Science, 332**,** 1097-1100.10.1126/science.1203980

Mendes AM, de Carvalho JE, Duarte MCT, Duran N and Bruns RE 2001. Factorial design and response surface optimization of crude violacein for *Chromobacterium violaceum* production. Biotechnol Lett23, 1963– 1969

Miller MB, Skorupski K, Lenz DH, Taylor RK & Bassler BL 2002. Parallel quorum sensing systems converge to regulate virulence in *Vibrio cholerae*. Cell, 110**,** 303-314.Doi 10.1016/S0092-8674(02)00829-2

Miyata ST, Bachmann V & Pukatzki S 2013. Type VI secretion system regulation as a consequence of evolutionary pressure. J Med Microbiol, 62**,** 663-76.10.1099/jmm.0.053983-0

Mojib N, Philpott R, Huang JP, Niederweis M & Bej AK 2010. Antimycobacterial activity *in vitro* of pigments isolated from Antarctic bacteria. Antonie Van Leeuwenhoek International Journal of General and Molecular Microbiology, 98**,** 531-540.DOI 10.1007/s10482-010-9470-0

Morohoshi T, Fukamachi K, Kato M, Kato N & Ikeda T 2010. Regulation of the violacein biosynthetic gene cluster by acylhomoserine lactone-mediated quorum sensing in *Chromobacterium violaceum* ATCC 12472. Biosci Biotechnol Biochem, 74**,** 2116-9.10.1271/bbb.100385

Nedoma J, Vrba J, Hejzlar J, Simek K & Straskrabova V 1994. N-Acetylglucosamine dynamics in fresh-water environments - concentration of amino-sugars, extracellular enzyme-activities, and microbial uptake. Limnology and Oceanography, 39**,** 1088-1100

Ng WL & Bassler BL 2009. Bacterial quorum-sensing network architectures. Annual Review of Genetics, 43**,** 197-222.10.1146/annurev-genet-102108-134304

Ng WL, Perez LJ, Wei YZ, Kraml C, Semmelhack MF & Bassler BL 2011. Signal production and detection specificity in *Vibrio* CqsA/CqsS quorum-sensing systems. Molecular Microbiology, 79**,** 1407-1417.10.1111/j.1365-2958.2011.07548.x

Ng WL, Wei YZ, Perez LJ, Cong JP, Long T, Koch M, Semmelhack MF, Wingreen NS & Bassler BL 2010. Probing bacterial transmembrane histidine kinase receptor-ligand interactions with natural and synthetic molecules. Proceedings of the National Academy of Sciences of the United States of America, 107**,** 5575-5580.10.1073/pnas.1001392107

Nirenberg HI 1981. A simplified method for identifying *Fusarium* spp occurring on wheat. Canadian Journal of Botany-Revue Canadienne De Botanique, 59**,** 1599-1609

Nykyri J, Mattinen L, Niemi O, Adhikari S, Koiv V, Somervuo P, Fang X, Auvinen P, Mae A, Palva ET & Pirhonen M 2013. Role and regulation of the Flp/Tad pilus in the virulence of *Pectobacterium atrosepticum* SCRI1043 and *Pectobacterium wasabiae* SCC3193. PLoS One, 8**,** e73718.10.1371/journal.pone.0073718

Osullivan J, Mccullough J, Johnson JH, Bonner DP, Clark JC, Dean L & Trejo WH 1990. Janthinocin-a, Janthinocin-B and Janthinocin-C, novel peptide lactone antibiotics produced by *Janthinobacterium lividum* .1. Taxonomy, Fermentation, Isolation, Physicochemical and Biological Characterization. Journal of Antibiotics, 43**,** 913-919

Pantanella F, Berlutti F, Passariello C, Sarli S, Morea C & Schippa S 2007. Violacein and biofilm production in *Janthinobacterium lividum*. J Appl Microbiol, 102**,** 992-9.10.1111/j.1365-2672.2006.03155.x

Paradkar A, Trefzer A, Chakraburtty R & Stassi D 2003. *Streptomyces* genetics: A genomic perspective. Critical Reviews in Biotechnology, 23**,** 1-27.Doi 10.1080/713609296

Peleg AY, Hogan DA & Mylonakis E 2010. Medically important bacterial-fungal interactions. Nat Rev Microbiol, 8**,** 340-9.10.1038/nrmicro2313

Poehlein A, Riegel K, Konig SM, Leimbach A, Daniel R & Durre P 2015. Genome sequence of *Clostridium sporogenes* DSM 795(T), an amino acid-degrading, nontoxic surrogate of neurotoxin-producing *Clostridium botulinum*. Stand Genomic Sci, 10**,** 40.10.1186/s40793-015-0016-y

Poplawsky AR, Urban SC & Chun W 2000. Biological role of xanthomonadin pigments in *Xanthomonas campestris* pv. *campestris*. Appl Environ Microbiol, 66**,** 5123-7

Rajagopal L, Sundari CS, Balasubramanian D & Sonti RV 1997. The bacterial pigment xanthomonadin offers protection against photodamage. Febs Letters, 415**,** 125-128.Doi 10.1016/S0014-5793(97)01109-5

Ramsey JP, Mercurio A, Holland JA, Harris RN & Minbiole KP 2015. The cutaneous bacterium *Janthinobacterium lividum* inhibits the growth of *Trichophyton rubrum in vitro*. Int J Dermatol, 54**,** 156-9.10.1111/ijd.12217

Reasoner DJ & Geldreich EE 1985. A new medium for the enumeration and subculture of bacteria from potable water. Appl Environ Microbiol, 49**,** 1-7

Richter M & Rossello-Mora R 2009. Shifting the genomic gold standard for the prokaryotic species definition. Proc Natl Acad Sci U S A, 106**,** 19126-31.10.1073/pnas.0906412106

Riemann L & Azam F 2002. Widespread N-acetyl-D-glucosamine uptake among pelagic marine bacteria and its ecological implications. Applied and Environmental Microbiology, 68**,** 5554-5562.10.1128/Aem.68.11.5554-5562.2002

Roest HP, Mulders IH, Spaink HP, Wijffelman CA & Lugtenberg BJ 1997. A *Rhizobium leguminosarum* biovar *trifolii* locus not localized on the sym plasmid hinders effective nodulation on plants of the pea cross-inoculation group. Mol Plant Microbe Interact, 10**,** 938-41.10.1094/MPMI.1997.10.7.938

Rossolini GM, Condemi MA, Pantanella F, Docquier JD, Amicosante G & Thaller MC 2001. Metallo-beta-lactamase producers in environmental microbiota: New molecular class B enzyme in *Janthinobacterium lividum*. Antimicrobial Agents and Chemotherapy, 45**,** 837-844.Doi 10.1128/Aac.45.3.837-844.2001

Ruiz B, Chavez A, Forero A, Garcia-Huante Y, Romero A, Sanchez M, Rocha D, Sanchez B, Rodriguez-Sanoja R, Sanchez S & Langley E 2010. Production of microbial secondary metabolites: Regulation by the carbon source. Critical Reviews in Microbiology, 36**,** 146-167.10.3109/10408410903489576

Sambrook JaR, D.W. 2001. Molecular Cloning: A Laboratory Manual. 3re ed. Cold Spring Harbor Laboratory Press, Cold Spring Harbor, New York,

Sanchez S & Olson B 2005. Ecology and industrial microbiology - Microbial diversity - the bright and promising future of microbial manufacturing. Current Opinion in Microbiology, 8**,** 229-233.10.1016/j.mib.2005.04.016

Sauer K, Camper AK, Ehrlich GD, Costerton JW & Davies DG 2002. *Pseudomonas aeruginosa* displays multiple phenotypes during development as a biofilm. Journal of Bacteriology, 184**,** 1140-1154.DOI 10.1128/jb.184.4.1140-1154.2002

Schell U, Kessler A & Hilbi H 2014. Phosphorylation signalling through the *Legionella* quorum sensing histidine kinases LqsS and LqsT converges on the response regulator LqsR. Molecular Microbiology, 92**,** 1039-1055.10.1111/mmi.12612

Schell U, Simon S, Sahr T, Hager D, Albers MF, Kessler A, Fahrnbauer F, Trauner D, Hedberg C, Buchrieser C & Hilbi H 2015. The alpha-hydroxyketone LAI-1 regulates motility, Lqs-dependent phosphorylation signaling and gene expression of *Legionella pneumophila*. Mol Microbiol.10.1111/mmi.13265

Schloss PD, Allen HK, Klimowicz AK, Mlot C, Gross JA, Savengsuksa S, Mcellin J, Clardy J, Ruess RW & Handelsman J 2010. Psychrotrophic strain of *Janthinobacterium lividum* from a cold Alaskan soil produces prodigiosin. DNA Cell Biol, 29**,** 533-41.10.1089/dna.2010.1020

Schluter JP, Czuppon P, Schauer O, Pfaffelhuber P, Mcintosh M & Becker A 2015. Classification of phenotypic subpopulations in isogenic bacterial cultures by triple promoter probing at single cell level. Journal of Biotechnology, 198**,** 3-14.10.1016/j.jbiotec.2015.01.021

Schuster M, Lostroh CP, Ogi T & Greenberg EP 2003. Identification, timing, and signal specificity of *Pseudomonas aeruginosa* quorum-controlled genes: a transcriptome analysis. J Bacteriol, 185**,** 2066-79

Sheng L, Gu D, Wang Q, Liu Q & Zhang Y 2012. Quorum sensing and alternative sigma factor RpoN regulate type VI secretion system I (T6SSVA1) in fish pathogen *Vibrio alginolyticus*. Arch Microbiol, 194**,** 379-90.10.1007/s00203-011-0780-z

Shoemaker WR, Muscarella ME & Lennon JT 2015. Genome sequence of the soil bacterium *Janthinobacterium* sp. KBS0711. Genome Announc, 3.10.1128/genomeA.00689-15

Sijbrandi R, Urbanus ML, Ten Hagen-Jongman CM, Bernstein HD, Oudega B, Otto BR & Luirink J 2003. Signal recognition particle (SRP)-mediated targeting and Sec-dependent translocation of an extracellular *Escherichia coli* protein. J Biol Chem, 278**,** 4654-9.10.1074/jbc.M211630200

Simon R, Priefer U & Puhler A 1983. A broad host range mobilization system for *in vivo* genetic-engineering - transposon mutagenesis in gram-negative bacteria. Bio-Technology, 1**,** 784-791.Doi 10.1038/Nbt1183-784

Simon S, Schell U, Heuer N, Hager D, Albers MF, Matthias J, Fahrnbauer F, Trauner D, Eichinger L, Hedberg C & Hilbi H 2015. Inter-kingdom signaling by the *Legionella* quorum sensing molecule LAI-1 modulates cell migration through an IQGAP1-Cdc42-ARHGEF9-Dependent pathway. PLoS Pathog, 11**,** e1005307.10.1371/journal.ppat.1005307

Skerman VBD, McGowan V, Sneath PHA 1980. Approved lists of bacterial names. Int.J.Syst.Bacteriol. **30** : 225-420

Smith H, Akiyama T, Foreman C, Franklin M, Woyke T, Teshima H, Davenport K, Daligault H, Erkkila T, Goodwin L, Gu W, Xu Y & Chain P 2013. Draft genome sequence and description of *Janthinobacterium* sp. strain CG3, a psychrotolerant Antarctic supraglacial stream bacterium. Genome Announc, 1.10.1128/genomeA.00960-13

Smith HJ, Foreman CM, Akiyama T, Franklin MJ, Devitt NP & Ramaraj T 2016. Genome sequence of *Janthinobacterium* sp. CG23_2, a violacein-producing isolate from an Antarctic supraglacial stream. Genome Announc, 4.10.1128/genomeA.01468-15

Sneath PHA 1956. Cultural and biochemical characteristics of the genus *Chromobacterium*. Journal of General Microbiology, 15**,** 70-98.10.1099/00221287-15-1-70

Sneath PHA 1984. Genus *Janthinobacterium*, p. 376-377. In N.R. Krieg and J. G. Holt (ed.), Bergey´s manual of systematic bacteriology- The Williams & Wilkins Co., Baltimore.

Song C, Schmidt R, De Jager V, Krzyzanowska D, Jongedijk E, Cankar K, Beekwilder J, Van Veen A, De Boer W, Van Veen JA & Garbeva P 2015. Exploring the

genomic traits of fungus-feeding bacterial genus *Collimonas*. BMC Genomics, 16**,** 1103.10.1186/s12864-015-2289-3

Spirig T, Tiaden A, Kiefer P, Buchrieser C, Vorholt JA & Hilbi H 2008. The *Legionella* autoinducer synthase LqsA produces an alpha-hydroxyketone signaling molecule. J Biol Chem, 283**,** 18113-23.10.1074/jbc.M801929200

Stamatakis A 2014. RAxML version 8: a tool for phylogenetic analysis and post-analysis of large phylogenies. Bioinformatics, 30**,** 1312-3.10.1093/bioinformatics/btu033

Stingele F, Neeser JR & Mollet B 1996. Identification and characterization of the eps (Exopolysaccharide) gene cluster from *Streptococcus thermophilus* Sfi6. J Bacteriol, 178**,** 1680-90

Suckow G, Seitz P & Blokesch M 2011. Quorum sensing contributes to natural transformation of *Vibrio cholerae* in a species-specific manner. J Bacteriol, 193**,** 4914-24.10.1128/JB.05396-11

Sun SY, Tay QXM, Kjelleberg S, Rice SA & Mcdougald D 2015. Quorum sensing-regulated chitin metabolism provides grazing resistance to *Vibrio cholerae* biofilms. Isme Journal, 9**,** 1812-1820.10.1038/ismej.2014.265

Tamura K, Peterson D, Peterson N, Stecher G, Nei M & Kumar S 2011. MEGA5: molecular evolutionary genetics analysis using maximum likelihood, evolutionary distance, and maximum parsimony methods. Mol Biol Evol, 28**,** 2731-9.10.1093/molbev/msr121

Tarkka MT, Sarniguet A & Frey-Klett P 2009. Inter-kingdom encounters: recent advances in molecular bacterium-fungus interactions. Curr Genet, 55**,** 233-43.10.1007/s00294-009-0241-2

Tatusova T, Ciufo S, Fedorov B, O'neill K & Tolstoy I 2014. RefSeq microbial genomes database: new representation and annotation strategy. Nucleic Acids Res, 42**,** D553-9.10.1093/nar/gkt1274

Tiaden A & Hilbi H 2012. alpha-Hydroxyketone synthesis and sensing by *Legionella* and *Vibrio*. Sensors (Basel), 12**,** 2899-919.10.3390/s120302899

Tiaden A, Spirig T & Hilbi H 2010. Bacterial gene regulation by alpha-hydroxyketone signaling. Trends Microbiol, 18**,** 288-97.10.1016/j.tim.2010.03.004

Tsai CS & Winans SC 2011. The quorum-hindered transcription factor YenR of *Yersinia enterocolitica* inhibits pheromone production and promotes motility via a small non-coding RNA. Mol Microbiol, 80**,** 556-71.10.1111/j.1365-2958.2011.07595.x

Urbanczyk H, Ast JC, Higgins MJ, Carson J & Dunlap PV 2007. Reclassification of *Vibrio fischeri*, *Vibrio logei*, *Vibrio salmonicida* and *Vibrio wodanis* as *Aliivibrio fischeri* gen. nov., comb. nov., *Aliivibrio logei* comb. nov., *Aliivibrio salmonicida* comb. nov. and *Aliivibrio wodanis* comb. nov. Int J Syst Evol Microbiol, 57**,** 2823-9.10.1099/ijs.0.65081-0

Valdes N, Soto P, Cottet L, Alarcon P, Gonzalez A, Castillo A, Corsini G & Tello M 2015. Draft genome sequence of *Janthinobacterium lividum* strain MTR reveals its mechanism of capnophilic behavior. Stand Genomic Sci, 10**,** 110.10.1186/s40793-015-0104-z

Vendeville A, Winzer K, Heurlier K, Tang CM & Hardie KR 2005. Making 'sense' of metabolism: Autoinducer-2, LuxS and pathogenic bacteria. Nature Reviews Microbiology, 3**,** 383-396.10.1038/nrmicro1146

Verma SC & Miyashiro T 2013. Quorum sensing in the squid-*Vibrio* symbiosis. Int J Mol Sci, 14**,** 16386-401.10.3390/ijms140816386

Wagner VE, Bushnell D, Passador L, Brooks AI & Iglewski BH 2003. Microarray analysis of *Pseudomonas aeruginosa* quorum-sensing regulons: effects of growth phase and environment. J Bacteriol, 185**,** 2080-95

Wallden K, Rivera-Calzada A & Waksman G 2010. Type IV secretion systems: versatility and diversity in function. Cell Microbiol, 12**,** 1203-12.10.1111/j.1462-5822.2010.01499.x

Wei YZ, Perez LJ, Ng WL, Semmelhack MF & Bassler BL 2011. Mechanism of *Vibrio cholerae* autoinducer-1 biosynthesis. Acs Chemical Biology, 6**,** 356-365.10.1021/cb1003652

Weller DM, Raaijmakers JM, Gardener BBM & Thomashow LS 2002. Microbial populations responsible for specific soil suppressiveness to plant pathogens. Annual Review of Phytopathology, 40**,** 309-+.10.1146/annurev.phyto.40.030402.110010

Wheeler TJ, Clements J & Finn RD 2014. Skylign: a tool for creating informative, interactive logos representing sequence alignments and profile hidden Markov models. Bmc Bioinformatics, 15.Artn 710.1186/1471-2105-15-7

Wiggins PJ, Smith JM, Harris RN & Minbiole KPC 2011. Gut of red-backed salamanders (*Plethodon cinereus*) may serve as a reservoir for an antifungal cutaneous bacterium. Journal of Herpetology, 45**,** 329-332

Williams TC, Ayrapetyan M & Oliver JD 2015. Molecular and physical factors that influence attachment of *Vibrio vulnificus* to chitin. Appl Environ Microbiol, 81**,** 6158-65.10.1128/AEM.00753-15

Yasumiba K, Bell S & Alford R 2016. Cell density effects of frog skin bacteria on their capacity to inhibit growth of the chytrid fungus, *Batrachochytrium dendrobatidis*. Microb Ecol, 71**,** 124-30.10.1007/s00248-015-0701-9

Yin C, Hulbert SH, Schroeder KL, Mavrodi O, Mavrodi D, Dhingra A, Schillinger WF & Paulitz TC 2013. Role of bacterial communities in the natural suppression of Rhizoctonia solani bare patch disease of wheat (Triticum aestivum L.). Appl Environ Microbiol, 79**,** 7428-38.10.1128/AEM.01610-13

8 Acknowledgements

First of all, I would like to thank Prof. Dr. Wolfgang R. Streit for giving me the opportunity to work on this project. I would like to thank you for supporting me during all stages of the project and always being open for discussion to solve upcoming challenges.

Second, I would like to thank Prof. Dr. Wilhelm Schäfer for reviewing this work and the inspiring and successful cooperation.

I would like to thank Prof. Dr. Helge B. Bode and PD Dr. Andreas Pommerening-Röser for beeing part of my examination committee. Furthermore, I would like to thank all the cooperation partners involved in this project.

I thank Katrin Petersen and Philipp Jenike for the contribution to this PhD thesis with their master thesis. Thank you Katrin for the ongoing help in the lab, discussions and fun time we had.

I thank Angela Jordan and Ursula Reinitz for their help with lab and material problems and organizational matters.

I thank Cathrin Kröger for all her help contributing to fungal questions, how to work with *Fusarium* and supplying me with lots of conidia.

Beyond that I would like to thank all members of the microbiology and biotechnology department for helpful discussions, nice lab atmosphere and the great moments at the workplace.

My special thanks go to Jessica Grote, my favorite postdoc. Thank you for discussing everything with me: work and non-work stuff. You’re the best seatmate I could have asked for.

And last but not least I want to thank my family and friends. Thank you for all the support and hurly-burly. Yes, I meant you: Annkathrin, Mareike, Lasse, Elke, Roland and Birgit.

9 Appendix

Table 9.1 Secondary metabolites synthesized by the 14 investigated strains

HH01					HH103					MP5059B				
Type	**Contig**	**From**	**To**	**Size**	**Type**	**Contig**	**From**	**To**	**Size**	**Type**	**Contig**	**From**	**To**	**Size**
Bacteriocin	1	1942509	1954215	11706	Terpene	1.27	56033	77794	21761	Bacteriocin	51	49008	60231	11223
Nrps	1	2850161	2905861	55700	Indole	1.27	196314	219328	23014	Terpene	58	15221	36988	21767
Nrps	2	1	81644	81643	Bacteriocin	1.27	281534	292478	10944	Bacteriocin	72	25338	37338	12000
Terpene	2	715227	738567	23340	Bacteriocin	14.78	67297	78922	11625	Indole	83	79200	102433	23233
Nrps-t1pks	2	863733	993446	129713	Bacteriocin	51.59	1	5823	5822	Bacteriocin	94	147313	158230	10917
Indole	2	1127178	1150198	23020					**73166**	Bacteriocin	95	33314	44369	11055
Nrps	2	1154166	1207247	53081	**HH104**									**90195**
Bacteriocin	2	2691674	2701961	10287	**Type**	**Contig**	**From**	**To**	**Size**	***J. lividum***				
Bacteriocin	2	4095570	4106421	10851	Indole	2.27	255396	278413	23017	**Type**	**Contig**	**From**	**To**	**Size**
Nrps	2	4170843	4208813	37970	Terpene	4.2	229832	251593	21761	Nrps	1116	1	3157	3156
				437311	Bacteriocin	20.5	77416	88318	10902	Hserlactone	1109	1	6477	6476
HH100					Bacteriocin	21.4	24135	35064	10929	T1pks-Trans	1088	1	71114	71113
Type	**Contig**	**From**	**To**	**Size**	Bacteriocin	21.4	80977	91906	10929	Bacteriocin	1070	89267	114209	24942
Bacteriocin	1.6	297386	308618	11232	Bacteriocin	27.37	34265	45893	11628	Bacteriocin	1068	65691	77313	11622
Indol	1.6	370675	393902	23227					**89166**	Indole	1062	6357	29377	23020
Terpene	9.142	72442	94209	21767	**HH105**					Bacteriocin	1061	97971	112925	14954
Bacteriocin	53.47	1	5882	5881	Type	Contig	From	To	Size	Terpene	1057	2379	24140	21761
Bacteriocin	116.7	1	7336	7335	Nrps		245159	298240	53081	Nrps	1043	1	10869	10868
				69442	Indole		299508	322528	23020	T1pks	1031	31062	62781	31719
HH101					Nrps - t1pks		514613	586000	71387	Nrps	1010	1	6465	6464
Type	**Contig**	**From**	**To**	**Size**	Terpene		720290	743630	23340	Nrps	1008	1	4167	4166
Terpene	2.9	67162	90082	22920	Nrps		812344	879101	66757	Bacteriocin	1003	12988	23917	10929
Nrps	2.9	222076	255211	33135	Nrps		242851	274494	31643					**241190**
Nrps-t1pks	11	1	38330	38329	Nrps		1	52104	52103	***J. agaricidamnosum***				
Nrps	12.6	1	9723	9722	Bacteriocin		74563	98069	23506	**Type**	**Contig**	**From**	**To**	**Size**
Nrps	12.9	1	9927	9926	Butyrolactone		44475	55245	10770	Nrps		172517	246041	73524
Nrps	14.2	1	7256	7255	t1pks		1	36978	36977	Bacteriocin		264017	274907	10890
Nrps	15.3	1	5473	5472	Nrps		1	16334	16333	Linaridin		691531	711619	20088
Nrps	15.6	1	5811	5810	Nrps		1	13583	13582	Indole		1188768	1211818	23050
Nrps	15.6	1	5171	5170	Nrps		1	13376	13375	Nrps-T1pks		1500808	1558071	57263
Bacteriocin	16.6	49875	60726	10851	Nrps		1	12549	12548	Nrps		1875131	1945825	70694
Nrps	17.5	1	3298	3297	Nrps		1	10190	10189	Terpene		2601041	2622818	21777
Nrps	17.7	1	2659	2658	Nrps		1	9035	9034	Nrps		3319919	3367445	47526
Nrps	18.5	1	2181	2180	Bacteriocin		1	8796	8795	Nrps		3360651	3407242	46591
Nrps	18.8	1	2505	2504	Nrps		1	6905	6904	Bacteriocin		4462389	4474032	11643
Nrps	19.1	1	1610	1609	Nrps		1	5790	5789	Nrps		5611727	5667113	55386
Nrps	19.2	1	1924	1923	Bacteriocin		1	4505	4504	Thiopeptide-Lantipept		5696297	5731458	35161
Nrps	20.1	1	1204	1203	Nrps		1	3765	3764	Bacteriocin		5741483	5752382	10899
Nrps	20.2	1	1275	1274	Nrps		1	3127	3126					**484492**
Nrps	21.1	1	111	110	Nrps		1	1457	1456	***D. phyllosphaerae***				
Nrps	21.2	1	1113	1112	Nrps		1	875	874	**Type**	**Contig**	**From**	**To**	**Size**
Bacteriocin	21.4	90098	98908	8810					**502857**	Bacteriocin		1	4532	4531
Nrps	21.7	1	1126	1125	**HH106**					Terpene		63457	85180	21723
Nrps	37.5	1	31961	31960	**Type**	**Contig**	**From**	**To**	**Size**	Terpene		145922	170014	24092
Indol	37.5	33306	64046	30740	Terpene	1.2	345867	367628	21761	Siderophore		1	9751	9750
Nrps	62.4	1	22288	22287	Indole	1.2	483596	506610	23014	Arylpolyene		8652	39110	30458
Other	76.2	5660	27119	21459	Bacteriocin	1.2	575510	586454	10944					**90554**
				282841	Bacteriocin	10	39389	50288	10899	***D. zoogloeoides***				
HH102					Bacteriocin	18.7	68846	80471	11625	**Type**	**Contig**	**From**	**To**	**Size**
Type	**Contig**	**From**	**To**	**Size**					**78243**	T1pks-Trans	2	52582	96922	44340
Bacteriocin	30.3	57951	68580	10629	**HH107**					Terpene	2	475793	497531	21738
Bacteriocin	1.35	90206	101150	10944	**Type**	**Contig**	**From**	**To**	**Size**	Bacteriocin	3	482188	494086	11898
Indol	1.35	163420	186434	23014	Bacteriocin	5.6	67406	79031	11625	Arylpolyene	5	15379	59029	43650
Terpene	1.35	304954	326715	21761	Indole	7.3	61830	84844	23014	Terpene	7	142677	167375	24698
Bacteriocin	36.9	39622	54216	14594	Bacteriocin	35.7	7409	18308	10899					**146324**
				80942	Bacteriocin	37.9	17739	28683	10944					
					Terpene	55.1	9135	35063	25928					
									82410					

Shown are the secondary metabolite type, the contig as known, the start and end positions and the size of the contig. The contig coding for the indole violacein is marked dark gray and for the arylpolyene xanthomonadin is marked bright gray.

Table 9.2 Genes potentially involved in protein secretion in all isolates and type strains

	Name	KEGG number	HH100	HH102	HH103	HH104	HH106	HH107	5059	1522	9268	HH01	HH101	HH105	23865	16928
	SecD/F	K03072	+	+	+	+	+	+	+	+	+	+	+	+	+	
	SecE	K03073			+			+			+	+	+	+	+	
	SecG	K03073	+	+	+	+	+	+	+	+	+	+	+	+	+	
	SecY	K03076	+	+	+	+	+	+	+	+	+	+	+	+	+	+
	YajC	K03210	+	+	+	+	+	+	+	+	+	+	+	+	+	+
sec	YidC	K03217	+	+	+	+	+	+	+	+	+	+	+	+	+	+
	SecA	K03070	+	+	+	+	+	+	+	+	+	+	+	+	+	+
	SecM															
	FtsY	K03110	+	+	+	+	+	+	+	+	+	+	+	+	+	+
	SecB	K03071	+	+	+	+	+	+	+	+	+	+	+	+	+	+
	ffh	K03106	+	+	+	+	+	+	+	+	+	+	+	+	+	+
	TatA	K03116	+	+	+	+	+	+	+	+	+	+	+	+	+	+
tat	TatB	K03117	+	+	+	+	+	+	+	+	+	+	+	+	+	+
	TatC	K03118	+	+	+	+	+	+	+	+	+	+	+	+	+	+
	TolC	K12340	+	+	+	+	+	+	+	+	+	+	+	+	+	+
1	HlyD	K11003		+	+	+	+	+	+							
	HlyB	K11004	+	+	+	+	+	+	+	+			+			
	GspD	K02453	+	+	+	+	+	+	+	+	+	+	+	+	+	+
	GspS															
	GspC	K02452	+	+	+	+	+	+	+	+	+	+	+		+	+
	GspF	K02455	+	+	+	+	+	+	+	+	+	+	+	+	+	+
	GspG	K02456	+	+	+	+	+	+	+	+	+	+	+	+	+	+
	GspH	K02457	+	+	+	+	+	+	+	+	+	+	+	+	+	+
2	GspI	K02458	+	+	+	+	+	+	+	+	+	+	+	+	+	+
	GspJ	K02459	+	+	+	+	+	+	+	+	+	+	+	+	+	+
	GspK	K02460	+	+	+	+	+	+	+	+	+	+	+	+	+	+
	GspL	K02461	+	+	+	+	+	+	+	+	+	+	+	+	+	+
	GspM	K02462	+	+	+	+	+	+	+	+	+	+	+	+	+	+
	GspE	K02454	+	+	+	+	+	+	+	+	+	+	+	+	+	+
	GspO	EC:2.1.- EC:3.4.23.43	++	++	++	++	++	++	++	++	++	++	++	++	++	++
	YscF															
	YscO															
	YscP															
	YscX															
	YscC	K03219									+					
	YscW															
	YscJ	K03222									+					
3	YscR	K03226									+					
	YscS	K03227									+					
	YscT	K03228									+					
	YscU	K03229									+					
	YscV	K03230									+					
	YscN	Ec:3.6.3.14	+	+	+	+	+	+	+	+	++	+	+	+	+	+
	YscQ	K03225									+					
	YscL															
	VirB1	K03194		+												
	VirB2	K03197											+	+	+	
	VirB3	K03198											+	+	+	
	VirB5	K03200		+									+	+	+	
	VirB7															
4	VirB9	K03204		+						+			+	+	+	
	VirB6	K03201		+									+	+		
	VirB8	K03203											+	+		
	VirB10	K03195		+						+			+	+	+	
	VirB4	K03199								+			+	+		
	VirB11	K03196		+									+	+	+	
	VirD4	K03205											+	+	+	
	VgrG	K11904	+	+	+	+	+	+	+	+	+	+	+	+	+	+
	Hcp	K11903	+	+	+	+	+	+	+	+	+	+	+	+	+	+
	Lip	K11906	+	+	+	+	+	+	+	+		+				
	IcmF	K11891	+	+	+	+	+	+	+	+	+	+	+	+	+	+
6	DotU	K11892	+	+	+	+	+	+	+	+	+	+	+	+	+	+
	ClpV	K11907	+	+	+	+	+	+	+	+	+	+	+	+	+	+
	PpkA	EC:2.7.11	+	+	+	+	+	+	+	+	+	+	+	+	+	+
	FhaI										+					
	PppA	EC:3.1.3.16	+	+	+		+	+	+	+	+	+	+	+		
Summe			66	73	67	69	65	66	71	81	92	71	84	83	64	58

Table 9.3 Annotated, predicted and potentially secreted α-amylases of all isolates and type strains

Locus Tag	Gene Product Name	Genome
DUPY_33670	alpha-amylase	*D.phyllosphaerae*
DUPY_51990	alpha-amylase	*D.phyllosphaerae*
F460DRAFT_01174	alpha-amylase	*D. zoogloeoides*
F460DRAFT_03410	alpha-amylase	*D. zoogloeoides*
JALI_48240	alpha-amylase	*J. lividum*
Jab_1c09720	Alpha amylase, catalytic domain	*D*. sp. HH01
Jab_2c03620	alpha-amylase	*D*. sp. HH01
Jab_2c25890	alpha-amylase	*D*. sp. HH01
JAB1_10200	alpha-amylase	*J*. sp. MP5059B
JAB2_58430	alpha-amylase	*J.* sp. HH100
JAB3_20440	alpha-amylase	*D.* sp. HH101
JAB3_47370	Alpha amylase, catalytic domain	*D.* sp. HH101
JAB3_55200	alpha-amylase	*D.* sp. HH101
JAB4_21770	alpha-amylase	*J.* sp. HH102
JAB5_04530	alpha-amylase	*J.* sp. HH103
JAB6_40950	alpha-amylase	*J.* sp. HH104
JAB7_36460	alpha-amylase	*D.* sp. HH105
JAB7_39670	alpha-amylase	*D.* sp. HH105
JAB7_47690	Alpha amylase, catalytic domain	*D.* sp. HH105
JAB8_25260	alpha-amylase	*J.* sp. HH106
JAB9_24720	alpha-amylase	*J.* sp. HH107

Homologous genes in dark and medium gray are present in all *Duganella* affiliated strains. Bright gray is one α-amylase gene of *J. lividum* with homologies to HH101 and HH105.

Table 9.4 Annotated, predicted and potentially secreted esterases and lipases of all isolates and type strains

Locus Tag	Gene Product Name	Genome
DUPY_12930	Acetyl esterase/lipase	*D.phyllosphaerae*
DUPY_17460	Acetyl esterase/lipase	*D.phyllosphaerae*
DUPY_47010	triacylglycerol lipase	*D.phyllosphaerae*
DUPY_52210	Secretory lipase	*D.phyllosphaerae*
F460DRAFT_01580	Acetyl esterase/lipase	*D. zoogloeoides*
F460DRAFT_04739	Acetyl esterase/lipase	*D. zoogloeoides*
F460DRAFT_05327	Acetyl esterase/lipase	*D. zoogloeoides*
GJA_1870	Acetyl esterase/lipase	*J. agaricidamnosum*
GJA_1872	Acetyl esterase/lipase	*J. agaricidamnosum*
GJA_2455	Acetyl esterase/lipase	*J. agaricidamnosum*
Jab_1c09330	Acetyl esterase/lipase	*D*. sp. HH01
Jab_2c14910	Acetyl esterase/lipase	*D*. sp. HH01
Jab_2c25040	Acetyl esterase/lipase	*D*. sp. HH01
Jab_2c30880	putative lipase/esterase	*D*. sp. HH01
Jab_2c03290	triacylglycerol lipase	*D*. sp. HH01

Locus Tag	Gene Product Name	Genome
JAB1_01500	Esterase/lipase superfamily enzyme	*J.* sp. MP5059B
JAB1_19800	Acetyl esterase/lipase	*J.* sp. MP5059B
JAB1_27280	Acetyl esterase/lipase	*J.* sp. MP5059B
JAB1_43450	Phospholipase/lecithinase/hemolysin	*J.* sp. MP5059B
JAB1_47960	triacylglycerol lipase	*J.* sp. MP5059B
JAB2_00480	triacylglycerol lipase	*J.* sp. HH100
JAB2_04100	phospholipase A1	*J.* sp. HH100
JAB2_04190	Acetyl esterase/lipase	*J.* sp. HH100
JAB2_07720	phospholipase C	*J.* sp. HH100
JAB2_26480	Esterase/lipase superfamily enzyme	*J.* sp. HH100
JAB2_29650	Acetyl esterase/lipase	*J.* sp. HH100
JAB2_55980	Phospholipase/lecithinase/hemolysin	*J.* sp. HH100
JAB3_02020	phospholipase A1	*D.* sp. HH101
JAB3_54910	triacylglycerol lipase	*D.* sp. HH101
JAB4_05670	Acetyl esterase/lipase	*J.* sp. HH102
JAB4_09580	Phospholipase/lecithinase/hemolysin	*J.* sp. HH102
JAB4_29180	Acetyl esterase/lipase	*J.* sp. HH102
JAB4_29270	phospholipase A1	*J.* sp. HH102
JAB4_33370	Esterase/lipase superfamily enzyme	*J.* sp. HH102
JAB4_42030	triacylglycerol lipase	*J.* sp. HH102
JAB4_43370	phospholipase C	*J.* sp. HH102
JAB5_04970	Acetyl esterase/lipase	*J.* sp. HH103
JAB5_05060	phospholipase A1	*J.* sp. HH103
JAB5_20090	triacylglycerol lipase	*J.* sp. HH103
JAB5_22490	Phospholipase/lecithinase/hemolysin	*J.* sp. HH103
JAB5_24890	phospholipase C	*J.* sp. HH103
JAB5_36820	Acetyl esterase/lipase	*J.* sp. HH103
JAB5_38530	Predicted acylesterase/phospholipase RssA	*J.* sp. HH103
JAB6_02370	Lysophospholipase L1	*J.* sp. HH104
JAB6_18420	Acetyl esterase/lipase	*J.* sp. HH104
JAB6_18460	phospholipase A1	*J.* sp. HH104
JAB6_47750	triacylglycerol lipase	*J.* sp. HH104
JAB6_48340	Acetyl esterase/lipase	*J.* sp. HH104
JAB6_53390	Predicted acylesterase/phospholipase RssA	*J.* sp. HH104
JAB7_04800	phospholipase A1	*D.* sp. HH105
JAB7_36780	triacylglycerol lipase	*D.* sp. HH105
JAB8_00030	phospholipase C	*J.* sp. HH106
JAB8_06890	Acetyl esterase/lipase	*J.* sp. HH106
JAB8_06970	phospholipase A1	*J.* sp. HH106
JAB8_25070	Acetyl esterase/lipase	*J.* sp. HH106
JAB8_34260	Acetyl esterase/lipase	*J.* sp. HH106
JAB8_37520	Phospholipase/lecithinase/hemolysin	*J.* sp. HH106
JAB8_46050	triacylglycerol lipase	*J.* sp. HH106
JAB9_20150	Phospholipase/lecithinase/hemolysin	*J.* sp. HH107

JAB9_23260	Acetyl esterase/lipase	*J.* sp. HH107
JAB9_23340	phospholipase A1	*J.* sp. HH107
JAB9_25060	phospholipase C	*J.* sp. HH107
JAB9_26430	triacylglycerol lipase	*J.* sp. HH107
JAB9_40850	Predicted acylesterase/phospholipase RssA	*J.* sp. HH107
JAB9_45780	Acetyl esterase/lipase	*J.* sp. HH107
JALI_04100	Acetyl esterase/lipase	*J. lividum*
JALI_04190	phospholipase A1	*J. lividum*
JALI_09110	triacylglycerol lipase	*J. lividum*
JALI_13950	Acetyl esterase/lipase	*J. lividum*
JALI_55310	triacylglycerol lipase	*J. lividum*
Locus Tag	**Gene Product Name**	**Genome**

Table 9.5 Annotated, predicted and potentially secreted chitinases of all strains and type strains

Locus Tag	**Gene Product Name**	**Genome**
GJA_1462	chitinase	*J. agaricidamnosum*
GJA_3469	chitinase	*J. agaricidamnosum*
GJA_4040	chitinase	*J. agaricidamnosum*
GJA_4156	chitinase	*J. agaricidamnosum*
Jab_1c17130	chitinase	*D*. sp. HH01
Jab_2c26460	chitinase	*D*. sp. HH01
Jab_2c26470	chitinase	*D*. sp. HH01
Jab_2c26490	chitinase	*D*. sp. HH01
JAB1_14790	putative chitinase	*J*. sp. MP5059B
JAB1_19120	chitinase	*J*. sp. MP5059B
JAB1_29670	putative chitinase	*J*. sp. MP5059B
JAB1_53330	chitinase	*J*. sp. MP5059B
JAB2_04990	chitinase	*J.* sp. HH100
JAB2_07660	chitinase family 18	*J.* sp. HH100
JAB2_50500	putative chitinase	*J.* sp. HH100
JAB3_10240	chitinase	*D.* sp. HH101
JAB3_19810	chitinase family 18	*D.* sp. HH101
JAB3_19830	chitinase family 18	*D.* sp. HH101
JAB4_28380	chitinase	*J.* sp. HH102
JAB4_38260	chitinase family 18	*J.* sp. HH102
JAB4_38270	chitinase class family 19	*J.* sp. HH102
JAB5_10110	chitinase	*J.* sp. HH103
JAB5_10920	putative chitinase	*J.* sp. HH103
JAB5_14470	chitinase family 18	*J.* sp. HH103
JAB6_11140	chitinase	*J.* sp. HH104
JAB6_48230	chitinase family 18	*J.* sp. HH104
JAB7_25400	chitinase	*D.* sp. HH105
JAB7_54080	chitinase family 18	*D.* sp. HH105
JAB7_54100	chitinase family 18	*D.* sp. HH105

JAB8_51920	chitinase	*J.* sp. HH106
JAB9_09060	chitinase	*J.* sp. HH107
JAB9_25790	chitinase family 18	*J.* sp. HH107
JALI_17800	chitinase	*J. lividum*
JALI_33250	chitinase	*J. lividum*
Locus Tag	**Gene Product Name**	**Genome**

Table 9.6 Annotated, predicted and potentially secreted chitin deacetylases of all strains and type strains

Locus Tag	**Gene Product Name**	**Genome**
DUPY_04600	Peptidoglycan/xylan/chitin deacetylase	*D.phyllosphaerae*
DUPY_31930	Peptidoglycan/xylan/chitin deacetylase	*D.phyllosphaerae*
F460DRAFT_01065	Predicted xylanase/chitin deacetylase	*D. zoogloeoides*
F460DRAFT_01971	Peptidoglycan/xylan/chitin deacetylase	*D. zoogloeoides*
F460DRAFT_02186	Peptidoglycan/xylan/chitin deacetylase	*D. zoogloeoides*
Jab_1c09510	Peptidoglycan/xylan/chitin deacetylase	*D*. sp. HH01
Jab_1c15070	Peptidoglycan/xylan/chitin deacetylase	*D*. sp. HH01
Jab_1c18190	Peptidoglycan/xylan/chitin deacetylase	*D*. sp. HH01
Jab_2c10030	Peptidoglycan/xylan/chitin deacetylase	*D*. sp. HH01
Jab_2c35190	Peptidoglycan/xylan/chitin deacetylase	*D*. sp. HH01
JAB1_33750	Peptidoglycan/xylan/chitin deacetylase	*J*. sp. MP5059B
JAB2_27690	Peptidoglycan/xylan/chitin deacetylase	*J.* sp. HH100
JAB3_08200	Peptidoglycan/xylan/chitin deacetylase	*D.* sp. HH101
JAB3_29740	Peptidoglycan/xylan/chitin deacetylase	*D.* sp. HH101
JAB3_47190	Peptidoglycan/xylan/chitin deacetylase	*D.* sp. HH101
JAB3_63710	Peptidoglycan/xylan/chitin deacetylase	*D.* sp. HH101
JAB4_36950	Peptidoglycan/xylan/chitin deacetylase	*J.* sp. HH102
JAB5_15100	Peptidoglycan/xylan/chitin deacetylase	*J.* sp. HH103
JAB6_19790	Peptidoglycan/xylan/chitin deacetylase	*J.* sp. HH104
JAB6_28930	Peptidoglycan/xylan/chitin deacetylase	*J.* sp. HH104
JAB7_01170	Peptidoglycan/xylan/chitin deacetylase	*D.* sp. HH105
JAB7_21720	Peptidoglycan/xylan/chitin deacetylase	*D.* sp. HH105
JAB7_27530	Peptidoglycan/xylan/chitin deacetylase	*D.* sp. HH105
JAB7_62770	Peptidoglycan/xylan/chitin deacetylase	*D.* sp. HH105
JAB8_40250	Peptidoglycan/xylan/chitin deacetylase	*J.* sp. HH106
JAB9_38060	Peptidoglycan/xylan/chitin deacetylase	*J.* sp. HH107
JALI_54300	Peptidoglycan/xylan/chitin deacetylase	*J. lividum*

Table 9.7 Gene sizes and intergenic regions of the JQS system of 21 *Oxalobacteraceae;* [bp]

Strain	*jqsA gene length*	*jqsA-jqsS* intergenic region	*jqsS gene length*	*jqsS-jqsR* intergenic region	*jqsR gene length*
HH100	1244	43	1442	4	1007
HH102	1244	43	1442	4	1007
HH103	1244	43	1442	4	1007
HH104	1244	164	1319	4	1007
HH106	1244	43	1442	4	1007
HH107	1244	43	1442	4	1007
5059	1247	153	1298	4	1007
1522	1247	153	1298	4	1007
9628	1247	160	1319	9	1001
25724	1247	153	1313	4	1007
RA13	1247	153	1298	4	1007
CG3	1253	184	1271	9	995
OK676	1244	42	1430	4	1007
344	1244	166	1316	4	1013
551a	1244	166	1316	4	1013
RIT308	1244	164	1319	4	1007
HH101	1259	172	1280	4	1010
HH105	1259	172	1280	4	1010
23865	1256	168	1280	3	1091
16928	1259	167	1280	3	1076
HH01	1259	172	1280	4	1010

Table 9.8 JAI-1 motif of the 5' gene regions of the chitinase *chiA*, the AI synthase *jqsA* and the violacein operon *vioA*

gene name	strain	gene number	JAI-1 motif in 5' gene region
chiA	HH01	Jab_2c26490	**TTGG** TACGCG **TCAA**
	HH100, HH102, HH103, HH104, HH107, 5059, 1522	JAB2_53050, JAB4_02140, JAB5_43070, JAB6_08700, JAB9_00320, JAB1_49050, JALI_07700	**TTAG** AGGCCACT **TCAA**
	HH101	JAB3_19810	**TTGG** TATTCG **TCAA**
	HH105	JAB7_54080	**TTGG** TACTCG **TCAA**
	9628	GJA_3469	**TTGA** TACCACT **TCGA**
jqsA	HH01, HH101, HH105	Jab_2c24330, JAB3_22080, JAB7_46330	**TTGA** TCAGCG **TCAA**
	HH100, HH102, HH103, HH104, HH106, HH107	JAB2_10110, JAB4_14950, JAB5_52650, JAB6_32140,JAB8_15610, JAB9_28750	**TTGA** GCTGTA **TCAA**
	5059, 1522	JAB1_37310, JALI_03530	**TTGA** TATACG **TCAA**
	9628	GJA_1197	**TTGA** TGTAGA **TCAA**
	16928	F460DRAFT_03279	**TTGA** TTTTGA **TCAA**
	9628	DUPY_10350	**TTGA** CCTTGA **TCAA**
vioA	HH01	Jab_2c08810	**TTGA** CATTTA **TCAA**
	HH100 - 107, 5059	JAB2_05300, JAB3_04810, JAB4_20530, JAB5_09800, JAB6_20840, JAB7_02320, JAB8_05560, JAB9_09370, JAB1_31660	**TTGA** TATTTA **TCAA**
	1522	JALI_28730	**TTGA** TATTTA **TCAA**

Table 9.9 Relative fluorescence (RFU) of the *F. graminearum* control (*F. g.*) and HH102 and HH102Δ*jqsA* NADG pretreated bacterial strains coincubated with *F. graminearum*

Experiment	*F. g.*	HH102	HH102Δ*jqsA*	p-value	statistically significant
V5	16958	5195	15384	0.0005	yes
	12524	3886			
	14691	5265	14853		
	14471				
V7	15302	6370	9264	0.0335	yes
	11973	6379	11106		
	11635		12859		
	13088	8497			
qRT1	5932	5338	14196	0.0001	yes
	5595	6733	10637		
	5885	4947	13154		
	5191	5847	11187		
	7717	5170	10319		
qRT2	6200	8862	8558	0.3579	no
	5300	8273	9184		
	6818	8807	10128		
	5736	9141	8774		
	7775				
qRT3	6659	1579	11419	0.0001	yes
	7410	1639	11274		
	8527	1450	8340		
	7654	1397	9470		
	9101	1419	8118		
P1	6517	376	896	0.0001	yes
	6988	380	793		
	6363	344	781		
	6592	307	810		
P2	7496	638	2151	0.0001	yes
	6560	643	2440		
	6882	511	2545		
	6409	402	1984		
P3		1174	3033	0.0062	yes
	10889	2592	3452		
		1693	3128		
	12161	1705	4273		

Shown are the RFUs of the eight independent experiments, the p-value of an unpaired t test and the resulting statistically significance.

Table 9.10 Relative fluorescence (RFU) of the *F. graminearum* control (*F. g.*) and HH102, HH102Δ*jqsA* and HH102Δ*jqsA* harboring *jqsA* gene on a self replicable pBBR1MCS-2 plasmid. 180 µl of filtered bacterial supernatant was coincubated with 400 *F. graminearum* conidia as described.

	F.graminearum			
	F.g.	**HH102**	**HH102Δ*jqsA***	**HH102Δ*jqsA* pBBR1MCS-2::*jqsA***
E1	6837 ± 417.2	549 ± 99.8	2280 ± 223.7	801 ± 93.3
E2	16862 ± 548.4	5528 ± 879.0	6030 ± 1741.3	751 ± 270.9
E3	11352 ± 1884.6	1580 ± 53.0	13926 ± 4035.2	4742 ± 1992.7

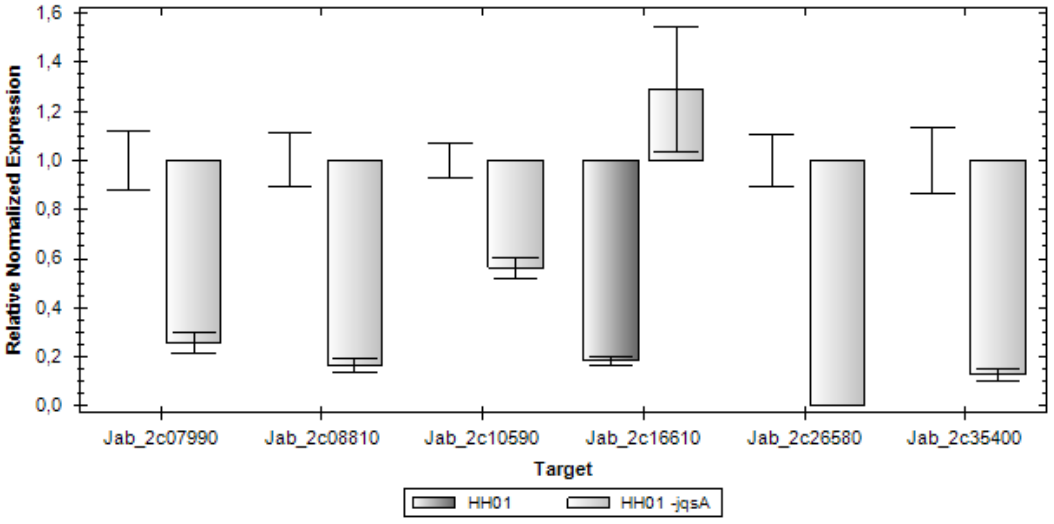

Figure 9.1 **qRT-PCR to verify the RNA-seq data of strains HH01 / HH01Δ*jqsA* at early stationary phase**. Shown is the normalized expression of three technical and three biological samples. The graph is shown with data relative to control (2.9.3).

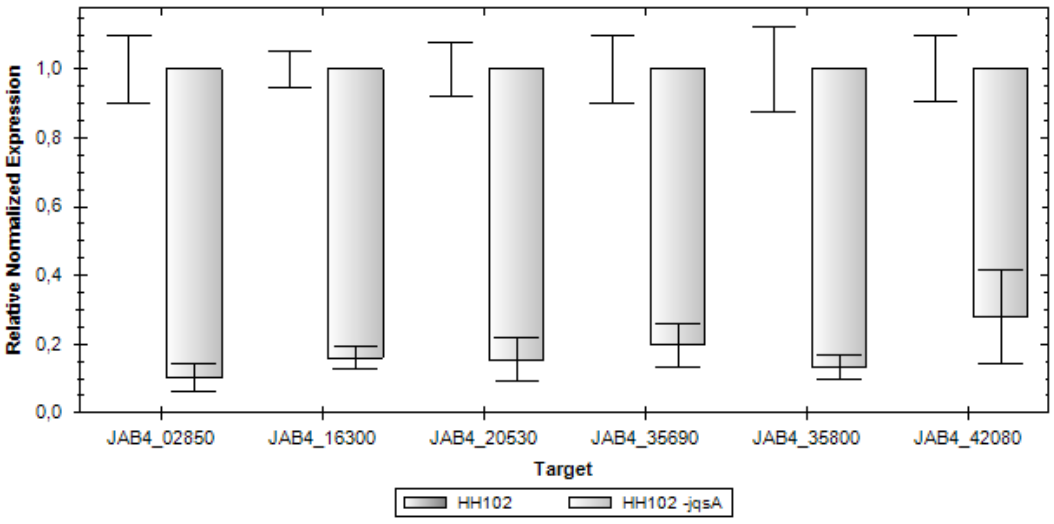

Figure 9.2 **qRT-PCR to verify the RNA-seq data of strains HH102 / HH102Δ*jqsA* at early stationary phase**. Shown is the normalized expression of three technical samples. For strain HH102 only jan4t1 and jan4t2 RNA was used, graphs of strain HH102ΔjqsA composes of three technical and three biological samples.The graph is shown with data relative to control (2.9.3).

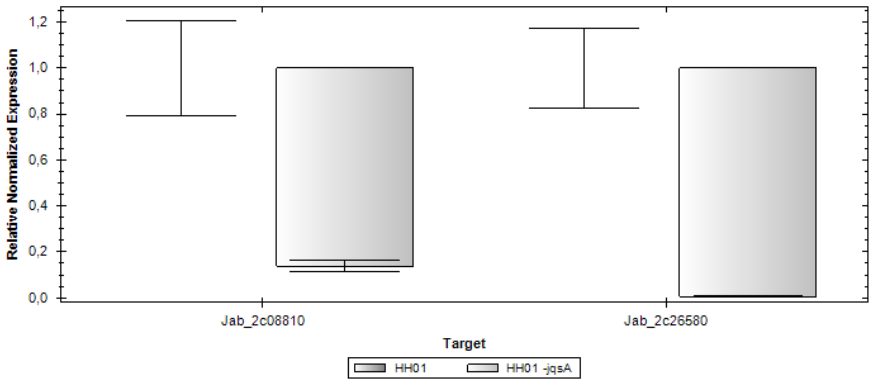

Figure 9.3 **qRT-PCR to verify the RNA-seq data of strains HH01 / HH01Δ*jqsA* at late stationary phase**. Shown is the normalized expression of three technical and three biological samples. The graph is shown with data relative to control (2.9.3).

Figure 9.4 **5' region of the *vioA* gene of strain HH107**. Shown are the primers for amplification of the promoter region (Pvio107+JAI-1-FP-BamHI; oFH91, Pvio107-JAI-1-FP-XhoI; oFH105, Pvio107+JAI-1-RP-EcoRI; oFH92; written in gray and gray boxed) and the JAI-1 motif highlighted in gray and written in white with the conserved bases bold and underlined. The -35 box and -10 box are both bright gray boxed. The translational start (ATG) is written in black withing primer Pvio107+JAI-1-RP-EcoRI. Numbers refer to the position in matters of the translational start.

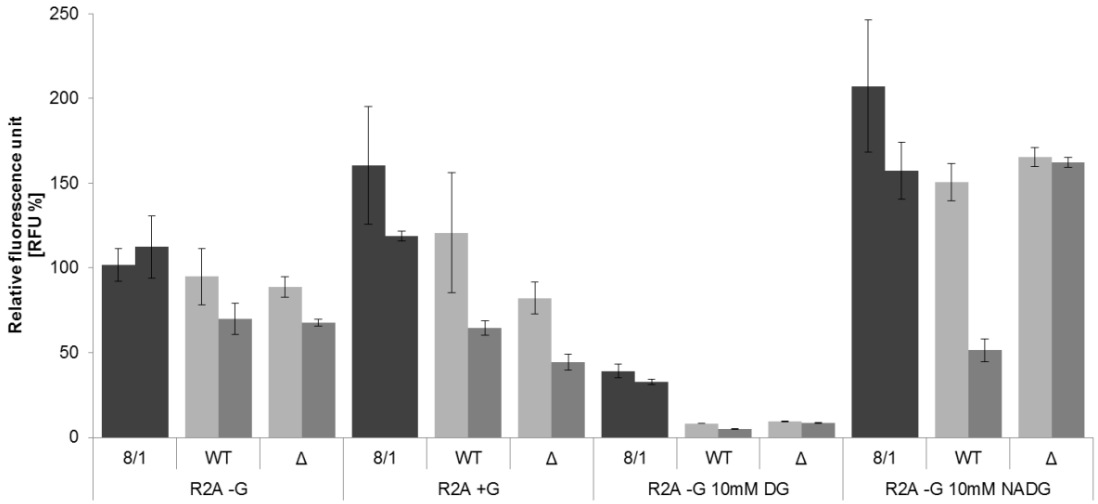

Figure 9.5 **Bacterial growth inhibition of *F. graminearum* 8/1** (8/1, dark gray)**.** Bright gray are either HH01 (WT) or HH01Δ*jqsA* (Δ) and gray are HH102 (WT) or HH102Δ*jqsA* (Δ). R2A –G media were supplemented with 0.05% G, 10 mM DG or 10 mM NADG. Bacteria were incubated at 22 °C for 24 h. 180 µl of filtered supernatant (1 x 10^9 cells/ml) and 400 fungal conidia were incubated for 72 h at 28 °C. Expression of chromosomally integrated *gfp* in 8/1 was detected at 485/20; 528/20 nm. Experiments were performed at least thrice in quadruples. One individual experiment is shown. RFU results of coincubated bacteria with fungi were normalized to fungal samples without bacteria in respective media (set as 100%).